Structural Brain Connectivity in Aging and Neurodegeneration

L.G.M. Cremers

Structural Brain Connectivity in Aging and Neurodegeneration

L.G.M. Cremers

ISBN: 978-94-6361-109-1
Printing: Optima Grafische Communicatie, Rotterdam, The Netherlands
Cover: Optima Grafische Communicatie, Rotterdam, The Netherlands

Structural Brain Connectivity in Aging and Neurodegeneration

Structurele brein connectiviteit in veroudering en neurodegeneratie

Proefschrift

ter verkrijging van de graad van doctor aan de
Erasmus Universiteit Rotterdam
op gezag van de
rector magnificus

Prof.dr. H.A.P. Pols

en volgens besluit van het College voor Promoties.

De openbare verdediging zal plaatsvinden op
dinsdag 26 juni 2018 13.30

door

Lotte G.M. Cremers

geboren te Boxmeer

Erasmus University Rotterdam

PROMOTIECOMMISSIE

Promotoren:	Prof.dr. M.W. Vernooij Prof.dr. M.A. Ikram
Overige leden:	Prof.dr. F-E. de Leeuw Prof.dr. P.J. Koudstaal Dr. S. Klein
Paranimfen:	Selma Andrade Pauline Croll

ACKNOWLEDGEMENTS

The work described in this thesis was conducted at the Department of Epidemiology in collaboration with the Department of Radiology and Nuclear Medicine at the Erasmus Medical Center, Rotterdam, the Netherlands.
The studies described in this thesis are embedded in the Rotterdam Study. The contribution of the study participants, the staff from the Rotterdam Study, and participating general practitioners and pharmacists is gratefully acknowledged. The Rotterdam Study is supported by the Erasmus University Medical Center and Erasmus University Rotterdam; the Netherlands Organization for Scientific Research (NWO); The Netherlands Organization for Health Research and Development (ZonMW); the Research Institute for Diseases in the Elderly (RIDE); the Netherlands Genomics Initiative (NGI); the Ministry of Education, Culture and Science; the Ministry of Health, Welfare and Sports; the European Commission (DG XII); and the Municipality of Rotterdam. The funders had no role in design or conduct of the studies; collection, management, analysis, or interpretation of the data; or preparation, review or approval of the manuscripts described in this thesis.

Publication of this thesis was kindly supported by the Department of Epidemiology and Radiology and Nuclear Medicine of the Erasmus University Medical Center and by the Erasmus University Rotterdam, The Netherlands.

TABLE OF CONTENTS

MANUSCRIPTS THAT FORM THE BASIS OF THIS THESIS

Chapter 2 Determinants of white matter microstructural changes

White matter degeneration with aging: longitudinal diffusion MR imaging analysis: de Groot M**, Cremers LGM**, Ikram MA., Hofman A., Krestin GP, van der Lugt A., Niessen WJ, Vernooij MV. Radiology 2016 May 279 (2): 532-41

Kidney function and microstructural integrity of brain white matter: Sedaghat S, **Cremers LGM**, de Groot M, Hoorn EJ, Hofman A, van der Lugt A, Franco OH, Vernooij MW, Dehghan A, Ikram MA. Neurology 2015 Jul 14: 85(2):154-61.

Retinal microvasculature and white matter microstructure: The Rotterdam Study. Mutlu U, **Cremers LGM**, de Groot M, Hofman A, Niessen WJ, van der Lugt A, Klaver CC, Ikram MA, Vernooij MW, Ikram MK. Neurology 2016 sept 6; 87(10):1003-10..

Reduced lung function is associated with poorer brain white matter microstructure. **Cremers LGM**, Lahousse L, de Groot M, Roshchupkin GV, Krestin GP, Niessen WJ, Stricker BH, Ikram MA, Brussele GG, Vernooij MW. *Submitted*

Age dependent association of thyroid function with brain morphology and microstructural organization: evidence from brain imaging.
Cremers LGM*,Chaker L*, Korevaar TIM, de Groot M, Dehghan A, Franco OH, Niessen WJ, Ikram MA, Peeters RP, Vernooij MW. Neurobiology of Aging 2018 Jan;61:44-51.

Chapter 3 White matter microstructural integrity and age-related brain diseases

Determinants, MRI correlates, and prognosis of mild cognitive impairment: The Rotterdam Study.
Cremers LGM*, de Bruijn RF*, Akoudad S*, Hofman A, Niessen WJ, van der Lugt A, Koudstaal PJ, Vernooij MW, Ikram MA. Journal of Alzheimers disease 2014;42 Suppl 3:S239-49.

Altered tract-specific white matter microstructure is related to poorer cognitive performance: The Rotterdam Study.
Cremers LGM, de Groot M, Hofman A, Krestin GP, van der Lugt A, Niessen WJ, Vernooij MW, Ikram MA. Neurobiology of Aging 2016 mar;39:108-17.

Structural connectivity relates to risk of dementia in the general population: evidence for the disconnectivity hypothesis.
Cremers LGM, Wolters FJ, de Groot M, Ikram MK, van der Lugt A, Niesesn WJ, Vernooij MW*, Ikram MA*. *Submitted*

White matter microstructure and hearing acuity in older adults: a population-based cross-sectional DTI study.
Rigters SC, **Cremers LGM**, Ikram MA, van der Schroeff MP, de Groot M, Roshchupkin GV, Niessen WJ, Baatenburg de Jong RJ, Goedegebure A, Vernooij MW. Neurobiology of aging 2018 Jan;61:124-131.

Lower microstructural integrity of brain white matter is related to higher mortality.
Cremers LGM*, Sedaghat S*, de Groot A, van der Lugt A, Niessen WJ, Franco OH, Dehghan A, Ikram MA, Vernooij MW. Neurology 2016 Aug 30; 87(9);927-34

Genetic variation underlying cognition and its relation with neurological outcomes.
Cremers LGM*, Knol MJ*, Heshmatollah A*, Ikram MK, Uitterlinden AG, van Duijn CM, Niessen WJ, Vernooij MW, Ikram MA, Adams HHH. *Submitted*

Predicting global cognitive decline in the general population using the Disease State Index.
Cremers LGM*, Huizinga W*, Niessen WJ, Krestin GP, Poot DHJ, Ikram MA, Lötjönen J, Klein S**, Vernooij MW**.
Submitted

Chapter 4 General Discussion

Structural connectivity relates to risk of dementia in the general population: evidence for the disconnectivity hypothesis.
Cremers LGM, Wolters FJ, de Groot M, Ikram MK, van der Lugt A, Niesesn WJ, Vernooij MW*, Ikram MA*. *Submitted*

* *Denotes equal contribution*
** *Denotes shared last author*

CHAPTER 1

Introduction

CHAPTER 1.1

General Introduction and outline

GENERAL INTRODUCTION

Worldwide, populations are aging. As a result, this will lead to an increase in prevalence of common age-related brain diseases such as cognitive decline, dementia and neurovascular diseases. These diseases pose a high burden on our society, both in terms of suffering as well as financially. From a perspective of disease prevention, the search for potentially modifiable etiologic factors and a better understanding of the pathophysiological pathways of age-related brain diseases is of major importance. One approach in this is to study brain disease in its earliest stage, before clinical symptoms arise. Subclinical brain changes are thought to occur years, if not decades, prior to onset of clinical symptoms of many age-related diseases[1], and with advanced, non-invasive imaging methods we are able to study these subclinical brain changes directly. In the past, research has mainly focused on cerebral grey matter in age-related diseases. Nowadays, also an important role of cerebral white matter in age-related diseases has been established. White matter constructs approximately 50% of the brain volume and consumes 43.8% of brain's total energy.[2] White matter is important for the connection of, and the communication between different cortical regions and consists of different white matter tracts, which play a different role in different brain functions. Macrostructural white matter damage such as white matter atrophy and white matter hyperintensity load, is visible on a conventional MRI. However these macrostructural changes constitute only the tip of the iceberg of the white matter pathology that have occurred.[3] To improve understanding of the pathophysiology and pathways of age-related brain diseases it is important to identify white matter pathology in an early and preclinical phase. More recently, microstructural white matter changes, not visible for the naked eye has therefore gained interest and is thought of as an earlier and potentially more sensitive marker of white matter damage.[3]

Diffusion tensor imaging (DTI) is a non-invasive magnetic resonance imaging suitable to quantitatively assessing white matter microstructural changes.[4] DTI is sensitive to the random movement of water molecules, which is dependent on the underlying tissue properties or microstructure. DTI can not only be used to characterize the underlying white matter microstructure, but also to reveal the anatomical paths of white matter tracts by connecting voxels with analogous directional diffusion-profiles, the so called tractography.[5]

Imaging data of white matter microstructural changes from the general population might help to disambiguate between normal and abnormal, help to understand underlying mechanisms of pathology and may help to identify persons at risk for a certain disease. However, population data on determinants of white matter microstructural changes globally but in particular in specific white matter tracts in the middle-aged and elderly are scarce.

AIM OF THIS THESIS

The objectives of this thesis were two-fold: Firstly, to study determinants of white matter microstructural changes. The brain is not an organ on itself but is connected with all other organs in our body and therefore we are in particular interested in the systemic influences on the brain of different organs. Secondly, to investigate the link between white matter microstructural and age-related brain diseases. In both aims, I focused both on the white matter microstructural changes across the whole brain, but also across different white matter tracts. My research was embedded within the Rotterdam Study, which is a population-based cohort study since 1990, investigating causes and consequences of diseases in the elderly.[6] From 2005 onwards, MRI scanning including DTI was added to the core study protocol.[7] The entire Rotterdam Study population undergoes regular cognitive assessments and is continuously monitored for major events, including dementia and vascular brain disease.

OUTLINE OF THIS THESIS

Chapter 2 discusses determinants of white matter microstructural damage. In **chapter 2.1** I describe the change in DTI-measures in aging. In **chapter 2.2 and 2.3** I focus on the association between kidney function and white matter microstructural integrity and retinal microvasculature and white matter microstructural changes respectively. **Chapter 2.4** is dedicated to the relation between lung function and white matter microstructure. In **chapter 2.5** I examined the association between thyroid function and white matter microstructural changes.

In **chapter 3** I present the association of global white matter microstructural changes but also in specific tracts with different age-related brain diseases. In **chapter 3.1** I focus on a transitional stage between normal aging and dementia, namely mild cognitive impairment and studied the determinants, MRI markers and prognosis of mild cognitive impairment. **Chapter 3.2** describes the link between tract-specific white matter microstructural integrity and cognitive functioning. In **chapter 3.3** I examined the relation between white matter microstructural integrity and risk of dementia in a longitudinal study. **Chapter 3.4** describes the association of white matter tract microstructural integrity and hearing impairment in the elderly. **Chapter 3.5** addresses the relation between white matter microstructural integrity and risk of mortality. **Chapter 3.6** focuses on the genetic variation underlying cognition and the relation with clinical outcomes and imaging markers. In **chapter 3.7** I applied a previously proposed prediction tool, namely the Disease State Index, to evaluate the prediction of cognitive decline using several features including DTI-measures.

Finally, in **chapter 4** the main findings of this thesis are summarized. Additionally, I discuss in more detail possible underlying pathways and methodological considerations of the performed studies and of diffusion tensor imaging in general. Furthermore, I will consider implications of the findings with respect to clinical practice, after which I will discuss future perspectives.

CHAPTER REFERENCES

1. Jack CR, Jr., Knopman DS, Jagust WJ, et al. Hypothetical model of dynamic biomarkers of the Alzheimer's pathological cascade. *Lancet Neurol.* 2010;9(1):119-128.
2. Fields RD. White matter matters. *Sci Am.* 2008;298(3):42-49.
3. de Groot M, Verhaaren BF, de Boer R, et al. Changes in normal-appearing white matter precede development of white matter lesions. *Stroke.* 2013;44(4):1037-1042.
4. Huisman TA. Diffusion-weighted and diffusion tensor imaging of the brain, made easy. *Cancer Imaging.* 2010;10 Spec no A:S163-171.
5. Jbabdi S, Sotiropoulos SN, Haber SN, Van Essen DC, Behrens TE. Measuring macroscopic brain connections in vivo. *Nat Neurosci.* 2015;18(11):1546-1555.
6. Ikram MA, Brusselle GGO, Murad SD, et al. The Rotterdam Study: 2018 update on objectives, design and main results. *Eur J Epidemiol.* 2017;32(9):807-850.
7. Ikram MA, van der Lugt A, Niessen WJ, et al. The Rotterdam Scan Study: design update 2016 and main findings. *Eur J Epidemiol.* 2015;30(12):1299-1315.

CHAPTER 2

Determinants of white matter microstructural changes

CHAPTER 2.1

White matter degeneration in aging, a longitudinal diffusion MRI analysis

Marius de Groot, Lotte G.M. Cremers, M. Arfan Ikram, Albert Hofman,Gabriel P. Krestin, Aad van der Lugt, Wiro J. Niessen, Meike W. Vernooij

Radiology 2016

ABSTRACT

Purpose To determine longitudinally the rate of change in diffusion tensor imaging (DTI) parameters of white matter microstructure in aging, and to investigate whether cardiovascular risk factors influence this longitudinal change.

Materials and methods A dedicated ethics committee overseen by national government approved this prospective, population-based cohort study and all participants gave written informed consent. Non-demented, community-dwelling participants were scanned using a research-dedicated 1.5T MRI scanner on two separate visits, on average 2.0 years apart. Out of 810 persons who were eligible for scanning at baseline, longitudinal imaging was available for 501 persons, mean age 69.9 years (range 64.1-91.1 years). Changes of normal-appearing white matter DTI characteristics in the tract-centers were analyzed first globally to investigate diffuse patterns of change, then locally using voxelwise multi-linear regressions. We assessed the influence of cardiovascular risk factors by treating them as additional determinants in both analyses.

Results Over the 2.0 year follow-up interval, global fractional anisotropy (FA) decreased by 0.0042 ($p<10^{-6}$), while mean diffusivity (MD) increased by 8.1 x $10^{-6}mm^2/s$ ($p<10^{-6}$). Voxelwise analysis of the brain white matter skeleton showed an average decrease of FA of 0.0082 ($p_{mean}= 0.002$) in 57% of skeleton voxels. The sensorimotor pathway, however, demonstrated an increase of FA of 0.0078 ($p_{mean}= 0.009$). MD increased on average 10.8 x $10^{-6}mm^2/s$ ($p_{mean}< 0.001$), in 79% of white matter skeleton voxels. Additionally, we found that white matter degeneration was more pronounced in higher age. Cardiovascular risk factors were generally not associated with longitudinal changes in white matter microstructure.

Conclusions Longitudinal diffusion analysis indicates widespread microstructural deterioration of the normal-appearing white matter in normal aging, with relative sparing of sensorimotor fibers.

INTRODUCTION

It has been recognized that not only grey matter loss, but also white matter deterioration plays an important role in brain aging and cognitive decline[1] and a vascular etiological pathway is often hypothesized.[2] Diffusion tensor imaging (DTI) is a non-invasive magnetic resonance imaging (MRI) technique that measures diffusion of water, and that can quantify subtle changes of white matter tissue organization not visible on structural MRI. DTI provides multiple descriptors of diffusion, with fractional anisotropy (FA) and mean diffusivity (MD) most widely used. FA describes the directionality of diffusion and a lower value typically reflects reduced microstructural organization in regions where white matter fibers are aligned. MD represents the overall magnitude of water diffusion and generally a higher value reflects reduced microstructural organization.[3] Reduced microstructural white matter organization possibly impedes communication within and between neurocognitive networks, which might result in cognitive impairment.[4] In order to identify persons at a higher risk of neurodegenerative disease, it is important to quantify changes in brain tissue in an early stage.[5] This however also requires characterization of baseline age-related changes. The quantitative nature makes DTI very suitable for longitudinal analyses, which are likely to be more sensitive in the early detection of changes in white matter microstructure. However, longitudinal data are still scarce and studies are mostly performed in small sample sizes and in patients with cognitive impairment or Alzheimer's disease.[6-9] The sparse longitudinal findings in 'normal' aging did however corroborate evidence from cross-sectional studies, which showed that during normal aging white matter demonstrates lower FA, with less uniform observations for regions with crossing fibers, combined with higher MD[6-11], and that those aging effects differ across brain regions.[8,9,12,13] Yet, these results need to be corroborated in larger longitudinal studies.

In the current study, we therefore aimed to longitudinally determine the rate of change in DTI parameters of white matter microstructure in aging, and to investigate whether cardiovascular risk factors influence this longitudinal change.[14-15]

METHODS

Study population

This study is based on participants from the Rotterdam Study, a prospective, population-based cohort study that investigates causes and consequences of age-related diseases.[16] The original study population consisted of 7983 participants aged 55 years and older within Ommoord, a suburb of Rotterdam. In 2000, the cohort was expanded with 3011 persons (≥55 years) living in the study area and not included before (16). Since 2005, brain MRI is incorporated in the core protocol of the study. In 2005 and 2006, a group of 1073 participants was randomly selected from the cohort expansion to participate in the Rotterdam Scan Study.[17] Participants were scanned three times, in 2005-2006, 2008-2009 and in 2011-2012. The latter two time points included an upgraded DTI acquisition that was used for the current analysis, defining the 2008-2009 scan as baseline, and the 2011-2012 scan as follow-up. We excluded individuals who (at either time point) were demented or had MRI contraindications (including claustrophobia). For the 2008-2009 scan, 899 out of the original 1073 persons could be invited, of whom 810 were eligible and 741 participated. At follow up in 2011-2012, 649 out of 741 were re-invited, 625 were eligible and 548 participated. We excluded participants with an incomplete acquisition (n=5), persons with MRI-defined cortical infarcts (n=20), and scans with artifacts hampering automated processing (n=22), resulting in 501 participants with longitudinal DTI data available for analysis. The Rotterdam Population Study Act Rotterdam Study, executed by the Ministry of Health, Welfare and Sports of the Netherlands. Written informed consent was obtained from all participants.

MRI acquisition

Multi-sequence MRI was performed with identical scan parameter settings at both time points on a 1.5T scanner (GE Signa Excite) dedicated to the study and maintained without major hardware or software updates.[17] In short, imaging included a T1-weighted 3D Fast RF Spoiled Gradient Recalled Acquisition in Steady State with an inversion recovery pre-pulse (FASTSPGR-IR) sequence, a proton density (PD) weighted sequence, and a T2-weighted fluid-attenuated inversion recovery (FLAIR) sequence.[17] For DTI, we performed a single shot, diffusion-weighted spin echo echo-planar imaging sequence (repetition time=8575 ms, echo time=82.6 ms, field-of-view=210×210 mm, matrix=96×64 (phase encoding) (zero-padded in k-space to 256×256) slice thickness=3.5 mm, 35 contig uous slices). Maximum b-value was 1000 s/mm^2 in 25 non-collinear directions; three volumes were acquired without diffusion weighting (b-value=0 s/mm^2).

Tissue segmentation

Baseline scans were segmented into grey matter, white matter, cerebrospinal fluid (CSF) and background tissue using an automatic segmentation method.[18] An automatic post-processing step distinguished normal-appearing white matter from white matter lesions (WML), based on the FLAIR image and the tissue segmentation.[19] Intracranial volume (ICV) (excluding the cerebellum with surrounding CSF) was estimated by summing total grey and white matter, and CSF volumes. The WML segmentation was mapped into DTI image space using boundary based registration[20] performed on the white matter segmentation, the b=0 and T1-weighted image.

DTI processing

Diffusion data was pre-processed using a standardized processing pipeline.[21] In short, DTI data was corrected for subject motion and eddy currents by affine co-registration of the diffusion-weighted volumes to the b=0 volumes, including correction of gradient vector directions. Diffusion tensors were estimated using a non-linear Levenberg-Marquardt estimator, available in ExploreDTI.[22] FA and MD, measures of tissue microstructure, were computed from the tensor images. Tensor fits were inspected for artifacts by reviewing axial slices of the FA images (MG, researcher with 5 years experience in diffusion image analysis and LGMC, radiologist in training with 2 years experience in diffusion image analysis).

Image registration

Intra-subject correspondence (between the two time points), and correspondence between subjects was achieved by image registration. Improved tract-based spatial statistics (TBSS) was used with optimized high degree-of-freedom registration in lieu of the two stage registration-projection approach implemented in the original TBSS method.[23,24] All registrations were inspected by reviewing axial compilations of super-positioned moving and target images (MG and LGMC). Following the registration, individual change in diffusion measures could be computed in standard space (MNI152, as provided with the FSL software[25]) by subtracting baseline from follow-up images.
A study specific white matter skeleton was constructed using the TBSS skeletonization procedure on the average FA image composed of all subject images at both time points combined in standard space; thresholding the FA skeleton at 0.25. This skeleton was then used to mask the difference images for longitudinal statistical analysis.

Assessment of risk factors

The following cardiovascular risk factors were assessed based on information derived from home interviews and physical examinations[16], at a single time point prior to baseline MRI-scanning. Blood pressure was measured twice in sitting position using a

random-zero sphygmomanometer. Use of anti-hypertensive drugs was recorded. Diabetes mellitus status was determined on fasting serum glucose level (>= 7.0 mmol/l), non-fasting serum glucose level (>=11.1 mmol/l) or the use of anti-diabetic medication. Smoking was assessed by interview and coded as never, former and current. Total and high-density lipoprotein (HDL) cholesterol were determined in blood serum, while recording the use of lipid lowering medication. *Apolipoprotein E (APOE)*-ε4 allele carriership was assessed on coded genomic DNA samples. Assessment of risk factors predated the baseline MRI on average 3 years.

Statistical analysis

Changes in diffusion characteristics were investigated in two ways: globally and locally, both using the skeletonized difference measurements. For the global analysis, we investigated the average change in FA and MD over the entire skeleton per subject, excluding voxels labeled as WML in the baseline scan. We assessed whether there was a global change in diffusion measures with multiple linear regression using three models. In model 1, we adjusted for age, sex, scan-interval and ICV. We additionally considered alternatives to model 1 in which we corrected for individual measures of white matter macrostructure: white matter atrophy (using normal-appearing white matter volume) or WML load (natural log-transformed to correct for the skewed volume distribution) instead of age. In model 2, we additionally adjusted for both white matter atrophy and WML load to identify changes to white matter microstructure, independent from the macrostructural white matter changes that may also affect the diffusivity measurements. In model 3, we added the different cardiovascular risk factors individually to model 1 to separately investigate the effect of these on change in white matter microstructure. For analyses with blood pressure and cholesterol, medication use was considered a confounder and added to the model. For the analysis of total cholesterol, HDL cholesterol was additionally included as a confounder. All global analyses were performed using SPSS (version 20).

For the localized TBSS analyses, we performed voxelwise multiple linear regressions for the same models as for the global analysis, also restricting the analyses to the (baseline) normal-appearing white matter. If significant associations were found for tests in model 3, we additionally performed an analysis correcting for measures of macrostructural white matter degeneration to rule out confounding by white matter atrophy and WML. We used threshold-free cluster enhancement[25] with default settings for skeletonized data to promote spatially clustered findings and controlled the family wise error rate by using a permutation based approach (using 5000 permutations).[27] All analyses were performed using an in-house adapted version of the Randomise tool available in FSL[25], effectively performing a voxelwise available-case analysis.

RESULTS

Table 1 shows the population characteristics of the 501 participants. Mean age at baseline MRI was 69.9 years (ranging from 64.1 to 91.1 years), and 253 (50.5%) participants were female. The global analyses, corrected for age, sex, scan interval and ICV, showed an average decrease of FA in the normal-appearing white matter skeleton of 0.0042 ($p<10^{-6}$) and an average increase of MD of 8.1 x $10^{-6}mm^2/s$ ($p<10^{-6}$) over the follow-up interval (model 1). The same changes were observed when additionally controlling for white matter atrophy and WML load (model 2). As can be seen in **Table 2**, these two additional confounding variables were also associated with changes in MD – higher WML load, less normal appearing white matter and higher age resulted in an additional increase in MD – but not with FA.

Table 1 Baseline characteristics of included participants

	N=501
Age (y)	69.9 (4.3)
Female	253 (50.5)
Follow up time (y)	2.0 (0.5)
NAWM baseline FA	0.322 (0.016)
NAWM baseline MD ($10^{-3}mm^2/s$)	0.726 (0.022)
Brain volume (mL)	1125 (114)
NAWM volume (mL)	394 (58)
WML volume (mL) †	3.74 (2.28-7.39)
Systolic blood pressure (mmHg)	142.3 (16.5)
Diastolic blood pressure (mmHg)	81.0 (9.7)
Use of blood pressure lowering medication	168 (33.7)
Diabetes mellitus	34 (6.9)
Smoking	
never	162 (32.7)
former	270 (54.4)
current	64 (12.9)
Total serum cholesterol (mmol/L)	5.73 (0.94)
Serum HDL cholesterol (mmol/L)	1.45 (0.40)
Use of lipid lowering medication	107 (21.4)
APOE-ε4 carriership	118 (23.1)

Data is presented as mean (SD) for continuous variables and number (%) for categorical variables. † White matter lesion volume presented as median (interquartile range). The following variables had missing data: cholesterol (n=3), lipid lowering medication (n=2, not overlapping with cholesterol), blood pressure (n=4), blood pressure lowering medication (n=2, overlapping with blood pressure) *APOE*-ε4 carriership (n=15), diabetes (n=5), smoking (n=5). NAWM indicates normal-appearing white matter; FA fractional anisotropy; MD mean diffusivity, WML white matter lesion.

Table 2. Demographic characteristics and global change in white matter microstructure

variable	**change in FA (x 10^{-3})**	***p* value**	**change in MD (x 10^{-6}mm^2/s)**	***p* value**
Age	*-0.12*	0.09	**0.20**	0.01
Sex	*0.37*	0.57	*-0.07*	0.93
Brain volume	*-0.18*	0.69	*0.91*	0.08
NAWM volume	*0.27*	0.51	**-1.43**	2 x 10^{-3}
ln(WML volume)	*-0.29*	0.31	**1.21**	2 x 10^{-4}

Voxelwise analyses, visualized in **Figure 1** for model 2, showed decrease in FA over the two-years follow-up interval in the majority of the brain white matter, except in most of the sensorimotor tracts. Change over time for models 1 and 2 was not materially different. Increase in FA was found in the motor tracts extending from the brain stem, through the internal capsule (both the anterior and posterior limbs) and the corona radiata up into the motor cortex (**Figure 1**). The MD increased throughout the brain, with most marked increase periventricularly and around the fornix. No voxels showed a significant decrease in MD. Amongst the voxels expressing increased FA, MD mostly increased. Constraining the voxelwise analysis to the normal-appearing white matter meant that the number of degrees-of-freedom of the analysis varied from voxel to voxel, but variation was smooth and the minimum number of subjects included per voxel for models 1 and 2 was 295.

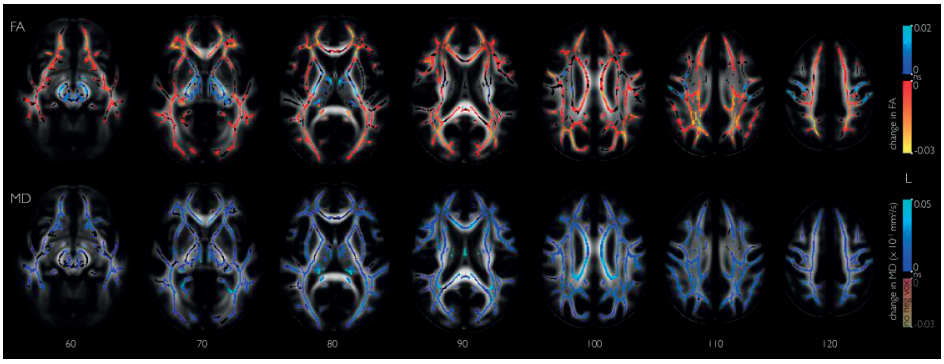

Figure 1. Change in diffusion characteristics over two-years of follow-up, corrected for age, sex, scan interval, intra cranial volume and macroscopic WM changes. The top row shows regions of significant change in fractional anisotropy (FA) over time, color coded blue to indicate increase, and red and yellow to indicate decrease in FA. The bottom row shows regions of significant change in mean diffusivity (MD), color-coded blue for increase (no voxels showed a significant decrease in MD). Results shown are $p<0.05$, the family wise error rate was controlled using a permutation approach. *P* values are presented in Supplementary Figure 2. Results are overlaid on a population specific average-FA image in MNI coordinates, showing non-significant (ns) skeleton voxels in black.

Figures 2 and 3 show how changes in FA (**Figure 2**) and MD (**Figure 3**) depended on various parameters included in models 1 and 2. For model 1, we observed associations between age and FA (decrease) or MD (increase). These associations were reduced both in strength and in extent, when additionally adding measures of macrostructural white matter changes (atrophy and WML load) in the model. The figures also show associations between white matter atrophy and WML load, and change in FA and MD in model 2 No difference in change in diffusion characteristics was observed for men and women.

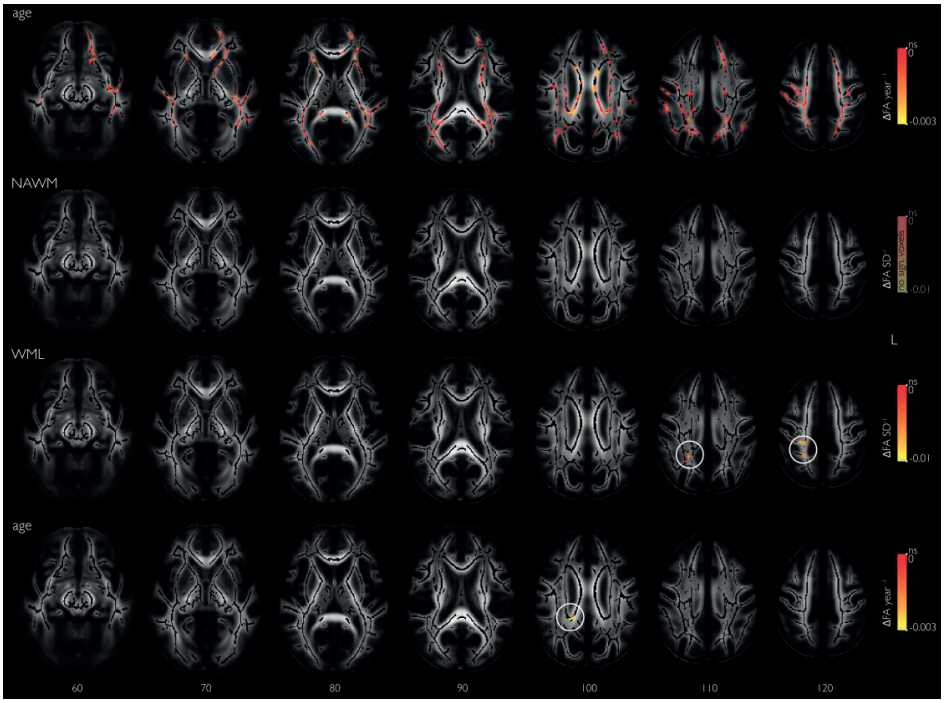

Figure 2. Age and macrostructural white matter changes at baseline and change in fractional anisotropy (FA) over two-years of follow-up. The top row shows in yellow-to-red regions of decrease in FA that relate to higher age at baseline (adjusted for sex, scan interval and intracranial volume (ICV)). The second and third row show FA changes that are associated with respectively a decrease in normal-appearing white matter (NAWM) volume and an increase in white matter lesion (WML) volume (both adjusted for age, sex, scan interval, ICV). The final row shows regions of decrease in FA related to higher age, when additionally adjusted for NAWM volume and WML volume. Inverse directions of association showed no significant voxels (not shown). Results shown are $p<0.05$, the family wise error rate was controlled using a permutation approach. *P* values are presented in Supplementary Figure 3. Results are overlaid on a population specific average-FA image in MNI coordinates, showing non-significant (ns) NAWM skeleton voxels in black.

Investigating cardiovascular risk factors in relation to longitudinal DTI changes, we only found associations for *APOE* ε4 carriership and for total serum cholesterol level. Specifically, ε4 carriers showed localized increases in FA in comparison to non-carriers, but no changes globally. These local differences were more prominent in the right than in the left hemisphere and primarily in the centrum semiovale and in the white matter adjacent to the trigone of the lateral ventricle. In contrast, we observed lower MD only in a small peritrigonal cluster in carriers compared to non-carriers. These observed associations persisted when additionally correcting for macrostructural measures of white matter degeneration. Similarly, we observed that global increase in MD to a lesser degree associated with *APOE* ε4 carriership (**Table 3**). Total serum cholesterol level was associated locally with more increase in MD in the left hemisphere. Regions included the corona radiata and white matter around the posterior and anterior horns of

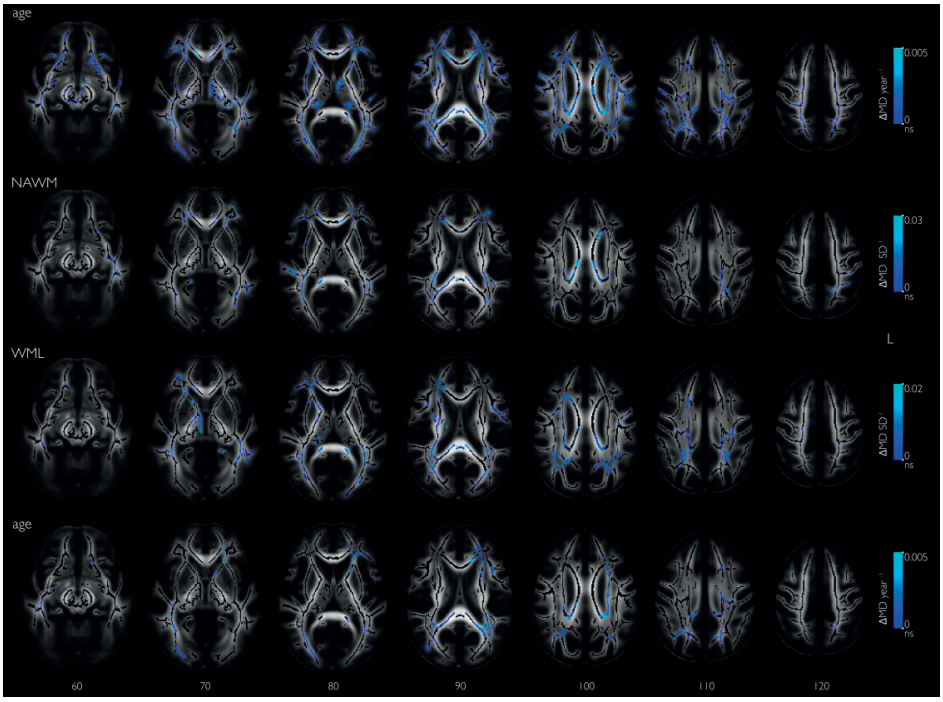

Figure 3. Age and macrostructural white matter changes at baseline and change in mean diffusivity (MD) over two-years of follow-up. The top row shows in blue regions of increase in MD that relate to higher age at baseline (adjusted for sex, scan interval and intracranial volume (ICV)). The second and third row show MD changes that are associated with respectively a decrease in normal-appearing white matter (NAWM) volume and an increase in white matter lesion (WML) volume (both adjusted for age, sex, scan interval, ICV). The final row shows regions of decrease in MD related to higher age, when additionally adjusted for NAWM volume and WML volume. Inverse directions of association showed no significant voxels (not shown). Results shown are $p<0.05$, the family wise error rate was controlled using a permutation approach. *P* values are presented in Supplementary Figure 4. Results are overlaid on a population specific average-FA image in MNI coordinates, showing non-significant (ns) NAWM skeleton voxels in black.

the lateral ventricle. These observed associations persisted when additionally correcting for macrostructural measures of white matter degeneration. Other cardiovascular risk factors were associated with neither global nor local changes in tissue microstructure. Results on global DTI characteristics are presented in **Table 3**.

Investigating cardiovascular risk factors in relation to longitudinal DTI changes, we only found associations for *APOE* ε4 carriership and for total serum cholesterol level. Specifically, ε4 carriers showed localized increases in FA in comparison to non-carriers, but no changes globally. These local differences were more prominent in the right than in the left hemisphere and primarily in the centrum semiovale and in the white matter adjacent to the trigone of the lateral ventricle. In contrast, we observed lower MD only in a small peritrigonal cluster in carriers compared to non-carriers. These observed associations persisted when additionally correcting for macrostructural measures of white matter degeneration. Similarly, we observed that global increase in MD to a lesser degree associated with *APOE* ε4 carriership (**Table 3**).

Table 3. Cardiovascular risk factors and global change in white matter microstructure

risk / protective factor	**change in FA ($x\ 10^{-3}$)**	***p* value**	**change in MD ($x\ 10^{-6} mm^2/s$)**	***p* value**
Systolic blood pressure	*-0.46*	0.09	*0.33*	0.29
Diastolic blood pressure	*-0.01*	0.98	*0.10*	0.76
Diabetes mellitus	*0.08*	0.77	*0.46*	0.13
Smoking (never - current)	*-0.15*	0.86	*0.22*	0.83
Total serum cholesterol	*-0.42*	0.15	*-0.09*	0.78
Serum HDL cholesterol	*0.31*	0.28	*-0.23*	0.49
APOE-ε4 carriership	*1.12*	0.07	**-1.51**	0.04

Cardiovascular risk factors and global change in white matter microstructure computed with respect to the population mean change of -0.0042 in FA ($p<10^{-6}$) and 8.1 x $10^{-6} mm^2/s$ in MD ($p<10^{-6}$). Values represent change in diffusion measure, per SD of change for continuous variables, or absolute for categorical variables. Significant results are shown in bold instead of italic.

Total serum cholesterol level was associated locally with more increase in MD in the left hemisphere. Regions included the corona radiata and white matter around the posterior and anterior horns of the lateral ventricle. These observed associations persisted when additionally correcting for macrostructural measures of white matter degeneration. Other cardiovascular risk factors were associated with neither global nor local changes in tissue microstructure. Results on global DTI characteristics are presented in **Table 3**.

DISCUSSION

In this large, population-based longitudinal sample of elderly persons, we found changes to microstructural tissue organization congruent with microstructural white matter deterioration. Over a two-year follow-up interval, loss of microstructure was globally reflected in decreases in FA and increases in MD, independent of severity of white matter atrophy and WML load. On a voxelwise level, we found regional differences in white matter changes, with decreased FA in most of the brain, but increased FA in most of the sensorimotor pathway, running from the brainstem up to the motor cortex. In contrast, MD was increased throughout the white matter skeleton, without any significant decreases. We found that white matter deterioration was locally more pronounced with higher age, indicating that older persons show more change in white matter microstructure over the same follow-up time than younger persons. This could partly be explained by macroscopic measures of white matter degeneration, i.e. white matter atrophy and WML load, which also increase with age. We only identified few associations between known (cardiovascular) determinants of white matter atrophy and WML load and changes in diffusion characteristics over time, both globally and locally. These findings contribute to our understanding of age related brain changes, and thereby may aid in the future identification of early pathology leading to disease.

Cross-sectional studies of normal aging of white matter have generally shown lower FA and higher MD with higher age[1,11,12] which is in line with our results. In a cross-sectional analysis of an earlier time point for the same population we found a similar effect with age itself, i.e. most of the associations with age were driven by macroscopic measures of white matter degeneration.[10] Both results indicate that white matter degeneration with aging is not intrinsically due to aging alone nor purely driven by macroscopic measures of white matter degeneration. Longitudinal analyses, which are necessary to reliably characterize change over time, have found reductions in FA and increases in MD.[6,9] Our findings confirm much of these longitudinal and cross sectional findings, and extend on these for the normal appearing white matter, in a larger population.

In the *sensorimotor* pathway, we identified a seemingly paradoxical increase of FA, which may relate to partial volume mixing of multiple fiber tracts (e.g. crossing or touching fibers) within these voxels. Selective degeneration of one fiber bundle with relative sparing of the other bundle may lead to an increase in FA, with concomitant increase in MD. This effect was previously observed in a study on Wallerian degeneration[28], and described in detail in a cross-sectional study on Alzheimer's disease.[29] The increased FA, ascending from the brain stem, through the internal capsule and the corona radiata up into the motor cortex – regions with either crossing fibers or closely spaced adjacent fibers[30-31] – thereby seems to indicate a relative sparing of sensorimotor fibers. Inside the *fornix* we found the strongest increase in MD. This may reflect

loss of microstructural organization in this limbic fiber, but we should note that this tract is small compared to our imaging matrix and surrounded by CSF. These findings therefore likely represent a combination of microstructural and macrostructural (i.e. tract thinning) changes.[32]

We did observe counter-intuitive associations with *APOE* ε4 carriership. Globally we observed a decrease in MD in carriers compared to non-carriers. Locally, we observed in *APOE* ε4 carriers increases in FA in comparison to non-carriers, in regions with a high prevalence of WML. These observations are in contrast to cross-sectional studies with *APOE* genotype, which have generally shown widespread deterioration of white matter microstructure associated with the ε4 allele.[33,34] On closer inspection this paradoxical increase in FA was largely explained by lower baseline FA for carriers, and a larger decrease in FA for non-carriers. Higher serum cholesterol was associated to stronger increases in MD over time in the left hemisphere. When investigating other cardiovascular risk factors, we observed associations with neither global nor local changes to white matter microstructure, which is in line with another longitudinal study[6] but in disagreement to cross-sectional observations.[2,35] These discrepancies, both for *APOE* and cardiovascular factors, might be due to the relatively short follow-up interval, which translates in the (clustered) voxelwise and global statistics being relatively underpowered. Another possibility is that changes induced by cardiovascular risk factors may be more prominent in the periphery of white matter tracts, whereas the TBSS method we used focused on tract centers. Most importantly however, our longitudinal design only probes differential effects, and not the difference accumulated over the total exposure time, which precludes the analysis from finding subtle differential changes with cardiovascular risk factors.

Limitations of our study are: 1. The relatively short follow-up interval, which may have limited the sensitivity to detect differences over time. Especially in the case of differential effects with risk factors (as mentioned above), this meant we could not disambiguate the risk factor-related changes from the large changes associated with aging. This also impedes direct translation of our findings to individual subjects, e.g. for use in clinical care. 2. The study protocol was defined in 2005-2006 and therefore the spatial resolution for the diffusion acquisition was relatively poor for current day standards.[23] Although the use of TBSS mitigates partial volume effects in the major white matter tracts and we adjusted for overall white matter atrophy, we will have been less sensitive to detect change in very thin tracts. We did nevertheless identify widespread deterioration of white matter microstructure within the studied interval. We excluded participants with dementia at either time point, but we did not exclude persons with mild cognitive impairment (MCI), since MCI contributes to the continuous spectrum of age related pathologies that we aim to investigate. This may have led

to inclusion of some persons with preclinical dementia, which could have affected our results.

In conclusion, in this large longitudinal analysis of brain white matter microstructure in normal aging, we found widespread microstructural deterioration of the normal-appearing white matter, with relative sparing of sensorimotor fibers**.** We found changes to be more prominent in older persons, which were partly explained by concomitant macroscopic white matter pathology. Cardiovascular risk factors did not generally relate to white matter microstructure. These insights into white matter degeneration in aging may help in understanding the pathophysiology of neurodegenerative diseases.

CHAPTER REFERENCES

1. Sullivan E V., Pfefferbaum A. Diffusion tensor imaging and aging. Neurosci Biobehav Rev. 2006;30(6):749–61.
2. Gons RAR, van Oudheusden LJB, de Laat KF, van Norden AGW, van Uden IWM, Norris DG, et al. Hypertension is related to the microstructure of the corpus callosum: the RUN DMC study. J. Alzheimers. Dis. 2012 Jan;32(3):623–31.
3. Beaulieu C. The basis of anisotropic water diffusion in the nervous system - a technical review. NMR Biomed. 2002;15(7-8):435–55.
4. O'Sullivan M, Jones DK, Summers PE, Morris RG, Williams SC, Markus HS. Evidence for cortical "disconnection" as a mechanism of age-related cognitive decline. Neurology. 2001 Aug;57(4):632–8.
5. Oishi K, Mielke MM, Albert M, Lyketsos CG, Mori S. DTI analyses and clinical applications in Alzheimer's disease. J. Alzheimers. Dis. 2011 Jan;26 Suppl 3:287–96.
6. Barrick TR, Charlton RA, Clark CA, Markus HS. White matter structural decline in normal ageing; a prospective longitudinal study using tract based spatial statistics. Neuroimage. 2010 Jun;51(2):565–77.
7. Teipel SJ, Meindl T, Wagner M, Stieltjes B, Reuter S, Hauenstein K-H, et al. Longitudinal changes in fiber tract integrity in healthy aging and mild cognitive impairment: a DTI follow-up study. J. Alzheimers. Dis. 2010 Jan;22(2):507–22.
8. Sullivan E V., Rohlfing T, Pfefferbaum A. Longitudinal study of callosal microstructure in the normal adult aging brain using quantitative DTI fiber tracking. Dev. Neuropsychol. 2010 Jan;35(3):233–56.
9. Sexton CE, Walhovd KB, Storsve AB, Tamnes CK, Westlye LT, Johansen-Berg H, et al. Accelerated Changes in White Matter Microstructure during Aging: A Longitudinal Diffusion Tensor Imaging Study. J. Neurosci. 2014 Nov 12;34(46):15425–36.
10. Vernooij MW, de Groot M, van der Lugt A, Ikram MA, Krestin GP, Hofman A, et al. White matter atrophy and lesion formation explain the loss of structural integrity of white matter in aging. Neuroimage. 2008 Nov;43(3):470–7.
11. Abe O, Aoki S, Hayashi N, Yamada H, Kunimatsu A, Mori H, et al. Normal aging in the central nervous system: quantitative MR diffusion-tensor analysis. Neurobiol Aging. 2002;23(3):433–41.
12. Burzynska AZ, Preuschhof C, Bäckman L, Nyberg L, Li S-C, Lindenberger U, et al. Age-related differences in white matter microstructure: region-specific patterns of diffusivity. Neuroimage. Elsevier Inc.; 2010 Feb 1;49(3):2104–12.
13. Nusbaum AO, Tang CY, Buchsbaum MS, Wei TC, Atlas SW. Regional and global changes in cerebral diffusion with normal aging. AJNR. Am. J. Neuroradiol. 2001 Jan;22(1):136–42.
14. Lee DY, Fletcher E, Martinez O, Zozulya N, Kim J, Tran J, et al. Vascular and degenerative processes differentially affect regional interhemispheric connections in normal aging, mild cognitive impairment, and Alzheimer disease. Stroke. 2010 Aug;41(8):1791–7.
15. Groot M De, Ikram MA, Akoudad S, Krestin GP, de Groot M, Ikram MA, et al. Tract-specific white matter degeneration in aging . The Rotterdam Study. Alzheimer's Dement. Elsevier Ltd; 2014 Sep 9;11(3):1–10.
16. Hofman A, Darwish Murad S, van Duijn CM, Franco OH, Goedegebure A, Ikram MA, et al. The Rotterdam Study: 2014 objectives and design update. Eur. J. Epidemiol. 2013 Nov;28(11):889–926.
17. Ikram MA, van der Lugt A, Niessen WJ, Krestin GP, Koudstaal PJ, Hofman A, et al. The Rotterdam Scan Study: design and update up to 2012. Eur. J. Epidemiol. 2011 Oct 16;26(10):811–24.

18. Vrooman HA, Cocosco CA, van der Lijn F, Stokking R, Ikram MA, Vernooij MW, et al. Multi-spectral brain tissue segmentation using automatically trained k-Nearest-Neighbor classification. Neuroimage. 2007 Aug;37(1):71–81.
19. De Boer R, Vrooman HA, van der Lijn F, Vernooij MW, Ikram MA, van der Lugt A, et al. White matter lesion extension to automatic brain tissue segmentation on MRI. Neuroimage. Elsevier Inc.; 2009 May 1;45(4):1151–61.
20. Greve DN, Fischl B. Accurate and robust brain image alignment using boundary-based registration. Neuroimage. Elsevier Inc.; 2009 Oct 15;48(1):63–72.
21. Koppelmans V, de Groot M, de Ruiter MB, Boogerd W, Seynaeve C, Vernooij MW, et al. Global and focal white matter integrity in breast cancer survivors 20 years after adjuvant chemotherapy. Hum. Brain Mapp. 2014 Dec 20;35(3):889–99.
22. Leemans A, Jeurissen B, Sijbers J, Jones DK. ExploreDTI: a graphical toolbox for processing, analyzing, and visualizing diffusion MR data. Proc. 17th Sci. Meet. Int. Soc. Magn. Reson. Med. 2009. p. 3537.
23. De Groot M, Vernooij MW, Klein S, Ikram MA, Vos FM, Smith SM, et al. Improving alignment in Tract-based spatial statistics: evaluation and optimization of image registration. Neuroimage. 2013 Aug 1;76:400–11.
24. Smith SM, Jenkinson M, Johansen-Berg H, Rueckert D, Nichols TE, Mackay CE, et al. Tract-based spatial statistics: voxelwise analysis of multi-subject diffusion data. Neuroimage. 2006 Jul;31(4):1487–505.
25. Jenkinson M, Beckmann CF, Behrens TEJ, Woolrich MW, Smith SM. FSL. Neuroimage. 2012 Aug 15;62(2):782–90.
26. Smith SM, Nichols TE. Threshold-free cluster enhancement: addressing problems of smoothing, threshold dependence and localisation in cluster inference. Neuroimage. 2009 Jan;44(1):83–98.
27. Nichols TE, Holmes AP. Nonparametric permutation tests for functional neuroimaging: a primer with examples. Hum Brain Mapp. 2002 Jan;15(1):1–25.
28. Pierpaoli C, Barnett A, Pajevic S, Chen R, Penix LR, Virta A, et al. Water diffusion changes in Wallerian degeneration and their dependence on white matter architecture. Neuroimage. 2001 Jun;13(6 Pt 1):1174–85.
29. Douaud G, Jbabdi S, Behrens TEJ, Menke RA, Gass A, Monsch AU, et al. DTI measures in crossing-fibre areas: increased diffusion anisotropy reveals early white matter alteration in MCI and mild Alzheimer's disease. Neuroimage. 2011 Apr 1;55(3):880–90.
30. Jeurissen B, Leemans A, Tournier J-D, Jones DK, Sijbers J. Investigating the prevalence of complex fiber configurations in white matter tissue with diffusion magnetic resonance imaging. Hum. Brain Mapp. 2013 Nov;34(11):2747–66.
31. Oishi K, Faria A V., Zijl PCM van, Mori S. MRI Atlas of Human White Matter, Second Edition. Academic Press; 2010.
32. Berlot R, Metzler-Baddeley C, Jones DK, O'Sullivan MJ. CSF contamination contributes to apparent microstructural alterations in mild cognitive impairment. Neuroimage. The Authors; 2014 Mar 3;92C:27–35.
33. Persson J, Lind J, Larsson A, Ingvar M, Cruts M, Van Broeckhoven C, et al. Altered brain white matter integrity in healthy carriers of the APOE epsilon4 allele: a risk for AD? Neurology. 2006 Apr 11;66(7):1029–33.
34. Westlye LT, Reinvang I, Rootwelt H, Espeseth T. Effects of APOE on brain white matter microstructure in healthy adults. Neurology. 2012 Nov 6;79(19):1961–9.

35. Salat DH, Williams VJ, Leritz EC, Schnyer DM, Rudolph JL, Lipsitz LA, et al. Inter-individual variation in blood pressure is associated with regional white matter integrity in generally healthy older adults. Neuroimage. Elsevier B.V.; 2012 Jan 2;59(1):181–92.

CHAPTER 2.2

Kidney function and microstructural integrity of brain white matter

Sanaz Sedaghat, Lotte G.M. Cremers, Marius de Groot, Ewout J. Hoorn, Albert Hofman, Aad van der Lugt, Oscar H. Franco, Meike W. Vernooij, Abbas Dehghan, M. Arfan Ikram

Neurology 2015

ABSTRACT

Objective To investigate the association of kidney function with white matter microstructural integrity.

Methods We included 2726 participants with a mean age of 56.6 years (45% men) from the population-based Rotterdam Study. Albumin-to-creatinine ratio, and glomerular filtration rate (eGFR), using serum cystatin C (eGFRcys) and creatinine (eGFRcr), were measured to evaluate kidney function. Diffusion-MRI was used to assess microstructural integrity of the normal-appearing white matter. Multiple linear regression models, adjusted for macrostructural MRI-markers and cardiovascular risk factors were used to model the association of kidney function with white matter microstructure.

Results Participants had average eGFRcr of 86.1 mL/min/1.73 m^2, average eGFRcys of 86.2 mL/min/1.73 m^2, and median albumin-to-creatinine ratio of 3.4 mg/g. Lower eGFRcys was associated with worse global white matter microstructural integrity, reflected as lower fractional anisotropy (FA) (standardized difference per SD: -0.053, 95%CI: -0.092, -0.014) and higher mean diffusivity (MD) (0.036, 95%CI: 0.001, 0.070). Similarly, higher albumin-to-creatinine ratio was associated with lower FA (-0.044, 95%CI: -0.078, -0.011). There was no linear association between eGFRcr and white matter integrity. Subgroup analyses showed attenuation of the associations after excluding subjects with hypertension. The associations with global DTI-measures didn't seem to be driven by particular tracts, but rather spread across multiple tracts in various brain regions.

Conclusions Reduced kidney function is associated with worse white matter microstructural integrity. Our findings highlight the importance for clinicians to consider concomitant macro- and microstructural changes of brain in subjects with impaired kidney function.

INTRODUCTION

The brain and the kidney are both vulnerable to vascular and hemodynamic alterations due to similar high flow and low resistance circulation.[1] Therefore, vascular damage in the kidney could mirror cerebrovascular changes in the brain.[1] Accordingly, a higher prevalence of cerebrovascular diseases such as stroke and vascular dementia among patients with chronic kidney disease (CKD) has been reported.[2, 3] Beyond clinically evident cerebrovascular diseases, previous studies showed an association between kidney function and subclinical cerebrovascular diseases including brain atrophy and white matter lesions.[2, 4, 5] However, subclinical cerebrovascular diseases have a wide spectrum and conventional MRI sequences are not capable of capturing this entire spectrum. Diffusion tensor imaging (DTI) is an advanced MRI technique that provides quantitative information of microscopic changes of the cerebral white matter. Recognition of early changes in white matter structural integrity is of importance as it might help to prevent further progression of brain pathologies before reaching an irreversible stage.[6] Despite the current evidence indicating that advanced impairments in kidney function are associated with brain pathologies,[2, 3] it is unknown whether changes in kidney function and glomerular integrity are linked to more subtle, microstructural changes in the brain. In this study, we hypothesized that loss of kidney function is associated with microstructural changes of the white matter.

METHODS

Study population

The present study is embedded within the second extension of the population-based Rotterdam Study (2005-2009), including participants of 45 years and older. For the current study, we included 2825 individuals with DTI data, of whom 2680 had urine albumin and urine creatinine measurements, 2717 had serum creatinine measurements, and 2726 had available data on serum cystatin C measurements (**Figure e-1**).

Standard Protocol Approvals, Registrations, and Patient Consents

The Rotterdam Study has been approved by the medical ethics committee according to the Population Study Act Rotterdam Study, executed by the Ministry of Health, Welfare and Sports of the Netherlands. Written informed consent was obtained from all participants.[7]

Kidney function

Estimated glomerular filtration rate (eGFR) was calculated for creatinine (eGFRcr) and cystatin C (eGFRcys) measurements separately as well as for both measurements

combined (eGFRcrcys), according to the Chronic Kidney Disease Epidemiology Collaboration (CKD-EPI) formula.[8] Albumin-to-creatinine ratio was estimated by dividing albumin by creatinine (mg/g).[9] Since measures of albumin-to-creatinine ratio were not normally distributed, albumin-to-creatinine ratio values were natural log transformed (further details about kidney function measurements in supplemental material). We defined three categories of kidney function using information from both eGFR and albumin-to-creatinine ratio. This categorization is based on the cutoffs of the Kidney Disease: Improving Global Outcomes (KDIGO) 2013,[10] and has been applied in the research setting before.[11] Categories were defined on the basis of two criteria: eGFR-crcys > 60 mL/min/1.73 m^2 and albumin-to-creatinine ratio < 30 mg/g. First category included participants that met both criteria. Second category included participants that met only one criterion. Participants that met none of the criteria were classified as the third category.[11]

Brain DTI-MRI

Brain MRI scanning was performed on a 1.5 tesla MRI scanner (GE Signa Excite). Scan protocol and sequence details are described extensively elsewhere.[12] For DTI, we performed a single shot, diffusion-weighted spin echo echo-planar imaging sequence. Maximum b-value was 1000 s/mm^2 in 25 non-collinear directions; three volumes were acquired without diffusion weighting (b-value = 0 s/mm^2).[12] All diffusion data were pre-processed using a standardized pipeline, including correction for motion and eddy currents, estimation of the diffusion tensor, and registration to tissue segmentation to obtain global mean DTI-measures in the normal-appearing white matter. These measures includes fractional anisotropy (FA), mean diffusivity (MD), and axial and radial diffusivities.[13] In general, lower values of FA and higher values of MD are indicative of worse microstructural integrity of the white matter. Next, white matter tracts were segmented using a diffusion tractography approach described previously.[14] We identified 14 different white matter tracts (11 tracts were defined for left and right hemispheres) in subject native space. Tracts were categorized into brainstem tracts, projection fibers association fibers, limbic system fibers and callosal fibers.[15] Tract-specific measurements of microstructure were obtained by taking median measures inside each white matter tract, with subsequent combination of left and right measures.[14] DTI values, both global and tract-specific, were measured using fully automated methods (no readers involved). Since these measures are not observer dependent, no observer bias was introduced. However, there might be some random measurement noise in the scan protocol. The average tract-specific reproducibility of our multi-step method was 87%. More details about the reproducibility of tract-specific DTI-parameters are provided elsewhere.[14]

Cardiovascular risk factors

Information related to smoking and alcohol consumption was acquired using questionnaires. Alcohol consumers were categorized into non, moderate and heavy drinkers. Smoking was categorized in never, former and current smoking. Information on medication use was based on home interviews. Hypertension was defined as a systolic blood pressure ≥140 mmHg or a diastolic blood pressure ≥ 90 mmHg or the use of antihypertensive medication. Cardiovascular disease was considered as a history of myocardial infarction, stroke or coronary revascularization procedures.[16] Diabetes mellitus was defined by use of blood glucose lowering medication and/or a fasting serum glucose level equal to or greater than 7.0 mmol/l.

Statistical analysis

Associations between kidney function markers and DTI-parameters were evaluated using multiple linear regression models. Subject-specific global and tract-specific DTI-parameters were standardized to z scores. Betas and 95% confidence intervals (CI) for difference in DTI parameters were estimated per standard deviation increase of measures of the kidney function. We performed the analyses in four steps. The first model was performed unadjusted. In the second model analyses were adjusted for age, sex, and macrostructural MRI-markers including white matter volume, intracranial volume, and WML (also known as white matter hyperintensities) volume. In the third model we additionally adjusted the analyses for cardiovascular risk factors (systolic blood pressure, diastolic blood pressure, alcohol intake, smoking, total cholesterol, high density lipoprotein cholesterol, diabetes mellitus, history of cardiovascular disease, and body mass index) and antihypertensive and lipid-lowering medication. In the fourth model, analyses with eGFR as determinants were adjusted for albumin-to-creatinine ratio, and analyses with albumin-to-creatinine ratio as determinant were further adjusted for eGFRcrcys. Based on previous literature[17] suggesting a U-shaped association between serum creatinine and brain outcomes, we further checked the non-linear association of eGFRcr with DTI-parameters of white matter integrity by including the quadratic term in the model. We performed an analysis of covariance where mean values of FA and MD were compared across three categories of kidney function. Moreover, we performed a series of sensitivity analyses, excluding subjects with chronic kidney disease (defined as eGFRcrcys < 60 mL/min/1.73 m^2), diabetes mellitus, hypertension, and with a history of cardiovascular disease. To investigate whether the association between kidney function and white matter integrity differs in participants with and without hypertension, we assessed the interactions between kidney function markers and hypertension in relation to DTI-parameters. In exploratory analyses, we evaluated if the associations between kidney function and white matter integrity is independent of C-reactive protein levels. Furthermore, to compare the magnitude of the association

with age, as an established risk factor for impairments in white matter integrity, we calculated the effect estimates for the association of age with FA and MD. Then, we divided the betas (per standard deviation) of kidney function markers by the betas of age in relation to DTI-parameters and reported the corresponding ratios.
In all analyses, we treated the phase encoding direction of the diffusion scan as a potential confounder. In tract specific analyses of the medial lemniscus, we additionally corrected for its varying coverage inside the field of view of the diffusion acquisition across participants. All analyses were carried out using SPSS 20.0.2 for windows or R version 2.15.0.

RESULTS

Table 1 presents the characteristics of the 2726 study participants. Average age of the participants was 56 ±6.4 years and 45 % were male. **Table 2** presents baseline characteristics of participants in different categories based on participants' kidney function.

The association between kidney function markers and global DTI-parameters of white matter microstructural integrity are presented in **Table 3**. In the unadjusted model, higher albumin-to-creatinine ratio was associated with lower FA and higher MD (standardized difference FA: -0.102, 95% confidence interval (CI): -0.139, -0.066; standardized difference MD: 0.096, 95%CI: 0.061, 0.132). Higher albumin-to-creatinine ratio was also associated with higher radial diffusivity (0.063, 95%CI: 0.027, 0.100) and higher axial diffusivity (0.103, 95%CI: 0.067, 0.139). Adjustments for age, sex, and macrostructural MRI-markers (white matter volume, intracranial volume, and WML volume) attenuated the association of albumin-to-creatinine ratio with FA, MD, and radial diffusivity (**Table 3**).There was no association between albumin-to-creatinine ratio and axial diffusivity in the second model. After further adjustments for cardiovascular risk factors, in the third model, associations of albumin-to-creatinine ratio with FA and radial diffusivity did not change, but the association with MD became non-significant (p: 0.09). Adjustment for eGFRcrcys in the fourth model didn't change the results (**Table 3**).

Table 1. Population Characteristics

Characteristics	n= 2726
Age, years	56.6 (6.4)
Men	1225 (44.9)
Systolic blood pressure, mmHg	131.9 (18.5)
Diastolic blood pressure, mmHg	82.3 (10.8)
Antihypertensive medication	595 (21.8)
Alcohol	
Moderate drinker	1640 (60.4)
Heavy drinker	806 (29.6)
Smoking	
Current	715 (26.2)
Former	1190 (43.7)
Total cholesterol, mmol/l	5.6 (1.0)
HDL cholesterol, mmol/l	1.4 (0.4)
Lipid-lowering medication	570 (20.9)
Diabetes mellitus	214 (7.9)
History of cardiovascular disease	128 (4.7)
Hypertension	1191 (43.7)
Body mass index, kg/m^2	27.5 (4.3)
Albumin-to-creatinine ratio, mg/g	3.4 (2.2, 6.2)
eGFRcr, mL/min/1.73 m^2	86.1 (13.5)
eGFRcys, mL/min/1.73 m^2	86.2 (16.0)
eGFRcrcys, mL/min/1.73 m^2	86.3 (13.4)
Intracranial volume, mL	1128.6 (122.0)
White matter volume, mL	416.8 (59.9)
White matter lesion volume, mL	2.0 (1.3, 3.5)
Fractional anisotropy	0.33 (0.01)
Mean diffusivity, 10^{-3} mm^2/s	0.74 (0.02)
Axial diffusivity, 10^{-3} mm^2/s	1.01 (0.03)
Radial diffusivity, 10^{-3} mm^2/s	0.60 (0.02)

Categorical variables are presented as numbers (percentages), continuous variables as means (standard deviations) and white matter lesions and albumin-to-creatinine ratio are presented as medians (interquartile ranges). The following variables had missing data: blood pressure (n=9), smoking (n=5), alcohol (n=12), lipid-lowering medication (n= 24), antihypertensive medication (n=24), HDL: high density lipoprotein cholesterol (n=7), Total cholesterol (n= 5), albumin-to-creatinine ratio (n=141), history of cardiovascular disease (n=28), body mass index (n=2), hypertension (n=24).

Abbreviations: eGFRcys: cystatin C based estimated glomerular filtration rate, eGFRcr: creatinine based estimated glomerular filtration rate, eGFRcrcys: creatinine and cystatin C based estimated glomerular filtration rate

Table 2. Population characteristics in categories of kidney function

Characteristics*	First category	Second category	Third category
	eGFR>60 and ACR<30 N=2320	eGFR<60 or ACR>30 N=179	eGFR<60 and ACR >30 N=14
Age, years	56.4 (5.9)	60.5 (9.6)	65.4 (9.2)
Men	1040 (44.8)	76 (42.5)	7 (50.0)
SBP, mmHg	131.4 (18.1)	139.6 (21.1)	145.5 (23.5)
DBP, mmHg	82.1 (10.7)	85.1 (12.0)	85.1 (11.2)
Anti-HTN Med	476 (20.5)	68 (38.0)	11 (78.6)
Alcohol			
Moderate drinker	1393 (60.0)	111 (62.0)	6 (42.9)
Heavy drinker	694 (29.0)	45 (25.1)	4 (28.6)
Smoking			
Current	590 (25.4)	49 (27.4)	4 (28.6)
Former	1014 (43.7)	80 (44.7)	7 (50.0)
Total chol, mmol/l	5.6 (1.0)	5.4 (1.1)	5.8 (1.3)
HDL chol, mmol/l	1.4 (0.4)	1.3 (0.4)	1.4 (0.5)
Lipid lowering Med	469 (20.2)	53 (29.6)	6 (42.9)
DM	155 (6.7)	34 (19.0)	2 (14.3)
CVD	99 (4.3)	19 (10.6)	2 (14.3)
HTN	982 (42.3)	116 (64.8)	14 (100)
BMI, kg/m^2	27.4 (4.2)	29.0 (5.1)	28.4 (4.6)
ACR, mg/g	3.3 (2.1, 5.5)	39.0 (8.4, 74.4)	130.1 (73.4, 229.1)
eGFRcr, mL/min/1.73 m^2	87.0 (11.9)	77.3 (18.9)	44.8 (16.7)
eGFRcys, mL/min/1.73 m^2	87.4 (14.3)	74.2 (21.4)	38.1 (13.3)
eGFRcrcys, mL/min/1.73 m^2	87.4 (11.7)	75.6 (20.0)	40.2 (13.9)
ICV, mL	1127.6 (121.1)	1125.3 (136.9)	1103.7 (133.5)
WMV, mL	417.3 (58.7)	408.7 (68.5)	385.9 (93.1)
WMLV, mL	2.0 (1.3, 3.4)	2.9 (1.6, 5.5)	8.9 (3.1, 13.0)
FA	0.33 (0.01)	0.33(0.01)	0.32 (0.02)
MD, 10^{-3} mm^2/s	0.74 (0.02)	0.75 (0.03)	0.76 (0.03)
Axial diffusivity, 10^{-3} mm^2/s	1.01 (0.03)	1.02 (0.03)	1.03 (0.03)
Radial diffusivity, 10^{-3} mm^2/s	0.60 (0.02)	0.61 (0.03)	0.63 (0.04)

*Sample size in this table is based on participants with available data for both eGFRcrcys and ACR (n=2513).
Categorical variables are presented as numbers (percentages), continuous variables as means (standard deviations) and white matter lesions and albumin-to-creatinine ratio are presented as medians (interquartile ranges).
Abbreviations: SBP: systolic blood pressure, DBP: diastolic blood pressure, Anti-HTN Med: antihypertensive medication, Total chol: total cholesterol, HDL chol: high density lipoprotein cholesterol, DM: diabetes mellitus, CVD: cardiovascular disease, HTN: hypertension, BMI: body mass index, ACR: Albumin-to-creatinine ratio, eGFRcys: cystatin C based estimated glomerular filtration rate, eGFRcr: creatinine based estimated glomerular filtration rate, eGFRcrcys: creatinine and cystatin C based estimated glomerular filtration rate, ICV: intracranial volume, WMV: white matter volume, WMLV: white matter lesion volume. FA: fractional anisotropy, MD: mean diffusivity.

Table 3. The association of kidney function parameters with DTI-parameters of white matter microstructural integrity

	Fractional anisotropy	Mean diffusivity	Axial diffusivity	Radial diffusivity
	Difference*(95% CI)	Difference*(95% CI)	Difference*(95% CI)	Difference*(95% CI)
Albumin-to-creatinine ratio N= 2680				
Model I	**-0.102 (-0.139, -0.066)**	**0.096 (0.061, 0.132)**	**0.063 (0.027, 0.100)**	**0.103 (0.067, 0.139)**
Model II	**-0.049 (-0.081, -0.016)**	**0.033(0.004, 0.062)**	0.018 (-0.015, 0.050)	**0.037 (0.008, 0.066)**
Model III	**-0.044 (-0.078, -0.011)**	0.026(-0.004, 0.056)	0.010 (-0.024, 0.044)	**0.031 (0.001, 0.061)**
Model IV	**-0.043 (-0.078, -0.008)**	0.027 (-0.004, 0.058)	0.013 (-0.022, 0.049)	**0.031 (0.001, 0.062)**
eGFRcys N=2726				
Model I	**0.204 (0.168, 0.240)**	**-0.248 (-0.283, -0.213)**	**-0.157 (-0.194, -0.120)**	**-0.268 (-0.303, -0.233)**
Model II	**0.053(0.016, 0.090)**	**-0.040 (-0.073, -0.007)**	-0.001 (-0.038, 0.036)	**-0.057 (-0.091, -0.024)**
Model III	**0.053(0.014, 0.092)**	**-0.036 (-0.070, -0.001)**	0.006 (-0.033, 0.045)	**-0.056 (-0.090, -0.021)**
Model IV	0.039 (-0.002, 0.079)	-0.033 (-0.069, 0.003)	0.003 (-0.038, 0.044)	**-0.050 (-0.087, -0.014)**
eGFRcr N= 2717				
Model I	**0.100 (0.063, 0.136)**	**-0.136 (-0.171, -0.100)**	**-0.092 (-0.129, -0.055)**	**-0.143 (-0.179, -0.107)**
Model II	-0.007 (-0.041, 0.027)	0.011 (-0.020, 0.041)	0.015 (-0.020, 0.049)	0.007 (-0.024, 0.038)
Model III	0.002 (-0.033, 0.036)	0.003 (-0.028, 0.034)	0.008 (-0.027, 0.043)	-0.001 (-0.032, 0.031)
Model IV	-0.013 (-0.049, 0.023)	0.009 (-0.023, 0.041)	0.008 (-0.029, 0.044)	0.009 (-0.024, 0.041)

*Differences (betas), and 95% CI are calculated using the per standard deviation increase in log-transformed albumin-to-creatinine ratio/ eGFRcys/ eGFRcr and subject-specific mean standardized z scores for fractional anisotropy, mean diffusivity, and axial and radial diffusivity. Model I: crude model. Model II: adjusted for age, sex, intracranial volume, white matter volume, and log transformed white matter lesion volume. Model III: additionally adjusted for systolic blood pressure, diastolic blood pressure, antihypertensive medication, alcohol intake, smoking, total cholesterol, high density lipoprotein cholesterol, lipid-lowering medication, diabetes mellitus, history of cardiovascular disease, and body mass index. Model IV: additionally adjusted for eGFRcrcys in analyses with albumin-to-creatinine ratio as determinant, and additionally adjusted for albumin-to-creatinine-ratio in analyses with eGFRcr or eGFRcys. *Abbreviations: CI: confidence interval, eGFRcys: cystatin C based estimated glomerular filtration rate, eGFRcr: creatinine based estimated glomerular filtration rate, eGFRcrcys: creatinine and cystatin C based estimated glomerular filtration rate.*

In the unadjusted model, each standard deviation higher eGFRcys was associated with higher FA and lower MD (FA: 0.204, 95% CI: 0.168, 0.240; MD: -0.248, 95%CI: -0.283, -0.213). Likewise, each standard deviation higher eGFRcys was associated with lower radial diffusivity (-0.268, 95%CI: -0.303, -0.233) and lower axial diffusivity (-0.157, 95%CI: -0.194, -0.120). The association of eGFRcys with FA, MD, and radial diffusivity attenuated after adjustment for age, sex, and macrostructural MRI-markers. There was no association between eGFRcys and axial diffusivity in the second model. Further adjustments for cardiovascular risk factors, in the third model, did not change the associations of eGFRcys with DTI-parameters of white matter integrity. After adjustment for albumin-to-creatinine ratio in the fourth model, the association of eGFRcys with FA and MD attenuated and became non-significant (p: 0.061 and 0.068, respectively) (**Table 3**). Each standard deviation higher eGFRcr was associated with higher FA, lower MD, and lower radial and axial diffusivity (all $p < 0.05$). There was no linear association be-

tween eGFRcr and DTI-parameters of white matter integrity after adjustment for age, sex, and macrostructural MRI-markers (all p>0.05) (**Table 3**). Including the quadratic term of eGFRcr in the model suggested a U-shaped association between eGFRcr and markers of white matter integrity (all P-values <0.05 for test of quadratic term) (**Table e-1**). After excluding the participants with 4 standard deviation lower/higher eGFRcr (n=9) the U-shaped association was not present anymore. Performing the analyses with eGFRcrcys as the determinant, the effect estimates were intermediate between two separate equations of eGFRcr and eGFRcys and resulted in borderline significant findings (**Table e-2**).

Figure 1 shows age and sex adjusted means of FA and MD in three categories of kidney function. We observed a linear trend between different categories of kidney function and white matter microstructural DTI-parameters, reflecting worse white matter microstructure in persons with worse kidney function (p for trend 0.001 for FA and 0.002 for MD).

Excluding individuals with chronic kidney disease, diabetes mellitus, or history of cardiovascular disease yielded similar findings. Excluding individuals with hypertension attenuated the association of kidney function with DTI parameters (**Figure e-2**). In the stratified analyses, the association between eGFRcys and MD was stronger in hypertensive participants (P for interaction, 0.001). A similar, borderline significant trend was observed for the interaction between albumin-to-creatinine ratio and hypertension in relation to FA (P for interaction 0.059) (**Table e-3**). Adjusting the association between markers of kidney function and DTI-parameters of white matter integrity for C-reactive protein didn't substantially change the associations (data not shown).
In an extra analysis, we observed that each year increase in age was associated with lower FA and higher MD (**Table e-4**). Comparing the effect estimates of age with eGFRcys in relation to FA, we showed that each standard deviation lower eGFRcys had the magnitude equal to 4.1 years of increase in age. Similarly, each standard deviation lower eGFRcys in relation to MD had the magnitude equal to 1.5 years increase in age.

Associations between kidney function and tract-specific diffusion measures are presented in **Figure 2** and **Table e-5**. Higher albumin-to-creatinine ratio was associated with higher MD in all tracts (projection fibers, association fibers, limbic system fibers, and callosal fibers). Likewise, higher eGFRcys was related to MD in all tracts, except for brain stem tracts. We did not observe any linear association between eGFRcr and tract-specific DTI-measures.

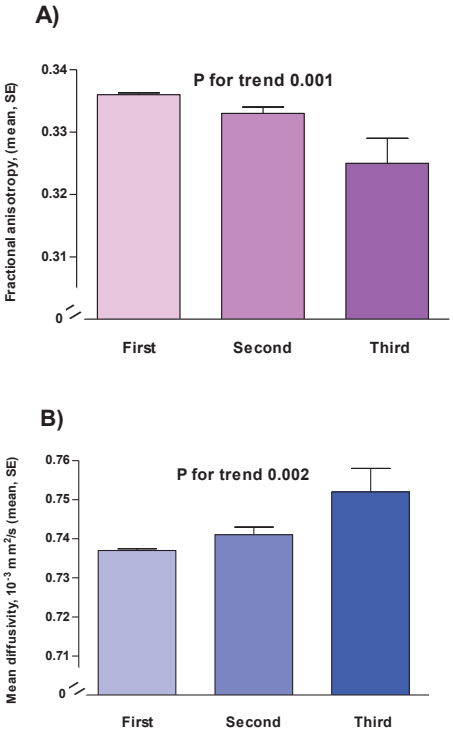

Figure 1. Means of **A)** fractional anisotropy **B)** and mean diffusivity in different categories of kidney function
First category: indicates eGFRcrcys > 60 mL/min/1.73 m^2 AND albumin-to-creatinine ratio < 30 mg/g (N=2320)
Second category: indicates eGFRcrcys > 60 mL/min/1.73 m^2 AND albumin-to-creatinine ratio > 30 mg/g OR eGFRcrcys < 60 mL/min/1.73 m^2 AND albumin-to-creatinine ratio < 30 mg/g (N=179)
Third category: indicates eGFRcrcys < 60 mL/min/1.73 m^2 AND albumin-to-creatinine ratio > 30 mg/g (N= 14)
Means are adjusted for age and sex.
Abbreviations: eGFRcrcys: creatinine and cystatin C based estimated glomerular filtration rate

DISCUSSION

In this cross-sectional study, we demonstrated that reduced kidney function was independently associated with worse microstructural integrity of cerebral white matter. The associations did not seem to be confined to specific white matter tracts.
Most of previous studies that investigated the association of kidney function with brain outcomes have focused either on cerebrovascular accidents, conventional macrostructural MRI-markers such as brain atrophy, or manifestations of cerebral small vessel disease.[2, 4, 5] In this study we show that reduced kidney function is related to loss of white matter microstructural integrity, which may be considered a more sensitive or subtle measure of white matter disease compared to macrostructural MRI-markers.

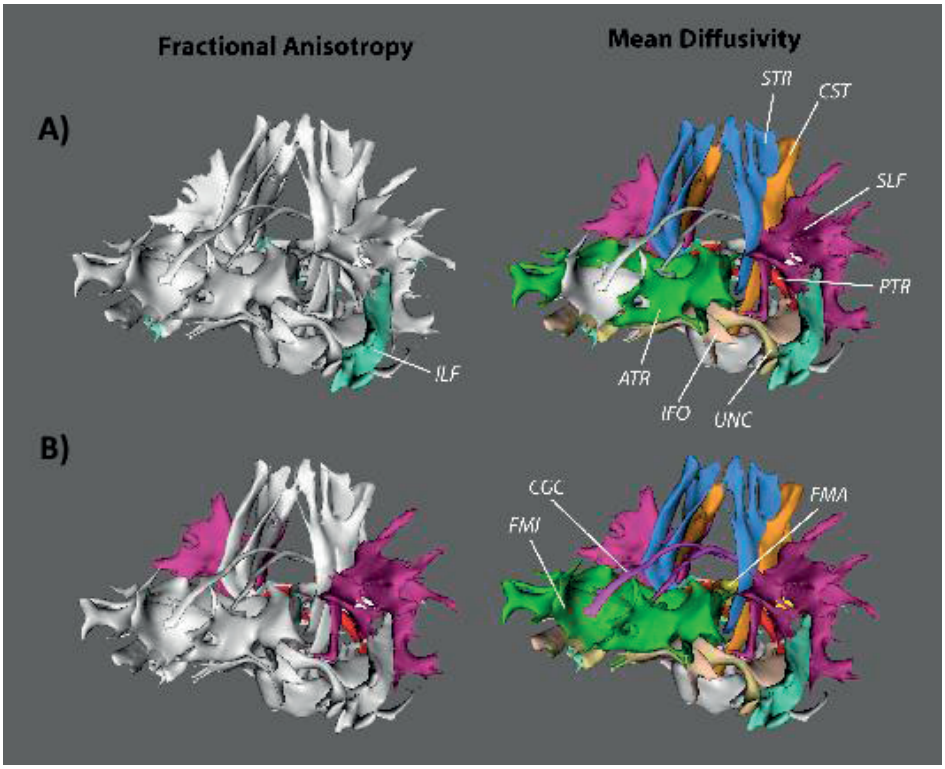

Figure 2. Association of **A)** ACR and **B)** eGFRcys with FA and MD in specific tracts. Adjusted for age, sex, white matter volume, intracranial volume, and log transformed white matter lesion volume.
Tracts with significant associations (after Bonferroni correction: $p<3.6\times10^{-3}$) are labelled and coloured.
Abbreviations: ACR: albumin-to-creatinine ratio, eGFRcys: cystatin C based estimated glomerular filtration rate, FA: fractional anisotropy, MD: mean diffusivity, ATR: anterior thalamic radiation, IFO: inferior fronto-occipital fasciculus, ILF: inferior longitudinal fasciculus, PTR: posterior thalamic radiation, SLF: superior longitudinal fasciculus, UNC: uncinate fasciculus, FMA: forceps major, FMI: forceps minor, CGC: cingulate gyrus part of cingulum, CGH: parahippocampal part of cingulum, CST: corticospinal tract, MCP: middle cerebellar peduncle, ML: medial lemniscus, STR: superior thalamic radiation.

The associations persisted after adjusting for history of stroke and conventional MRI-markers, indicating that decrease in kidney function might reflect early brain microstructural changes independent of co-existing comorbidities and pathologies.
A linear association between eGFRcys and white matter microstructure was present; however, we observed a U-shaped association between eGFRcr and DTI-parameters of white matter integrity. This discrepancy could be explained by the fact that subjects with very low creatinine are also at increased risk because of malnutrition and loss of muscle mass.[18] In line with this explanation, Seliger et al. reported a linear association between higher levels of serum cystatin C and prevalence of subclinical brain infarcts.[17] In contrast, they found that the prevalence of subclinical brain infarcts was higher in

both subjects with low and high serum creatinine suggesting a U-shaped association.[17] Levels of serum cystatin C are reported to be independent of muscle mass; nevertheless, some cardiovascular risk factors such as obesity and diabetes can be non-GFR determinants of serum cystatin C levels.[19] In addition, previous reports proposed that underlying inflammation can influence levels of cystatin C.[19] Since inflammation itself is a vascular risk factor, cystatin C may reflect inflammatory status independent of eGFR. However, in this study adjusting for cardiovascular risk factors as well as an inflammatory marker (C-reactive protein) did not change the associations.

Several explanations can be proposed for the association of kidney function with degeneration of white matter. First, kidney and the brain share several cardiovascular risk factors. Therefore, existence of these risk factors can simultaneously damage the vasculature of both kidney and brain.[1] While in this study adjusting for conventional cardiovascular risk factors such as blood pressure and excluding participants with diabetes, and cardiovascular disease did not change our findings, excluding participants with hypertension attenuated the associations. This might indicate that history of hypertension plays a role as an effect modifier and not as a confounder in the association between kidney function and white matter integrity. Future studies are needed to explore whether subjects with hypertension are more vulnerable to detrimental influences of impaired kidney function on white matter microstructural integrity. Second, it has been suggested that vascular damage is a diffuse phenomenon.[20] Given that the brain and kidney have similar circulation systems, and endothelial cells play a crucial role in both blood brain barrier and glomerular integrity,[1] it is possible that this association can originate from a systemic process affecting vascular beds in both organs.[20] Third, it is possible that impaired kidney function can lead to brain vascular injury via increase in pro-inflammatory factors and decrease in serum nitric oxide.[5] Nitric oxide regulates the function of the cerebral microcirculation and the blood brain barrier, which can contribute to cerebral hypoperfusion and subsequently white matter damage.[1]

In the tract-specific analyses, MD seemed to be a more sensitive marker for loss of white matter microstructural integrity in relation to kidney function. This might be explained by the prevailing theory that less uniform changes in FA are seen in deterioration of crossing fibers regions,[21] in contrast to MD that may show more consistent changes in areas of white matter loss. This is further supported by the considerable estimates for the prevalence of crossing fiber regions in the brain.[21]

The integrity of white matter is of great importance in normal functioning of the brain. Complex cognitive tasks are coordinated by interactions between different regions of the brain and intact white matter integrity plays an essential role in these interactions.[14, 22] In line with this notion, we previously showed that early changes in the white matter microstructure, as reflected in DTI-measures of the white matter, are associated with impaired cognitive function.[22] These associations were independent of

macrostructural brain abnormalities such as white matter lesions. Our findings might suggest that impairments in white matter integrity can be an underlying mechanism behind the association between impaired kidney function and cognitive dysfunction.

Strengths of our study include the large sample size and availability of extensive data on various cardiovascular risk factors, and macrostructural MRI-markers that enabled us to control for several potential confounders. Nevertheless, a number of limitations should be acknowledged. First, due to the cross-sectional design of the study, we cannot draw conclusions about the directionality and causality. Second, the cerebellum was not being fully incorporated in the field of view of the diffusion scan, making conclusion on brain stem tracts less reliable. In addition, our findings are based on a population-based study including relatively young and healthy individuals. Prevalence of kidney disease in this population is low and hence the associations are based on minor degrees of kidney dysfunction. Therefore, it is possible that the associations would be more prominent in older populations and in patients with kidney disease. In this study we did not have enough power to perform the analyses in participants with eGFR<60 mL/min/1.73 m^2.Further patient-based studies are needed to investigate this link in high risk individuals with lower eGFR levels.

In this study we showed that kidney function is related to impaired white matter microstructural integrity, suggesting that both kidney biomarkers and microstructural changes of white matter are biologically related. Our findings suggest that clinicians need to consider concomitant macro- and microstructural changes in the brain among subjects with impaired kidney function.

CHAPTER REFERENCES

1. Mogi M, Horiuchi M. Clinical Interaction between Brain and Kidney in Small Vessel Disease. Cardiol Res Pract 2011;2011:306189.
2. Bugnicourt JM, Godefroy O, Chillon JM, Choukroun G, Massy ZA. Cognitive disorders and dementia in CKD: the neglected kidney-brain axis. J Am Soc Nephrol 2013;24:353-363.
3. Krishnan AV, Kiernan MC. Neurological complications of chronic kidney disease. Nat Rev Neurol 2009;5:542-551.
4. Fabbian F, Casetta I, De Giorgi A, et al. Stroke and renal dysfunction: are we always conscious of this relationship? Clin Appl Thromb Hemost 2012;18:305-311.
5. Ikram MA, Vernooij MW, Hofman A, Niessen WJ, van der Lugt A, Breteler MM. Kidney function is related to cerebral small vessel disease. Stroke 2008;39:55-61.
6. Vermeer SE, Hollander M, van Dijk EJ, et al. Silent brain infarcts and white matter lesions increase stroke risk in the general population: the Rotterdam Scan Study. Stroke 2003;34:1126-1129.
7. Hofman A, Darwish Murad S, van Duijn CM, et al. The Rotterdam Study: 2014 objectives and design update. Eur J Epidemiol 2013;28:889-926.
8. Inker LA, Schmid CH, Tighiouart H, et al. Estimating glomerular filtration rate from serum creatinine and cystatin C. N Engl J Med 2012;367:20-29.
9. Rietveld I, Hofman A, Pols HA, van Duijn CM, Lamberts SW, Janssen JA. An insulin-like growth factor-I gene polymorphism modifies the risk of microalbuminuria in subjects with an abnormal glucose tolerance. Eur J Endocrinol 2006;154:715-721.
10. Kidney Disease: Improving Global Outcomes (KDIGO) CKD Work Group. KDIGO 2012 Clinical Practice Guideline for the Evaluation and Management of Chronic Kidney Disease. Kidney inter, Suppl 2013;3:1-150.
11. Mahmoodi BK, Yatsuya H, Matsushita K, et al. Association of kidney disease measures with ischemic versus hemorrhagic strokes: pooled analyses of 4 prospective community-based cohorts. Stroke 2014;45:1925-1931.
12. Ikram MA, van der Lugt A, Niessen WJ, et al. The Rotterdam Scan Study: design and update up to 2012. Eur J Epidemiol 2011;26:811-824.
13. Koppelmans V, de Groot M, de Ruiter MB, et al. Global and focal white matter integrity in breast cancer survivors 20 years after adjuvant chemotherapy. Hum Brain Mapp 2014;35:889-899.
14. de Groot M, Ikram MA, Akoudad S, et al. Tract-specific white matter degeneration in aging. The Rotterdam Study. Alzheimers Dement 2014.
15. de Groot M, Vernooij MW, Klein S, et al. Improving alignment in Tract-based spatial statistics: evaluation and optimization of image registration. Neuroimage 2013;76:400-411.
16. Leening MJ, Kavousi M, Heeringa J, et al. Methods of data collection and definitions of cardiac outcomes in the Rotterdam Study. Eur J Epidemiol 2012;27:173-185.
17. Seliger SL, Longstreth WT, Jr., Katz R, et al. Cystatin C and subclinical brain infarction. J Am Soc Nephrol 2005;16:3721-3727.
18. Seronie-Vivien S, Delanaye P, Pieroni L, et al. Cystatin C: current position and future prospects. Clin Chem Lab Med 2008;46:1664-1686.
19. Stevens LA, Schmid CH, Greene T, et al. Factors other than glomerular filtration rate affect serum cystatin C levels. Kidney Int 2009;75:652-660.
20. Thompson CS, Hakim AM. Living beyond our physiological means: small vessel disease of the brain is an expression of a systemic failure in arteriolar function: a unifying hypothesis. Stroke 2009;40:e322-330.

21. Jeurissen B, Leemans A, Tournier JD, Jones DK, Sijbers J. Investigating the prevalence of complex fiber configurations in white matter tissue with diffusion magnetic resonance imaging. Hum Brain Mapp 2013;34:2747-2766.
22. Vernooij MW, Ikram MA, Vrooman HA, et al. White matter microstructural integrity and cognitive function in a general elderly population. Arch Gen Psychiatry 2009;66:545-553.

SUPPLEMENTAL MATERIAL

CHAPTER 2.3

Retinal microvasculature and white matter microstructure: the Rotterdam Study

Unal Mutlu, Lotte G.M. Cremers, Marius de Groot, Albert Hofman, Wiro J. Niessen, Aad van der Lugt, Caroline C. Klaver, M. Arfan Ikram, Meike W. Vernooij, M. Kamran Ikram. ME*, Chaker L *, Niemeijer MN, Kors JA

Neurology 2016

ABSTRACT

Objective To investigate whether retinal microvascular damage is related to normal-appearing white matter microstructure on diffusion tensor MRI.

Methods We included 2,436 participants (age ≥45 years) from the population-based Rotterdam Study (2005-2009) who had gradable retinal images and brain MRI scans. Retinal arteriolar and venular calibers were measured semiautomatically on fundus photographs. White matter microstructure was assessed using diffusion tensor MRI. We used linear regression models to investigate the associations of retinal vascular calibers with markers of normal-appearing white matter microstructure, adjusting for age, sex, the fellow vascular caliber, and additionally for structural MRI markers and cardiovascular risk factors.

Results Narrower arterioles and wider venules were associated with poor white matter microstructure: adjusted difference in fractional anisotropy per standard deviation decrease in arteriolar caliber -0.061 (95% confidence interval (CI): -0.106; -0.016) and increase in venular caliber -0.054 (-0.096; -0.011), adjusted difference in mean diffusivity per standard deviation decrease in arteriolar caliber 0.048 (0.007; 0.088), and increase in venular caliber 0.047 (0.008; 0.085). The associations for venules were more prominent in women.

Conclusions Retinal vascular calibers are related to normal-appearing white matter microstructure. This suggests that microvascular damage in the white matter is more widespread than visually detectable as white matter lesions.

INTRODUCTION

With aging populations, the number of persons with age-related neurologic disorders such as stroke and dementia will rise substantially.[1] Vascular brain pathology has been recognized as an important contributor to the development of both these disorders.[2-4] Besides large vessel disease, pathology of the cerebral small vessels (<200 μm) has also been implicated as a crucial substrate.[5] However, the direct examination of cerebral small vessels is difficult with current neuroimaging modalities. Alternatively, the retinal microvasculature is thought to reflect the condition of the cerebral microvasculature, and is therefore increasingly being used to study vascular brain pathology.[6, 7] Indeed, several studies have shown a link of retinal vascular calibers with stroke and dementia.[8, 9] By extension, these retinal markers have also been associated with brain MRI markers such as white matter lesions, lacunar infarcts, and cerebral microbleeds.[10, 11] However, these structural MRI-markers of microvascular damage are considered the tip of the iceberg of a more widespread vascular brain pathology.[12] In the last decade, advanced MRI techniques such as diffusion tensor MRI (DT-MRI) have enabled us to visualize and quantify the microstructure of normal-appearing white matter, which is presumed to be affected already in earlier stages of vascular brain damage.[13] However, the exact link of microvascular damage with such microstructural MRI-markers has never been investigated.

Therefore, our primary aim was to investigate the relation between retinal vascular calibers and microstructure of normal-appearing white matter. As a secondary aim, we examined the association of retinal vascular calibers with structural MRI markers of cerebral microvascular damage.

METHODS

Study population

This study is embedded within the second extension of the Rotterdam Study (2005-2009), a prospective population-based cohort study in the Ommoord district in the city Rotterdam, the Netherlands, including 3,932 participants aged ≥45 years.[14] A total of 976 participants did not undergo a MRI for the following reasons: did not visited the research center (n=410), refused or physically/mentally unable to attend (n=277), nonrespondent (n=108), had MRI contraindications (n=154), or could not complete MRI (n=27). From the remaining 2,956 participants who underwent a multi-sequence MRI, we excluded persons with cortical infarcts (n=76) and those who had scans with artifacts that hampered automated analysis (n=55). This left 2,825 persons with available DT-MRI data, of whom a further 389 had no (gradable) fundus photographs. For

the current study, 2,436 persons were included With available DT-MRI and retinal data.

Standard protocol approvals, registrations, and patient consents

The Rotterdam Study has been approved by the medical ethics committee according to the Population Study Act Rotterdam Study, executed by the Ministry of Health, Welfare and Sports of the Netherlands. All participants gave written informed consent. Baseline home interviews and examinations were performed between 2005 and 2009.

Grading of retinal vascular calibers

A full ophthalmic examination was done including fundus color photography of the optic disc with a 20º visual field camera (TRC-50VT, Tokyo Optical Co., Tokyo, Japan) after pharmacological mydriasis. We analyzed for each participant the fundus photograph of one eye with the best quality with a semiautomated system (IVAN, University of Wisconsin-Madison, Madison, Wisconsin). Then we calculated one summary value for the arteriolar calibers (in μm) and one for the venular calibers (in μm) for each participant.[15] Subsequently, we adjusted these summary measures for refractive errors to approximate absolute measures.[11] We verified in a random sub-sample (n=100) that individual measurements in both eyes were similar. Measurements were performed by two trained raters masked for participant characteristics. Pearson correlation coefficients for interrater and intrarater reliability (n=100) were 0.85 and 0.86 for arteriolar calibers, and 0.87 and 0.87 for venular calibers, respectively.

Assessment of DT-MRI parameters

All brain MRI scanning was performed on a single 1.5 Tesla MRI scanner (Signa Excite, GE Healthcare, Milwaukee, Wisconsin). Scan protocol details are described extensively elsewhere.[16] For DT-MRI, we performed a single shot, diffusion-weighted spin echoplanar imaging sequence with maximum b value of 1,000 s/mm^2 in 25 non-collinear directions. A standardized pipeline was used to preprocess all diffusion data, including correction for motion and eddy currents, and registration to tissue segmentation to obtain global mean DT-MRI measures of the normal-appearing white matter. The normal-appearing white matter is being considered as the white matter volume without white matter lesion volumes. The global DT-MRI measures included fractional anisotropy (FA), mean diffusivity (MD), axial diffusivity (AxD), and radial diffusivity (RD). In general, lower values of FA and higher values of MD are indicative of poorer white matter microstructure. Besides, changes in AxD and RD values may give extra information about the underlying cause of poor white matter microstructure. In 1,338 participants, the diffusion acquisition scheme was rotated with the phase and frequency encoding directions swapped, which led to a mild ghost artifact in the phase

encoding direction. Therefore, we treated the phase encoding direction as a covariate in the analyses.[17]

Other MRI markers

Volumetric measures of normal-appearing white matter volume, intracranial volume, and white matter lesion volume (in milliliters) were obtained supratentorially, using a validated tissue segmentation approach that included conventional k-nearest-neighbor brain tissue classification and white matter lesion segmentation.[18, 19] The presence of cerebral microbleeds and lacunar infarcts was rated by 1 of 5 trained research physicians, blinded to the participants' data, on a 3D T2-weighted gradient-recalled echo MRI. The presence of lacunes of presumed ischemic origin was rated on fluid-attenuated inversion recovery, proton density-weighted and T1-weighted sequences.[20] We defined lacunes as focal lesions ≥3 and <15 mm in size with the same signal intensity as cerebrospinal fluid on all sequences and a hyperintense rim on fluid-attenuated inversion recovery.

Assessment of cardiovascular risk factors

We measured the systolic and diastolic blood pressure twice in sitting position at the right upper arm with a random-zero sphygmomanometer. The mean of these two readings was used for further analysis. We calculated the body mass index as weight divided by height squared. An automated enzymatic procedure measured the non-fasting serum concentrations of total and high-density lipoprotein cholesterol.[21] We defined diabetes mellitus as present if fasting serum glucose concentration was ≥7.0 mmol/L, or if participants reported anti-diabetic medication use. C-reactive protein serum concentration was measured by the Rate Near Infrared Particle Immunoassay method (Immage®, Beckman Coulter Inc., Brea, California). We determined the presence of atherosclerotic plaques at the carotid artery bifurcation, common carotid artery, and internal carotid artery on both sides by ultrasound. Presence of these plaques was defined as focal thickening of the vessel wall ≥2mm with or without calcified components relative to adjacent segments. We retrieved data on smoking (non, former, or current) and antihypertensive medication use by a computerized questionnaire.

Statistical analysis

We used analysis of covariance, adjusted for age and sex, to assess difference in population characteristics between participants and nonparticipants. White matter lesion volumes were transformed using natural logarithm to account for a skewed distribution. We calculated z-scores for retinal vascular calibers, log-transformed white matter lesion volumes, and DT-MRI parameters to better compare the arteriolar and venular effects on imaging parameters. Associations of retinal vascular calibers with DT-MRI

parameters were evaluated using linear regression models. Mean differences and corresponding 95% confidence intervals (CI) in DT-MRI parameters were estimated per standard deviation (SD) decrease in arteriolar caliber or increase in venular caliber, and in tertiles of retinal vascular calibers. We adjusted for age, sex, and the other vascular caliber (model 1), and additionally for white matter volume, intracranial volume, white matter lesion volume, lacunar infarcts, and cerebral microbleeds (model 2). We further adjusted for systolic and diastolic blood pressure, antihypertensive medication, body mass index, total and high-density lipoprotein cholesterol, diabetes mellitus, C-reactive protein, atherosclerotic plaque and smoking (model 3). We explored effect modification by stratifying for age (median: 56 years), sex, hypertension, diabetes mellitus, and smoking, and by adding interaction terms to the statistical models. In all analyses, we treated the phase encoding direction for the diffusion acquisition as a confounder. We compared the effect estimates of arterioles and venules with age – an established risk factor for poor white matter microstructure – to have an impression about the magnitude of these associations. First, we calculated the effect estimates for the association of age with FA and MD. Then, we divided the betas (per SD) of retinal vascular calibers by the betas of age in relation to DT-MRI measures and reported the corresponding ratios. Furthermore, to assess the relation of retinal vascular calibers with white matter lesion volumes, cerebral microbleeds and lacunar infarcts, we used linear and logistic regression models. Missing values, if present, were less than in 4% of the cases, which we dealt with using 5-fold multiple imputations based on determinant, outcome, and covariates. Given the Pearson correlation coefficient between systolic and diastolic blood pressure (r=0.77), we examined the possibility of collinearity by calculating the variance inflation factor, but none was identified (variance inflation factor <2.9). Statistical tests were performed at the 0.05 significance level (two-tailed) using SPSS 21.0 for Windows (IBM corp., Armonk, New York).

RESULTS

Table 1 shows the characteristics of the study population. Of the total 3,932 participants, 1,496 (38%) did not participate in this study. After adjusting for age and sex (if applicable), nonparticipants were on average older, had higher blood pressure, had higher body mass index, had higher C-reactive protein levels, and were more smokers compared to participants. Of the 2,436 (62%) participants, 56% were women and the average age was 56.5 years (SD: 6.2).

Table 2 shows the associations between retinal vascular calibers and white matter microstructure. Both narrower arterioles and wider venules were associated with lower FA, higher MD, higher AxD, and higher RD. After adjusting for other MRI markers,

the associations between retinal vascular calibers and DT-MRI parameters attenuated, but remained statistically significant. Additional adjustments for cardiovascular risk factors marginally changed the results.

Table 1. Characteristics of the eligible study cohort

Characteristics	Participants (n=2,436)	Non-participants (n=1,496)
Age, years	56.5 (6.2)	58.2 (8.6)*
Female	1374 (56)	878 (59)
Systolic blood pressure, mmHg	131.9 (18.5)	134.1 (20.3)*
Diastolic blood pressure, mmHg	82.3 (10.8)	83.2 (11.4)*
Antihypertensive medication	406 (28)	523 (22)*
Hypertension	1,117 (46)	726 (56)*
Body mass index, kg/m^2	27.5 (4.3)	28.4 (5.2)*
Total cholesterol, mmol/L	5.6 (1.1)	5.5 (1.1)
High-density lipoprotein cholesterol, mmol/L	1.4 (0.4)	1.4 (0.4)
Diabetes mellitus type 2	190 (8)	131 (9)
C-reactive protein, mg/L	2.5 (4.4)	3.0 (5.3)*
Atherosclerotic plaque	604 (25)	476 (32)
Smoking status		
Non-smoker	786 (32)	459 (31)
Former smoker	1,116 (46)	608 (41)*
Current smoker	534 (22)	417 (28)*
Arteriolar caliber, µm	158.7 (15.4)	-
Venular caliber, µm	239.8 (22.7)	-
White matter volume, ml	418.7 (57.3)	-
Intracranial volume, ml	1,129.0 (119.2)	-
White matter lesion volume†, ml	2.0 (1.3-3.5)	-
Cerebral microbleeds	302 (12)	-
Lacunar infarcts	87 (4)	-
Fractional anisotropy	0.34 (0.01)	-
Mean diffusivity, 10^{-3} mm^2/s	0.73 (0.02)	-
Axial diffusivity, 10^{-3} mm^2/s	1.01 (0.02)	-
Radial diffusivity, 10^{-3} mm^2/s	0.59 (0.02)	-

Values are presented as means (standard deviation) or as numbers (percentages). *Significantly different from included persons (age and sex adjusted p-value< 0.05). †Presented as median (interquartile range) because of skewed distribution. The following variables had missing values: systolic and diastolic blood pressure (n=7), use of antihypertensive medication (n=18), body mass index (n=2), total cholesterol (n=27), high-density lipoprotein cholesterol (n=29), diabetes mellitus (n=18), C-reactive protein (n=92), atherosclerotic plaque (n=6), smoking (n=5).

Table 2. The association between retinal vascular calibers and white matter microstructure

	Fractional anisotropy	Mean diffusivity	Axial diffusivity	Radial diffusivity
Arteriolar caliber, per SD decrease				
Model 1	-0.121 (-0.166; -0.077)	0.108 (0.065; 0.150)	0.065 (0.022; 0.108)	0.119 (0.075; 0.162)
Model 2	-0.061 (-0.104; -0.018)	0.054 (0.015; 0.092)	0.032 (-0.006; 0.070)	0.059 (0.019; 0.099)
Model 3	-0.061 (-0.106; -0.016)	0.048 (0.007; 0.088)	0.025 (-0.016; 0.065)	0.055 (0.013; 0.097)
Venular caliber, per SD increase				
Model 1	-0.086 (-0.130; -0.043)	0.080 (0.038; 0.123)	0.045 (0.003; 0.087)	0.090 (0.048; 0.133)
Model 2	-0.060 (-0.101; -0.019)	0.054 (0.016; 0.091)	0.027 (-0.010; 0.064)	0.062 (0.023; 0.101)
Model 3	-0.054 (-0.096; -0.011)	0.047 (0.008; 0.085)	0.023 (-0.016; 0.061)	0.054 (0.015; 0.094)

Values represent difference in z-scores of DT-MRI parameters with 95% confidence interval.
Model 1: adjusted for age, sex and the other vascular caliber.
Model 2: as model 1, additionally adjusted for white matter volume, intracranial volume, white matter lesion volume, lacunar infarcts and cerebral microbleeds.
Model 3: as model 2, additionally adjusted for systolic blood pressure, diastolic blood pressure, antihypertensive medication, body mass index, total cholesterol, high-density lipoprotein cholesterol, diabetes mellitus, C-reactive protein, plaque and smoking.
Abbreviations: SD=standard deviation.

Figure 1 shows absolute mean differences in FA and MD by tertiles of arteriolar and venular calibers (adjusted for age and sex). In stratified analyses (**Figure 2**), adjusted for variables in model 3, we found that the association for arterioles with MD was modified by hypertension (P-value for interaction=0.021), whereas for venules, the associations with FA and MD were in both cases modified by sex (P-value for interaction=0.006, and 0.034, respectively). With respect to diabetes mellitus, we observed that the effects of arterioles and venules on DT-MRI parameters were more pronounced in persons with diabetes mellitus. However, p-values for the formal interaction terms were not significant: for arterioles these were 0.180 for FA and 0.172 for MD, whereas for venules these were 0.091 for FA and 0.097 for MD.

In an additional analysis to compare the magnitude of the associations with age, we observed that each year increase in age was associated with lower FA (-0.009 (-0.016; -0.002)) and higher MD (0.023 (0.016; 0.029)). We found that each SD narrower arterioles and wider venules in relation to FA had the magnitude equal to 6.8 years and 6.0 years of increase in age, respectively. Similarly, each SD narrower arterioles and wider venules in relation to MD had the magnitude equal to 2.1 and 2.0 years increase in age, respectively.

Table 3 shows the associations between retinal vascular calibers and structural MRI markers of cerebral microvascular damage. Both narrower arterioles and wider venules were significantly associated with larger white matter lesion volumes. Additional adjustments for cardiovascular risk factors (model 3) attenuated these associations. Narrower arterioles and wider venules were also associated with the presence of cerebral microbleeds and lacunar infarcts in model 1. These associations disappeared after adjusting for other MRI markers and cardiovascular risk factors.

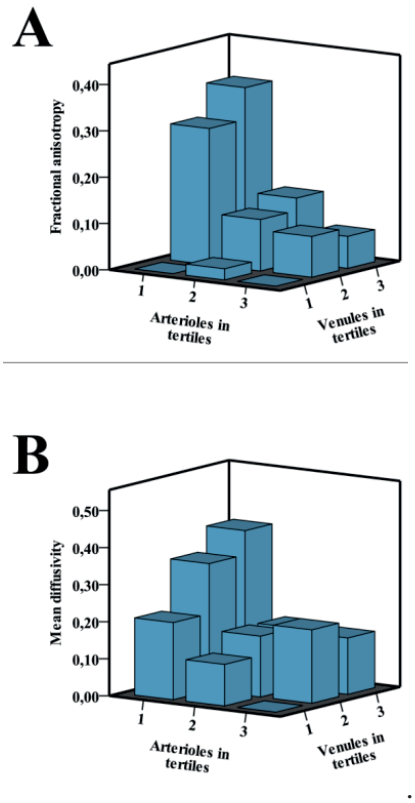

Figure 1. Absolute mean difference in (A) fractional anisotropy and (B) mean diffusivity by tertiles of retinal vascular calibers.

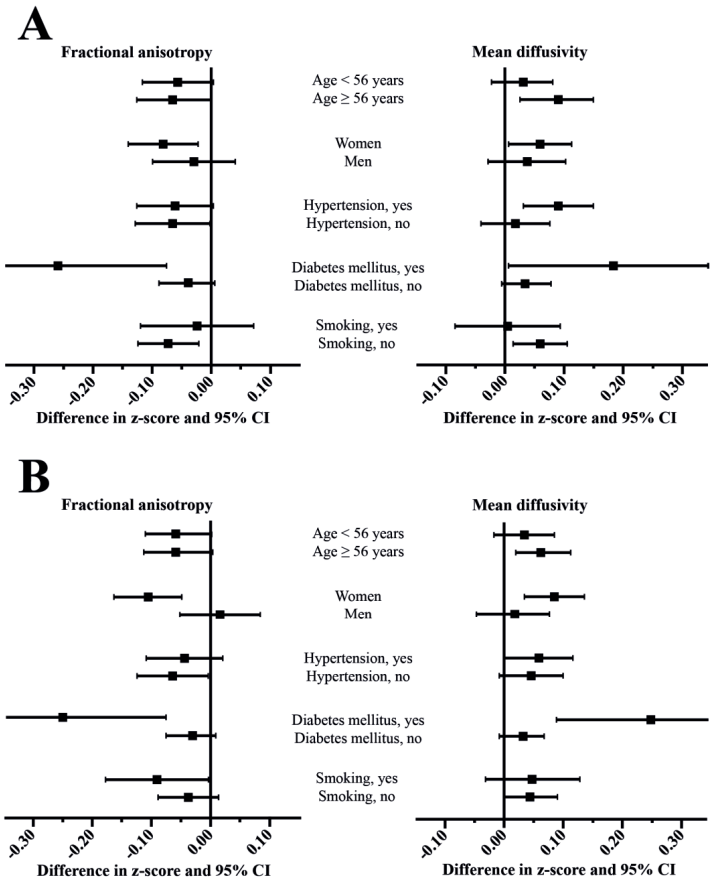

Figure 2. Stratified analyses on the association of (A) arteriolar and (B) venular calibers with white matter microstructure measures.

Table 3. The association between retinal vascular calibers and markers of cerebral small vessel disease.

	White matter lesion volume	Presence of cerebral microbleeds	Presence of lacunar infarcts
	Difference in z-score (95% CI)	Odds ratio (95% CI)	Odds ratio (95% CI)
Arteriolar caliber, per SD decrease			
Model 1	0.145 (0.100; 0.189)	1.20 (1.04; 1.40)	1.34 (1.03; 1.75)
Model 2	0.146 (0.104; 0.188)	1.15 (0.99; 1.34)	1.10 (0.84; 1.43)
Model 3	0.101 (0.057; 0.145)	1.14 (0.97; 1.33)	1.10 (0.83; 1.45)
Venular caliber, per SD increase			
Model 1	0.061 (0.018; 0.104)	1.09 (0.95; 1.26)	1.31 (1.02; 1.68)
Model 2	0.059 (0.018; 0.100)	1.07 (0.92; 1.24)	1.17 (0.90; 1.52)
Model 3	0.030 (-0.012; 0.071)	1.09 (0.94; 1.27)	1.15 (0.88; 1.51)

White matter lesion volumes are natural log transformed.
Abbreviations: CI=confidence interval; SD= standard deviation.
Model 1: adjusted for age, sex and the other vascular caliber.
Model 2: as model 1, additionally adjusted for intracranial volume, white matter lesion volume, lacunar infarcts and cerebral microbleeds (if applicable).
Model 3: as model 2, additionally adjusted for systolic blood pressure, diastolic blood pressure, antihypertensive medication, body mass index, total cholesterol, high-density lipoprotein cholesterol, diabetes mellitus, C-reactive protein, plaque and smoking.

DISCUSSION

In this study, we found that retinal microvascular pathology is related to poorer microstructure of normal-appearing cerebral white matter.

With respect to retinal vascular imaging as a tool in assessing vascular brain pathology, several large population-based studies have shown that retinal microvascular damage is related to subclinical and clinical vascular brain diseases. Community-based cohorts of predominantly healthy people have shown that retinopathy signs were associated with incident stroke, cognitive decline and dementia.[22, 23] Apart from clinical outcomes, these studies also showed that persons with retinopathy signs had more often subclinical microvascular brain damages such as white matter lesions, cerebral infarcts and cerebral microbleeds.[22-26] Overall these findings suggest that both retinal and cerebral microvascular damage may appear simultaneously as part of systemic microvascular disease with common pathogenesis.[26] However, signs of retinopathy are relatively late manifestations of organ damage and presumably reflect advanced stages of microvascular damage including blood-retina barrier disruption.[27] There are ongoing efforts to unravel earlier retinal markers (e.g. narrower arterioles and wider venules), as they likely represent a point in the pathophysiologic cascade that is potentially reversible, offering great potential for the development of preventive strategies or surrogate markers for trials.

Interestingly, cross-sectional data from the Rotterdam Study showed that the association of retinal vascular calibers with markers of cerebral small vessel disease was not significant.[28] In contrast, longitudinal data from the same study showed that wider venular caliber was associated with progression of white matter lesions in both periventricular and subcortical regions, and with incident lacunar infarcts on MRI.[28] Overall, these findings indicate that changes in retinal vascular calibers may precede the development of white matter lesions and lacunar infarcts. Findings from our current study are in line with these observations. We found that retinal vascular calibers were strongly related to markers of normal-appearing white matter on DT-MRI, independently of structural MRI markers of cerebral small vessel disease. Moreover, the joint effect of narrower arterioles and wider venules on white matter microstructure appears to be much stronger than their individual effect.

Pathophysiologically, a narrow retinal arteriolar caliber may reflect not only active vasoconstriction, but also systemic structural changes such as arteriolosclerosis.[29] These processes may concomitantly occur in the brain, where they affect the ability of cerebral arterioles to maintain control of local blood flow. Thus, predisposed areas as served by these vessels may lead to ischemic damage, and eventually to a state of chronic hypoperfusion of the white matter with subsequent demyelination and axonal damage.[12] It has been shown that subtle changes in the white matter due to demyelination and axonal damage can be detected using DT-MRI.[30] With respect to the venous system, several histopathological studies have reported venular abnormalities such as venous collagenosis in areas affected by white matter lesions.[31] In line with these observations, our findings show that subtle changes in retinal venular calibers are associated with DT-MRI markers of normal-appearing white matter.

A growing body of evidence now suggests that microvascular damage primarily affects women.[32] Indeed, narrower arterioles were found to increase the risk of coronary heart disease in women, but not in men.[33] In addition, cardiovascular risk factors typically associated with female sex such as an unfavorable lipid profile and inflammatory markers were also found to be associated with wider venules.[7] Our findings provide further evidence suggesting that the pathogenesis of vascular brain diseases is different in men and women.

Furthermore, we found that the relation of retinal microvasculature with white matter microstructure is more pronounced in persons with diabetes mellitus. It is well-known that diabetes mellitus primarily affects small vessels due to chronic exposure to hyperglycemia, which can lead to impaired function of endothelium as well as pericytes.[34] It is conceivable that such more severe damage to the microcirculation might translate into stronger associations among diabetics compared to nondiabetics. At the same time, persons with diabetes mellitus very often have other cardiometabolic comorbidities, such as dyslipidemia and subclinical inflammation, all of which can further aggravate

the small vessel damage.[35] Although we did adjust for covariates that are considered proxies for these processes, a substantial residual effect remains likely and may explain the stronger associations among diabetics compared to nondiabetics.

DT-MRI is highly sensitive to changes in water diffusion in the white matter microstructure and thus a robust method to detect microstructural changes.[30] Experimental studies have suggested that perpendicular diffusivity may reflect myelin loss, whereas axial diffusivity may point towards axonal degeneration.[36] Although it is not completely clear which pathophysiological processes underlie alterations in white matter DT-MRI measures, possible mechanisms besides microvascular lesions include inflammation, demyelination and blood-brain barrier disruption. Nevertheless, DT-MRI is a useful research tool to probe not only cerebrovascular pathology, but also other brain diseases such as multiple sclerosis and other inflammatory demyelinating diseases. With respect to our study, given the rarity of these other diseases, it is unlikely that our findings may have been affected by these conditions.

Several methodological issues need to be discussed. First, the cross-sectional design of our study prevented us from assessing the temporal link between the retinal microvasculature and white matter microstructure. Second, persons excluded from these analyses had a slightly worse cardiovascular risk profile, suggesting a limited role for selection bias. Third, retinal caliber measurements were assessed at a single timepoint and were not synchronized to the cardiac cycle. Hence, we were not able to assess dynamic changes in the microcirculation. This random misclassification suggests that the true effect sizes may have been larger. Fourth, we were unable to measure some confounding factors such as previous blood pressure or cholesterol levels, which could have influenced our associations by introducing residual confounding. Furthermore, participants in the Rotterdam Study are mainly middle-class white persons, which limits the generalizability of our findings. Also, due to the low number of incident clinical endpoints (stroke/dementia) in this extended cohort, we were not able to examine the association between retinal vascular calibers and DT-MRI-markers with these endpoints. Finally, we acknowledge that the sensitivity of DT-MRI to a broad spectrum of other factors (e.g. noise, artifacts, and crossing white matter tracts) makes interpretation difficult, thus inferences should be drawn carefully.

Strengths of our study are the population-based setting including relatively young and healthy individuals, the large study size and available data on macrostructural and microstructural brain imaging markers, enabling us to assess independent associations. In this study, we have shown that retinal vascular calibers are associated with poorer white matter microstructure in normal-appearing white matter. These findings suggest that microvascular damage in the white matter is more widespread than visually detectable on MRI. Future studies with longitudinal data on incident clinical cerebrovascular diseases are needed to examine the clinical implications of these retinal and DT-MRI markers.

CHAPTER REFERENCES

1. World Health Organization. Neurological disorders: Public health challenges. Geneva2006.
2. Akoudad S, Portegies ML, Koudstaal PJ, et al. Cerebral Microbleeds Are Associated With an Increased Risk of Stroke: The Rotterdam Study. Circulation 2015;132:509-516.
3. Kester MI, Goos JD, Teunissen CE, et al. Associations between cerebral small-vessel disease and Alzheimer disease pathology as measured by cerebrospinal fluid biomarkers. JAMA Neurol 2014;71:855-862.
4. Vermeer SE, Longstreth WT, Jr., Koudstaal PJ. Silent brain infarcts: a systematic review. Lancet Neurol 2007;6:611-619.
5. Thompson CS, Hakim AM. Living beyond our physiological means: small vessel disease of the brain is an expression of a systemic failure in arteriolar function: a unifying hypothesis. Stroke 2009;40:e322-330.
6. Wong TY, Klein R, Klein BE, Tielsch JM, Hubbard L, Nieto FJ. Retinal microvascular abnormalities and their relationship with hypertension, cardiovascular disease, and mortality. Surv Ophthalmol 2001;46:59-80.
7. Ikram MK, de Jong FJ, Vingerling JR, et al. Are retinal arteriolar or venular diameters associated with markers for cardiovascular disorders? The Rotterdam Study. Invest Ophthalmol Vis Sci 2004;45:2129-2134.
8. Ikram MK, de Jong FJ, Bos MJ, et al. Retinal vessel diameters and risk of stroke: the Rotterdam Study. Neurology 2006;66:1339-1343.
9. de Jong FJ, Schrijvers EM, Ikram MK, et al. Retinal vascular caliber and risk of dementia: the Rotterdam study. Neurology 2011;76:816-821.
10. Hilal S, Ong YT, Cheung CY, et al. Microvascular network alterations in retina of subjects with cerebral small vessel disease. Neurosci Lett 2014;577:95-100.
11. Littmann H. [Determining the true size of an object on the fundus of the living eye] Zur Bestimmung der wahren Grosse eines Objektes auf dem Hintergrund eines lebenden Auges. Klin Monbl Augenheilkd 1988;192:66-67.
12. Pantoni L. Cerebral small vessel disease: from pathogenesis and clinical characteristics to therapeutic challenges. Lancet Neurol 2010;9:689-701.
13. de Groot M, Verhaaren BF, de Boer R, et al. Changes in normal-appearing white matter precede development of white matter lesions. Stroke 2013;44:1037-1042.
14. Hofman A, Brusselle GG, Darwish Murad S, et al. The Rotterdam Study: 2016 objectives and design update. Eur J Epidemiol 2015;30:661-708.
15. Knudtson MD, Lee KE, Hubbard LD, Wong TY, Klein R, Klein BE. Revised formulas for summarizing retinal vessel diameters. Curr Eye Res 2003;27:143-149.
16. Ikram MA, van der Lugt A, Niessen WJ, et al. The Rotterdam Scan Study: design update 2016 and main findings. Eur J Epidemiol 2015;30:1299-1315.
17. de Groot M, Ikram MA, Akoudad S, et al. Tract-specific white matter degeneration in aging: the Rotterdam Study. Alzheimers Dement 2015;11:321-330.
18. Vrooman HA, Cocosco CA, van der Lijn F, et al. Multi-spectral brain tissue segmentation using automatically trained k-Nearest-Neighbor classification. Neuroimage 2007;37:71-81.
19. de Boer R, Vrooman HA, van der Lijn F, et al. White matter lesion extension to automatic brain tissue segmentation on MRI. Neuroimage 2009;45:1151-1161.

20. Vernooij MW, Ikram MA, Wielopolski PA, Krestin GP, Breteler MM, van der Lugt A. Cerebral microbleeds: accelerated 3D T2*-weighted GRE MR imaging versus conventional 2D T2*-weighted GRE MR imaging for detection. Radiology 2008;248:272-277.
21. Hofman A, van Duijn CM, Franco OH, et al. The Rotterdam Study: 2012 objectives and design update. Eur J Epidemiol 2011;26:657-686.
22. Wong TY, Klein R, Sharrett AR, et al. Cerebral white matter lesions, retinopathy, and incident clinical stroke. JAMA 2002;288:67-74.
23. Qiu C, Cotch MF, Sigurdsson S, et al. Cerebral microbleeds, retinopathy, and dementia: the AGES-Reykjavik Study. Neurology 2010;75:2221-2228.
24. Qiu C, Cotch MF, Sigurdsson S, et al. Microvascular lesions in the brain and retina: The age, gene/environment susceptibility-Reykjavik study. Ann Neurol 2009;65:569-576.
25. Cheung N, Mosley T, Islam A, et al. Retinal microvascular abnormalities and subclinical magnetic resonance imaging brain infarct: a prospective study. Brain 2010;133:1987-1993.
26. Cooper LS, Wong TY, Klein R, et al. Retinal microvascular abnormalities and MRI-defined subclinical cerebral infarction: the Atherosclerosis Risk in Communities Study. Stroke 2006;37:82-86.
27. Bergers G, Song S. The role of pericytes in blood-vessel formation and maintenance. Neuro Oncol 2005;7:452-464.
28. Ikram MK, De Jong FJ, Van Dijk EJ, et al. Retinal vessel diameters and cerebral small vessel disease: the Rotterdam Scan Study. Brain 2006;129:182-188.
29. Liew G, Wang JJ, Mitchell P, Wong TY. Retinal vascular imaging: a new tool in microvascular disease research. Circ Cardiovasc Imaging 2008;1:156-161.
30. Alexander AL, Lee JE, Lazar M, Field AS. Diffusion tensor imaging of the brain. Neurotherapeutics 2007;4:316-329.
31. Brown WR, Moody DM, Challa VR, Thore CR, Anstrom JA. Venous collagenosis and arteriolar tortuosity in leukoaraiosis. J Neurol Sci 2002;203-204:159-163.
32. Shaw LJ, Bugiardini R, Merz CN. Women and ischemic heart disease: evolving knowledge. J Am Coll Cardiol 2009;54:1561-1575.
33. Wong TY, Klein R, Sharrett AR, et al. Retinal arteriolar narrowing and risk of coronary heart disease in men and women. The Atherosclerosis Risk in Communities Study. JAMA 2002;287:1153-1159.
34. Armulik A, Genove G, Betsholtz C. Pericytes: developmental, physiological, and pathological perspectives, problems, and promises. Dev Cell 2011;21:193-215.
35. Fox CS, Coady S, Sorlie PD, et al. Trends in cardiovascular complications of diabetes. JAMA 2004;292:2495-2499.
36. Song SK, Sun SW, Ramsbottom MJ, Chang C, Russell J, Cross AH. Dysmyelination revealed through MRI as increased radial (but unchanged axial) diffusion of water. Neuroimage 2002;17:1429-1436.

CHAPTER 2.4

Reduced lung function is associated with poorer brain white matter microstructure

Lotte G.M. Cremers, Lies Lahousse, Marius de Groot, Gennady V. Roshchupkin, Gabriel.P Krestin, Wiro J. Niessen, Bruno H. Stricker, M. Arfan Ikram, Guy G. Brussele, Meike W. Vernooij

Submitted

ABSTRACT

Background Brain pathology is a presumed link between Chronic Obstructive Pulmonary Disease (COPD) and cognitive impairment. We assessed the association of lung function with the microstructural integrity of cerebral white matter tracts in an aging population. In addition, we studied the link between white matter microstructure and global cognition in participants with and without COPD.

Methods We included 2,405 participants free of stroke and dementia (mean age 68.4± 9.0 years, 52.6% female), who performed spirometry and diffusing capacity within the Rotterdam Study, a population-based cohort study. Diffusion-MRI and probabilistic tractography was used to assess the microstructural integrity of 15 different white matter tracts. We furthermore obtained a marker of global cognition (g-factor) using a cognitive test battery.

Results Out of 2,405 participants, 363 persons were classified as having COPD. In the overall population, lower forced expiratory volume in 1 second and a lower diffusing capacity were associated with reduced white matter microstructural integrity throughout the brain, but mainly in the association tracts. This remained after excluding persons with overt COPD. Persons with severe COPD had poorer tract-specific microstructural integrity than those without COPD, again particularly in the association tracts. Though formal interaction was absent, the link between white matter microstructural integrity and global cognition seemed stronger in persons with COPD versus persons without COPD.

Conclusions Reduced lung function (even within the normal range) is related to regional microstructural white matter damage throughout the brain, but especially in the association tracts. This may underlie the relation between COPD and reduced cognition.

INTRODUCTION

Patients with chronic obstructive pulmonary disease (COPD) have progressive and largely irreversible airflow limitation that is associated with an abnormal response of the lungs to noxious particles or gases[1]. However, COPD is not limited to the lungs and an important extrapulmonary effect is cognitive dysfunction[2-4]. Furthermore, patients with COPD have an increased risk of dementia.[5] The exact pathway linking COPD and cognitive impairment and dementia remains unclear. Brain changes may be considered an intermediate in the association between COPD and these endpoints.

Previous research found that total grey and white matter volumes seem to be similar between persons with and without COPD,[6,7] whereas other studies found reduced regional grey matter volume,[8,9] and a higher white matter lesion load,[10,11] in patients with COPD. Also, in patients with hypoxemic COPD there was evidence of hypoperfusion in the anterior and subcortical regions of the brain compared to healthy controls.[12] All these findings suggest a more regional degeneration pattern in COPD patients. Regional imaging markers may be therefore more insightful than global assessment of brain morphology. Previous studies investigating regional brain changes in COPD patients mainly focused on cerebral grey matter. Studies focusing on cerebral white matter are sparse and have been performed in small samples.[7,13,14] Regional white matter changes can be evaluated at a macrostructural level, such as by investigating atrophy and a higher white matter lesion load. However, regional white matter changes can also be assessed at a level not visible for the naked eye, by means of diffusion-MRI allowing quantitative evaluation of the microstructural integrity of white matter. Fractional anisotropy (FA) and mean diffusivity (MD) are the two measures most commonly derived from diffusion-MRI. In general lower values of FA and higher values of MD are indicative of a poorer white matter microstructural integrity. Also, white matter can be studied even more in depth by considering different white matter tracts.

The aim of this study was to determine the effect of reduced lung function (both within the normal range and overt COPD) on tract-specific white matter microstructural integrity in a large population of 2,405 middle aged and elderly persons from the population-based Rotterdam Study.[15] We hypothesized that reduced lung function is related to poor microstructural integrity, in particular in the association tracts, since these tracts are typically vulnerable to vascular damage.[16] Furthermore, we studied whether the relation between white matter microstructural integrity and global cognition differed between participants with and without COPD.

METHODS

Study population

This study was embedded within the framework of Rotterdam Study, an ongoing, prospective, population-based cohort study including participants of 45 years and older living in Ommoord, a suburb of Rotterdam.[15,17,18] Since 2005, MRI-scanning, including diffusion-MRI, was implemented in the study protocol.[18] For the current study we included 4,493 non-demented participants with lung function data. We excluded 468 participants with asthma. Out of 4,025 participants, 3,184 had an interpretable forced expiratory volume in one second (FEV_1) measurement. Of them, 2,700 had a good quality MRI scan. We additionally excluded participants with a history of clinical stroke (N=65), and MRI-defined cortical infarcts (N=13), resulting in 2,405 participants in the FEV_1 analysis. For the COPD analysis, we additionally excluded participants with a spirometry report suggestive of a restrictive syndrome [FEV_1/ forced expiratory vital capacity (FVC) $\geq$ 70% and FVC < 80% predicted] (N=91), so 2,314 persons were included in the COPD analysis. Out of 2,314 participants 363 persons had a diagnosis of COPD. Out of 2,405 participants 2,125 persons had analyzable diffusing data. The Rotterdam Study has been approved by the medical ethics committee according to the Population Study Act Rotterdam Study, executed by the Ministry of Health, Welfare and Sports of the Netherlands. Written informed consent was obtained from all participants.[15]

Assessment of COPD

Spirometry and diffusing capacity were performed around the time of the scan date using a Master Screen® PFT Pro (CareFusion, San Diego, CA) by trained paramedical personnel according to the ATS/ERS guidelines.[19,20,21] The diffusing capacity of the lungs measured using carbon monoxide was corrected for the haemoglobin concentration ($DL_{CO,c}$). Additional details on the assessment of COPD is provided in an online data supplement.

MRI acquisition and processing

Multi-sequence MR imaging was performed on a 1.5 tesla MRI scanner (GE Signa Excite). The imaging protocol, sequence details and segmentation methods have been described extensively elsewhere.[18] The conventional scan protocol consisted of a T1-weighted image, a T2-weighted fluid-attenuated inversion recovery (FLAIR) sequence, a proton density weighted image. For diffusion-MRI, we performed a single shot, diffusion-weighted spin echo echo-planar imaging sequence. Maximum b-value was 1000 s/mm^2 in 25 non-collinear directions and three volumes were acquired without diffusion weighting (b-value = 0 s/mm^2). Using a probabilistic diffusion tractography

approach 15 different white matter tracts (12 tracts were present in both left and right hemisphere) were segmented.[22] Participant specific mean FA and MD inside each white matter tract were obtained, and left and right measures were averaged.[22] Subsequently, we computed z-scores for the tract-specific parameters (by subtracting the mean and dividing by the SD) to facilitate comparison of associations. We combined the tissue and tract segmentations to obtain tract-specific white matter volumes and tract-specific WMH volumes (natural-log transformed to account for their skewed distribution). See the online data supplement for further details.

Voxel-based Analysis

We also performed voxel-based analyses on white matter tracts to investigate whether lung function was associated with the microstructure of sub-regions of specific tracts. Voxel-based analysis (VBA) of diffusion-MRI data was performed using the voxel-based morphometry method[23] as previously described.[24] See the online supplement for more details on the VBA data processing.

Assessment of global cognitive function

Global cognitive function was assessed constructing a g-factor using a principal component analysis based on 5 different cognitive tests tapping into different cognitive domains namely the delayed recall score of the 15-Word Learning Test, Stroop interference Test, Letter-Digit Substitution Task, Word Fluency Test, and the Purdue Pegboard test.[25] The explained variance was 50.4 %.

Other measurements

Cardiovascular risk factors (systolic and diastolic blood pressure, serum and HDL-cholesterol, medication use, smoking, diabetes) were assessed based on information derived from home interviews and physical examinations during the center visit as previously described.[15] We used the validated Dutch version of the Center for Epidemiology Depression Scale (CES-D) for assessment of depressive symptoms.[26] More details can be read in the online data supplement.

Statistical analysis

Associations of lung function and tract-specific diffusion measurements were evaluated using multivariable linear regression models. Z-scores and 95% confidence intervals (CI) of tract-specific diffusion-MRI measures were estimated per unit increase of lung function parameters. Also, the g-factor was estimated per unit increase of lung function measures using multivariable linear regression models. We furthermore assessed the relation between tract-specific diffusion-MRI measures and global cognition (g-factor) stratified based on COPD status. Analyses were adjusted for age, sex, intracranial vol-

ume, tract-specific white matter volume, log-transformed tract-specific WMH volume, CES-D score, smoking and other cardiovascular risk factors such as blood pressure, serum cholesterol, HDL-cholesterol, diabetes, antihypertensive medication and lipid-lowering medication. Since the cerebellum could not always be fully incorporated in the diffusion scan, leading to varying coverage of one of the 15 tracts (medial lemniscus), we additionally controlled for the varying field of view in the tract-specific analyses of the medial lemniscus, by treating this as a potential confounder.[22]
Missing covariates (< 2%) for all covariates were imputed using multiple imputations creating 5 data sets according to the Markov Chain Monte Carlo method and pooled subsequently (IBM SPSS Statistics for Windows, version 21.0. Armonk, NY).

Sensitivity analysis
We performed a sensitivity analysis repeating the tract-specific analysis with exclusion of all persons with COPD. We performed this analysis to investigate whether lung function measures within the normal range also associated with white matter microstructural damage. We also repeated the tract-specific analysis for FEV_1 and the diffusing capacity with the exclusion of the participants with a spirometry suggestive of a restrictive syndrome, to investigate whether the associations found with FEV1, diffusing capacity and white matter microstructure were driven by participants with a restrictive syndrome.
For the tract-specific analyses, we corrected the p-value (alpha level of 0.05) for multiple comparisons by estimating the number of independent tests by using the variance of the eigenvalues of the correlation matrix of the 33 variables used in the main analysis (FEV_1, DL_{COc}, COPD and FA and MD for the 15 tracts) with the following formula: M_{eff}= 1 +(M-1)(1-var (λ_{obs})/M) with M is number of variables, M_{eff} is the number of independent variables.[27,28] Based on this formula M_{eff} was 20.534. Afterwards, using the Šidák formula: α sidak = 1 - ((1 - α)^(1/M_{eff})) we calculated a significance level of p< 0.0025.[27] All analyses were carried out using R version 2.15.0.

RESULTS

Table 1 presents the characteristics of the study population. Mean age of the participants was 68.4 ± 9.0 years, and 52.6 % were women. Persons with COPD were older (mean age 69.8± 9.4), and more often used antihypertensive and lipid-lowering medication and had smoked significantly more pack-years than persons without COPD (median 31 ± 13.8-50.0 versus 12.1 ± 4.3-25.0).

Table 1. Population characteristics

Characteristic	n= 2,405
Age, years	68.4 (9.0)
Female	1,264 (52.6)
Systolic blood pressure, mmHg	142.1 (21.3)
Diastolic blood pressure, mmHg	83.1 (10.9)
Antihypertensive medication	865 (36.0)
Smoking	
Never	850
Former	1273
Current	282
Packyears in current and past smokers	15 (5.0-30.0)
Total cholesterol, mmol/l	5.5 (1.1)
HDL cholesterol, mmol/l	1.5 (0.4)
Lipid-lowering medication	687 (28.6)
Diabetes mellitus	327 (13.6)
CES-D score	12 (10.0-14.0)
COPD	363 (15.7)
GOLD A	186 (8.2)
GOLD B	114 (5.0)
GOLD C	11 (0.5)
GOLD D	20 (0.9)
FEV_1, L	2.7 (0.80)
$DL_{CO,c}$, mmol/min/kPa/L	1.5 (0.24)
Intracranial volume, mL	1141.6 (115.9)
White matter volume, mL	396.5 (58.9)
White matter hyperintensities volume, mL	3.42 (1.8-7.3)

Categorical variables are presented as numbers (percentages), continuous variables as means (standard deviations) and packyears, CES-D score and white matter lesions volume are presented as median(interquartile range). The following variables had missing data: $DL_{CO,c}$ (n=280), COPD classification (n=91), COPD GOLD classification (n=32)

Abbreviations: COPD: chronic obstructive pulmonary disease; GOLD: Global initiative for chronic Obstructive Lung Disease criteria; FEV_1: forced expiratory volume during the first second; $DL_{CO,c}$: diffusing capacity of the lungs using carbon monoxide corrected for the haemoglobin concentration; HDL: high-density lipoprotein; CES-D: Center for Epidemiology Depression Scale.

White matter tract-specific analysis

Figure 1 and **Table 2** present the association of lung function (FEV_1, diffusing capacity), and COPD status with tract-specific diffusion-MRI measures (FA, MD) after adjusting for age, sex, macrostructural MRI markers, CES-D score, smoking, and other cardiovascular risk factors. A higher FEV_1 and a higher diffusing capacity were associated with higher FA and lower MD throughout the brain, but most prominently in the association tracts (**Figure 2**). For FEV_1, the mean difference in FA (z-score) in the association tracts per

liter increase of FEV_1 ranged from 0.07 (CI:0.00;0.13) to 0.09 (CI: 0.03;0.15), the mean difference in MD (z-score) in the association tracts ranged from -0.06 (CI: -0.11;-0.01) to -0.10 (CI: -0.15;-0.04). For the diffusing capacity, the mean difference in FA (z-score) in the association tracts per unit increase of the diffusing capacity ranged from 0.21 (CI: 0.06;0.35) to 0.29 (CI:0.14;0.44), the mean difference in MD (z-score) ranged from -0.27 (CI: -0.39;-0.14) to -0.32 (CI: -0.46;-0.18). We found no statistically significant differences in white matter microstructure comparing persons with and without COPD (**Table 2**).

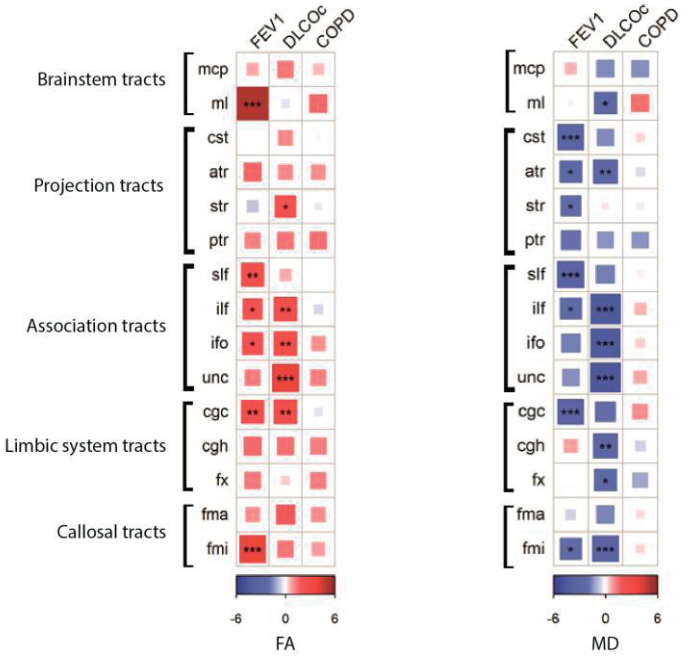

Figure 1. Association of lung function measures and tract-specific diffusion-MRI measures. Colors reflect t-values of the linear regression model per unit increase of the lung function marker after adjustments for age, sex, macrostructural MRI markers, CES-D, score, smoking pack-years and other cardiovascular risk factors. Higher strength of association is depicted in darker red for positive associations, darker blue for negative associations.

Abbreviations: *MCP: middle cerebellar peduncle, ML: medial lemniscus, CST: cortico-spinal tract, ATR: anterior thalamic radiation, STR: superior thalamic radiation, PTR: posterior thalamic radiation, SLF: superior longitudinal fasciculus, ILF: inferior longitudinal fasciculus, IFO: inferior-fronto-occipital fasciculus, UNC: uncinate fasciculus, CGC: cingulate gyrus part of cingulum, CGH: parahippocampal part of cingulum, FMA: forceps major, FMI: forceps minor. FA: fractional anisotropy, MD: mean diffusivity, FEV_1: forced expiratory volume in one second, DLCOc: diffusing capacity, COPD: chronic obstructive pulmonary disease, FA: fractional anisotropy, MD: mean diffusivity, CES-D: Center for Epidemiology Depression Scale.*

*p<0.05 **p<0.01 ***p<0.0025

Table 2. Lung function and tract-specific diffusion-MRI measures of white matter microstructural integrity

	Fractional anisotropy			Mean diffusivity		
	FEV_1	**DL_{COc}**	**COPD**	**FEV_1**	**DL_{COc}**	**COPD**
Brain stem tracts						
Middle cerebellar peduncle	0.03 (-0.04;0.10)	0.12 (-0.06;0.29)	0.03 (-0.08;0.14)	0.02 (-0.05;0.09)	-0.12 (-0.29;0.04)	-0.07 (-0.18;0.03)
Medial lemniscus [a]	**0.17 (0.10;0.23)***	-0.03 (-0.18;0.13)	0.08 (-0.02;0.17)	-0.01 (-0.08;0.07)	**-0.23 (-0.42;-0.05)**	0.09 (-0.03;0.20)
Projection tracts						
Corticospinal tract	0.00 (-0.07;0.07)	0.10 (-0.08;0.28)	0.01 (-0.10;0.12)	**-0.09 (-0.15;-0.04)***	-0.10 (-0.23;0.04)	0.01 (-0.07;0.10)
Anterior thalamic radiation	0.05 (-0.01;0.10)	0.07 (-0.06;0.20)	0.05 (-0.04;0.13)	**-0.04 (-0.08;-0.01)**	**-0.13 (-0.22;-0.04)**	-0.01 (-0.07;0.05)
Superior thalamic radiation	-0.02 (-0.09;0.04)	**0.19 (0.03;0.35)**	-0.01 (-0.11;0.09)	**-0.06 (-0.13;0.00)**	0.02 (-0.14;0.18)	-0.01 (-0.11;0.08)
Posterior thalamic radiation	0.04 (-0.02;0.10)	0.11 (-0.04;0.25)	0.07 (-0.02;0.16)	-0.05 (-0.11;0.00)	-0.09 (-0.23;0.04)	-0.06 (-0.14;0.03)
Association tracts						
Superior longitudinal fasciculus	**0.09 (0.03;0.15)**	0.05 (-0.10;0.21)	0.00 (-0.10;0.09)	**-0.10 (-0.15;-0.04)***	-0.11 (-0.24;0.02)	0.01 (-0.08;0.09)
Inferior longitudinal fasciculus	**0.07 (0.00;0.13)**	**0.22 (0.06;0.38)**	-0.02 (-0.12;0.07)	**-0.06 (-0.11;-0.01)**	**-0.29 (-0.41;-0.16)***	0.03 (-0.05;0.11)
Inferior fronto-occipital fasciculus	**0.07 (0.01;0.13)**	**0.21 (0.06;0.35)**	0.05 (-0.04;0.13)	-0.04 (-0.09;0.01)	**-0.27 (-0.39;-0.14)***	0.02 (-0.06;0.09)
Uncinate fasciculus	0.04 (-0.02;0.10)	**0.29 (0.14;0.44)***	0.06 (-0.03;0.15)	-0.04 (-0.10;0.02)	**-0.32 (-0.46;-0.18)***	0.04 (-0.05;0.12)
Limbic system tracts						
Cingulate gyrus part of cingulum	**0.09 (0.03;0.16)**	**0.24 (0.07;0.41)**	-0.02 (-0.12;0.09)	**-0.12 (-0.19;-0.05)***	-0.17 (-0.34;0.00)	0.06 (-0.05;0.17)
Parahippocampal part of cingulum	0.05 (-0.01;0.12)	0.12 (-0.04;0.29)	0.07 (-0.03;0.17)	0.03 (-0.04;0.11)	**-0.26 (-0.44;-0.08)**	-0.03 (-0.14;0.08)
Fornix	0.05 (-0.02;0.11)	0.03 (-0.13;0.20)	0.07 (-0.04;0.17)	0.00 (-0.05;0.05)	**-0.14 (-0.25;-0.02)**	-0.04 (-0.11;0.03)
Callosal tracts						
Forceps major	0.03 (-0.03;0.08)	0.13 (-0.01;0.26)	0.04 (-0.04;0.13)	-0.02 (-0.07;0.04)	-0.11 (-0.25;0.03)	0.01 (-0.07;0.10)
Forceps minor	**0.11 (0.05;0.16)***	0.09 (-0.04;0.23)	0.04 (-0.05;0.12)	**-0.08 (-0.14;-0.01)**	**-0.26 (-0.42;-0.11)***	0.02 (-0.08;0.11)

Data are presented as differences in Z-scores of tract-specific diffusion-MRI measures (95% CI). Results in bold were significant after $p<0.05$. Results in bold and * were significant after correction for multiple testing ($p<0.0025$). Adjusted for age, sex, intracranial volume, WM and log-transformed WMH volumes of the investigated tract, and additionally for CES-D score, smoking pack-years and other cardiovascular risk factors (systolic blood pressure, diastolic blood pressure, antihypertensive medication, serum cholesterol, HDL-cholesterol, lipid lowering medication, diabetes).

Abbreviations: COPD: chronic obstructive pulmonary disease; FEV_1: forced expiratory volume during the first second in l; DL_{COc}= diffusing capacity of the lungs using carbon monoxide corrected for the haemoglobin concentration; CI: confidence interval; WM: white matter; WMH: white matter hyperintensities; CES-D: Center for Epidemiology Depression Scale.

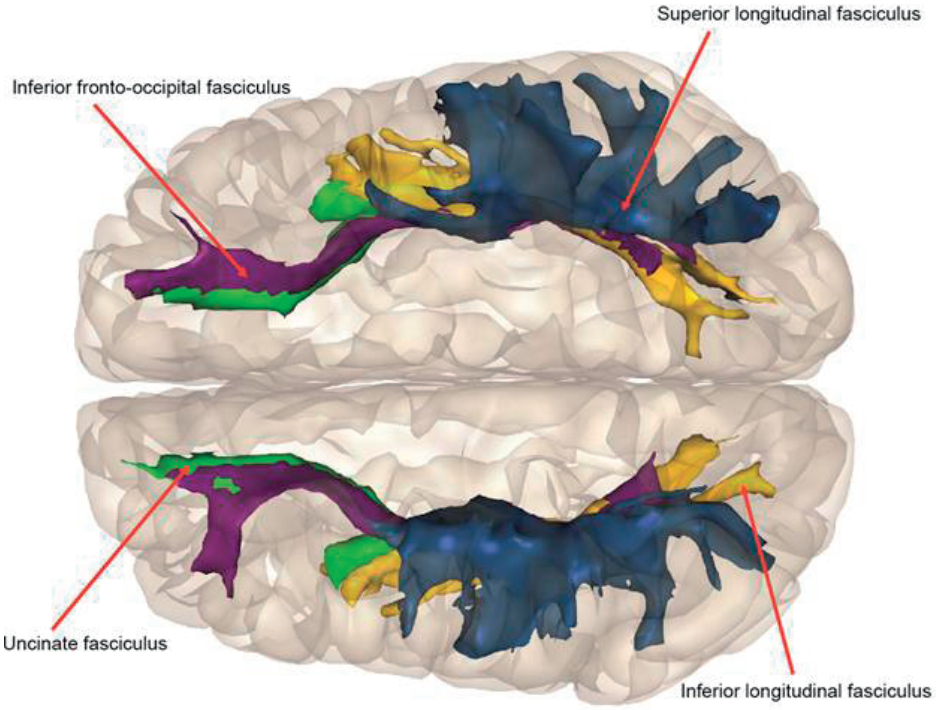

Figure 2. Overview of the association tracts (top view)

Voxel-based analysis

In the voxel-based analyses, a higher FEV_1 associated with both a higher FA and a lower MD in voxels of the corticospinal tract, anterior thalamic radiation, superior thalamic radiation, (all projection tracts), inferior longitudinal fasciculus (association tract), forceps major (callosal tract), and with the cingulate gyrus (limbic system tract). Furthermore, a higher FEV_1 associated with a lower MD in voxels of the posterior thalamic radiation (projection tract), superior longitudinal fasciculus, inferior fronto-occipital fasciculus, uncinate fasciculus (all association tracts), and with voxels of the forceps minor (callosal tract) (**Figure 3, panel A and B, Supplementary Table 3**).

A higher diffusing capacity associated with a higher FA in voxels in periventricular and subcortical white matter, and with a lower MD in subcortical white matter (**Figure 3, panel C and D**). However, these voxels did not belong to one of the predefined tracts of the anatomical template. We found no voxels significantly associated with COPD (**Supplementary Table 3**).

Table 3 presents the results for the association between COPD severity based on the 2013 GOLD classification and mean diffusivity after adjusting for age, sex, macro-structural MRI markers, CES-D score, smoking and other cardiovascular risk factors. We observed that persons with severe COPD (GOLD group D) compared to persons

without COPD had poorer tract-specific microstructural integrity throughout the brain, again most prominently in the association tracts.

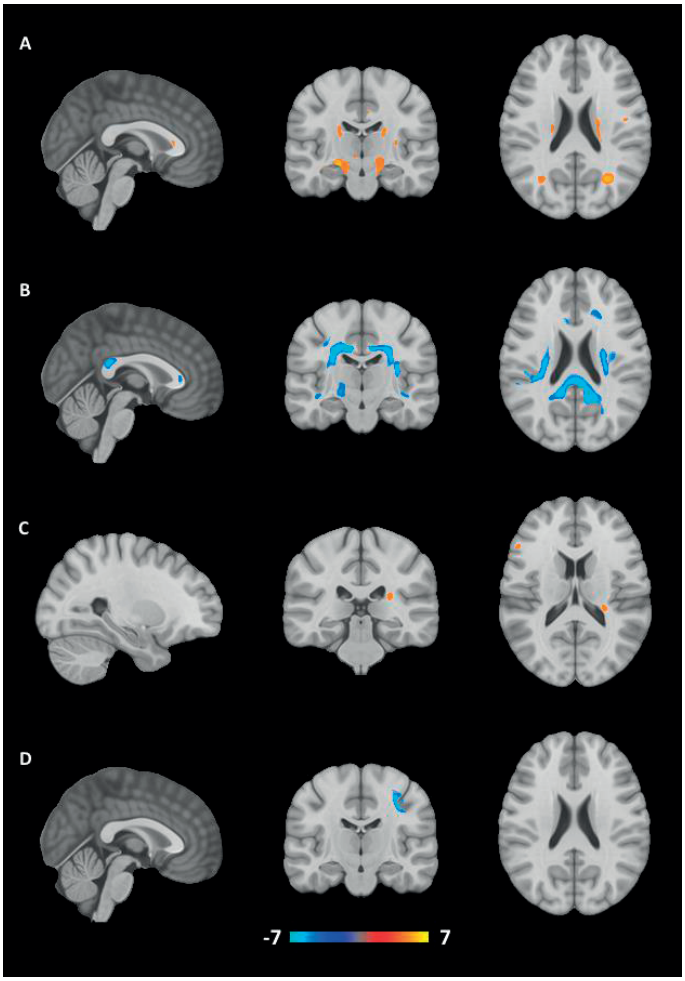

Figure 3. Association of lung function measures and voxel-wise diffusion-MRI measures. (voxel-wise linear regression analysis) with adjustments for age, sex, macrostructural MRI markers, CES-D score, smoking pack-years and other cardiovascular risk factors). P-value threshold for significance was defined based on permutation tests. Significant voxels (for FA $p< 5.91 \times 10^{-8}$ for MD $p< 6.49 \times 10^{-8}$) are color-coded. Colors reflect t-values and higher strength of association is depicted in darker red/yellow for positive associations, lighter blue for negative associations. Significant voxels cluster mainly in association and projection tracts.
Panel A: Association of FEV_1 and voxel-wise fractional anisotropy.
Panel B: Association of FEV_1 and voxel-wise mean diffusivity.
Panel C: Association of diffusing capacity and voxel-wise fractional anisotropy.
Panel D: Association of diffusing capacity and voxel-wise mean diffusivity.

Table 3. COPD severity and tract-specific diffusion-MRI measures of white matter microstructural integrity

Mean diffusivity				
	GOLD A	**GOLD B**	**GOLD C**	**GOLD D**
Brainstem tracts				
Middle cerebellar peduncle	-0.04 (-0.18;0.09)	-0.05 (-0.21;0.12)	0.27 (-0.24;0.78)	0.01 (-0.37;0.39)
Medial lemniscus	0.02 (-0.13;0.17)	0.13 (-0.06;0.32)	0.31 (-0.27;0.89)	**0.62 (0.18;1.06)**
Projection tracts				
Corticospinal tract	-0.02(-0.13;0.09)	0.07 (-0.04;0.15)	0.10 (-0.31;0.51)	0.39 (0.08;0.71)
Anterior thalamic radiation	-0.04 (-0.11;0.03)	0.05 (-0.04;0.15)	-0.25 (-0.53;0.03)	0.08 (-0.13;0.30)
Superior thalamic radiation	-0.03 (-0.16;0.09)	0.04 (-0.12;0.20)	-0.06 (-0.54;0.42)	0.18 (-0.18;0.54)
Posterior thalamic radiation	-0.03 (-0.14;0.08)	-0.07 (-0.21;0.06)	0.03 (-0.39;0.45)	0.10 (-0.21;0.42)
Association tracts				
Superior longitudinal fasciculus	-0.04 (-0.14;0.07)	0.03 (-0.11;0.16)	-0.09 (-0.52;0.35)	**0.49 (0.18;0.80)***
Inferior longitudinal fasciculus	0.02 (-0.08;0.12)	-0.01 (-0.14;0.12)	0.23 (-0.17;0.62)	**0.37 (0.07;0.67)**
Inferior fronto-occipital fasciculus	0.00 (-0.10;0.11)	0.05 (-0.08;0.17)	-0.11 (-0.49;0.28)	**0.36 (0.08;0.66)**
Uncinate fasciculus	-0.02 (-0.13;0.10)	0.10 (-0.04;0.25)	-0.19 (-0.64;0.26)	**0.48 (0.14;0.81)**
Limbic system tracts				
Cingulate gyrus part of cingulum	0.02 (-0.12;0.15)	0.09 (-0.09;0.26)	-0.25 (-0.79;0.28)	**0.69 (0.28;1.09)***
Parahippocampal part of cingulum	-0.01 (-0.15;0.14)	-0.03 (-0.21;0.15)	-0.01 (-0.57;0.55)	0.01 (-0.42;0.43)
Fornix	-0.03 (-0.12;0.06)	0.00 (-0.11;0.11)	-0.06 (-0.40;0.29)	-0.07 (-0.34;0.20)
Callosal tracts				
Forceps major	0.03 (-0.08;0.14)	0.00 (-0.14;0.14)	0.11 (-0.32;0.54)	0.11 (-0.22;0.43)
Forceps minor	0.00 (-0.13;0.12)	0.01 (-0.17;0.14)	-0.09 (-0.57;0.40)	**0.48 (0.11;0.84)**

Data are presented as differences in Z-scores of tract-specific diffusion-MRI measures (95% CI). Results in bold were significant after $p<0.05$. Results in bold and * were significant after correction for multiple testing ($p<0.0025$). Adjusted for age, sex, intracranial volume, WM and log-transformed WMH volumes of the investigated tract and additionally adjusted for CES-D score, smoking pack-years and other cardiovascular risk factors (systolic blood pressure, diastolic blood pressure, antihypertensive medication, serum cholesterol, HDL-cholesterol, lipid lowering medication, diabetes).

Abbreviations: GOLD:Global Initiative for Chronic Obstructive Lung Disease criteria; CI: confidence interval; WM: white matter; WMH: white matter hyperintensities; CES-D: Center for Epidemiology Depression Scale; HDL: high-density lipoprotein.

Global cognition

Table 4 presents the results of the association between lung function (FEV_1, diffusing capacity), COPD and global cognition. Higher lung function measures associated with a better global cognition. Per liter increase of FEV_1, the g-factor increased: β (95% CI) 0.19 (0.13;0.26). Per unit increase of the diffusing capacity the g-factor increased with β (95% CI): 0.18 (0.02;0.35), after adjustments for after adjusting for age, sex, intracranial volume, CES-D score, smoking, and other cardiovascular risk factors. Participants with COPD had a lower global cognition: β (95% CI) -0.11 (-0.21;0.00). **Table 5** presents the results of the association between tract-specific mean diffusivity and global cognition stratified based on COPD status Though formal interaction

was absent (**Supplementary Table 1**), the link between white matter microstructural integrity and global cognition seemed stronger in persons with COPD versus persons without COPD.

Table 4. Association of lung function and global cognition (g-factor)

Variable	G-factor Model 1 β (95% CI)	G-factor Model 2 β (95% CI)
fev	0.25 (0.18;0.31)	0.19 (0.13;0.26)
DL_{COc}	0.24 (0.08;0.40)	0.18 (0.02;0.35)
COPD	-0.18 (-0.28;-0.08)	-0.11 (-0.21;0.00)

Values represent the mean differences (95% CI) of the g-factor per unit increase of lung function parameters. Model I: Adjusted for age, sex, intracranial volume. Model II: Model I and additionally for CES-D score, smoking pack-years and other cardiovascular risk factors (systolic blood pressure, diastolic blood pressure, antihypertensive medication, serum cholesterol, HDL-cholesterol, lipid lowering medication, diabetes).
Abbreviations: COPD: Chronic Obstructive Pulmonary disease; CI: confidence interval; DL_{COc}= diffusing capacity of the lungs using carbon monoxide corrected for the haemoglobin concentration; FEV_1: forced expiratory volume during the first second in l; DL_{COc}= diffusing capacity of the lungs using carbon monoxide corrected for the haemoglobin concentration. WM: white matter; WMH: white matter hyperintensities;

Sensitivity analysis

We repeated the tract-specific analysis with exclusion of all participants with COPD. Reduced lung function within the normal range associated with tract-specific microstructural damage throughout the brain, but again most prominently in the association tracts. The estimates changed only slightly compared to the analysis including persons with COPD, however some of the associations were not (*statistically*) significant anymore upon multiple comparisons correction (**Supplementary Table 2**).

We furthermore repeated the tracts-specific analysis with FEV_1 and the diffusing capacity as determinant, with the exclusion of all participants with a spirometry suggestive of a restrictive syndrome (N=91). The estimates did not change substantially. However, again, some of the associations were not statistically significant anymore (**Supplementary Table 3).**

Table 5. Tract-specific mean diffusivity and global cognition (g-factor)

	Model I		Model II	
	G-factor in COPD +	**G-factor in COPD –**	**G-factor in COPD +**	**G-factor in COPD -**
Brainstem tracts				
Middle cerebellar peduncle	-0.05 (-0.15;0.06)	0.01 (-0.04;0.05)	-0.05 (-0.15;0.05)	0.00 (-0.05;0.04)
Medial lemniscus	-0.07 (-0.17;0.02)	0.00 (-0.04;0.04)	-0.06 (-0.15;0.04)	0.00 (-0.04;0.04)
Projection tracts				
Corticospinal tract	**-0.23 (-0.36;-0.10)***	**-0.08 (-0.14;-0.02)**	**-0.21 (-0.35;-0.07)**	**-0.06 (-0.12;0.00)**
Anterior thalamic radiation	**-0.28 (-0.49;-0.08)**	**-0.16 (-0.25;-0.07)***	**-0.27 (-0.47;-0.07)**	**-0.15 (-0.23;-0.06)***
Superior thalamic radiation	**-0.32 (-0.54;-0.11)**	**-0.11 (-0.19;-0.02)**	**-0.27 (-0.47;-0.06)**	-0.08 (-0.17;0.01)
Posterior thalamic radiation	-0.13 (-0.27;0.00)	-0.05 (-0.10;0.01)	-0.12 (-0.25;0.01)	-0.04 (-0.10;0.01)
Association tracts				
Superior longitudinal fasciculus	**-0.14 (-0.28;-0.01)**	**-0.07 (-0.12;-0.01)**	-0.13 (-0.26;0.01)	-0.05 (-0.11;0.00)
Inferior longitudinal fasciculus	-0.11 (-0.24;0.03)	**-0.11 (-0.17;-0.06)***	-0.10 (-0.23;0.03)	**0.10 (0.16;0.04)***
Inferior fronto-occipital fasciculus	-0.10 (-0.23;0.03)	**-0.10 (-0.15;-0.04)***	-0.11 (-0.24;0.03)	**-0.08 (-0.14;-0.03)***
Uncinate fasciculus	**-0.14 (-0.25;-0.02)**	**-0.10 (-0.15;-0.05)***	-0.12 (-0.24;0.00)	**-0.09 (-0.14;-0.04)***
Limbic system tracts				
Cingulate gyrus part of cingulum	**-0.14 (-0.24;-0.04)**	**-0.07 (-0.11;-0.03)***	**-0.13 (-0.23;-0.03)**	**-0.06 (-0.10;-0.01)**
Parahippocampal part of cingulum	-0.06 (-0.17;0.04)	**-0.06 (-0.10;-0.02)**	-0.06 (-0.16;0.04)	**-0.06 (-0.10;-0.02)**
Fornix	**-0.21 (-0.38;-0.04)**	-0.07 (-0.13;0.00)	**-0.19 (-0.36;-0.03)**	-0.06 (-0.13;0.01)
Callosal tracts				
Forceps major	-0.04 (-0.17;0.09)	-0.05 (-0.10;0.01)	-0.07 (-0.20;0.05)	-0.04 (-0.10;0.01)
Forceps minor	**-0.13 (-0.25;-0.01)**	**-0.11 (-0.16;-0.06)***	-0.11 (-0.21;0.01)	**-0.10 (-0.15;-0.05)***

Values represent the mean differences in g-factor (95% CI) per SD increase of mean diffusivity. Results in bold were significant after $p<0.05$. Results in bold and * were significant after correction for multiple testing ($p<0.0027$). Model I is adjusted for age, sex, intracranial volume, WM and log-transformed WMH volumes of the investigated tract. Model II is model I, and additionally adjusted for CES-D score, smoking pack-years and other cardiovascular risk factors (systolic blood pressure, diastolic blood pressure, antihypertensive medication, serum cholesterol, HDL-cholesterol, lipid lowering medication, diabetes).

DISCUSSION

We showed that in middle aged and elderly persons reduced lung function (even within the normal range) indicated by a lower FEV_1 and a lower diffusing capacity was related to lower FA and higher MD indicating a reduced microstructural integrity throughout the brain. More specifically, among the 15 white matter tracts examined, reduced lung function most strongly associated with poorer tract-specific white matter microstructure in the association tracts. We observed significant differences in white matter microstructure, again mainly in the associations tracts, comparing persons with *severe* COPD classified as GOLD D to persons without COPD. In the voxel-based analyses, FEV_1 most strongly associated with the microstructure of the voxels of association and projection tracts. All associations were independent from age, sex, macrostructural white matter pathology, CES-D score, smoking pack-years and other cardiovascular risk factors. We also found that the link between white matter microstructural integrity and global cognition seemed stronger among COPD patients than in persons without COPD, however there was no significant interaction on the multiplicative scale.

Research focusing on the relation of lung function and cerebral white matter microstructural integrity using diffusion-MRI is limited. In line with our results, a previous study showed reduced white matter integrity throughout the brain in 25 COPD patients compared to 25 controls.[29] However, the differences in white matter microstructural damage between these COPD patients and controls were no longer significant after adjustments for smoking, cerebrovascular comorbidity and cognition. Two other diffusion-MRI studies, using a voxel-based approach concluded that COPD could affect white matter microstructural integrity mainly in frontoparietal periventricular white matter,[13] mainly in the visual cortex of the occipital lobe, the posterior part of the parietal lobe as well in the temporal lobe.[14] However, differences between COPD cases and controls were not statistically significant, which might be due to the small number of participants in these studies.

The pathophysiology of white matter damage in persons with COPD is not fully elucidated. Possible mechanisms are neuronal damage caused by free radicals generated in chronic hypoxia.[30] Furthermore metabolic decreases and decline of cerebral perfusion due to hypoxia may cause morphologic brain changes.[12] Another possible mechanism is systemic inflammation which may induce chronic inflammation in the vascular wall contributing to both microvascular and macrovascular damage.[31] However, it is not known to what extent these mechanisms can also explain the association we found between reduced lung function parameters within the normal range and poorer white matter microstructure.

The main novelty of our paper is that we investigated the association between lung function measures (spirometry and diffusing capacity) as well as COPD and white

matter microstructure of functionally different white matter tracts obtained with tractography, but also on a voxel-wise level. In the tract-specific analysis, we showed that a lower FEV_1 and lower diffusing capacity had a varying effect on different white matter tracts, and were associated with a lower microstructural integrity in particular of the association tracts. In our study we did not find significant associations comparing participants with and without COPD and only observed significant differences in white matter microstructure comparing persons with *severe* COPD to persons without COPD. This may be explained by the fact that this is a population-based study in which most persons classified as having COPD only have mild COPD. Also, as a consequence of this population-based setting only 20 COPD patients were classified as GOLD D. In this GOLD D group we observed significant differences in white matter microstructure (mainly in the association tracts) compared to persons without COPD. This finding, together with the fact that the strongest associations between diffusing capacity and white matter microstructure are seen in the association tracts, points toward hypoxia/ischemia as a plausible underlying mechanism. Another underlying mechanism explaining why persons with COPD GOLD D have a poorer white matter microstructure compared to persons without COPD, may be that persons with severe COPD (GOLD D) have a high exacerbation rate (2 or more/year) and it is possible that in particular these exacerbations may cause brain changes, since especially exacerbations of COPD have been correlated with cognitive decline.[32-34] However, it must be noted that in our study only 20 participants with COPD were classified as GOLD D.

For MD, we found similar results with FEV_1 and white matter microstructure comparing the results of the tract-specific analysis with the voxel-based analysis. For FA, however, we found in the tract-specific analysis different significant associations between FEV_1 and white matter microstructure compared to the voxel-based analysis (mainly no significant associations with the projection tracts, but more significant associations with the associations tracts and callosal tracts). Furthermore, for both FA and MD, we found in the tract-specific analysis with diffusing capacity significant associations, in particular in the association tracts, and there we no significant associations in the voxel-based analysis. Explanations for these differences may be that by averaging positive and negative voxels, as we did in the tract-specific analysis, significant associations can go undetected. On the other hand, a major downside of exploring associations on a voxel-wise level is multiple comparisons corrections, making this method less sensitive to very small changes. Therefore, we chose to conduct both methods and present them in parallel, as we feel they convey complementary information.

Different white matter tracts have a variable susceptibility to decline,[35,36] possibly caused by the location of different tracts. Association tracts connect different cortical regions of the same hemisphere and arise in watershed areas which means that

their blood supply relies on small and deep lenticulostriate arteries. Association tracts may therefore be more vulnerable to insult and vascular damage.[16] This is in line with previous studies which showed that COPD patients are particularly prone to vascular damage.[37] Association tracts, but also the projection tracts play a critical role in cognitive performance.[38] Poor white matter microstructural integrity of these tracts may therefore be an important link between COPD and cognitive impairment.

Strengths of our study include the population-based design, the large sample size and the ability to control for several potential confounders due to the availability of extensive data on cardiovascular risk factors and macrostructural MRI-markers. We performed a tract-specific analysis in 15 main white matter tracts, and, the tract-specific measurements were performed with fully automated, publicly available methods.[39] Furthermore, we also included a voxel-based analysis. However, also some limitations should be acknowledged. Due to the cross-sectional design, no conclusions can be drawn on the directionality of causality of the associations.. We used mean FA and MD aggregated over each white matter tract eventually missing some spatial information which is retained in voxel-based techniques. Also, tractography in general is influenced by crossing fiber regions, possibly resulting in unreliable diffusion-MRI measures in some areas, in particular for fractional anisotropy.[40] The cerebellum could not be fully incorporated in the field of view, making analyses on brain stem tracts less reliable. Furthermore, we cannot exclude residual confounding, even with adjustments for the large number of potential confounders performed in our analyses. Finally, only a very small proportion of our participants presented with clinically abnormal lung function and only 20 COPD patients were classified as GOLD D.

In conclusion, we show that tract-specific diffusion-MRI parameters and voxel-based analyses provide additional insight into the association between reduced lung function and the patterns of microstructural white matter damage beyond global diffusion-MRI parameters. We found that persons with reduced lung function (even within the normal range) have more regional microstructural white matter damage, especially in the association tracts. Further studies should evaluate whether cognitive impairment in COPD patients is mediated through poorer regional white matter microstructural integrity.

CHAPTER REFERENCES

1. Brusselle GG, Joos GF, Bracke KR. New insights into the immunology of chronic obstructive pulmonary disease. *Lancet.* 2011;378(9795):1015-1026.
2. Dalal AA, Shah M, Lunacsek O, Hanania NA. Clinical and economic burden of patients diagnosed with COPD with comorbid cardiovascular disease. *Respir Med.* 2011;105(10):1516-1522.
3. Xu W, Collet JP, Shapiro S, et al. Independent effect of depression and anxiety on chronic obstructive pulmonary disease exacerbations and hospitalizations. *Am J Respir Crit Care Med.* 2008;178(9):913-920.
4. Laurin C, Moullec G, Bacon SL, Lavoie KL. Impact of anxiety and depression on chronic obstructive pulmonary disease exacerbation risk. *Am J Respir Crit Care Med.* 2012;185(9):918-923.
5. Liao KM, Ho CH, Ko SC, Li CY. Increased Risk of Dementia in Patients With Chronic Obstructive Pulmonary Disease. *Medicine (Baltimore).* 2015;94(23):e930.
6. Borson S, Scanlan J, Friedman S, et al. Modeling the impact of COPD on the brain. *Int J Chron Obstruct Pulmon Dis.* 2008;3(3):429-434.
7. Taki Y, Kinomura S, Ebihara S, et al. Correlation between pulmonary function and brain volume in healthy elderly subjects. *Neuroradiology.* 2013;55(6):689-695.
8. Zhang H, Wang X, Lin J, et al. Reduced regional gray matter volume in patients with chronic obstructive pulmonary disease: a voxel-based morphometry study. *AJNR Am J Neuroradiol.* 2013;34(2):334-339.
9. Wang C, Ding Y, Shen B, et al. Altered Gray Matter Volume in Stable Chronic Obstructive Pulmonary Disease with Subclinical Cognitive Impairment: an Exploratory Study. *Neurotox Res.* 2016.
10. van Dijk EJ, Vermeer SE, de Groot JC, et al. Arterial oxygen saturation, COPD, and cerebral small vessel disease. *J Neurol Neurosurg Psychiatry.* 2004;75(5):733-736.
11. Spilling CA, Jones PW, Dodd JW, Barrick TR. White matter lesions characterise brain involvement in moderate to severe chronic obstructive pulmonary disease, but cerebral atrophy does not. *BMC Pulm Med.* 2017;17(1):92.
12. Antonelli Incalzi R, Marra C, Giordano A, et al. Cognitive impairment in chronic obstructive pulmonary disease--a neuropsychological and spect study. *J Neurol.* 2003;250(3):325-332.
13. Ryu CW, Jahng GH, Choi CW, et al. Microstructural change of the brain in chronic obstructive pulmonary disease: a voxel-based investigation by MRI. *COPD.* 2013;10(3):357-366.
14. Zhang H, Wang X, Lin J, et al. Grey and white matter abnormalities in chronic obstructive pulmonary disease: a case-control study. *BMJ Open.* 2012;2(2):e000844.
15. Hofman A, Brusselle GG, Darwish Murad S, et al. The Rotterdam Study: 2016 objectives and design update. *Eur J Epidemiol.* 2015;30(8):661-708.
16. Rosano C, Abebe KZ, Aizenstein HJ, et al. Longitudinal systolic blood pressure characteristics and integrity of white matter tracts in a cohort of very old black and white adults. *Am J Hypertens.* 2015;28(3):326-334.
17. Hofman A, Brusselle GG, Darwish Murad S, et al. The Rotterdam Study: 2016 objectives and design update. *Eur J Epidemiol.* 2015;28(11):889-926.
18. Ikram MA, van der Lugt A, Niessen WJ, et al. The Rotterdam Scan Study: design update 2016 and main findings. *Eur J Epidemiol.* 2015;30(12):1299-1315.
19. Lahousse L, Vernooij MW, Darweesh SK, et al. Chronic obstructive pulmonary disease and cerebral microbleeds. The Rotterdam Study. *Am J Respir Crit Care Med.* 2013;188(7):783-788.
20. Celli BR, MacNee W, Force AET. Standards for the diagnosis and treatment of patients with COPD: a summary of the ATS/ERS position paper. *Eur Respir J.* 2004;23(6):932-946.

21. Macintyre N, Crapo RO, Viegi G, et al. Standardisation of the single-breath determination of carbon monoxide uptake in the lung. *Eur Respir J.* 2005;26(4):720-735.
22. de Groot M, Ikram MA, Akoudad S, et al. Tract-specific white matter degeneration in aging: the Rotterdam Study. *Alzheimers Dement.* 2015;11(3):321-330.
23. Ashburner J, Friston KJ. Voxel-based morphometry--the methods. *Neuroimage.* 2000;11(6 Pt 1):805-821.
24. Roshchupkin GV, Adams HH, van der Lee SJ, et al. Fine-mapping the effects of Alzheimer's disease risk loci on brain morphology. *Neurobiol Aging.* 2016;48:204-211.
25. Hoogendam YY, Hofman A, van der Geest JN, van der Lugt A, Ikram MA. Patterns of cognitive function in aging: the Rotterdam Study. *Eur J Epidemiol.* 2014;29(2):133-140.
26. Mirza SS, de Bruijn RF, Direk N, et al. Depressive symptoms predict incident dementia during short- but not long-term follow-up period. *Alzheimers Dement.* 2014;10(5 Suppl):S323-S329 e321.
27. Galwey NW. A new measure of the effective number of tests, a practical tool for comparing families of non-independent significance tests. *Genet Epidemiol.* 2009;33(7):559-568.
28. Nyholt DR. A simple correction for multiple testing for single-nucleotide polymorphisms in linkage disequilibrium with each other. *Am J Hum Genet.* 2004;74(4):765-769.
29. Dodd JW, Chung AW, van den Broek MD, Barrick TR, Charlton RA, Jones PW. Brain structure and function in chronic obstructive pulmonary disease: a multimodal cranial magnetic resonance imaging study. *Am J Respir Crit Care Med.* 2012;186(3):240-245.
30. Sin DD, Man SF. Why are patients with chronic obstructive pulmonary disease at increased risk of cardiovascular diseases? The potential role of systemic inflammation in chronic obstructive pulmonary disease. *Circulation.* 2003;107(11):1514-1519.
31. Rocha VZ, Libby P. Obesity, inflammation, and atherosclerosis. *Nat Rev Cardiol.* 2009;6(6):399-409.
32. Zhang X, Cai X, Shi X, et al. Chronic Obstructive Pulmonary Disease as a Risk Factor for Cognitive Dysfunction: A Meta-Analysis of Current Studies. *J Alzheimers Dis.* 2016;52(1):101-111.
33. Dodd JW, Charlton RA, van den Broek MD, Jones PW. Cognitive dysfunction in patients hospitalized with acute exacerbation of COPD. *Chest.* 2013;144(1):119-127.
34. Ambrosini V, Cancellieri A, Chilosi M, et al. Acute exacerbation of idiopathic pulmonary fibrosis: report of a series. *Eur Respir J.* 2003;22(5):821-826.
35. Bender AR, Volkle MC, Raz N. Differential aging of cerebral white matter in middle-aged and older adults: A seven-year follow-up. *Neuroimage.* 2016;125:74-83.
36. Kochunov P, Williamson DE, Lancaster J, et al. Fractional anisotropy of water diffusion in cerebral white matter across the lifespan. *Neurobiol Aging.* 2012;33(1):9-20.
37. Lahousse L, van den Bouwhuijsen QJ, Loth DW, et al. Chronic obstructive pulmonary disease and lipid core carotid artery plaques in the elderly: the Rotterdam Study. *Am J Respir Crit Care Med.* 2013;187(1):58-64.
38. Cremers LG, de Groot M, Hofman A, et al. Altered tract-specific white matter microstructure is related to poorer cognitive performance: The Rotterdam Study. *Neurobiol Aging.* 2016;39:108-117.
39. de Groot M, Vernooij MW, Klein S, et al. Improving alignment in Tract-based spatial statistics: evaluation and optimization of image registration. *NeuroImage.* 2013;76:400-411.
40. Jeurissen B, Leemans A, Tournier JD, Jones DK, Sijbers J. Investigating the prevalence of complex fiber configurations in white matter tissue with diffusion magnetic resonance imaging. *Hum Brain Mapp.* 2013;34(11):2747-2766.

SUPPLEMENTAL MATERIAL

CHAPTER 2.5

Age-dependent association of thyroid function with brain morphology and microstructure

Lotte G.M. Cremers*, Layal Chaker*, Tim Korevaar, Marius de Groot, Abbas Dehghan, Oscar H. Franco, Wiro J. Niessen, M.Arfan Ikram, Robin P. Peeters, Meike W. Vernooij

Neurobiology of Aging 2018

**Denotes equal contribution*

ABSTRACT

Background Thyroid hormone (TH) is crucial during neurodevelopment but high levels of TH have been linked to neurodegenerative disorders. No data on the association of thyroid function with brain imaging in the general population are available.

Methods We therefore investigated the association of thyroid-stimulating hormone and free thyroxine (FT4) with MRI-derived total intracranial volume, brain tissue volumes and diffusion tensor imaging (DTI) measures of white matter microstructure in 4,683 dementia- and stroke-free participants (mean age 60.2, range 45.6-89.9 years).

Results Higher FT4 levels were associated with larger total intracranial volumes (β=6.73mL, 95% confidence interval 2.94-9.80). Higher FT4 levels were also associated with larger total brain and white matter volumes in younger individuals, but with smaller total brain and white matter volume in older individuals (p-interaction 0.02). There was a similar interaction by age for the association of FT4 with mean diffusivity on DTI (p-interaction 0.026).

Conclusions These results are in line with differential effects of TH during neurodevelopmental and neurodegenerative processes and can improve understanding of the role of thyroid function in neurodegenerative disorders.

INTRODUCTION

Thyroid hormone impacts different essential neuronal processes including neurogenesis, myelination, and neural differentiation in childhood and throughout adulthood.[1,2] Already during intrauterine neurodevelopment, thyroid hormone impacts on several processes including neuronal cell proliferation, differentiation and migration.[1,3] Suboptimal thyroid hormone availability during early life can have profound impact on brain function later in life. This is illustrated by the link between congenital hypothyroidism and cretinism, a condition characterized by severely impaired physical and mental development. Mild forms of both low and high thyroid function during the gestational period have been associated with a lower child IQ and differences in brain morphology during later life.[4]

However, the effects of thyroid hormone on the brain are age dependent because in addition to its effects during development, thyroid hormone is also related to neurodegeneration. In older adults, higher thyroid function has been associated with a higher risk of neurodegenerative disorders and poorer cognition.[5,6] A meta-analysis of cohort studies showed that higher thyroid function is associated with higher risk of cognitive impairment.[7] We previously described an increased risk of dementia with high-normal to high thyroid function and a protective effect of low and low-normal thyroid function.[8] This risk did not seem to be explained by cardiovascular risk factors or subclinical vascular brain damage. The underlying mechanisms explaining the link between thyroid function and dementia are yet unclear, but possible and yet unexplored pathways are through subclinical changes in microstructural organization or brain tissue atrophy.

Owing to the link with cognitive impairment, we hypothesized that thyroid hormone could have adverse effects on processes affecting brain volumes and white matter microstructure in older age. We also hypothesized that this effect could be age-dependent, due to the different effects of thyroid hormone during the neurodevelopmental period. Therefore, we investigated the association of thyroid function with intracranial brain volume (as a marker of development), total brain, white matter and grey matter volumes on MRI (as markers of neurodegeneration). Furthermore, we tested whether the association of thyroid function and diffusion tensor imaging (DTI) measures related to white matter microstructural organization were different in younger versus older participants.

METHODS

Setting

The study was performed in the context of the Rotterdam Study (RS), a prospective population-based cohort study that investigates determinants and occurrence of cardiovascular, neurological, ophthalmologic, psychiatric, and endocrine diseases in the middle-aged and elderly population. The aims and design of the Rotterdam Study have been described in detail elsewhere.[9] We included participants from three independent cohorts within the Rotterdam Study. The RS Cohort 1 (RSI) includes participants aged 55 years and older and baseline data were collected during 1990-1993. RS Cohort II (RSII) includes participants aged 55 years and older and baseline data were collected from 2000-2001. For the RS Cohort 3 (RSIII), persons included were aged 45 years and over and baseline data were collected from 2006 to 2008. Thyroid function assessment was determined in a random subset of 9,689 participants in all three cohorts and brain MRI was included in the core protocol of the Rotterdam Study since 2005. The study protocol was approved by the Medical Ethics Committee of the Erasmus University and by the Ministry of Health, Welfare and Sport of the Netherlands, implementing the "Wet Bevolkingsonderzoek: ERGO (Population Studies Act: Rotterdam Study)". All included participants provided a written informed consent in accordance with the Declaration of Helsinki to participate in the study and to obtain information from their family physicians.

Study population

We included all participants from the Rotterdam Study, cohort I wave 3, cohort II wave I and cohort III wave I, with thyroid function measurements, MRI measurements and free of dementia at baseline (n=5104). We excluded 248 participants with prevalent stroke and with MRI-defined cortical infarcts and 173 participants using thyroid function altering medication (levothyroxine, anti-thyroid drugs, amiodarone or corticosteroids). Final study population included 4,683 participants of which 3,852 also had DTI measurements.

Assessment of thyroid function

Thyroid function was measured through thyroid-stimulating hormone (TSH) and free thyroxine (FT4) using the same methods and assay for all cohorts (The electrochemiluminescence immunoassay for thyroxine and thyrotropine, "ECLIA", Roche) in serum samples stored at -80°C. We determined the reference values for normal range TSH as 0.4-4.0 mIU/L and FT4 as 11-25 pmol/L (= 0.85-1.95 ng/dL) according to national guidelines as well as our previous studies.[8,10]

MRI acquisition and analysis

Multi-sequence brain MR Imaging was performed on a 1.5 tesla MRI scanner (GE Signa Excite). The imaging protocol and sequence details were described extensively elsewhere.[11] Scans were automatically segmented supra tentorially into grey matter, white matter, cerebrospinal fluid (CSF) and background tissue. Intracranial volume (ICV) (excluding the cerebellum and surrounding CSF) was estimated by summing total grey and white matter and CSF volumes.[12] Total brain volume was estimated by summing total grey and white matter volumes.[12] A post-processing white matter lesion classification, based on the FLAIR image and the tissue segmentation, was used to obtain white matter lesion volumes (natural-log transformed to account for their skewed distribution).[13] All segmentations were visually inspected and were corrected if needed. Cortical infarcts were visually rated on structural sequences, and were classified as cortical infarcts in case of involvement of cortical grey matter. In a subset of our study population (N=2,449) cerebellar volume was processed automatically using FreeSurfer 4.5. This procedure, based on probabilistic information obtained from a manually labeled training set, assigns a neuroanatomical label to each voxel in an MRI volume. This is explained in more detail elsewhere.[14] In this subset we computed intracranial volume, including cerebellar volume, and total cerebellar volume.

Diffusion-MRI processing

For characterization of white matter microstructural organization with DTI, a single shot, diffusion-weighted spin echo echo-planar imaging sequence was performed. Maximum b-value was 1000 s/mm^2 in 25 non-collinear directions and three volumes were acquired without diffusion weighting (b-value = 0 s/mm^2). For the diffusion acquisition, due to technical issues 1165 participants were scanned with the phase and frequency encoding directions swapped leading to a mild ghost artifact.[15] We corrected for this potential confounder in our analyses. Diffusion data were pre-processed using a standardized pipeline (including correction for motion and eddy currents) as previously described.[16] A diffusion tensor model was estimated in each voxel, and co-registration between structural imaging and diffusion image space was performed.[15] Through averaging of the diffusion measurements inside the normal appearing white matter (voxels with white matter lesions were excluded from the analysis) we obtained global mean fractional anisotropy (FA), mean diffusivity (MD), radial diffusivity, and axial diffusivity.[15] The median time between thyroid function measurement and MRI scan was 0.21 years (interquartile range: 0.06-10.16).

Assessment of other variables

Blood pressure was measured at the right brachial artery using a random-zero sphygmomanometer after 5 minutes of rest with the participants in sitting position. The mean

of two consecutive measurements was used. Information regarding the use of blood pressure lowering medication for the indication of hypertension was derived from structured home interviews and linkage to pharmacy records. Serum total and high density lipoprotein (HDL) cholesterol were measured in fasting serum by enzymatic method. Smoking information was derived from baseline questionnaires and categorized in never, previous and current smokers. Alcohol consumption was documented as intake in grams per day. Body-mass index (BMI) was calculated as weight kilograms divided by height in meters squared. History of diabetes mellitus was defined by a repeated (two measurements within one year) impaired fasting glucose ≥ 7 mmol/L or a non-fasting glucose of ≥ 11 mmol/L (when fasting samples were absent) or use of anti-glycemic medication at baseline.[17] Educational level was assessed during a baseline home interview and people were classified into 7 categories: from low level of education (primary only) to high (university). Prevalent dementia and clinical stroke were ascertained as previously described.[18,19] In short, participants were evaluated for dementia using a three strep protocol. All participants were screened using the Mini-Mental State Examination (MMSE)[20] and Geriatric Mental State schedule (GMS).[21] Persons scoring ≤ 25 on the MMSE or >0 on the GMS underwent an examination and informant interview with the Cambridge Examination for Mental Disorders of the Elderly. Persons suspicious of having dementia underwent further neuropsychological testing if necessary. Furthermore, in addition to the above screening method, persons were continuously monitored for the dementia diagnosis through computerized linkage of the study database and medical records of the general practitioner's office and Regional Institute for Outpatient Mental Health Care (RIAGG). The accepted DSM-III-R criteria were used for the dementia diagnosis[22].

Statistical analysis

We used ordinary least squares linear regression models with restricted cubic splines at three knots,[23] which provided the best fit with the data without overfitting, for all analyses, to account for possible non-linear associations. Primary analyses for brain volume measurements were adjusted for age, sex, cohort, time between laboratory measurement and MRI scan and intracranial volume. We included intracranial volume as a covariate in our model to correct for the inter-individual variability in head size.[24] In a second model, we additionally adjusted for several cardiovascular risk factors including total cholesterol, HDL-cholesterol, systolic blood pressure, diastolic blood

pressure, smoking, prevalent diabetes mellitus, BMI, alcohol use and educational level. For the analyses of intracranial volume, we did not adjust for the variable itself. Primary analyses for diffusion measurements adjusted for age, sex, cohort, time between laboratory measurement and MRI scan, intracranial volume, white matter volume and white matter lesion volume. A second model additionally adjusted for total cholesterol, HDL-cholesterol, systolic blood pressure, diastolic blood pressure, smoking, prevalent diabetes, BMI, alcohol use and educational level. TSH was natural log-transformed for all analyses to approximate normality and interaction of TSH or FT4 with age (as a continuous measure) or sex was tested for all analyses. We conducted sensitivity analyses 1) constricting analyses to the reference range of thyroid function (n=4141) and 2) excluding participants with time interval above 1 year between laboratory measurement and MRI scan (n=2527). In order to quantify the effects in different age groups we additionally stratified our main analyses by the mean age of our population (~ 60 years of age). Missing covariates (< 5% for all covariates but alcohol [6.7%]) were imputed using multiple imputations creating 5 data sets according to the Markov Chain Monte Carlo method and pooled subsequently (IBM SPSS Statistics for Windows, version 21.0. Armonk, NY). In our multiple comparisons correction we took the main analyses (FT4, TSH with the 9 different outcomes (intracranial volume, total brain volume, total white matter volume, total grey matter volume, cerebellar volume, FA, MD, radial diffusivity, and axial diffusivity) into account. We estimated the number of independent tests by using the variance of the eigenvalues of the correlation matrix of the 11 variables used in our main analyses. We calculated the number of independent tests using the following formula: M_{eff}= 1 +(M-1)(1-var (λ_{obs})/M) with M is number of tests, M_{eff} is the number of independent tests.[25,26] Based on this formula M_{eff} was 5.668331474. Afterwards, using the Šidák formula: α sidak = 1 - ((1 - α)^(1/M_{eff})) our corrected significance level was p< 0.0081.[25] Statistical analyses were conducted and plots were produced using R statistical software (rms, Himsc, visreg packages, R-project, Institute for Statistics and Mathematics, R Core Team (2013), Vienna, Austria, version 3.0.2).

RESULTS

We included a total of 4683 participants, with an average age of 60.2 years (range 45.6-89.9) of which 54.9% were female (**Table 1**). As the results of the two tested models are comparable we present both for illustration, but only report the most adjusted model in the manuscript. Linearity assumption was met for all main analyses and indicated in tables if otherwise.

Table 1 Characteristics of the 4,683 study participants

Variable	Mean (SD) [a]
Age, years	60.2 (7.3)
Female sex n, %	2,571 (54.9)
TSH, ImU/L median (IQR)	1.97 (1.36 - 2.78)
FT4, pmol/L	15.5 (2.1)
Intracranial volume, mL	1140.0 (115.5)
Grey matter volume, mL	529.4 (53.6)
White matter volume, mL	409.2 (59.1)
White matter lesion volume, mL, median, IQR	2.9 (1.7-6.0)
Mean fractional anisotropy	0.34 (0.02)
Mean diffusivity, 10^{-3} mm^2/s	0.74 (0.03)
BMI, kg/m^2	27.1 (4.0)
Total cholesterol, mmol/L	5.70 (1.02)
HDL-cholesterol, mmol/L	1.42 (0.41)
Systolic blood pressure, mmHg	134.8 (19.3)
Diastolic blood pressure, mmHg	79.9 (10.9)
Prevalent diabetes n, %	399 (8.5)
Smoking	
Current n, %	1,029 (22.0)
Past n, %	2,211 (47.2)
Never n, %	1,443 (30.8)
Alcohol use, grams per day, median, IQR	15.0 (6.3-21.4)
Time between thyroid function measurement and scan (in years) median, IQR	0.21 (0.06-10.16)

[a] Values are means and (standard deviation) unless otherwise specified.
There were 13 participants with missing values for BMI, 5 total cholesterol, 17 HDL-cholesterol, 14 systolic and diastolic, 17 smoking, 18 for prevalent diabetes and 313 for alcohol use.
Abbreviations: BMI = body-mass index; TSH = thyroid-stimulating hormone, FT4 = free thyroxine; SD = Standard deviation; IQR = inter-quartile range

Brain tissue volumes and intracranial volume

Higher FT4 levels were associated with larger intracranial volume with a beta (β) of 6.23 mL per one unit increase of FT4 pmol/L (95% Confidence Interval [CI], 2.80, 9.66, **Table 2**), and the association was not different according to age (**Figure 1**, **Supplemental Table 1**, **Supplemental Table 2**). There was no association of TSH levels with intracranial volume. Higher FT4 levels were associated with larger brain volume overall (β 2.26, CI, 1.10, 3.43, **Table 2**) and white matter volume in particular (β 1.43, CI, 0.25, 2.62, **Table 2**), but not in elderly (**Figure 1**, **Supplemental Table 2**). The p for interaction of age with total brain volume was 0.002 and for age with white matter volume was 0.038 (**Supplemental Table 1**). The associations of FT4 and TSH with total brain volume were mainly attributable to white matter and not gray matter volume (**Table 2**). Higher levels of TSH were associated with smaller brain volumes (β -1.35, CI, -2.26,

-0.45, **Table 2**). Higher FT4 levels were associated with a larger white matter volume (β 1.43, CI, 0.24, 2.62), but not gray matter volume (β 0.78, CI, -0.25, 1.80). Higher TSH levels were associated with a smaller white matter volume (β - 1.58, CI,-2.50, - 0.67), but not grey matter volume (β 0.19, CI, -0.61, 0.99). Constricting analyses to the reference range of thyroid function or excluding participants with time interval between laboratory measurement and MRI scan > 1 year did not change effect estimates (**Table 3**). There was no significant interaction of FT4 or TSH with sex on the association with any of the studied outcomes (p> 0.10). There was no significant interaction of TSH with age on the association with any of the studied outcomes (p> 0.35, **Supplemental Table 1**).

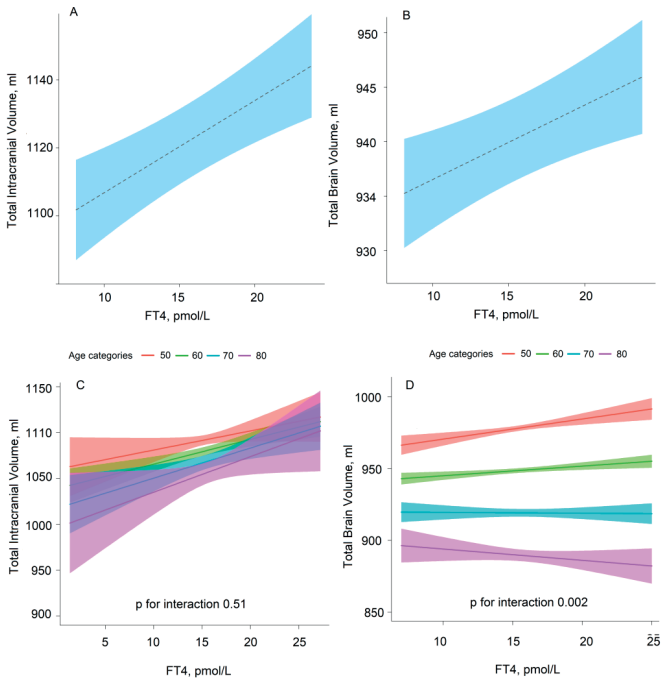

Figure 1. Total intracranial and brain volume according to FT4 serum values
Plot A) depicts the association of FT4with intracranial volume and plot B) depicts the association of FT4 with total brain volume. Plot C) depicts the interaction of FT4 with age continuously for the intracranial volume analysis and D) depicts interaction of FT4 with age continuously for the total brain volume analysis. All analyses are adjusted for age, sex, cohort and time between laboratory measurements and MRI scan, and the analyses with brain volume were additionally adjusted for intracranial volume.

Total cerebellar volume

The additional analysis using a subgroup of 2249 persons with cerebellar volume data measured with FreeSurfer, yielded a similar albeit a more pronounced association of FT4 with intracranial volume (β 10.13, CI, 3.61, 16.64, **Supplemental Table 3**). FT4 was positively associated with cerebellar volume (β 0.68.13, CI, 3.61, 16.64, **Supple-**

mental table 3). No associations were observed for TSH with intracranial volume or cerebellar volume (**Supplemental Table 3**).

Table 2 Association of TSH or FT4 with intracranial, total, white and grey matter brain volume measurements

Variable	Total intracranial volume β (95% CI)	Total brain volume β (95% CI)	Total white matter volume β (95% CI)	Total grey matter volume β (95% CI)
TSH				
Model 1	0.39 (-2.32, 3.09)	-1.37 (-2.28, -0.46)	-1.58 (-2.50, -0.67)	0.21 (-0.59, 1.01)
Model 2	0.64 (-2.04, 3.32)	-1.37 (-2.27, -0.47)	-1.55 (-2.47, -0.63)	0.18 (-0.61, 0.98)
FT4				
Model 1	7.23 (3.78, 10.67)	1.95 (0.78, 3.12)*	1.43 (0.25, 2.61)	0.47 (-0.55, 1.49)
Model 2	6.23 (2.80, 9.66)	2.26 (1.10, 3.43)	1.43 (0.25, 2.62)	0.78 (-0.24, 1.81)

Model 1: age, sex, cohort, time between laboratory measurement and MRI scan and intracranial volume Model 2= Model 1 + total cholesterol, HDL-cholesterol, systolic blood pressure, diastolic blood pressure, smoking, prevalent diabetes, BMI, alcohol use and educational level. * p for non-linearity 0.054; Abbreviations: CI = confidence interval; FT4 = free thyroxine; MRI= Magnetic resonance imaging; OR = odds ratio; TSH = thyroid stimulating hormone

Table 3 Sensitivity analyses of association of TSH or FT4 with MRI intracranial and brain volume measurements

Variable		Total intracranial volume β (95% CI)	Total brain volume β (95% CI)	Total white matter volume β (95% CI)	Total grey matter volume β (95% CI)
Reference range (n= 4,141)*					
TSH	Model 1	-0.91 (-5.40, 3.58)	-1.40 (-2.89, 0.09)	-1.88 (-3.40, -0.35)	0.48 (-0.84, 1.81)
	Model 2	-0.87 (-5.34, 3.59)	-1.30 (-2.78, 0.17)	-1.76 (-3.28, -0.22)	0.45 (-0.87, 1.78)
FT4	Model 1	8.31 (4.25, 12.36)	2.32 (0.87, 3.76)**	1.56 (0.07, 3.04)	0.60 (-0.60, 1.80)
	Model 2	7.17 (3.12, 11.22)	2.53 (1.09, 3.97)**	1.41 (-0.08, 2.90)	0.99 (-0.22, 2.20)
Excluding participants with time interval between laboratory measurement and MRI scan > 1 years (n= 2,527)					
TSH	Model 1	1.42 (-2.7, 5.56)	-1.41 (-2.74, -0.08)	-1.22 (-2.55, 0.11)	-0.24 (-1.42, 0.49)
	Model 2	1.54 (-2.57, 5.65)	-1.50 (-2.82, -0.17)	-1.23 (-2.57, 0.11)	-0.30 (-1.48, 0.88)
FT4	Model 1	6.78 (1.95, 11.61)	2.57 (1.01, 4.13)**	2.36 (0.79, 3.93)	0.08 (-1.29, 1.46)
	Model 2	5.40 (0.57, 10.22)	2.95 (1.39, 4.52)**	2.42 (0.83, 4.00)	0.43 (-0.96, 1.82)

Model 1: age, sex, cohort, time between laboratory measurement and MRI scan and intracranial volume Model 2= Model 1 + total cholesterol, HDL-cholesterol, systolic blood pressure, diastolic blood pressure, blood pressure lowering medication with indication of hypertension, smoking, prevalent diabetes, BMI, alcohol use and educational level.

* Reference ranges for TSH were 0.4-4.0 mIU/L and for FT4 were 11-25 pmol/L. ** non-linearity of association $p < 0.05$. Abbreviations: CI = confidence interval; FT4 = free thyroxine; MRI= Magnetic resonance imaging; OR = odds ratio; TSH = thyroid stimulating hormone

White matter microstructural organization

There was no overall association of TSH or FT4 with diffusion properties of white matter, neither FA nor MD (**Table 4**). However, there was a significant interaction with age for the association of FT4 and MD (p for interaction 0.026, **Figure 2**, **Supplemental Table 1**). In older participants, higher FT4 values were associated with a lower FA (albeit not statistically significant interaction, p = 0.052, **Supplemental Table 1**) and higher MD, generally indicating reduced matter microstructural integrity (**Supplemental Table 4**). In contrast, in younger participants, higher FT4 levels were associated with a higher FA and lower MD, generally indicating increased white matter integrity. The associations for radial and axial diffusivity followed the same pattern as mean diffusivity (**Figure 2**). All results survive the threshold for significance after multiple comparisons correction except for the association of FT4 in the full range with white matter volume.

Table 4 Association of full range TSH or FT4 with Z-scores of Diffusion Tensor Imaging parameters of white matter (n=3,852)

	FA β (95% CI)	**MD β (95% CI)**	**RD β (95% CI)**	**AD β (95% CI)**
TSH				
Model 1	-0.00(-0.03, 0.03)	0.01(-0.01, 0.03)	0.01(-0.01, 0.03)	0.01(-0.01, 0.03)
Model 2	-0.00(-0.03, 0.03)	0.01(-0.01, 0.03)	0.01(-0.01, 0.03)	0.01(-0.01, 0.03)
FT4				
Model 1	-0.01(-0.05, 0.02)	0.02(-0.01, 0.04)	0.01(-0.01, 0.04)	0.02(-0.01, 0.04)
Model 2	-0.01(-0.04, 0.03)	0.01(-0.02, 0.04)	0.01(-0.02, 0.04)	0.01(-0.01, 0.04)

Model 1: age, sex, cohort, time between laboratory measurement and MRI scan, intracranial volume, white matter volume and white matter lesions. Model 2= Model 1 + total cholesterol, HDL-cholesterol, systolic blood pressure, diastolic blood pressure, blood pressure lowering medication with indication of hypertension, smoking, prevalent diabetes, BMI, alcohol use and educational level. *Abbreviations: CI = confidence interval; FA = fractional anisotropy; FT4 = free thyroxine; MD = mean diffusivity; RD = radial diffusivity; AD = axial diffusivityTSH = thyroid stimulating hormone*

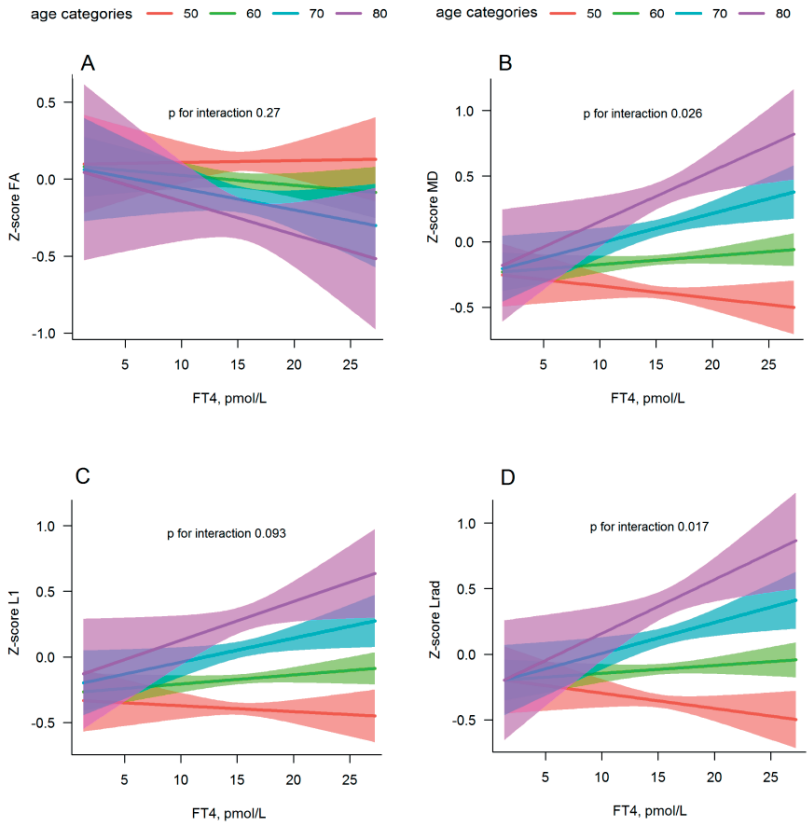

Figure 2. DTI measurements according to FT4 serum values

Plot depicting the interaction of FT4 with age for z-scores of A) fractional anisotropy, B) mean diffusivity, C) radial diffusivity and D) axial diffusivity . All analyses are adjusted for age, sex, cohort, time between laboratory measurements and MRI scan, intracranial volume, white matter and white matter lesion volume.

DISCUSSION

We report an association of higher FT4 with larger intracranial volume, independent of age. Higher FT4 levels are also associated with a larger total brain volume, mainly attributable to white matter volume. However this association was age-dependent. In older participants (over ~70 years old) higher FT4 levels were associated with a smaller total brain volume, primarily white matter. We also found a differential effect of age on the association of FT4 with DTI measures that can be linked to white matter integrity. In older participants, higher FT4 were associated with DTI measures reflecting poorer white matter integrity. In younger participants (especially those <50 years), higher FT4 levels were associated with DTI measures reflecting better white matter integrity, primarily lower MD. These findings could indicate an age-dependent effect of thyroid hormone on brain morphology and microstructural organization, beneficial in younger

age and deleterious in older age. To our knowledge, there are no previous studies assessing the association of thyroid function with brain volumes and white matter microstructure in the general population. Based on our results, we hypothesize that the findings in younger participants could reflect a positive role of thyroid hormone balance in myelination, sustainability and protection of neurons during early stages of life. In contrast, in older age, high thyroid function could be deleterious by causing neuronal damage and in turn neurodegeneration.

Thyroid hormone is important for growth, development and metabolism in virtually all organs and effects on the brain are numerous. Fetal neurogenesis is thyroid hormone dependent and both lack and excess of thyroid hormone availability can hamper brain development and has deleterious effects on brain morphology.[1,2,27] In older age, mainly high thyroid function has been linked to neurodegeneration and cognitive impairment.[6,7,10] Higher thyroid hormone levels are related to a higher basal metabolic rate and oxygen consumption. In turn, this can affect oxidative stress, either due to increased reactive oxygen species production or lower activity of antioxidants, potentially leading to oxidative damage.[28,29] These effects are reported to be tissue specific, but oxidative damage may be most pronounced in metabolic active organs such as the brain possibly leading to negative effects on neuronal integrity.[29] Free radical injury has been suggested to associate with white matter changes on DTI.[30] With microstructural changes thought to accumulate to macrostructural tissue change, this could be one of the pathways explaining the association of thyroid function with lower white matter volume and poorer integrity in elderly, potentially also the previously described relation with the risk of dementia. The pathophysiology of dementia is multifactorial, but implication of oxidative stress has also been proposed.[31,32] Alternatively, a common genetic predisposition could underlie the association of thyroid function with dementia and white matter integrity.

Thyroid function is known to affect several cerebrovascular risk factors. However, deleterious cardiovascular risk factors, such as dyslipidemia and increased blood pressure, are mainly consequences observed in hypothyroidism. Furthermore, we previously described lack of association of thyroid function with small vessel disease on MRI, including white matter lesions, lacunar infarcts and cerebral microbleeds.[8] Also, adjusting for various cardiovascular risk factors in the current study did not change the associations meaningfully. This, together with the current results, suggests that the association of thyroid function with measures of white matter microstructure in elderly is independent of these risk factors and mediated through other pathways (e.g. oxidative stress). Thyroid hormone also has distinct effects on myelin formation and regeneration.[33,34] However, thyroid hormone and thyroid hormone repletion is mainly associated with acceleration of myelination and remyelination in different animal studies and patient populations.[33-35] This demonstrates the potential complexity of the

pathophysiology[2] and more research is needed to unravel the exact pathophysiological link between thyroid function, white matter microstructure and dementia. Discovery of underlying pathways is not only needed to understand the pathophysiology of dementia, but also to identify persons at risk and determine promising treatment targets. Another implication of our study may lie in the possible effects of overtreatment of hypothyroidism. In recent years, physicians have commenced levothyroxine treatment in people at lower serum TSH thresholds, i.e. milder cases of hypothyroidism.[36] It was found that in patients treated with levothyroxine for hypothyroidism, a substantial proportion was not within treatment target, with over 10% being overtreated and actually classifying as iatrogenic hyperthyroidism.[36] Our study results suggest that endogenous high FT4 values may negatively affect brain volume and brain tissue in older age. Although we have not investigated whether high thyroid function due to levothyroxine (i.e. exogenous thyroxine) use has comparable effects on brain volumes and DTI measurements as endogenous thyroid hormone, we speculate that this is plausible. Further research is needed to confirm this hypothesis.

Strengths of our study include the large sample size and availability of detailed phenotypical information. Also, we were able to adjust for a wide variety of confounders. Nevertheless, residual confounding cannot be excluded in an observational study, even with adjustments for the large number of potential confounders performed in our analyses. Another limitation of our study is that thyroid function was measured only once, which is a limitation for most observational cohort studies, and therefore changes over time could not be assessed. A sensitivity analysis limited to participants with thyroid function within the reference range (n=4141), which are known to be relatively stable over time,[37,38] yielded similar results. Nevertheless, our results need to be confirmed in study preferably with a longitudinal design. Furthermore; no conclusions can be drawn on the causality of the associations due to the cross-sectional design. We used averaged diffusion parameters, aggregated over all the normal-appearing white matter voxels. This did not allow us to assess brain changes on a more regional level. Finally, the Rotterdam Study constitutes of mainly Caucasian participants of 45 years and older, so our results may be less generalizable to younger or other ethnic populations.

Conclusions

In summary, our study shows that higher FT4 levels are associated with larger brain volumes and higher white matter microstructural integrity in younger individuals, but not in elderly. Furthermore, our results highlight the need for caution in overtreatment in mild hypothyroidism. Thyroid hormone excess is a risk factor for dementia and further studies should evaluate whether this is indeed mediated through poorer white matter microstructural integrity.

CHAPTER REFERENCES

1. Calza L, Fernandez M, Giardino L. Role of the Thyroid System in Myelination and Neural Connectivity. *Comprehensive Physiology.* 2015;5(3):1405-1421.
2. Bernal J. Thyroid Hormones in Brain Development and Function. 2000.
3. Kapoor R, Desouza LA, Nanavaty IN, Kernie SG, Vaidya VA. Thyroid hormone accelerates the differentiation of adult hippocampal progenitors. *J Neuroendocrinol.* 2012;24(9):1259-1271.
4. Korevaar TI, Peeters RP. The continuous spectrum of thyroid hormone action during early life. *Lancet Diabetes Endocrinol.* 2016;4(9):721-723.
5. Cappola AR, Arnold AM, Wulczyn K, Carlson M, Robbins J, Psaty BM. Thyroid function in the euthyroid range and adverse outcomes in older adults. *J Clin Endocrinol Metab.* 2015;100(3):1088-1096.
6. Pasqualetti G, Pagano G, Rengo G, Ferrara N, Monzani F. Subclinical Hypothyroidism and Cognitive Impairment: Systematic Review and Meta-Analysis. *J Clin Endocrinol Metab.* 2015;100(11):4240-4248.
7. Rieben C, Segna D, da Costa BR, et al. Subclinical Thyroid Dysfunction and the Risk of Cognitive Decline: a Meta-Analysis of Prospective Cohort Studies. *J Clin Endocrinol Metab.* 2016:jc20162129.
8. Chaker L, Wolters FJ, Bos D, et al. Thyroid function and the risk of dementia: The Rotterdam Study. *Neurology.* 2016.
9. Hofman A, Brusselle GG, Darwish Murad S, et al. The Rotterdam Study: 2016 objectives and design update. *Eur J Epidemiol.* 2015;30(8):661-708.
10. Chaker L, Heeringa J, Dehghan A, et al. Normal Thyroid Function and the Risk of Atrial Fibrillation: the Rotterdam Study. *J Clin Endocrinol Metab.* 2015;100(10):3718-3724.
11. Ikram MA, van der Lugt A, Niessen WJ, et al. The Rotterdam Scan Study: design update 2016 and main findings. *Eur J Epidemiol.* 2015;30(12):1299-1315.
12. Vrooman HA, Cocosco CA, van der Lijn F, et al. Multi-spectral brain tissue segmentation using automatically trained k-Nearest-Neighbor classification. *Neuroimage.* 2007;37(1):71-81.
13. de Boer R, Vrooman HA, van der Lijn F, et al. White matter lesion extension to automatic brain tissue segmentation on MRI. *Neuroimage.* 2009;45(4):1151-1161.
14. Hoogendam YY, van der Geest JN, van der Lijn F, et al. Determinants of cerebellar and cerebral volume in the general elderly population. *Neurobiol Aging.* 2012;33(12):2774-2781.
15. de Groot M, Ikram MA, Akoudad S, et al. Tract-specific white matter degeneration in aging: the Rotterdam Study. *Alzheimers Dement.* 2015;11(3):321-330.
16. Koppelmans V, de Groot M, de Ruiter MB, et al. Global and focal white matter integrity in breast cancer survivors 20 years after adjuvant chemotherapy. *Hum Brain Mapp.* 2014;35(3):889-899.
17. Ligthart S, van Herpt TT, Leening MJ, et al. Lifetime risk of developing impaired glucose metabolism and eventual progression from prediabetes to type 2 diabetes: a prospective cohort study. *Lancet Diabetes Endocrinol.* 2016;4(1):44-51.
18. Bos MJ, Koudstaal PJ, Hofman A, Ikram MA. Modifiable etiological factors and the burden of stroke from the Rotterdam study: a population-based cohort study. *PLoS Med.* 2014;11(4):e1001634.
19. Schrijvers EM, Verhaaren BF, Koudstaal PJ, Hofman A, Ikram MA, Breteler MM. Is dementia incidence declining?: Trends in dementia incidence since 1990 in the Rotterdam Study. *Neurology.* 2012;78(19):1456-1463.
20. Folstein MF, Folstein SE, McHugh PR. "Mini-mental state". A practical method for grading the cognitive state of patients for the clinician. *J Psychiatr Res.* 1975;12(3):189-198.

21. Copeland JR, Kelleher MJ, Kellett JM, et al. A semi-structured clinical interview for the assessment of diagnosis and mental state in the elderly: the Geriatric Mental State Schedule. I. Development and reliability. *Psychol Med.* 1976;6(3):439-449.
22. American Psychiatric Association. *Diagnostic and Statistical Manual of Mental Disorders*. Washington, DC1987.
23. *rms: S functions for biostatistical/epidemiologic modeling, testing, estimation, validation, graphics, and prediction* [computer program]. 2009.
24. Pintzka CW, Hansen TI, Evensmoen HR, Haberg AK. Marked effects of intracranial volume correction methods on sex differences in neuroanatomical structures: a HUNT MRI study. *Front Neurosci.* 2015;9:238.
25. Galwey NW. A new measure of the effective number of tests, a practical tool for comparing families of non-independent significance tests. *Genet Epidemiol.* 2009;33(7):559-568.
26. Nyholt DR. A simple correction for multiple testing for single-nucleotide polymorphisms in linkage disequilibrium with each other. *Am J Hum Genet.* 2004;74(4):765-769.
27. Korevaar TI, Muetzel R, Medici M, et al. Association of maternal thyroid function during early pregnancy with offspring IQ and brain morphology in childhood: a population-based prospective cohort study. *Lancet Diabetes Endocrinol.* 2016;4(1):35-43.
28. Schwartz HL, Oppenheimer JH. Ontogenesis of 3,5,3'-triiodothyronine receptors in neonatal rat brain: dissociation between receptor concentration and stimulation of oxygen consumption by 3,5,3'-triiodothyronine. *Endocrinology.* 1978;103(3):943-948.
29. Villanueva I, Alva-Sanchez C, Pacheco-Rosado J. The role of thyroid hormones as inductors of oxidative stress and neurodegeneration. *Oxid Med Cell Longev.* 2013;2013:218145.
30. Back SA, Kroenke CD, Sherman LS, et al. White matter lesions defined by diffusion tensor imaging in older adults. *Ann Neurol.* 2011;70(3):465-476.
31. Zhou X, Li Y, Shi X, Ma C. An overview on therapeutics attenuating amyloid beta level in Alzheimer's disease: targeting neurotransmission, inflammation, oxidative stress and enhanced cholesterol levels. *Am J Transl Res.* 2016;8(2):246-269.
32. von Arnim CAF, Gola U, Biesalski HK. More than the sum of its parts? Nutrition in Alzheimer's disease. *Nutrition.* 2010;26(7-8):694-700.
33. Adamo AM, Aloise PA, Soto EF, Pasquini JM. Neonatal hyperthyroidism in the rat produces an increase in the activity of microperoxisomal marker enzymes coincident with biochemical signs of accelerated myelination. *J Neurosci Res.* 1990;25(3):353-359.
34. Noguchi T, Sugisaki T. Hypomyelination in the cerebrum of the congenitally hypothyroid mouse (hyt). *J Neurochem.* 1984;42(3):891-893.
35. Harsan LA, Steibel J, Zaremba A, et al. Recovery from chronic demyelination by thyroid hormone therapy: myelinogenesis induction and assessment by diffusion tensor magnetic resonance imaging. *J Neurosci.* 2008;28(52):14189-14201.
36. Taylor PN, Iqbal A, Minassian C, et al. Falling threshold for treatment of borderline elevated thyrotropin levels-balancing benefits and risks: evidence from a large community-based study. *JAMA Intern Med.* 2014;174(1):32-39.
37. Andersen S, Pedersen KM, Bruun NH, Laurberg P. Narrow individual variations in serum T(4) and T(3) in normal subjects: a clue to the understanding of subclinical thyroid disease. *J Clin Endocrinol Metab.* 2002;87(3):1068-1072.
38. Chaker L, Korevaar TI, Medici M, et al. Thyroid Function Characteristics and Determinants: The Rotterdam Study. *Thyroid.* 2016;26(9):1195-1204.

SUPPLEMENTAL MATERIAL

CHAPTER 3

White matter microstructural changes in aging and neurodegeneration

CHAPTER 3.1

Determinants, MRI correlates, and prognosis of mild cognitive impairment: The Rotterdam Study

Lotte G.M. Cremers, Renee F.A. de Bruijn, Saloua Akoudad, Albert Hofman, Wiro J. Niessen, Aad van der Lugt, Peter J. Koudstaal, Meike W. Vernooij, M. Arfan Ikram

Journal of Alzheimer's Disease 2014

ABSTRACT

Mild cognitive impairment (MCI) marks a transitional stage between healthy aging and dementia, but the understanding of MCI in the general population remains limited. We investigated determinants, MRI-correlates, and prognosis of MCI within the population-based Rotterdam Study. Firstly, we studied age, *APOE*-ε4 carriership, waist circumference, hypertension, diabetes mellitus, total and HDL-cholesterol levels, smoking, and stroke as potential determinants of MCI. Determinants were assessed cross-sectionally at baseline (2002-2005) and up to 7 years prior to baseline (1997-2001). Secondly, we compared volumetric, microstructural, and focal MRI-correlates in persons with and without MCI. Thirdly, we followed participants for incident dementia and mortality until 2012. Out of 4,198 participants, 417 had MCI, of whom 163 amnestic and 254 non-amnestic MCI. At baseline, older age, *APOE*-ε4 carriership, lower total cholesterol levels, and stroke were associated with MCI. Additionally, lower HDL-cholesterol levels and smoking were related to MCI when assessed 7 years prior to baseline. Persons with MCI, particularly those with non-amnestic MCI, had larger white matter lesion volumes, worse microstructural integrity of normal-appearing white matter, and a higher prevalence of lacunes, compared to cognitively healthy participants. MCI was associated with an increased risk of dementia (hazard ratio (HR) 3.98, 95% confidence interval (CI) 2.97;5.33), Alzheimer's disease (HR 4.03, 95% CI 2.92;5.56), and mortality (HR 1.54, 95% CI 1.28;1.85). In conclusion, we found that several vascular risk factors and MRI-correlates of cerebrovascular disease were related to MCI in the general population. Participants with MCI had an increased risk of dementia, including Alzheimer's disease, and mortality.

INTRODUCTION

Although the etiology of dementia is largely unknown, it is well established that neuropathology related to dementia slowly accumulates over decades. Consequently, identifying persons at a higher risk of dementia could postpone or even prevent dementia by timely targeting modifiable risk factors.[1] In this light, mild cognitive impairment (MCI) has been identified as the transitional stage between normal aging and dementia. Thus far, several studies have focused on identifying determinants, magnetic resonance imaging (MRI)-correlates, and prognosis of MCI. Various studies have established the role of amyloid pathology in MCI, but emerging evidence also implicates vascular factors as risk factors for MCI.[2-4] However, findings on determinants, MCI-correlates, and prognosis of MCI vary greatly due to differences in study populations, definitions of MCI, and determinants under investigation.[2, 5-11] Studying MCI in the general population may strengthen previous findings on determinants and prognosis of MCI. More importantly, clinical studies may suffer from referral bias and reverse causality. In the general population referral bias is less present and investigating determinants years before MCI could overcome the problem of reverse causality.

In the population-based Rotterdam Study we investigated determinants, MRI-correlates, and prognosis of MCI. Firstly, we focused on several vascular risk factors that were measured not only cross-sectionally, but also up to 7 years prior to diagnosis of MCI. Secondly, we investigated the relation between MCI and volumetric, microstructural, and focal imaging markers. Thirdly, we followed participants over a period of 9 years to determine the risk of incident dementia, Alzheimer's disease, and mortality.

METHODS

Setting and study population

The Rotterdam Study is a prospective population-based cohort that started in 1990. Inhabitants, aged 55 years and older, of Ommoord, a district of Rotterdam, the Netherlands were invited to participate in the study.[12] Out of 10,215 invited inhabitants, 7,983 (78%) agreed to participate. In 2000, this cohort was extended with 3,011 participants (67% of invitees) who had become 55 years of age or had moved into the district since the start of the study. Every 4 years, participants are re-invited to undergo home interviews and various examinations at the research center.[12]

Between 2002-2005, which was the fourth examination round of the original cohort and the second examination round of the extended cohort, an extensive neuropsychological test battery was implemented in the Rotterdam Study.[12] Given that extensive neuropsychological testing is required to assess MCI, 2002-2005 was set as baseline for MCI screening in our study. Of the 6,061 study participants that underwent examinations

between 2002-2005, 192 participants were excluded because they were demented, 67 because they were not sufficiently screened for dementia, and another 250 participants because they did not answer the questions regarding subjective cognitive complaints. An additional 1,354 participants were excluded because they missed one or more cognitive test scores or had unreliable test scores. Eventually, 4,198 persons were eligible to participate in this study. Because MRI was implemented from 2005 onwards,[13] only a random subset of 697 out of 4,198 persons underwent MRI, which was on average 1.01 years (0.46 standard deviation (SD)) after MCI screening. Persons with cortical infarcts were excluded (N=15) as tissue loss and gliosis surrounding cortical infarcts may cause unreliable white matter lesion segmentations. Eventually, 682 participants were included in the analyses of MRI-correlates.

Determinants of MCI and other measurements

Determinants of MCI were selected based on biological plausibility and literature on established risk factors of dementia.[14-18] Educational level was assessed at study entry by interview and categorized into seven groups: primary education only or primary education with an unfinished higher education, lower vocational education, lower secondary education, intermediate vocational education, general secondary education, higher vocational education, and university. Since educational level was required for assessment of the MCI diagnosis, we imputed missing values for education (1.8%) based on age and sex.

Information on *APOE* genotype was obtained using polymerase chain reaction on coded DNA samples without knowledge of MCI diagnosis. This method has been described in detail previously.[19, 20] *APOE*-ε4 carrier status was defined as carrier of one or two ε4 alleles. Waist circumference was measured in centimeters at the level midway between the lower rib margin and the iliac crest, with participants in standing position without heavy outer garments and with emptied pockets while breathing out gently. Blood pressure was measured in sitting position on the right arm and calculated as the average of two measurements using a random-zero sphygmomanometer. Hypertension was defined as a blood pressure ≥140/90 mmHg or use of blood pressure lowering medication, prescribed for the indication of hypertension. Diabetes mellitus was defined as a fasting serum glucose level ≥7.0 mmol/L, non-fasting serum glucose level ≥11.1 mmol/L, or use of anti-diabetic medication. Serum glucose, total cholesterol, and HDL-cholesterol levels were acquired by an automated enzymatic procedure (Boehringer Mannheim System). Smoking habits were assessed by interview and categorized as current, former, and never smoking. At study entry, history of stroke was assessed using home interviews and confirmed by reviewing medical records. After entering the Rotterdam Study, participants were continuously followed-up for stroke through automatic linkage of general practitioner files with the study database. For

potential strokes, additional information was collected from hospital, nursing home, and general practitioner records. An experienced neurologist adjudicated the strokes using standardized definitions, as described in detail previously.[21]
Apart from educational level and *APOE*-ε4 carrier status, all measurements were assessed at each examination round of the Rotterdam Study. We used the measurements that were assessed at the baseline of this study (2002-2005), and the measurements that were assessed at the previous examination round, which was up to 7 years (mean 4.4 years, SD 0.55) prior to baseline (1997-2001) (**Supplementary Figure 1**).

Assessment of MCI
MCI was defined using the following criteria: 1) presence of subjective cognitive complaints, 2) presence of objective cognitive impairment, and 3) absence of dementia.
Subjective cognitive complaints were evaluated by interview. This interview included three questions on memory (difficulty remembering, forgetting what one had planned to do, and difficulty finding words), and three questions on everyday functioning (difficulty managing finances, problems using a telephone, and difficulty getting dressed). Subjective cognitive complaints were scored positive when a subject answered "yes" to at least one of these questions. We assessed objective cognitive impairment using a cognitive test battery comprising letter-digit substitution task, Stroop test, verbal fluency test, and 15-word verbal learning test based on Rey's recall of words.[22] To obtain more robust measures, we constructed compound scores for various cognitive domains including memory function, information-processing speed, and executive function.[22, 23] Briefly, compound score for memory was calculated as the average of Z-scores for the immediate and delayed recall of the 15-word verbal learning test. For information processing speed averaged Z-scores for the Stroop reading and Stroop colour-naming subtask and the letter-digit substitution task were used. Finally, executive function included Z-scores of the Stroop interference subtask, the letter-digit substitution task, and the verbal fluency test. We classified persons as cognitively impaired if they scored below 1.5 SD of the age and education adjusted means of the study population. We subsequently classified the MCI subtypes amnestic and non-amnestic MCI. Amnestic MCI was defined as persons with MCI who had an impaired test score on memory function (irrespective of other domains). Non-amnestic MCI was defined as persons with MCI having normal memory function, but an impaired test score on executive function or information-processing speed.

Brain MRI and post-processing
We performed a multisequence MRI protocol on a 1.5-Tesla scanner (GE Healthcare). The sequences in the imaging protocol consisted of three high resolution axial scans, i.e., a T1-weighted sequence (slice thickness 1.6 mm, zero-padded to 0.8), a proton

density-weighted sequence (slice thickness 1.6 mm), and a fluid-attenuated inversion recovery (FLAIR) sequence (slice thickness 2.5 mm).[13] For cerebral microbleed detection, we used a custom-made accelerated three-dimensional T2*-weighted gradient-recalled echo (3D T2* GRE (slice thickness 1.6 mm, zero-padded to 0.8).[24] For diffusion tensor imaging scans we used a 2D acquisition and EPI readout (slice thickness for DTI was 3.5 mm). Maximum b-value was 1000 s/mm^2 in 25 non-collinear directions (number of excitations (NEX)=1) and one volume was acquired without diffusion weighting (b-value= 0 s/mm^2).

We used an automated tissue segmentation, including conventional k-nearest-neighbor brain tissue classifier extended with white matter lesion (WML) segmentation,[25] to segment scans into grey matter volume, white matter volume, WML volume, cerebrospinal fluid, and background. Total brain volume was defined as the sum of total grey matter volume, white matter volume, and WML volume. Hippocampal volume was determined using an automated method, as described extensively before.[26]

The segmentation was brought to the DTI image space using boundary based registration performed on the white matter segmentation,[27] the b=0 and T1-weighted images.

Diffusion data was pre-processed using a standardized processing pipeline.[28] In short, DTI data was corrected for subject motion and eddy currents by affine co-registration of the diffusion weighted volumes to the b=0 volume, including correction of gradient vector directions. Diffusion tensors were estimated using a non-linear Levenberg Marquadt estimator, available in ExploreDTI.[29] Global fractional anisotropy (FA) and mean diffusivity (MD), measures of microstructural integrity, were computed from the estimated tensor images over the entire normal-appearing white matter in each subject. The final registration result of each scan was checked visually for errors.[30, 31] Partial volume effects and presence of multiple white matter fibre orientation within a voxel were thus minimized. Sixteen subjects had to be excluded from the white matter microstructural integrity analyses due to scanning artifacts or excessive motion. FA and MD were standardized to echo time (TE) values, because TE was not constant for all participants.

All scans were rated by 1 of 5 trained research-physicians to determine presence of microbleeds and lacunes of presumed vascular origin.[32] Microbleeds were rated as focal areas of signal loss, on 3D T2* Gradient Recalled Echo-weighted MR imaging. Lacunes were rated on FLAIR, proton-density-weighted and T1-weighted sequences, and were defined as focal lesions ≥3mm and <15mm in size, with the same signal intensity as cerebrospinal fluid on all sequences and a hyperintense rim on the FLAIR (when located supratentorially).[33] Infarcts showing involvement of grey matter were classified as cortical infarcts.

Assessment of dementia

Participants were screened for dementia at baseline and at follow-up examinations using a three-step protocol. Screening was done using the Mini-Mental State Examination (MMSE) and the Geriatric Mental Schedule (GMS) organic level.[34, 35] Screen-positives (MMSE <26 or GMS organic level >0) subsequently underwent an examination and informant interview with the Cambridge Examination for Mental Disorders in the Elderly (CAMDEX).[36] During this interview, more information on functional status and cognitive performance was collected. Participants who were suspected of having dementia underwent extra neuropsychological testing if necessary. Additionally, for persons not visiting the research center, the total cohort was continuously monitored for dementia through computerized linkage of the study database and digitized medical records from general practitioners and the Regional Institute for Outpatient Mental Health Care. When information on neuroimaging was required and available, it was used for decision making on the diagnosis. In the end, a consensus panel, led by a neurologist, decided on the final diagnosis in accordance with standard criteria for dementia (Diagnostic and Statistical Manual of Mental Disorders, Third Edition, Revised (DSM-III-R)) and Alzheimer's Disease (National Institute of Neurological and Communicative Diseases and Stroke/Alzheimer's Disease and Related Disorders Association (NINCDS-ADRDA)).[37, 38] Follow-up for incident dementia was complete until January 1st, 2012.

Assessment of mortality

Deaths were continuously reported through automatic linkage with general practitioner files. In addition, municipal health records were checked bimonthly for information on vital status. Information about cause and circumstances of death was obtained from general practitioner and hospital records.[39] Follow-up for mortality was complete until January 1st, 2012.

Statistical analysis

Firstly, we examined whether risk factors of dementia were related to MCI using multivariate logistic regression models adjusted for age and sex cross-sectionally. Since vascular risk factors often correlate,[17] we estimated the independent effect of each risk factor by including all risk factors into the same model. Age was included per 5 year increase into the model and waist circumference, total and HDL-cholesterol levels were included per SD increase into the model. Persons with missing values were excluded from these analyses. We investigated whether excluded persons had different characteristics than persons who were included in the analysis using Univariate Analysis of Variance, adjusting for age and sex where appropriate. The same models as in the cross-sectional analysis were used to examine the relation with risk factors assessed

up to 7 years prior to MCI diagnosis. Secondly, we used linear and logistic regression to investigate the relation of MCI with volumetric markers (i.e., total brain volume, hippocampal volume, WML volume), microstructural integrity markers (i.e., mean FA, MD) and focal markers (i.e, cerebral microbleeds, lacunes) of brain pathology on MRI cross-sectionally. Hippocampal volume was studied as the mean of the left and right hippocampal volume. WML was log-transformed due to the skewed distribution. Volumetric and microstructural measures were modeled continuously. Microbleeds and lacunes were dichotomized into present versus absent. These analyses were adjusted for age and sex (model 1), and additionally for *APOE*-ε4 carriership, waist circumference, hypertension, diabetes mellitus, total and HDL-cholesterol levels, and smoking (model 2). In model 2 we investigated whether irrespective of the presence of vascular risk factors, persons with MCI had more volumetric, microstructural, and focal changes in the brain compared to cognitively healthy participants. Analyses of volumetric and microstructural integrity measures were also adjusted for intracranial volume. In addition we performed a sensitivity analysis for the imaging correlates, excluding participants who became demented in the period between MCI screening and MRI scanning (N=12). Thirdly, we used Cox proportional hazards to study the association between MCI and risk of dementia, Alzheimer's disease, and mortality longitudinally. These models were adjusted for the same determinants as described in model 2 but with addition of prevalent stroke and educational level. All analyses were repeated investigating the amnestic and non-amnestic MCI subtypes separately. Analyses were performed using statistical software package SPSS 20.0, using an α-value of 0.05.

RESULTS

Characteristics of the study population are presented in **Table 1**. Out of 4,198 participants, 417 (9.9%) had MCI. Of these, 163 had amnestic MCI and 254 had non-amnestic MCI. Missing values for determinants of MCI occurred in 268 participants (6.4%) in 2002-2005 (baseline) and in 615 participants (14.6%) in 1997-2001. Participants excluded from the baseline analyses were more often female, suffered more from hypertension, and had a larger waist circumference than participants included in the analyses. Participants excluded due to missing data in 1997-2001 were also more often female and more often hypertensive but had lower cholesterol levels than participants included in our analyses (**Supplementary Table 1**).

At baseline, older age (odds ratio (OR) per 5 year increase in age 1.20, 95% confidence interval (CI) 1.11;1.29), *APOE*-ε4 carriership (OR 1.26, 95% CI 1.00;1.59), lower total cholesterol levels (OR 0.87, 95% CI 0.78;0.98), and stroke (OR 2.12, 95% CI 1.40;3.19) were independently related to MCI (**Table 2**). Male gender and *APOE*-ε4

carriership were only related to amnestic MCI, whereas older age and lower total cholesterol levels were only related to non-amnestic MCI.

Older age (OR per 5 year increase in age 1.18, 95% CI 1.11;1.29), *APOE*-ε4 carriership (OR 1.35, 95% CI 1.06;1.72), lower HDL-cholesterol levels (OR 0.86, 95% CI 0.75;0.98), current smoking (OR 1.49, 95% CI 1.06;2.09) and prevalent stroke (OR 2.50, 95% CI 1.48;4.23) were related to MCI when assessed up to 7 years (mean 4.4 years, SD 0.55) prior to MCI diagnosis (**Table 3**). *APOE*-ε4 carriership and former and current smoking were related to amnestic MCI, whereas older age and lower HDL-cholesterol levels were related to non-amnestic MCI.

Out of 682 participants with MRI scanning, 49 screened positive for MCI. Participants with MCI, particularly those with non-amnestic MCI, had larger WML volumes compared to cognitively healthy participants (mean difference in log-transformed WML volume: 0.36, 95% CI 0.05;0.68). Persons with non-amnestic MCI also had worse microstructural integrity of normal-appearing white matter after adjustments for cardiovascular risk (mean difference in mean FA: -0.007, 95% CI -0.014;-0.001, mean difference in mean MD: 0.013, 95% CI 0.001;0.024) (**Table 4**, model II). As for focal markers of vascular brain pathology, microbleeds were more frequent in persons with MCI, however this association was not significant. Lacunes however, were more frequent in participants with MCI, again particularly in those with non-amnestic MCI (age and sex adjusted OR 3.16, 95% CI 0.98;10.19) (**Table 4**). MRI scanning was performed on average 1.0 years (SD 0.46) after MCI screening. During this time-interval, 12 of 682 participants who underwent MRI were diagnosed with dementia. Out of these, 6 were initially screened as having MCI. Excluding participants with dementia at time of MRI scanning did not change our results (data not shown).

During 24,934 person-years of follow-up, 215 participants developed incident dementia, of whom 177 had Alzheimer's disease. During 29,096 persons-years of follow-up, 827 persons died. Participants with MCI had an increased risk of dementia (age and sex adjusted hazard ratio (HR) 3.98, 95% CI 2.97;5.33) (**Table 5**). The risk of dementia was especially increased in persons with amnestic MCI (HR 6.89, 95% CI 4.74;10.01), but was also increased in persons with non-amnestic MCI (HR 2.65, 95% CI 1.79;3.92). Results were similar for Alzheimer's disease. We found that participants with MCI also had an increased risk of mortality (HR 1.54, 95% CI 1.28;1.85) (**Table 5**). These results did not change across MCI-subtypes and additional adjustments did not change our results.

Table 1. Characteristics of the study population

	Examinations at baseline 2002-2005		Examinations before baseline 1997-2001	
	No MCI N=3,781	**MCI N=417**	**No MCI[a] N=3,730**	**MCI[a] N=401**
Age, years	71.5 (7.1)	73.5 (7.5)	67.1 (7.0)	68.9 (7.4)
Females	58.2%	52.0%	58.1%	51.1%
APOE-ε4 carrier	26.2%	29.7%	26.2%	30.8%
Educational level				
Primary education	16.8%	24.8%	16.4%	23.8%
Lower vocational education	20.2%	22.4%	20.3%	22.5%
Lower secondary education	17.5%	9.2%	17.6%	9.4%
Intermediate vocational education	26.7%	28.2%	26.8%	28.6%
General secondary education	4.6%	1.9%	4.7%	2.0%
Higher vocational education	12.7%	11.4%	12.7%	11.6%
University	1.6%	1.9%	1.6%	2.0%
Waist circumference, cm	93.4 (11.8)	94.6 (12.4)	93.0 (11.5)	94.1 (11.9)
Hypertension	80.6%	83.0%	65.2%	70.9%
Diabetes mellitus	14.1%	19.2%	8.3%	9.6%
Cholesterol, mmol/l	5.65 (1.00)	5.43 (0.96)	5.84 (0.97)	5.75 (0.90)
HDL-cholesterol, mmol/l	1.46 (0.40)	1.41 (0.40)	1.40 (0.39)	1.32 (0.36)
Smoking				
Former	55.1%	55.6%	50.4%	50.6%
Current	15.1%	17.5%	19.0%	23.4%
Stroke	3.4%	8.2%	2.0%	5.0%
MRI imaging markers[b]				
Total brain volume, ml	923.9 (89.6)	906.3 (119.9)	NA	NA
Hippocampal volume, ml	3.0 (0.3)	3.0 (0.4)	NA	NA
White matter lesions, ml	3.5 (2.0-6.5)	4.5 (2.6-12.4)	NA	NA
Fractional anisotropy	0.35 (0.02)	0.34 (0.02)	NA	NA
Mean diffusivity, 10^{-3} mm^2/sec	0.77 (0.05)	0.79 (0.05)	NA	NA
Cerebral microbleeds	20.9%	28.6%	NA	NA
Lacunes	5.7%	16.3%	NA	NA

[a]MCI as assessed at baseline (2002-2005) [b]MR imaging was performed in a randomly selected subset (N=682). Continuous variables are presented as means (standard deviations) and categorical variables as percentages. White matter lesions are presented as median (interquartile range).

Abbreviations: MCI=mild cognitive impairment, N=number of participants, *APOE*=apolipoprotein E, HDL=high-density lipoprotein.

Table 2. Associations between risk factors of dementia and MCI at baseline (cross-sectional).

	MCI	Amnestic MCI	Non-amnestic MCI
	Odds ratio (95% CI) n/N 389/3,541	**Odds ratio (95% CI) n/N 154/3,541**	**Odds ratio (95% CI) n/N 235/3,541**
Age, per 5 years	1.20 (1.11;1.29)	1.04 (0.92;1.17)	1.30 (1.19;1.43)
Females	0.91 (0.70;1.17)	0.66 (0.45;0.98)	1.11 (0.80;1.54)
APOE-ε4 carrier	1.26 (1.00;1.59)	1.43 (1.01;2.02)	1.17 (0.86;1.58)
Waist circumference, per SD	1.04 (0.92;1.18)	1.03 (0.84;1.25)	1.05 (0.90;1.24)
Hypertension	0.94 (0.70;1.25)	1.03 (0.66;1.59)	0.88 (0.61;1.28)
Diabetes mellitus	1.24 (0.93;1.65)	1.44 (0.94;2.20)	1.11 (0.77;1.59)
Cholesterol, per SD	0.87 (0.78;0.98)	0.94 (0.79;1.11)	0.84 (0.73;0.97)
HDL-cholesterol, per SD	0.94 (0.83;1.06)	1.02 (0.84;1.23)	0.88 (0.75;1.04)
Smoking			
Former	0.96 (0.74;1.25)	1.08 (0.71;1.66)	0.90 (0.65;1.25)
Current	1.21 (0.86;1.70)	1.37 (0.81;2.31)	1.13 (0.73;1.74)
Stroke	2.12 (1.40;3.19)	2.68 (1.51;4.76)	1.78 (1.04;3.03)

Values represent odds ratios and 95% confidence intervals, adjusted for all other risk factors.
Abbreviations: MCI=mild cognitive impairment, CI=confidence interval, n=number of cases, N=number of controls, APOE=apolipoprotein E, SD=standard deviation, HDL=high-density lipoprotein.

Table 3. Associations between risk factors of dementia, assessed 7 years prior, and MCI.

	MCI	Amnestic MCI	Non-amnestic MCI
	Odds ratio (95% CI) n/N 348/3,235	**Odds ratio (95% CI) n/N 140/3,235**	**Odds ratio (95% CI) n/N 208/3,235**
Age, per 5 years	1.18 (1.11;1.29)	1.08 (0.95;1.23)	1.25 (1.13;1.38)
Females	0.93 (0.71;1.21)	0.75 (0.50;1.11)	1.08 (0.77;1.51)
APOE-ε4 carrier	1.35 (1.06;1.72)	1.54 (1.08;2.22)	1.23 (0.90;1.69)
Waist circumference, per SD	1.02 (0.90;1.16)	1.02 (0.84;1.24)	1.03 (0.87;1.21)
Hypertension	1.17 (0.90;1.52)	1.00 (0.68;1.45)	1.33 (0.94;1.87)
Diabetes mellitus	1.05 (0.72;1.54)	0.87 (0.46;1.62)	1.16 (0.73;1.84)
Total cholesterol, per SD	0.95 (0.85;1.07)	0.94 (0.78;1.12)	0.96 (0.83;1.11)
HDL-cholesterol, per SD	0.86 (0.75;0.98)	0.95 (0.78;1.16)	0.80 (0.67;0.95)
Smoking			
Former	1.12 (0.84;1.49)	1.66 (1.01;2.73)	0.92 (0.65;1.31)
Current	1.49 (1.06;2.09)	2.45 (1.41;4.24)	1.12 (0.73;1.73)
Stroke	2.50 (1.48;4.23)	2.91 (1.40;6.06)	2.22 (1.14;4.33)

Values represent odds ratios and 95% confidence intervals, adjusted for all other risk factors and additionally for time between measurements and MCI diagnosis. *Abbreviations: MCI=mild cognitive impairment, CI=confidence interval, n=number of cases, N=number of controls, APOE=apolipoprotein E, SD=standard deviation, HDL=high-density lipoprotein.*

Table 4. Association between MCI and MRI markers of brain pathology (cross-sectional).

	Volumetric measures Mean difference (95% CI)			Microstructural integrity measures Mean difference (95% CI)		Focal measures Odds ratio (95% CI)	
Model I	**Total brain**	**Hippocampus**	**WML**	**FA**	**MD**	**Microbleeds**	**Lacunes**
No MCI	Reference	Reference	Reference	Reference	Reference	Reference	Reference
MCI	-6.66 (-15.61;2.28)	0.01 (-0.07;0.08)	0.34 (0.11;0.58)	-0.003 (-0.008;0.001)	0.007 (-0.001;0.016)	1.42 (0.73-2.75)	2.68 (1.11-6.45)
Amnestic	-8.37 (-21.16;4.42)	0.05 (-0.06;0.15)	0.32 (-0.02;0.65)	-0.001 (-0.007;0.006)	0.003 (-0.009;0.016)	1.55 (0.61-3.95)	2.31 (0.69-7.68)
Non-amnestic	-5.04 (-17.10;7.01)	-0.03 (-0.13;0.07)	0.36 (0.05;0.68)	-0.006 (-0.012;0.001)	0.010 (-0.001;0.022)	1.35 (0.55-3.31)	3.16 (0.98-10.19)
Model II	**Total brain**	**Hippocampus**	**WML**	**FA**	**MD**	**Microbleeds**	**Lacunes**
No MCI	Reference	Reference	Reference	Reference	Reference	Reference	Reference
MCI	-6.37 (-15.31;2.57)	-0.01 (-0.08;0.07)	**0.35 (0.11;0.58)**	**-0.004 (-0.009;0.001)**	**0.007 (-0.001;0.016)**	**1.51 (0.77-2.98)**	**2.55 (0.99-6.54)**
Amnestic	-6.78 (-19.57;6.01)	0.04 (-0.07;0.15)	0.21 (-0.13;0.55)	-0.000 (-0.007;0.007)	0.001 (-0.012;0.013)	1.51 (0.58-3.97)	1.77 (0.49-6.36)
Non-amnestic	-5.77 (-17.86;6.32)	-0.03 (-0.13;0.07)	0.46 (0.14;0.78)	-0.007 (-0.014;-0.001)	0.013 (0.001;0.024)	1.55 (0.62-3.89)	3.83 (1.08 13.61)

Model I: adjusted for age and sex.

Model II: adjusted for age, sex, *apolipoprotein E*-ε4 carriership, waist circumference, hypertension, diabetes mellitus, total and high-density lipoprotein cholesterol, and smoking. Model II was a complete case analysis Analyses involving volumetric or microstructural integrity measures were additionally adjusted for intracranial volume.

Volumetric measures were expressed in milliliter (ml), FA has no unit, and MD is expressed in 10^{-3} mm^2/sec. Focal measures were expressed as present versus absent.

Abbreviations: MCI= mild cognitive impairment, MRI=magnetic resonance imaging, CI=confidence interval, WML= white matter lesions volume, FA= fractional anisotropy, MD= mean diffusivity.

Table 5. Associations between MCI and risk of dementia, Alzheimer's disease, and mortality (longitudinal)

	Dementia		Alzheimer's disease		Mortality	
	n/N	Hazard ratio (95% CI)	n/N	Hazard ratio (95% CI)	n/N	Hazard ratio (95% CI)
Model I						
No MCI	149/3,781	Reference	122/3,781	Reference	695/3,781	Reference
MCI	66/417	3.98 (2.97;5.33)	55/417	4.03 (2.92;5.56)	132/417	1.54 (1.28;1.85)
Amnestic MCI	35/163	6.89 (4.74;10.01)	29/163	7.21 (4.77;10.89)	50/163	1.74 (1.30;2.31)
Non-amnestic MCI	31/254	2.65 (1.79;3.92)	26/254	2.69 (1.75;4.12)	82/254	1.44 (1.14;1.81)
Model II						
No MCI	140/3,541	Reference	114/3,541	Reference	653/3,541	Reference
MCI	59/389	3.70 (2.70;5.05)	49/389	3.75 (2.66;5.30)	123/389	1.48 (1.22;1.80)
Amnestic MCI	33/154	6.76 (4.55;10.03)	27/154	7.20 (4.64;11.18)	46/154	1.58 (1.17;2.14)
Non-amnestic MCI	26/235	2.30 (1.50;3.54)	22/235	2.38 (1.49;3.80)	77/235	1.41 (1.12;1.80)

Model I: adjusted for age and sex. Model II: adjusted for age, sex, *apolipoprotein E*-ε4 carriership, waist circumference, hypertension, diabetes mellitus, total and high-density lipoprotein cholesterol, smoking, stroke, and educational level. Values represent hazard ratios and 95% confidence intervals.
Abbreviations: n=number of cases, N=number of persons at risk, CI=confidence interval, MCI=mild cognitive impairment.

DISCUSSION

We found that in the general population, older age, *APOE*-ε4 carriership, lower total cholesterol levels, and prevalent stroke were associated with MCI. Lower HDL-cholesterol levels and current smoking were only related to MCI when assessed up to 7 years prior to MCI screening. Compared to cognitively healthy participants, participants with MCI had larger WML volumes, worse microstructural integrity of normal-appearing white matter, and a higher frequency of lacunes. MCI was associated with an increased risk of dementia, Alzheimer's disease, and mortality.

Major strengths of our study are its population-based setting, large sample size, and extensive data collection. Some limitations of our study need to be considered. Firstly, the extensive neuropsychological test battery required for the MCI diagnosis was implemented in 2002-2005 (baseline), and therefore we were not able to assess MCI status on the examination rounds prior to baseline. Therefore, it is possible that some persons may already have had MCI at the previous examination round. Secondly, the cross-sectional setting in the analyses of risk factors prevented inferring causality. However, the extensive data collection enabled us to investigate determinants both cross-sectionally at baseline and 7 years prior to baseline, overcoming reverse causality in our study. Thirdly, we did not measure visuospatial ability, and could therefore not include this component in our diagnostic criteria for MCI. Finally, MRI scanning was performed on average 1.01 years (SD 0.46) later than the initial screening for

MCI, and misclassification of participants may be present. Nonetheless, 90% of our study participants underwent MRI within 1.5 years of MCI screening, and if present this non-differential misclassification would have led to an underestimation of the true association. Also, we repeated the analyses after excluding incident dementia cases, and found that results did not change materially. We found that some determinants of MCI differed over time. Lower HDL-cholesterol levels and current smoking were only related to MCI when assessed up to 7 years prior to MCI screening. There is a possibility that persons with a declining cognitive ability change their daily habits, including dietary and smoking habits, which could result in reverse causality in cross-sectional analysis. Another explanation is that these associations indeed differ over time, as has been shown for several risk factors for dementia.[4, 40]

In line with previous clinical and population-based studies, we found that people with MCI had larger WML volumes, worse microstructural integrity of normal-appearing white matter, and a higher prevalence of lacunes compared to cognitively healthy participants.[23, 41-43] As regional measurements of DTI were not available in our study, we examined DTI measures averaged over the entire normal appearing white matter. For future investigations however, it would be interesting to study regional differences in FA and MD. MCI was not associated with total brain volume, hippocampal volume, and cerebral microbleeds. These imaging markers have been implicated in persons with MCI before,[44-49] but relatively small sample size hampered our ability to investigate these associations more thoroughly. Also, smaller total brain volume, hippocampal volume and microbleeds may mark more downstream neuropathology and as such would be a better marker for clinical dementia rather than the transitional stage of MCI.[50]

Participants with MCI had an increased risk of dementia and an increased risk of mortality, independently of several risk factors of dementia. Because of this poorer prognosis, our findings underline the importance of identifying persons with MCI.

It is hypothesized that different subtypes of dementia are preceded by different subtypes of MCI. Amnestic MCI is supposed to especially increase the risk of Alzheimer's disease, whereas non-amnestic MCI more likely increases the risk of vascular dementia and other dementia subtypes, such as Lewy body dementia and frontotemporal dementia.[51, 52] This would suggest that determinants might also differ per subtype of MCI. However, our findings propose that this distinction is not as unambiguous. On the one hand, we found that there are indeed some differences in determinants for amnestic and non-amnestic subtypes; e.g. *APOE*-ε4 carriership and smoking were related to amnestic MCI only and MRI-correlates of vascular damage, such as larger WML load, altered diffusion tensor imaging measures, and lacunes, were more strongly related to non-amnestic MCI. On the other hand, we found that persons with MCI who converted to dementia, most often converted to Alzheimer's disease, regardless of

the MCI subtype. Moreover, stroke was related to both subtypes of MCI. Our results therefore suggest that accumulating vascular damage plays a role in both amnestic and non-amnestic MCI. This is consistent with the fact that vascular disease not only plays an important role in vascular dementia, but also in Alzheimer's disease.[2-4, 17, 53, 54] Therefore, we propose that timely targeting modifiable vascular risk factors might contribute to the prevention of MCI and dementia. Nonetheless, it should be kept in mind that the cross-sectional setting of our study in the analyses of risk factors prevents us from drawing any conclusions regarding causality.

We found that persons with amnestic MCI had a larger risk of dementia than persons with non-amnestic MCI. This difference might be a consequence of the definitions of the MCI subtypes. Study participants with amnestic MCI may have experienced difficulties on other cognitive domains besides memory alone, while participants with non-amnestic MCI per definition did not experience any memory problems. Hence, persons with amnestic MCI may have been cognitively more impaired than persons with non-amnestic MCI.

In conclusion, in our population-based study we found that several vascular risk factors and MRI-correlates of cerebrovascular disease were associated with MCI. Persons with MCI had an increased risk of dementia, Alzheimer's disease, and mortality.

CHAPTER REFERENCES

1. Petersen RC, Roberts RO, Knopman DS, Boeve BF, Geda YE, Ivnik RJ, Smith GE, Jack CR, Jr. Mild cognitive impairment: ten years later. Arch Neurol. 2009 Dec;66(12):1447-55.
2. Wiesmann M, Kiliaan AJ, Claassen JA. Vascular aspects of cognitive impairment and dementia. J Cereb Blood Flow Metab. 2013 Nov;33(11):1696-706.
3. Gorelick PB, Scuteri A, Black SE, Decarli C, Greenberg SM, Iadecola C, Launer LJ, Laurent S, Lopez OL, Nyenhuis D, Petersen RC, Schneider JA, Tzourio C, Arnett DK, Bennett DA, Chui HC, Higashida RT, Lindquist R, Nilsson PM, Roman GC, Sellke FW, Seshadri S, American Heart Association Stroke Council CoE, Prevention CoCNCoCR, Intervention, Council on Cardiovascular S, Anesthesia. Vascular contributions to cognitive impairment and dementia: a statement for healthcare professionals from the american heart association/american stroke association. Stroke. 2011 Sep;42(9):2672-713.
4. Duron E, Hanon O. Vascular risk factors, cognitive decline, and dementia. Vasc Health Risk Manag. 2008;4(2):363-81.
5. Farias ST, Mungas D, Reed BR, Harvey D, DeCarli C. Progression of mild cognitive impairment to dementia in clinic- vs community-based cohorts. Arch Neurol. 2009 Sep;66(9):1151-7.
6. Ward A, Arrighi HM, Michels S, Cedarbaum JM. Mild cognitive impairment: disparity of incidence and prevalence estimates. Alzheimers Dement. 2012 Jan;8(1):14-21.
7. Palmer K, Backman L, Winblad B, Fratiglioni L. Mild cognitive impairment in the general population: occurrence and progression to Alzheimer disease. Am J Geriatr Psychiatry. 2008 Jul;16(7):603-11.
8. Ahl RE, Beiser A, Seshadri S, Auerbach S, Wolf PA, Au R. Defining MCI in the Framingham Heart Study Offspring: Education Versus WRAT-based Norms. Alzheimer Dis Assoc Disord. 2013 Oct-Dec;27(4):330-6.
9. Ganguli M, Fu B, Snitz BE, Hughes TF, Chang CC. Mild cognitive impairment: incidence and vascular risk factors in a population-based cohort. Neurology. 2013 Jun 4;80(23):2112-20.
10. Roberts R, Knopman DS. Classification and epidemiology of MCI. Clin Geriatr Med. 2013 Nov;29(4):753-72.
11. Panza F, Frisardi V, Capurso C, Imbimbo BP, Vendemiale G, Santamato A, D'Onofrio G, Seripa D, Sancarlo D, Pilotto A, Solfrizzi V. Metabolic syndrome and cognitive impairment: current epidemiology and possible underlying mechanisms. J Alzheimers Dis. 2010;21(3):691-724.
12. Hofman A, Darwish Murad S, van Duijn CM, Franco OH, Goedegebure A, Ikram MA, Klaver CC, Nijsten TE, Peeters RP, Stricker BH, Tiemeier HW, Uitterlinden AG, Vernooij MW. The Rotterdam Study: 2014 objectives and design update. Eur J Epidemiol. 2013 Nov;28(11):889-926.
13. Ikram MA, van der Lugt A, Niessen WJ, Krestin GP, Koudstaal PJ, Hofman A, Breteler MM, Vernooij MW. The Rotterdam Scan Study: design and update up to 2012. Eur J Epidemiol. 2011 Oct;26(10):811-24.
14. Richard E, Moll van Charante EP, van Gool WA. Vascular risk factors as treatment target to prevent cognitive decline. J Alzheimers Dis. 2012;32(3):733-40.
15. Middleton LE, Yaffe K. Targets for the prevention of dementia. J Alzheimers Dis. 2010;20(3):915-24.
16. Middleton LE, Yaffe K. Promising strategies for the prevention of dementia. Arch Neurol. 2009 Oct;66(10):1210-5.
17. Iadecola C. The pathobiology of vascular dementia. Neuron. 2013 Nov 20;80(4):844-66.

18. Verghese PB, Castellano JM, Holtzman DM. Apolipoprotein E in Alzheimer's disease and other neurological disorders. Lancet Neurol. 2011 Mar;10(3):241-52.
19. Wenham PR, Price WH, Blandell G. Apolipoprotein E genotyping by one-stage PCR. Lancet. 1991 May 11;337(8750):1158-9.
20. Slooter AJ, Cruts M, Kalmijn S, Hofman A, Breteler MM, Van Broeckhoven C, van Duijn CM. Risk estimates of dementia by apolipoprotein E genotypes from a population-based incidence study: the Rotterdam Study. Arch Neurol. 1998 Jul;55(7):964-8.
21. Wieberdink RG, Ikram MA, Hofman A, Koudstaal PJ, Breteler MM. Trends in stroke incidence rates and stroke risk factors in Rotterdam, the Netherlands from 1990 to 2008. Eur J Epidemiol. 2012 Apr;27(4):287-95.
22. Bos D, Vernooij MW, Elias-Smale SE, Verhaaren BF, Vrooman HA, Hofman A, Niessen WJ, Witteman JC, van der Lugt A, Ikram MA. Atherosclerotic calcification relates to cognitive function and to brain changes on magnetic resonance imaging. Alzheimers Dement. 2012 Oct;8(5 Suppl):S104-11.
23. Prins ND, van Dijk EJ, den Heijer T, Vermeer SE, Jolles J, Koudstaal PJ, Hofman A, Breteler MM. Cerebral small-vessel disease and decline in information processing speed, executive function and memory. Brain. 2005 Sep;128(Pt 9):2034-41.
24. Vernooij MW, Ikram MA, Wielopolski PA, Krestin GP, Breteler MM, van der Lugt A. Cerebral microbleeds: accelerated 3D T2*-weighted GRE MR imaging versus conventional 2D T2*-weighted GRE MR imaging for detection. Radiology. 2008 Jul;248(1):272-7.
25. de Boer R, Vrooman HA, van der Lijn F, Vernooij MW, Ikram MA, van der Lugt A, Breteler MM, Niessen WJ. White matter lesion extension to automatic brain tissue segmentation on MRI. Neuroimage. 2009 May 1;45(4):1151-61.
26. van der Lijn F, den Heijer T, Breteler MM, Niessen WJ. Hippocampus segmentation in MR images using atlas registration, voxel classification, and graph cuts. Neuroimage. 2008 Dec;43(4):708-20.
27. Koppelmans V, de Groot M, de Ruiter MB, Boogerd W, Seynaeve C, Vernooij MW, Niessen WJ, Schagen SB, Breteler MM. Global and focal white matter integrity in breast cancer survivors 20 years after adjuvant chemotherapy. Hum Brain Mapp. 2014 Mar;35(3):889-99.
28. Leemans A, Jones DK. The B-matrix must be rotated when correcting for subject motion in DTI data. Magn Reson Med. 2009 Jun;61(6):1336-49.
29. de Groot M, Vernooij MW, Klein S, Leemans A, de Boer R, van der Lugt A, Breteler MM, Niessen WJ. Iterative co-linearity filtering and parameterization of fiber tracts in the entire cingulum. Med Image Comput Comput Assist Interv. 2009;12(Pt 1):853-60.
30. Akoudad S, de Groot M, Koudstaal PJ, van der Lugt A, Niessen WJ, Hofman A, Ikram MA, Vernooij MW. Cerebral microbleeds are related to loss of white matter structural integrity. Neurology. 2013 Oct 30.
31. Wardlaw JM, Smith EE, Biessels GJ, Cordonnier C, Fazekas F, Frayne R, Lindley RI, O'Brien JT, Barkhof F, Benavente OR, Black SE, Brayne C, Breteler M, Chabriat H, Decarli C, de Leeuw FE, Doubal F, Duering M, Fox NC, Greenberg S, Hachinski V, Kilimann I, Mok V, Oostenbrugge R, Pantoni L, Speck O, Stephan BC, Teipel S, Viswanathan A, Werring D, Chen C, Smith C, van Buchem M, Norrving B, Gorelick PB, Dichgans M, nEuroimaging STfRVco. Neuroimaging standards for research into small vessel disease and its contribution to ageing and neurodegeneration. Lancet Neurol. 2013 Aug;12(8):822-38.
32. Vernooij MW, van der Lugt A, Ikram MA, Wielopolski PA, Niessen WJ, Hofman A, Krestin GP, Breteler MM. Prevalence and risk factors of cerebral microbleeds: the Rotterdam Scan Study. Neurology. 2008 Apr 1;70(14):1208-14.

33. Folstein MF, Folstein SE, McHugh PR. "Mini-mental state". A practical method for grading the cognitive state of patients for the clinician. J Psychiatr Res. 1975 Nov;12(3):189-98.
34. Copeland JR, Kelleher MJ, Kellett JM, Gourlay AJ, Gurland BJ, Fleiss JL, Sharpe L. A semi-structured clinical interview for the assessment of diagnosis and mental state in the elderly: the Geriatric Mental State Schedule. I. Development and reliability. Psychol Med. 1976 Aug;6(3):439-49.
35. Roth M, Tym E, Mountjoy CQ, Huppert FA, Hendrie H, Verma S, Goddard R. CAMDEX. A standardised instrument for the diagnosis of mental disorder in the elderly with special reference to the early detection of dementia. Br J Psychiatry. 1986 Dec;149:698-709.
36. American Psychiatric Association: Diagnostic and Statistical Manual of Mental Disorders. 3rd rev. ed.: Washington, DC, American Psychiatric Association 1987.
37. McKhann G, Drachman D, Folstein M, Katzman R, Price D, Stadlan EM. Clinical diagnosis of Alzheimer's disease: report of the NINCDS-ADRDA Work Group under the auspices of Department of Health and Human Services Task Force on Alzheimer's Disease. Neurology. 1984 Jul;34(7):939-44.
38. Leening MJ, Kavousi M, Heeringa J, van Rooij FJ, Verkroost-van Heemst J, Deckers JW, Mattace-Raso FU, Ziere G, Hofman A, Stricker BH, Witteman JC. Methods of data collection and definitions of cardiac outcomes in the Rotterdam Study. Eur J Epidemiol. 2012 Mar;27(3):173-85.
39. Johnson KC, Margolis KL, Espeland MA, Colenda CC, Fillit H, Manson JE, Masaki KH, Mouton CP, Prineas R, Robinson JG, Wassertheil-Smoller S, Women's Health Initiative Memory S, Women's Health Initiative I. A prospective study of the effect of hypertension and baseline blood pressure on cognitive decline and dementia in postmenopausal women: the Women's Health Initiative Memory Study. J Am Geriatr Soc. 2008 Aug;56(8):1449-58.
40. Jokinen H, Lipsanen J, Schmidt R, Fazekas F, Gouw AA, van der Flier WM, Barkhof F, Madureira S, Verdelho A, Ferro JM, Wallin A, Pantoni L, Inzitari D, Erkinjuntti T, Group LS. Brain atrophy accelerates cognitive decline in cerebral small vessel disease: the LADIS study. Neurology. 2012 May 29;78(22):1785-92.
41. van der Flier WM, van Straaten EC, Barkhof F, Ferro JM, Pantoni L, Basile AM, Inzitari D, Erkinjuntti T, Wahlund LO, Rostrup E, Schmidt R, Fazekas F, Scheltens P, group Ls. Medial temporal lobe atrophy and white matter hyperintensities are associated with mild cognitive deficits in non-disabled elderly people: the LADIS study. J Neurol Neurosurg Psychiatry. 2005 Nov;76(11):1497-500.
42. Schmidt R, Ropele S, Enzinger C, Petrovic K, Smith S, Schmidt H, Matthews PM, Fazekas F. White matter lesion progression, brain atrophy, and cognitive decline: the Austrian stroke prevention study. Ann Neurol. 2005 Oct;58(4):610-6.
43. Staekenborg SS, Koedam EL, Henneman WJ, Stokman P, Barkhof F, Scheltens P, van der Flier WM. Progression of mild cognitive impairment to dementia: contribution of cerebrovascular disease compared with medial temporal lobe atrophy. Stroke. 2009 Apr;40(4):1269-74.
44. Kirsch W, McAuley G, Holshouser B, Petersen F, Ayaz M, Vinters HV, Dickson C, Haacke EM, Britt W, 3rd, Larseng J, Kim I, Mueller C, Schrag M, Kido D. Serial susceptibility weighted MRI measures brain iron and microbleeds in dementia. J Alzheimers Dis. 2009;17(3):599-609.
45. Werring DJ, Frazer DW, Coward LJ, Losseff NA, Watt H, Cipolotti L, Brown MM, Jager HR. Cognitive dysfunction in patients with cerebral microbleeds on T2*-weighted gradient-echo MRI. Brain. 2004 Oct;127(Pt 10):2265-75.
46. Pettersen JA, Sathiyamoorthy G, Gao FQ, Szilagyi G, Nadkarni NK, St George-Hyslop P, Rogaeva E, Black SE. Microbleed topography, leukoaraiosis, and cognition in probable Alzheimer disease from the Sunnybrook dementia study. Arch Neurol. 2008 Jun;65(6):790-5.

47. Desikan RS, Cabral HJ, Hess CP, Dillon WP, Glastonbury CM, Weiner MW, Schmansky NJ, Greve DN, Salat DH, Buckner RL, Fischl B, Alzheimer's Disease Neuroimaging I. Automated MRI measures identify individuals with mild cognitive impairment and Alzheimer's disease. Brain. 2009 Aug;132(Pt 8):2048-57.
48. Farias ST, Park LQ, Harvey DJ, Simon C, Reed BR, Carmichael O, Mungas D. Everyday cognition in older adults: associations with neuropsychological performance and structural brain imaging. J Int Neuropsychol Soc. 2013 Apr;19(4):430-41.
49. Jack CR, Jr., Albert MS, Knopman DS, McKhann GM, Sperling RA, Carrillo MC, Thies B, Phelps CH. Introduction to the recommendations from the National Institute on Aging-Alzheimer's Association workgroups on diagnostic guidelines for Alzheimer's disease. Alzheimers Dement. 2011 May;7(3):257-62.
50. Roberts RO, Geda YE, Knopman DS, Cha RH, Pankratz VS, Boeve BF, Tangalos EG, Ivnik RJ, Mielke MM, Petersen RC. Cardiac disease associated with increased risk of nonamnestic cognitive impairment: stronger effect on women. JAMA Neurol. 2013 Mar 1;70(3):374-82.
51. Petersen RC, Morris JC. Mild cognitive impairment as a clinical entity and treatment target. Arch Neurol. 2005 Jul;62(7):1160-3; discussion 7.
52. Daviglus ML, Plassman BL, Pirzada A, Bell CC, Bowen PE, Burke JR, Connolly ES, Jr., Dunbar-Jacob JM, Granieri EC, McGarry K, Patel D, Trevisan M, Williams JW, Jr. Risk factors and preventive interventions for Alzheimer disease: state of the science. Arch Neurol. 2011 Sep;68(9):1185-90.
53. Silvestrini M, Viticchi G, Altamura C, Luzzi S, Balucani C, Vernieri F. Cerebrovascular assessment for the risk prediction of Alzheimer's disease. J Alzheimers Dis. 2012;32(3):689-98.

Supplementary Table 1. Characteristics of the included and excluded participants

	Examinations at baseline 2002-2005		Examinations before baseline 1997-2001	
	Included in analysis N=3,930	**Excluded from analysis N=268**	**Included in analysis N=3,583**	**Excluded from analysis N=615**
Age, years	71.8 (7.2)	71.2 (7.2)	67.5 (7.0)	67.3 (7.0)
Females	57.0%	66.0% [a]	56.3%	64.4% [a]
APOE-ε4 carrier	26.5%	26.3%	26.9%	23.9%
Waist circumference, cm	93.5 (11.8)	94.5 (12.8)[a]	93.0 (12.3)	93.1 (11.5)
Hypertension	80.4%	86.9% [a]	64.9%	72.1% [a]
Diabetes mellitus	14.4%	17.9%	8.6%	7.5%
Cholesterol, mmol/l	5.62 (0.99)	5.79 (1.03)	5.84 (0.96)	5.76 (1.00) [a]
HDL-cholesterol, mmol/l	1.45 (0.40)	1.45 (0.40)	1.40 (0.39)	1.33 (0.36)
Smoking				
Former	55.5%	50.0%	51.2%	44.8%
Current	15.2%	18.3%	19.0%	22.7%
Stroke	3.9%	3.0%	2.3%	1.6%

[a] Significantly different ($p<0.05$) between included participants and excluded participants, after sex and age adjustment – if applicable. Participants excluded from the analysis missed at least one value of the determinants mentioned in the table.

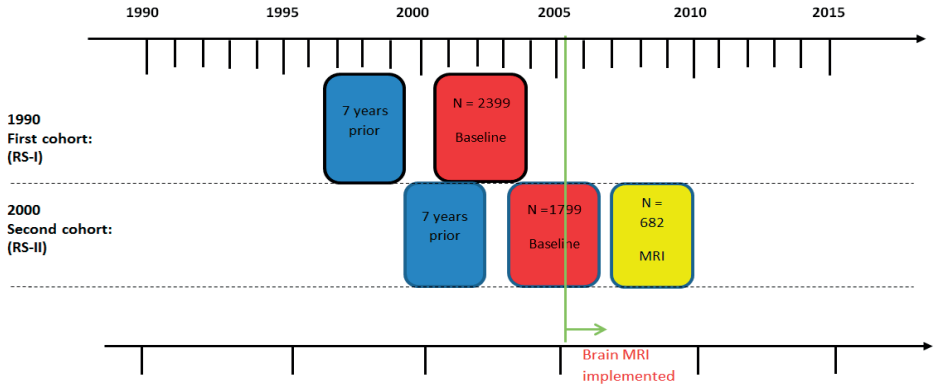

Supplementary Figure 1. Assessment of determinants, MCI and MRI examination
In red: baseline measurement of determinants and MCI assessed in 2002-2005. In blue: measurement of determinants assessed in the examination round 7 years prior to baseline. In yellow: a random subset of 682 persons with MCI screening at baseline and brain MRI examination performed on average 1.01 years after baseline (2005 onwards). Abbreviations: MCI= mild cognitive impairment, MRI=magnetic resonance imaging, RS = Rotterdam Study.

CHAPTER 3.2

Altered tract-specific white matter microstructure is related to poorer cognitive performance. The Rotterdam Study.

Lotte G.M Cremers, Marius de Groot, Albert Hofman, Gabriel P. Krestin, Aad van der Lugt, Wiro J. Niessen, Meike W. Vernooij, M. Arfan Ikram

Neurobiology of Aging 2016

ABSTRACT

White matter microstructural integrity has been related to cognition. Yet, the potential role of specific white matter tracts on top of a global white matter effect remains unclear, especially when considering specific cognitive domains. Therefore, we determined the tract-specific effect of white matter microstructure on global cognition and specific cognitive domains. In 4,400 nondemented and stroke-free participants (mean age 63.7, 55.5% female) we obtained diffusion magnetic resonance imaging parameters (fractional anisotropy and mean diffusivity) in 14 white matter tracts using probabilistic tractography and assessed cognitive performance with a cognitive test battery. Tract-specific white matter microstructure in all supratentorial tracts was associated with poorer global cognition. Lower fractional anisotropy in association tracts, primarily the inferior-fronto-occipital fasciculus, and higher mean diffusivity in projection tracts, in particular the posterior thalamic radiation, most strongly related to poorer cognition. Altered white matter microstructure related to poorer information processing speed, executive functioning, and motor speed, but not to memory. Tract-specific microstructural changes may aid in better understanding the mechanism of cognitive impairment and neurodegenerative diseases.

INTRODUCTION

Brain white matter damage is increasingly recognized as an important factor in the pathophysiology of cognitive impairment and dementia.[1-4] Evidence shows that macrostructural white matter changes, such as white matter lesions, white matter atrophy and lacunes relate to poorer cognitive performance. Studies have already suggested a regional pattern of association between these macrostructural white matter changes and specific cognitive domains.[5-7] At the same time, it is thought that such conventional markers only represent the tip of the iceberg of white matter changes. Focusing on microstructural changes by means of the microstructural integrity of the white matter, may provide a more in-depth insight of alterations in the white matter. Perhaps more importantly, the white matter is not a bulk substance but consists of different white matter tracts, which are important for the connection of different cortical regions.[8] Changes in white matter microstructural integrity are accompanied by changes in diffusion magnetic resonance imaging (diffusion-MRI) parameters. Fractional anisotropy (FA) is generally lower, mean diffusivity (MD) is generally higher (with exceptions) in older or diseased brains, which is thought to reflect reduced white matter microstructure.[9,10]

Altered microstructure of white matter tracts, e.g. as a result of aging or pathologic processes, is presumed to lead to loss of communication between cortical regions, resulting in poorer cognitive performance, the so-called "disconnection hypothesis".[6,11-14] Information processing speed and executive function are the most consistently impaired cognitive functions that have been related to white matter damage.[15-17] However the potential role of specific white matter tracts on top of a global white matter effect in cognitive performance remains unclear, especially when considering specific cognitive domains. It is necessary to investigate these potential roles for specific white matter tracts to elucidate probable mechanism of cognitive impairment and neurodegenerative diseases. Therefore, the purpose of this study was to determine the tract-specific effect of white matter microstructure on global cognition and specific cognitive domains in a large, middle aged and elderly population of 4400 persons from the population-based Rotterdam Study,[18] using diffusion-MRI.

METHODS

Study population

This study is based on participants from the Rotterdam Study, an ongoing, prospective, population-based cohort study including participants of 45 years and older living in Ommoord, a suburb of Rotterdam.[19] From 2005 onwards, MRI-scanning was included in the study protocol.[20] Between 2006 and 2011, 5,430 nondemented participants with-

out contraindications for MRI (including claustrophobia) were eligible for scanning. Among these persons, 4,841 underwent a multi-sequence MRI acquisition of the brain, including diffusion-weighted MRI-scanning. We excluded scans with incomplete acquisitions (N=53), scans with artifacts hampering automated processing (N=112), and scans with MRI-defined cortical infarcts (N=160). We additionally excluded 116 participants with history of clinical stroke. This resulted in 4400 individuals with analyzable MRI data. Of these, 3876 participants had fully available cognition data. MRI-scanning and cognitive assessment took place at the same visit, apart from 677 participants who underwent MRI-scanning on average 1.9 years (standard deviation (SD) 0.6) before cognitive assessment. The Rotterdam Study has been approved by the medical ethics committee according to the Population Study Act Rotterdam Study, executed by the Ministry of Health, Welfare and Sports of the Netherlands. All participants gave written informed consent.

MRI acquisition and processing

We performed multi-sequence MR imaging on a 1.5 tesla MRI scanner (GE Signa Excite), undergoing a QA protocol keeping the system unchanged (no major updates or upgrades) for the period of inclusion. The imaging protocol was described extensively elsewhere.[20] Due to a technical problem between February 2007 and May 2008, 1338 subjects were scanned with the phase and frequency encoding directions swapped for the diffusion acquisition, which led to a mild ghosting artifact in the phase encoding direction.[21] This was treated as a potential confounder in the analysis (see statistical analysis). An automated tissue segmentation approach was used to classify scans into grey matter, white matter, cerebrospinal fluid (CSF) and background tissue. Intracranial volume (ICV) (excluding the cerebellum and surrounding CSF) was estimated by summing total grey and white matter and CSF volumes, and used to correct for head size.[22] White matter lesions (WML) were identified using an automated post-processing step based on the FLAIR image and the tissue segmentation.[23] We visually assessed the presence of infarcts on structural MRI sequences, and in case of involvement of cortical grey matter we classified them as cortical infarcts.

Diffusion-MRI processing and tractography

For diffusion-MRI, we performed a single shot, diffusion-weighted spin echo echo-planar imaging sequence. Maximum b-value was 1000 s/mm^2 in 25 non-collinear directions; three volumes were acquired without diffusion weighting (b-value = 0 s/mm^2). All diffusion data were pre-processed using a standardized pipeline.[24] In short, eddy current and head-motion correction were performed on the diffusion data. The resampled data was used to fit diffusion tensors, allowing (in combination with the

tissue segmentation) computation of global mean FA and MD in the normal-appearing white matter .

The diffusion data was also used to segment white matter tracts using a diffusion tractography approach described previously.[21] For 14 different white matter tracts (11 of which segmented bilaterally) tract-specific white matter microstructural diffusion-MRI parameters (median FA, and MD) were obtained with subsequent combination of left and right measures (**Figure 1**).[21] The average reproducibility of our tract-specific measurements was 87%, which is good.[21] We standardized tract-specific diffusion-MRI parameters (zero mean, unit SD) to facilitate comparison of associations. Tracts were categorized, based on anatomy, into brainstem tracts, projection tracts, association tracts, limbic system tracts and callosal tracts.[21]

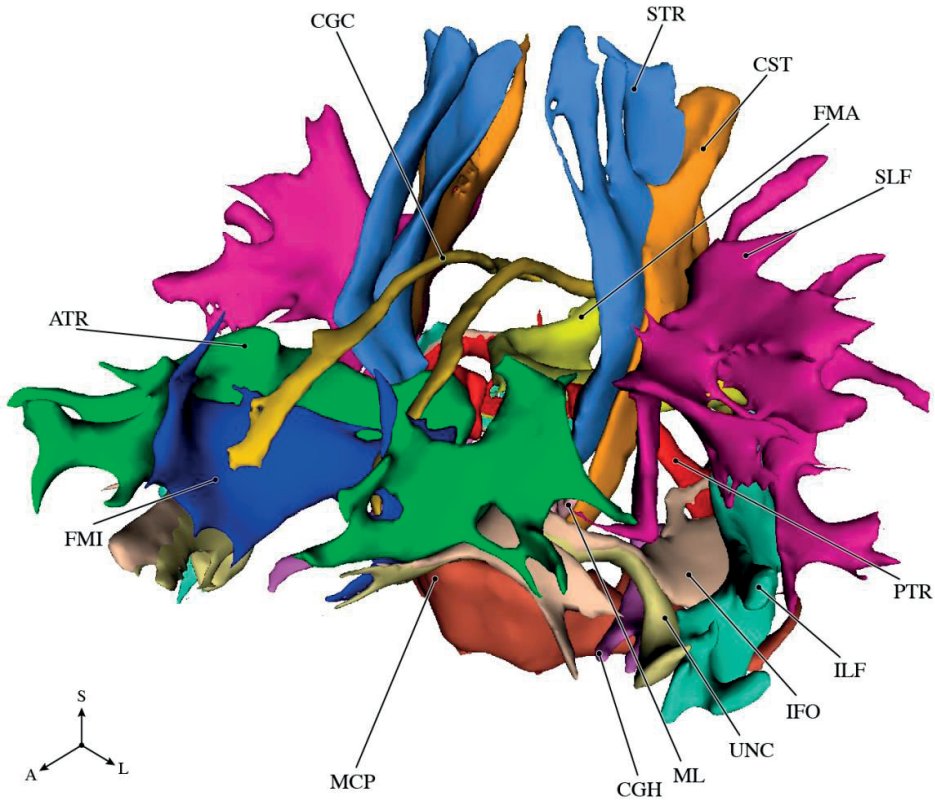

Figure 1. Overview of white matter tracts

Abbreviations: MCP: middle cerebellar peduncle, ML: medial lemniscus, CST: cortico-spinal tract, ATR: anterior thalamic radiation, STR: superior thalamic radiation, PTR: posterior thalamic radiation, SLF: superior longitudinal fasciculus, ILF: inferior longitudinal fasciculus, IFO: inferior-fronto-occipital fasciculus, UNC: uncinated fasciculus, CGC: cingulate gyrus part of cingulum, CGH: parahippocampal part of cingulum, FMA: forceps major, FMI: forceps minor. A=anterior, S=superior, L=lateral.

Tract segmentations were also used to acquire tract-specific white matter volumes, and- by combining the tissue and tract segmentations- tract-specific WML volumes. Tract-specific WML volumes were natural-log transformed, to account for their skewed distribution.
The cerebellum could not be fully incorporated in the field of view of the diffusion-MRI scan, resulting in partial coverage of the medial lemniscus at the lower border of the scan. To overcome this problem alternative seed masks for tractography were selected until reasonable coverage was achieved.[21] This correction was treated as a potential confounder in all models that included the medial lemniscus (see statistical analysis).

Assessment of cognitive function
Cognitive function was assessed in all participants with the following cognitive test battery: 15-Word Learning Test (15-WLT), which tests immediate and delayed recall to investigate memory;[25] Stroop tests (reading, color-naming, interference), which tap into information processing speed and executive function;[26,27] Letter-Digit Substitution Task and[28] Word Fluency Test (WFT);[29], which both test executive function, and the Purdue Pegboard test to measure fine motor speed.[30]
To aid comparison across cognitive tests we generated z-scores for each cognitive test. The z-scores for the Stroop tests were inverted: higher scores on the Stroop test indicate a poorer performance, while higher scores on the other cognitive tests indicate better cognitive performance. In addition, we also investigated global cognition by constructing a g-factor using a principal component analysis on the delayed recall score of the 15-Word Learning Test, Stroop interference Test, Letter-Digit Substitution Task, Word Fluency Test, and the Purdue Pegboard test.[31]

Ascertainment of dementia and clinical stroke
Prevalent dementia and clinical stroke were ascertained as previously described,[32-34] and these patients were excluded.

Other measurements
The following cardiovascular risk factors, based on information derived from home interviews and physical examinations during the center visit, were assessed. Blood pressure was measured twice in sitting position using a random-zero sphygmomanometer and the average of two measurements was used in the analyses. Information on the use of antihypertensive medication was collected by using questionnaires and by checking the medication cabinets of the participants. Total serum cholesterol and high-density lipoprotein (HDL) cholesterol were determined in blood serum, taking lipid-lowering medication into account. Smoking was assessed by interview and coded

as never, former and current. Diabetes mellitus status was determined based on fasting serum glucose level (>= 7.0 mmol/l) or, if unavailable, non-fasting serum glucose level (>=11.1 mmol/l) or the use of anti-diabetic medication.[19] The participants' attained level of education was collected and was categorized into 7 categories, ranging from primary education only to university level.

Missing values on cardiovascular risk factors and education (<3% for all variables) were imputed by multiple imputation (n=5), based on age, sex, education, serum cholesterol level, HDL cholesterol level, systolic blood pressure, diastolic blood pressure, antihypertensive medication, lipid-lowering medication, smoking and diabetes.

Apolipoprotein E (APOE)-ε4 allele carriership was assessed on coded genomic DNA samples.[35] APOE genotype was in Hardy-Weinberg equilibrium.

Statistical analysis

First, we created scatterplots correlating tract-specific diffusion parameters with global cognition (g-factor), adjusted for age and sex, to explore linearity of the associations. Next, associations of tract-specific diffusion measurements with cognitive performance were evaluated using multivariable linear regression models. Standardized betas and 95% confidence intervals (CI) were estimated on standardized FA or MD within each tract. We performed analyses in three models. In model I, analyses were adjusted for age, sex, education, intracranial volume, tract-specific white matter volume, and tract-specific WML volume. In model II we additionally adjusted for cardiovascular risk factors and *APOE-ε4 allele* carriership, to study whether there were pathways relating white matter microstructure to cognition, other than those involving these factors. This is relevant since vascular factors may be considered either confounders or part of the causal chain from vascular factors through white matter microstructure to cognition. We furthermore applied model III, which additionally adjusted for global FA (for analyses with tract-specific FA as determinant) or for global MD (for analyses with tract-specific MD as determinant) on top of model II, to study whether specific tracts provided additional information above global white matter diffusion-MRI parameters. In all analyses, we treated the phase encoding direction of the diffusion scan as a potential confounder. For analyses in which the medial lemniscus was studied we additionally adjusted for the variable position of seed masks, as explained before.

We compared effect sizes across associations of different tracts and cognitive tests using Z-tests ($beta_1$–$beta_2$)/(sqrt(standard $error_1^2$+standard $error_2^2$) to investigate whether the association with cognition in certain tracts was significantly different across tracts. See Supplementary Table A.1 for all betas and standard errors. Moreover, we performed a series of sensitivity analyses, excluding the participants who underwent MRI-scanning on average 1.9 years prior to cognitive assessment, and we also excluded participants with a Mini Mental State Examination (MMSE) lower than 26. We corrected the

p-value (alpha level of 0.05) for multiple comparisons using Šidák correction, after estimating the number of independent tests, resulting in a threshold for significance of $p<0.0006$.[36,37] All analyses were carried out using R version 2.15.0.

RESULTS

Table 1 presents the characteristics of the study population. Mean age of the participants was 63.7 ±11.1 years, and 55.5 % were women. Scatterplots correlating tract-specific diffusion parameters with global cognition (g-factor), adjusted for age and sex are shown in **Supplementary Fig. A.1 & A.2**.

The association of tract-specific diffusion parameters and global cognition is presented in **Table 2** and in **Figure 2**. Lower FA and higher MD in all tracts (except for brainstem tracts) were associated with lower global cognition. For FA, white matter microstructure in the association tracts followed by the callosal tracts was most strongly related with global cognition. After adjusting for cardiovascular risk factors and *APOE-ε4* allele carriership (model II), the mean difference in g-factor (z-score) per SD increase of FA in the association tracts ranged from 0.09 (CI:0.06;0.12) to 0.12 (CI:0.09;0.16), in the callosal tracts from 0.09 (CI:0.05;0.12) to 0.11 (CI:0.08;0.14). For MD, white matter microstructure in the projection tracts, followed by the association tracts was most strongly related with global cognition. Mean difference in z-score for the g-factor per SD increase of MD in the projection tracts, after adjusting for cardiovascular risk factors and *APOE-ε4* allele carriership, ranged from -0.16 (CI:-0.20;-0.13) to -0.18 (CI:-0.22;-0.14), in the association tracts from -0.11 (CI:-0.14;-0.08) to -0.16 (CI:-0.20;-0.12). After controlling for global FA or global MD (model III), the associations attenuated but, the majority of the associations remained significant.

Table 3 presents the associations of white matter microstructure with cognitive performance on separate cognitive tests after adjustment for age, sex, education, intracranial volume, tract-specific white matter volume, tract-specific WML volume, cardiovascular risk factors and *APOE-ε4* allele carriership (model II). Higher values of FA, in all tracts (except the brain stem tracts), but mainly in the inferior fronto-occipital fasciculus, inferior longitudinal fasciculus (association tracts), forceps minor (callosal tract) and the posterior thalamic radiation (projection tract), were generally associated with a better performance on the Stroop tests, Letter-Digit Substitution Task, and the Purdue Pegboard test and to a lesser degree on the Word Fluency Test. Higher values of MD in all tracts, but mainly in the projection tracts, (especially in the posterior thalamic radiation) and in the association tracts, in particular in the inferior fronto-occipital fasciculus were associated with poorer performance on the Stroop tests, Letter-Digit Substitution Task, and the Purdue Pegboard test, and also to a lesser degree on the Word Fluency Test. Additionally adjusting for global FA or global MD

Table 1. Population characteristics

Characteristic	Total (N = 4400)
Age, yrs	63.7 (11.1)
Sex, women	2444 (55.5)
Cognitive tests results[a]	
Word Learning Test immediate recall (sum of 3 trials)	23.3 (6.5)
Word Learning Test delayed recall	7.7 (2.9)
Stroop test	
Reading subtask of Stroop test, s	17.0 (3.4)
Color naming subtask of Stroop test, s	23.2 (4.6)
Interference subtask of Stroop test, s	47.7 (17.2)
Letter-Digit Substitution Task, number of correct digits	30.4 (7.1)
Word Fluency Test, number of animals	23.0 (6.0)
Purdue Pegboard test, number of pins placed	10.5 (1.9)
Education[b]	3 (1-4)
Systolic blood pressure, mmHg	139.3 (21.5)
Diastolic blood pressure, mmHg	83.1 (10.8)
Blood pressure lowering medication	1555 (35.3)
Serum cholesterol, mmol/l	5.5 (1.1)
HDL-cholesterol, mmol/l	1.5 (0.4)
Lipid lowering medication	1231 (28.0)
Smoking	
Never	1363 (31.0)
Former	2130 (48.4)
Current	907 (20.6)
Diabetes mellitus	413 (9.4)
Apolipoprotein E-ε4 allele carriership	1184 (28.8)
Normal appearing white matter volume, ml	404.1 (61.6)
Intra-cranial volume, ml	1340.0 (133.1)
White matter lesion volume[b], ml	2.9 (1.6-6.0)
Mean FA	0.3 (0.02)
Mean MD, 10^{-3} mm^2/sec	0.7 (0.03)

Continuous variables are presented as means (standard deviations) and categorical variables as n (percentages). Data on *apolipoprotein E-ε4 allele* carriership were missing in 287 persons. Global FA and global MD were missing in 173 participants, due to failed segmentation.

[a]Cognitive tests were available for Word Learning Test immediate recall in n=4186, Word Learning Test delayed recall in n=4134, reading subtask of Stroop test in n=4207, color naming subtask of Stroop test in n=4207, interference subtask of Stroop test in n=4200, Letter-Digit Substitution Task in n=4234, Word Fluency Test in n= 4272, and Purdue Pegboard test in n= 4087.

[b]Education and white matter lesion volume are presented as median (inter-quartile range).

Abbreviations: N;number of participants, HDL;high-density lipoprotein, s;seconds, FA;fractional anisotropy, MD;mean diffusivity x 10^{-3} mm^2/sec.

Table 2. Associations of fractional anisotropy and mean diffusivity with global cognition (g-factor)

	Fractional Anisotropy			*Mean Diffusivity*		
White matter tracts	**Model I**	**Model II**	**Model III**	**Model I**	**Model II**	**Model III**
Tracts in brainstem						
Middle cerebellar peduncle	-0.01 (-0.05;0.03)	-0.01 (-0.05;0.03)	-0.01 (-0.05;0.03)	-0.01 (-0.04;0.02)	0.00 (-0.03;0.03)	0.02 (-0.01;0.05)
Medial lemniscus [a]	0.03 (0.00;0.06)	0.03 (0.00;0.06)	0.01 (-0.02;0.05)	**-0.05 (-0.08;-0.02)**	-0.04 (-0.07;-0.01)	0.00 (-0.03;0.03)
Projection tracts						
Corticospinal tract	0.01 (-0.02;0.03)	0.01 (-0.02;0.04)	-0.02 (-0.05;0.01)	**-0.17 (-0.20;-0.13)**	**-0.16 (-0.19;-0.12)**	**-0.11 (-0.17;-0.06)**
Anterior thalamic radiation	**0.07 (0.04;0.10)**	**0.07 (0.04;0.10)**	0.04 (0.00;0.08)	**-0.17 (-0.21;-0.13)**	**-0.16 (-0.20;-0.12)**	**-0.13 (-0.19;-0.07)**
Superior thalamic radiation	0.01 (-0.02;0.04)	0.01 (-0.01;0.04)	-0.02 (-0.05;0.01)	**-0.17 (-0.21;-0.13)**	**-0.16 (-0.20;-0.13)**	**-0.13 (-0.19;-0.07)**
Posterior thalamic radiation	**0.11 (0.08;0.14)**	**0.10 (0.07;0.14)**	**0.09 (0.05;0.13)**	**-0.19 (-0.23;-0.15)**	**-0.18 (-0.22;-0.14)**	**-0.14 (-0.19;-0.09)**
Association tracts						
Superior longitudinal fasciculus	**0.09 (0.06;0.12)**	**0.09 (0.06;0.12)**	0.06 (0.01;0.11)	**-0.13 (-0.16;-0.09)**	**-0.13 (-0.16;-0.09)**	-0.06 (-0.13;0.00)
Inferior longitudinal fasciculus	**0.11 (0.08;0.14)**	**0.10 (0.07;0.13)**	**0.09 (0.05;0.13)**	**-0.14 (-0.18;-0.10)**	**-0.13 (-0.17;-0.10)**	-0.10 (-0.16;-0.04)
Inferior fronto-occipital fasciculus	**0.13 (0.10;0.16)**	**0.12 (0.09;0.16)**	**0.11 (0.07;0.15)**	**-0.17 (-0.20;-0.13)**	**-0.16 (-0.20;-0.12)**	**-0.13 (-0.20;-0.07)**
Uncinate fasciculus	**0.06 (0.03;0.09)**	0.06 (0.02;0.09)	-0.01 (-0.05;0.04)	**-0.11 (-0.14;-0.08)**	**-0.11 (-0.14;-0.08)**	-0.02 (-0.08;0.04)
Limbic system tracts						
Cingulate gyrus part of cingulum	**0.07 (0.05;0.10)**	**0.07 (0.04;0.10)**	0.04 (0.01;0.07)	**-0.09 (-0.11;-0.06)**	**-0.08 (-0.11;-0.05)**	0.00 (-0.04;0.04)
Parahippocampal part of cingulum	**0.05 (0.02;0.08)**	**0.05 (0.02;0.08)**	0.03 (0.00;0.06)	**-0.07 (-0.10;-0.04)**	**-0.07 (-0.10;-0.04)**	-0.03 (-0.06;0.00)
Callosal tracts						
Forceps major	**0.09 (0.06;0.12)**	**0.09 (0.05;0.12)**	0.06 (0.02;0.10)	**-0.12 (-0.16;-0.09)**	**-0.12 (-0.16;-0.08)**	-0.07 (-0.12;-0.02)
Forceps minor	**0.12 (0.09;0.15)**	**0.11 (0.08;0.14)**	0.07 (0.03;0.11)	**-0.15 (-0.18;-0.12)**	**-0.14 (-0.18;-0.11)**	-0.07 (-0.13;-0.02)

Values represent the mean differences in z-score (95% CI) of the g-factor per SD increase of fractional anisotropy or mean diffusivity. Results in bold were significant after correction for multiple testing ($p<6.0*10^{-4}$). Model I: Adjusted for age, sex, education, intracranial volume, WM and log-transformed WML volumes of the investigated tract. Model II: Model I, and additionally adjusted for cardiovascular risk factors (systolic blood pressure, diastolic blood pressure, antihypertensive medication, serum cholesterol, HDL-cholesterol, lipid lowering medication, smoking, diabetes), and *apolipoprotein E-ε4* allele carriership. Model III: Model II, and additionally adjusted for mean global FA or mean global MD.

[a] Additionally adjusted for the variable position of the seed mask.

Abbreviations: g-factor; general cognitive factor (incorporating Word Learning Test delayed recall, interference subtask of Stroop test, Letter-Digit Substitution Test, Word Fluency Test and Purdue Pegboard test), WM; white matter, WML; white matter lesion volume, FA; fractional anisotropy, MD; mean diffusivity x 10^{-3} mm^2/sec. G-factor available in N=3876.

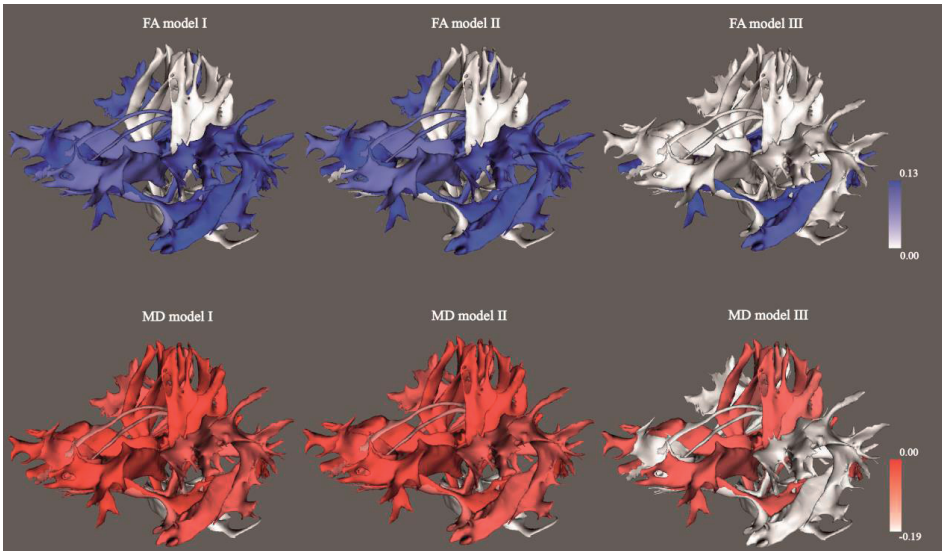

Figure 2. Diffusion-MRI measures and global cognition
Mean differences in z-score of global cognition for all 14 white matter tracts in the population, presented in a single subject anatomy for visualization. Colors reflect the mean differences in z-score per SD increase of FA (row1) or MD (row2), adjusted for age, sex, education, intracranial volume, tract-specific WM volume, and tract-specific WML volume (model I). Model II is model I and additionally adjusted for cardiovascular risk factors, and *apolipoprotein E-ε4* allele carriership. Model III adjusts for global FA or global MD on top of model II.
Higher strength of association is depicted in darker blue for positive associations, darker red for negative associations, with non-significant associations displayed in white.
Abbreviations: FA; fractional anisotropy, MD; mean diffusivity, ICV; intracranial volume, WM; white matter, WML; white matter lesion.

(**Table 4**) attenuated most of the associations, but the majority of the projection and association tracts remained significant, with again the strongest associations for the inferior fronto-occipital fasciculus and the posterior thalamic radiation. We did not find any association between tract-specific microstructure and memory (15-Word Learning Tests). Overall, the effect sizes of the projection, association and callosal tracts with the different cognitive tests were significantly larger than the effect sizes of the brain stem and the limbic system (data not shown). This was particularly true for the posterior thalamic radiation and the inferior fronto-occipital fasciculus, which showed strongest effects among all tracts.
Excluding 677 participants who underwent MRI-scanning on average 1.9 years prior to cognitive assessment yielded similar findings (data not shown). Also, excluding participants with a Mini Mental State Examination lower than 26 yielded similar results (data not shown). There was no significant interaction between the microstructure of any of the tracts and *APOE-ε4* allele carriership after correction for multiple testing.

Table 3. Associations of tract-specific fractional anisotropy and mean diffusivity with separate cognitive tests

White matter tracts FA	Immediate memory	Delayed memory	Stroop 1	Stroop 2	Stroop 3	LDST	Word Fluency	Pudue Pegboard
Brainstem tracts								
Middle cerebellar peduncle	0.01	0.01	-0.03	-0.01	0.03	0.01	-0.02	0.02
Medial lemniscus[a]	0.01	0.01	0.04	0.03	0.01	0.05	0.04	-0.01
Projection tracts								
Corticospinal tract	-0.02	-0.01	0.00	0.02	0.01	0.03	-0.01	0.01
Anterior thalamic radiation	0.03	0.02	0.05	0.08	0.07	0.07	0.02	0.05
Superior thalamic radiation	0.00	0.01	0.01	0.02	0.03	0.02	0.00	0.01
Posterior thalamic radiation	0.01	-0.01	0.06	0.09	0.10	0.12	0.05	0.12
Association tracts								
Superior longitudinal fasciculus	0.01	0.00	0.09	0.10	0.10	0.09	0.04	0.09
Inferior longitudinal fasciculus	0.01	-0.01	0.07	0.10	0.11	0.10	0.05	0.09
Inferior fronto-occipital fasciculus	0.01	-0.01	0.10	0.12	0.12	0.13	0.09	0.11
Uncinate fasciculus	-0.01	-0.01	0.03	0.05	0.05	0.06	0.03	0.05
Limbic system tracts								
Cingulate gyrus part of cingulum	0.00	-0.03	0.06	0.09	0.09	0.07	0.04	0.05
Parahippocampal part of cingulum	-0.01	0.00	0.04	0.05	0.06	0.03	0.08	0.04
Callosal tracts								
Forceps major	0.03	0.01	0.08	0.08	0.09	0.08	0.05	0.09
Forceps minor	0.01	0.00	0.10	0.13	0.11	0.11	0.05	0.11
MD								
Brainstem tracts								
Middle cerebellar peduncle	0.00	0.00	-0.01	-0.01	-0.04	-0.01	0.00	0.01
Medial lemniscus[a]	0.01	0.01	0.00	-0.02	-0.06	0.05	-0.02	-0.01
Projection tracts								
Corticospinal tract	-0.04	-0.03	-0.09	-0.13	-0.13	-0.15	-0.10	-0.13
Anterior thalamic radiation	-0.05	-0.05	-0.10	-0.13	-0.16	-0.14	-0.10	-0.10
Superior thalamic radiation	-0.03	-0.03	-0.10	-0.13	-0.15	-0.15	-0.10	-0.12
Posterior thalamic radiation	-0.05	-0.04	-0.11	-0.16	-0.18	-0.16	-0.11	-0.13
Association tracts								
Superior longitudinal fasciculus	-0.01	-0.02	-0.09	-0.11	-0.12	-0.13	-0.07	-0.09
Inferior longitudinal fasciculus	-0.03	-0.02	-0.09	-0.12	-0.15	-0.12	-0.08	-0.10
Inferior fronto-occipital fasciculus	-0.04	-0.03	-0.11	-0.14	-0.17	-0.14	-0.10	-0.14
Uncinate fasciculus	0.01	-0.01	-0.04	-0.07	-0.10	-0.11	-0.07	-0.08
Limbic system tracts								
Cingulate gyrus part of cingulum	0.01	0.01	-0.02	-0.04	-0.07	-0.07	-0.05	-0.06
Parahippocampal part of cingulum	-0.02	-0.04	-0.01	-0.02	-0.07	-0.04	-0.06	-0.02
Callosal tracts								
Forceps major	-0.01	-0.02	-0.09	-0.08	-0.11	-0.10	-0.07	-0.09
Forceps minor	-0.03	-0.03	-0.09	-0.13	-0.13	-0.14	-0.09	-0.13

Values represent the mean differences in Z-score of each cognitive test per SD increase of fractional anisotropy or mean diffusivity. The colored cells represent significant associations surviving multiple testing ($p<6.0*10^{-4}$) and the intensity in red and blue reflects the magnitude of the associations whereby darker colors reflect stronger associations. Results are adjusted for age, sex, education, intracranial volume, WM and log-transformed WML volumes of the investigated tract, cardiovascular risk factors (systolic blood pressure, diastolic blood pressure, antihypertensive medication, serum cholesterol, HDL-cholesterol, lipid lowering medication, smoking, diabetes, and *apolipoprotein E-ε4* allele carriership.[a] Additionally adjusted for the variable position of the seed mask.
Abbreviations: LDST;Letter-Digit Substitution Task, SD; standard deviation, WM; white matter, WML;white matter volume, HDL; high-density lipoprotein.
Abbreviations of diffusion measurements: FA. fractional anisotropy; MD. mean diffusivity x 10^{-3} mm^2/sec.

Table 4. Associations of tract-specific fractional anisotropy and mean diffusivity with separate cognitive tests adjusted for global DTI

White matter tracts FA	Immediate memory	Delayed memory	Stroop 1	Stroop 2	Stroop 3	LDST	Word Fluency	Purdue Pegboard
Brainstem tracts								
Middle cerebellar peduncle	0.02	0.02	-0.03	-0.01	0.03	0.01	-0.02	-0.03
Medial lemniscus[a]	0.01	0.01	0.03	0.01	-0.01	0.03	0.03	-0.03
Projection tracts								
Corticospinal tract	-0.02	-0.01	-0.03	-0.02	-0.02	0.00	-0.01	-0.02
Anterior thalamic radiation	0.04	0.04	0.03	0.05	0.04	0.04	0.01	0.00
Superior thalamic radiation	0.00	0.01	-0.01	-0.01	0.01	0.00	-0.01	-0.03
Posterior thalamic radiation	0.02	0.00	0.04	0.06	0.08	0.10	0.05	0.08
Association tracts								
Superior longitudinal fasciculus	-0.01	0.01	0.07	0.08	0.06	0.08	0.05	0.05
Inferior longitudinal fasciculus	0.02	0.00	0.04	0.07	0.11	0.10	0.05	0.06
Inferior fronto-occipital fasciculus	0.01	-0.01	0.09	0.10	0.10	0.12	0.11	0.08
Uncinate fasciculus	-0.04	-0.02	-0.02	-0.02	-0.01	0.00	0.02	-0.01
Limbic system tracts								
Cingulate gyrus part of cingulum	-0.01	-0.03	0.03	0.06	0.06	0.05	0.03	0.01
Parahippocampal part of cingulum	-0.02	-0.01	0.03	0.03	0.04	0.01	0.07	0.02
Callosal tracts								
Forceps major	0.02	0.02	0.06	0.05	0.07	0.05	0.06	0.05
Forceps minor	-0.01	-0.01	0.07	0.08	0.07	0.08	0.03	0.07
MD								
Brainstem tracts								
Middle cerebellar peduncle	0.01	0.00	0.00	0.00	-0.02	0.01	0.01	0.02
Medial lemniscus[a]	0.01	0.01	0.02	0.02	-0.03	0.00	-0.01	0.03
Projection tracts								
Corticospinal tract	-0.05	-0.04	-0.11	-0.09	-0.11	-0.10	-0.08	-0.11
Anterior thalamic radiation	-0.09	-0.08	-0.10	-0.10	-0.18	-0.09	-0.08	-0.08
Superior thalamic radiation	-0.06	-0.06	-0.12	-0.11	-0.17	-0.10	-0.09	-0.10
Posterior thalamic radiation	-0.06	-0.06	-0.11	-0.14	-0.18	-0.10	-0.10	-0.09
Association tracts								
Superior longitudinal fasciculus	-0.01	-0.05	-0.08	-0.06	-0.09	-0.06	-0.06	-0.05
Inferior longitudinal fasciculus	-0.04	-0.06	-0.10	-0.08	-0.19	-0.05	-0.04	-0.07
Inferior fronto-occipital fasciculus	-0.08	-0.09	-0.13	-0.11	-0.20	-0.06	-0.10	-0.13
Uncinate fasciculus	0.04	-0.01	0.01	0.03	-0.03	-0.02	-0.03	-0.01
Limbic system tracts								
Cingulate gyrus part of cingulum	0.05	0.03	0.05	0.06	0.00	0.02	-0.02	0.01
Parahippocampal part of cingulum	-0.02	-0.06	0.01	0.02	-0.04	0.02	-0.04	0.00
Callosal tracts								
Forceps major	-0.02	-0.02	-0.09	-0.04	-0.09	-0.04	-0.06	-0.04
Forceps minor	-0.03	-0.05	-0.07	-0.07	-0.06	-0.06	-0.03	-0.11

Values represent the mean differences in Z-score of each cognitive test per SD increase of fractional anisotropy or mean diffusivity. The colored cells represent significant associations surviving multiple testing ($p<6.0*10^{-4}$), and the intensity in red and blue reflects the magnitude of the associations whereby darker colors reflect stronger associations. Results are adjusted for age, sex, education, intracranial volume, WM and log-transformed WML volumes of the investigated tract, cardiovascular risk factors (systolic blood pressure, diastolic blood pressure, antihypertensive medication, serum cholesterol, HDL-cholesterol, lipid lowering medication, smoking, diabetes, *apolipoprotein E-ε4* allele carriership, and additionally for global DTI parameters (global FA or global MD).[a] Additionally adjusted for the variable position of the seed mask. *Abbreviations:* LDST;Letter-Digit Substitution Task, SD; standard deviation, WM; white matter, WML;white matter volume, HDL; high-density lipoprotein. *Abbreviations of diffusion measurements:* FA. fractional anisotropy; MD. mean diffusivity x 10^{-3} mm^2/sec.

DISCUSSION

In this study among middle-aged and elderly persons, altered tract-specific white matter microstructure in all supratentorial tracts, was associated with poorer cognitive performance, independent from age and macrostructural white matter pathology. Specifically, we found that these associations were driven by lower FA and higher MD, which have been suggested to reflect reduced white matter microstructural integrity.[10] Altered supratentorial tract-specific white matter microstructure was related to poorer information processing speed, executive function and motor speed, but not to memory. We found tract-specific differences for associations with cognitive function: among the fourteen white matter tracts the microstructural integrity in the posterior thalamic radiation (projection tract) and the inferior fronto-occipital fasciculus (association tract) were most strongly associated with cognitive performance.

Strengths of this study include the large sample size and the population-based setting. Furthermore, we performed a tract-specific analysis in fourteen main white matter tracts, and, the tract-specific measurements were performed with fully automated, publicly available methods.[38] Some limitations need to be considered. Due to the cross-sectional design, no conclusions can be drawn on the directionality of causality of the associations. Furthermore, the evaluation of cognitive performance in this study is less extensive compared to some other studies. However, we constructed a g-factor as a marker of global cognition using 5 different cognitive test variables, under the assumption that these tests are representative of various cognitive domains. This facilitates comparison with other studies, even when the incorporated cognitive tests are slightly different, since g-factors constructed of different cognitive tests across different test batteries are highly correlated and can be interpreted as stable factors in a variety of cognitive domains.[39] We performed a complete-case analysis to construct a g-factor and this might have caused some selection bias, as persons who did not have values for all cognitive tests were not included. Another aspect to note is that we used median FA and MD in each white matter tract. While the median is more robust to variation in the tails of the measurement distributions compared to the mean, capturing an entire tract in a single measurement discards spatial information that is retained in voxel-based techniques. Finally, the cerebellum could not be fully incorporated in the field of view, making analyses on brain stem tracts less reliable. Several papers have studied the association of white matter microstructure and cognition.[6,40-42] A global white matter effect has already been associated with cognition. The main novelty of our paper is that we show that tract-specific diffusion MRI measures (when adjusted for global diffusion-MRI measures) provide more information above global diffusion-MRI measures. Furthermore, by using a cognitive test battery rather than a single test, our study is not limited to a specific cognitive domain.

In a previous study investigating the association of age and white matter microstructure, in the same community-dwelling population, a widespread altered (except for the sensorimotor tracts, including brainstem tracts) white matter microstructural integrity with age was found.[21] In extension to this study, we now demonstrate that altered microstructural integrity of the same supratentorial tracts is associated with poorer cognitive performance, independent from age and cardiovascular risk factors. Also, after excluding participants with possible mild cognitive impairment (MMSE<26), the associations remained significant. The association between tract-specific white matter microstructure and global cognition was particularly driven by information processing speed, executive function and motor speed, but not by memory. Only few tract-specific studies investigated the association of microstructural integrity of brain white matter with cognition in asymptomatic participants.[43-49] Some studies concluded that white matter throughout the brain was associated with cognitive performance and reported no specific role for any white matter tract.[49] Other studies found a tract-specific effect in which altered microstructural integrity in association and callosal tracts associated with poorer information processing speed and executive function,[43-45,47,48] and with poorer motor speed,[45] which is in line with our findings. However, some previous studies associated altered tract-specific white matter microstructure with memory, in contrast to our results.[45,46,50] Our study differs from these studies in that we investigated a larger sample, and we took white matter atrophy and white matter lesion volume into account, and thus adjusted for macrostructural white matter changes, which may have driven the association with memory function in previous research. Furthermore, other studies incorporated different memory tests and cognitive domains (e.g. impaired error monitoring) and different white matter tracts (e.g. fornix).[50]

We did not find similar associations with cognitive function across all tracts. We found the strongest associations between white matter microstructure and cognition in the posterior thalamic radiation and the inferior-occipital fasciculus. This is largely in line with previous studies performed in specific patient-populations such as in secondary-progressive multiple sclerosis, subcortical ischemic vascular disease,[51,52] and coronary artery disease.[16] We can hypothesize on the basis of this finding using the previously described 'disconnection hypothesis'[53]. The posterior thalamic radiation connects the thalamus with the posterior parietal and occipital lobe[54] and plays a key role connecting visual and motor processes. The inferior fronto-occipital fasciculus connects frontal cortical regions with posterolateral temporal and occipital regions and is involved in language function and in visual spatial function which influences coordinative abilities.[45,55] Information processing speed and executive function are partly dependent on language function and on visual capabilities; motor speed depends on coordinative abilities. Damage to the tracts integrating these processes may therefore lead to poorer cognitive performance in these domains.

The role of *APOE-ε4* allele carriership in white matter microstructural integrity and cognition is still under debate. We found no significant interaction between *APOE-ε4* allele carriership and white matter microstructural integrity in the association with cognition, in line with previous studies.[56,57] This may indicate that although *APOE-ε4* allele carriership is a major genetic risk factor for cognitive impairment and Alzheimer's disease, this may not be mediated by altered white matter microstructural integrity. Lower values of FA in the association tracts were most strongly associated with poorer cognitive performance. In contrast, higher values of MD in the projections tracts were most strongly associated with impaired cognition. The disparity in associations between FA, MD and cognitive performance might indicate that FA and MD reflect different pathophysiology. The lack of specificity in the interpretation of diffusion-MRI parameters prevents clear-cut conclusions on the exact mechanisms underlying the changes in diffusion-MRI parameters. It can be hypothesized that FA is dominated by tract coherence and axonal loss, and MD by (volume of) extracellular fluid.[6,9] Apart from a biological difference, MD seems to be more sensitive to changes in regions with crossing tracts,[58] and since voxels of projection tracts (corticospinal tract, superior thalamic radiation) contain large volumes of crossing-tract anatomy, this might explain part of the disparity observed.[21] Our observation that after adjustments for global diffusion parameters, the various associations remained significant, at least indicates that there is variation in tracts beyond global diffusion-MRI parameters, and suggests local or functional differences in patterns of white matter neurodegeneration.

Conclusions

In conclusion, tract-specific diffusion-MRI parameters provide insight into the association between white matter tracts and cognitive performance beyond global diffusion-MRI parameters. This study provides novel etiological insight into the relation of the location of brain damage and cognitive performance; in other words it provides insight in which tract influences which specific cognitive domain. Second, our findings may also have clinical implications. For instance, knowledge on tract-specific effects on cognition may inform clinicians to predict which cognitive domains may be most affected depending on the location of a stroke. Finally, given the importance of recognizing pathways leading to cognitive impairment and dementia, our results may aid in developing new biomarkers for cognitive impairment and neurodegenerative diseases and may lead to better recognition of persons at risk**.**

CHAPTER REFERENCES

1. Pievani M, Agosta F, Pagani E, et al. Assessment of white matter tract damage in mild cognitive impairment and Alzheimer's disease. *Hum Brain Mapp.* 2010;31(12):1862-1875.
2. Sexton CE, Kalu UG, Filippini N, Mackay CE, Ebmeier KP. A meta-analysis of diffusion tensor imaging in mild cognitive impairment and Alzheimer's disease. *Neurobiol Aging.* 2011;32(12):2322 e2325-2318.
3. Wang Y, West JD, Flashman LA, et al. Selective changes in white matter integrity in MCI and older adults with cognitive complaints. *Biochim Biophys Acta.* 2012;1822(3):423-430.
4. Brun A, Englund E. A white matter disorder in dementia of the Alzheimer type: a pathoanatomical study. *Ann Neurol.* 1986;19(3):253-262.
5. Benjamin P, Lawrence AJ, Lambert C, et al. Strategic lacunes and their relationship to cognitive impairment in cerebral small vessel disease. *Neuroimage Clin.* 2014;4:828-837.
6. Vernooij MW, Ikram MA, Vrooman HA, et al. White matter microstructural integrity and cognitive function in a general elderly population. *Arch Gen Psychiatry.* 2009;66(5):545-553.
7. Smith EE, O'Donnell M, Dagenais G, et al. Early cerebral small vessel disease and brain volume, cognition, and gait. *Ann Neurol.* 2015;77(2):251-261.
8. Doricchi F, Thiebaut de Schotten M, Tomaiuolo F, Bartolomeo P. White matter (dis)connections and gray matter (dys)functions in visual neglect: gaining insights into the brain networks of spatial awareness. *Cortex.* 2008;44(8):983-995.
9. Maclullich AM, Ferguson KJ, Reid LM, et al. Higher systolic blood pressure is associated with increased water diffusivity in normal-appearing white matter. *Stroke.* 2009;40(12):3869-3871.
10. Beaulieu C. The basis of anisotropic water diffusion in the nervous system - a technical review. *NMR Biomed.* 2002;15(7-8):435-455.
11. O'Sullivan M, Jones DK, Summers PE, Morris RG, Williams SC, Markus HS. Evidence for cortical "disconnection" as a mechanism of age-related cognitive decline. *Neurology.* 2001;57(4):632-638.
12. Salat DH, Tuch DS, Greve DN, et al. Age-related alterations in white matter microstructure measured by diffusion tensor imaging. *Neurobiol Aging.* 2005;26(8):1215-1227.
13. Teipel SJ, Grothe MJ, Filippi M, et al. Fractional anisotropy changes in Alzheimer's disease depend on the underlying fiber tract architecture: a multiparametric DTI study using joint independent component analysis. *J Alzheimers Dis.* 2014;41(1):69-83.
14. Nazeri A, Chakravarty MM, Rajji TK, et al. Superficial white matter as a novel substrate of age-related cognitive decline. *Neurobiol Aging.* 2015;36(6):2094-2106.
15. Zhang R, Liu K, Yang L, et al. Reduced white matter integrity and cognitive deficits in maintenance hemodialysis ESRD patients: a diffusion-tensor study. *Eur Radiol.* 2015;25(3):661-668.
16. Santiago C, Herrmann N, Swardfager W, et al. White Matter Microstructural Integrity Is Associated with Executive Function and Processing Speed in Older Adults with Coronary Artery Disease. *Am J Geriatr Psychiatry.* 2015;23(7):754-763.
17. Tuladhar AM, van Norden AG, de Laat KF, et al. White matter integrity in small vessel disease is related to cognition. *Neuroimage Clin.* 2015;7:518-524.
18. Hofman A, Brusselle GG, Darwish Murad S, et al. The Rotterdam Study: 2016 objectives and design update. *Eur J Epidemiol.* 2015;30(8):661-708.
19. Hofman A, Brusselle GG, Darwish Murad S, et al. The Rotterdam Study: 2016 objectives and design update. *Eur J Epidemiol.* 2015;28(11):889-926.
20. Ikram MA, van der Lugt A, Niessen WJ, et al. The Rotterdam Scan Study: design and update up to 2012. *Eur J Epidemiol.* 2011;26(10):811-824.

21. de Groot M, Ikram MA, Akoudad S, et al. Tract-specific white matter degeneration in aging: The Rotterdam Study. *Alzheimer's & dementia : the journal of the Alzheimer's Association.* 2015;11(3):321-330.
22. Vrooman HA, Cocosco CA, van der Lijn F, et al. Multi-spectral brain tissue segmentation using automatically trained k-Nearest-Neighbor classification. *Neuroimage.* 2007;37(1):71-81.
23. de Boer R, Vrooman HA, van der Lijn F, et al. White matter lesion extension to automatic brain tissue segmentation on MRI. *Neuroimage.* 2009;45(4):1151-1161.
24. Koppelmans V, de Groot M, de Ruiter MB, et al. Global and focal white matter integrity in breast cancer survivors 20 years after adjuvant chemotherapy. *Hum Brain Mapp.* 2014;35(3):889-899.
25. Bleecker ML, Bolla-Wilson K, Agnew J, Meyers DA. Age-related sex differences in verbal memory. *J Clin Psychol.* 1988;44(3):403-411.
26. Golden CJ. Identification of brain disorders by the Stroop Color and Word Test. *J Clin Psychol.* 1976;32(3):654-658.
27. Goethals I, Audenaert K, Jacobs F, et al. Cognitive neuroactivation using SPECT and the Stroop Colored Word Test in patients with diffuse brain injury. *J Neurotrauma.* 2004;21(8):1059-1069.
28. Lezak MD. Neuropsychological assessment in behavioral toxicology--developing techniques and interpretative issues. *Scand J Work Environ Health.* 1984;10 Suppl 1:25-29.
29. Welsh KA, Butters N, Mohs RC, et al. The Consortium to Establish a Registry for Alzheimer's Disease (CERAD). Part V. A normative study of the neuropsychological battery. *Neurology.* 1994;44(4):609-614.
30. Desrosiers J, Hebert R, Bravo G, Dutil E. The Purdue Pegboard Test: normative data for people aged 60 and over. *Disabil Rehabil.* 1995;17(5):217-224.
31. Hoogendam YY, Hofman A, van der Geest JN, van der Lugt A, Ikram MA. Patterns of cognitive function in aging: the Rotterdam Study. *Eur J Epidemiol.* 2014;29(2):133-140.
32. Roth M, Tym E, Mountjoy CQ, et al. CAMDEX. A standardised instrument for the diagnosis of mental disorder in the elderly with special reference to the early detection of dementia. *Br J Psychiatry.* 1986;149:698-709.
33. Schrijvers EM, Verhaaren BF, Koudstaal PJ, Hofman A, Ikram MA, Breteler MM. Is dementia incidence declining?: Trends in dementia incidence since 1990 in the Rotterdam Study. *Neurology.* 2012;78(19):1456-1463.
34. Akoudad S, Portegies ML, Koudstaal PJ, et al. Cerebral Microbleeds are Associated With an Increased Risk of Stroke: The Rotterdam Study. *Circulation.* 2015;132(6):509-516.
35. Wenham PR, Price WH, Blandell G. Apolipoprotein E genotyping by one-stage PCR. *Lancet.* 1991;337(8750):1158-1159.
36. Nyholt DR. A simple correction for multiple testing for single-nucleotide polymorphisms in linkage disequilibrium with each other. *Am J Hum Genet.* 2004;74(4):765-769.
37. Nyholt DR. Evaluation of Nyholt's procedure for multiple testing correction - author's reply. *Hum Hered.* 2005;60(1):61-62.
38. de Groot M, Vernooij MW, Klein S, et al. Improving alignment in Tract-based spatial statistics: evaluation and optimization of image registration. *NeuroImage.* 2013;76:400-411.
39. Johnson W, te Nijenhuis J, Bouchard TJ. Still just 1 g: Consistent results from five test batteries. *Intelligence.* 2008;36(1):81-95.
40. Penke L, Munoz Maniega S, Murray C, et al. A general factor of brain white matter integrity predicts information processing speed in healthy older people. *J Neurosci.* 2010;30(22):7569-7574.

41. Burzynska AZ, Wong CN, Voss MW, Cooke GE, McAuley E, Kramer AF. White matter integrity supports BOLD signal variability and cognitive performance in the aging human brain. *PLoS One.* 2015;10(4):e0120315.
42. Metzler-Baddeley C, Jones DK, Steventon J, Westacott L, Aggleton JP, O'Sullivan MJ. Cingulum microstructure predicts cognitive control in older age and mild cognitive impairment. *J Neurosci.* 2012;32(49):17612-17619.
43. Salami A, Eriksson J, Nilsson LG, Nyberg L. Age-related white matter microstructural differences partly mediate age-related decline in processing speed but not cognition. *Biochim Biophys Acta.* 2012;1822(3):408-415.
44. Ystad M, Hodneland E, Adolfsdottir S, et al. Cortico-striatal connectivity and cognition in normal aging: a combined DTI and resting state fMRI study. *Neuroimage.* 2011;55(1):24-31.
45. Voineskos AN, Rajji TK, Lobaugh NJ, et al. Age-related decline in white matter tract integrity and cognitive performance: a DTI tractography and structural equation modeling study. *Neurobiol Aging.* 2012;33(1):21-34.
46. Charlton RA, Barrick TR, McIntyre DJ, et al. White matter damage on diffusion tensor imaging correlates with age-related cognitive decline. *Neurology.* 2006;66(2):217-222.
47. Lopez-Oloriz J, Lopez-Cancio E, Arenillas JF, et al. Diffusion tensor imaging, intracranial vascular resistance and cognition in middle-aged asymptomatic subjects. *Cerebrovasc Dis.* 2014;38(1):24-30.
48. Laukka EJ, Lovden M, Kalpouzos G, et al. Associations between white matter microstructure and cognitive performance in old and very old age. *PLoS One.* 2013;8(11):e81419.
49. Kuznetsova KA, Maniega SM, Ritchie SJ, et al. Brain white matter structure and information processing speed in healthy older age. *Brain Struct Funct.* 2015.
50. Metzler-Baddeley C, Jones DK, Belaroussi B, Aggleton JP, O'Sullivan MJ. Frontotemporal connections in episodic memory and aging: a diffusion MRI tractography study. *J Neurosci.* 2011;31(37):13236-13245.
51. Lin L, Xue Y, Duan Q, et al. Microstructural White Matter Abnormalities and Cognitive Dysfunction in Subcortical Ischemic Vascular Disease: an Atlas-Based Diffusion Tensor Analysis Study. *J Mol Neurosci.* 2015;56(2):363-370.
52. Yu HJ, Christodoulou C, Bhise V, et al. Multiple white matter tract abnormalities underlie cognitive impairment in RRMS. *Neuroimage.* 2012;59(4):3713-3722.
53. Hogan AM, Vargha-Khadem F, Saunders DE, Kirkham FJ, Baldeweg T. Impact of frontal white matter lesions on performance monitoring: ERP evidence for cortical disconnection. *Brain.* 2006;129(Pt 8):2177-2188.
54. Aralasmak A, Ulmer JL, Kocak M, Salvan CV, Hillis AE, Yousem DM. Association, commissural, and projection pathways and their functional deficit reported in literature. *J Comput Assist Tomogr.* 2006;30(5):695-715.
55. Schmahmann JD, Smith EE, Eichler FS, Filley CM. Cerebral white matter: neuroanatomy, clinical neurology, and neurobehavioral correlates. *Ann N Y Acad Sci.* 2008;1142:266-309.
56. Wang R, Fratiglioni L, Laukka EJ, et al. Effects of vascular risk factors and APOE epsilon4 on white matter integrity and cognitive decline. *Neurology.* 2015;84(11):1128-1135.
57. Nyberg L, Salami A. The APOE epsilon4 allele in relation to brain white-matter microstructure in adulthood and aging. *Scand J Psychol.* 2014;55(3):263-267.
58. Jeurissen B, Leemans A, Tournier JD, Jones DK, Sijbers J. Investigating the prevalence of complex fiber configurations in white matter tissue with diffusion magnetic resonance imaging. *Hum Brain Mapp.* 2013;34(11):2747-2766.

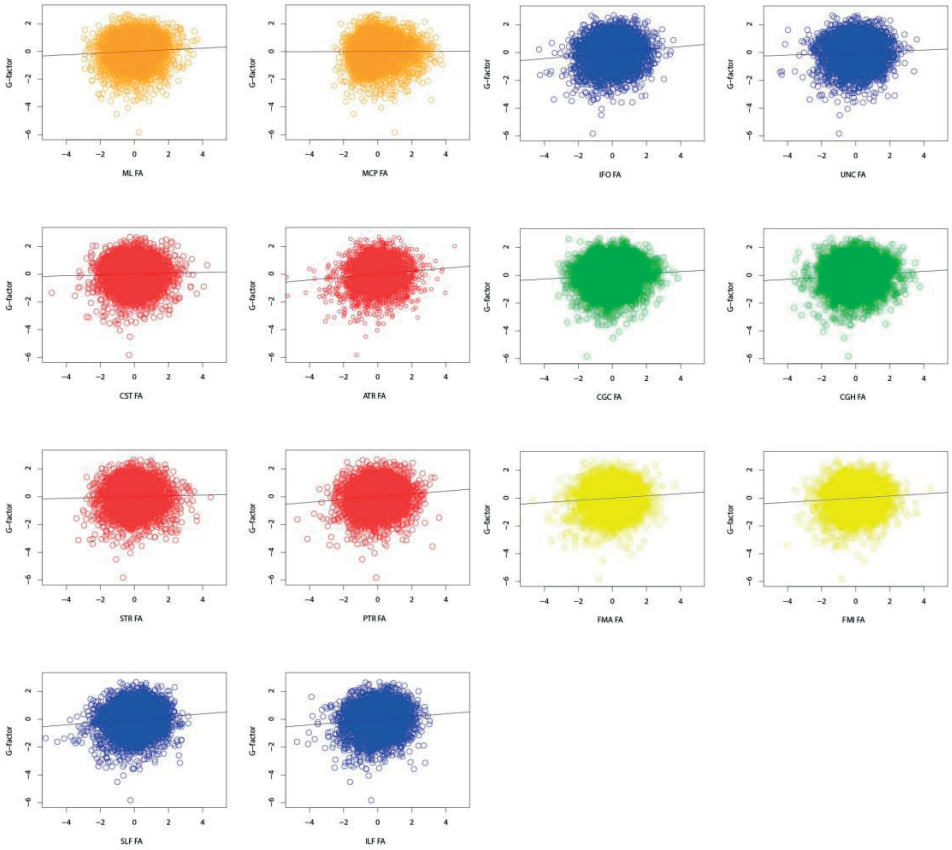

Supplementary Figure A1 Scatterplot correlating tract-specific fractional anisotropy with global cognition (g-factor), adjusted for age and sex.

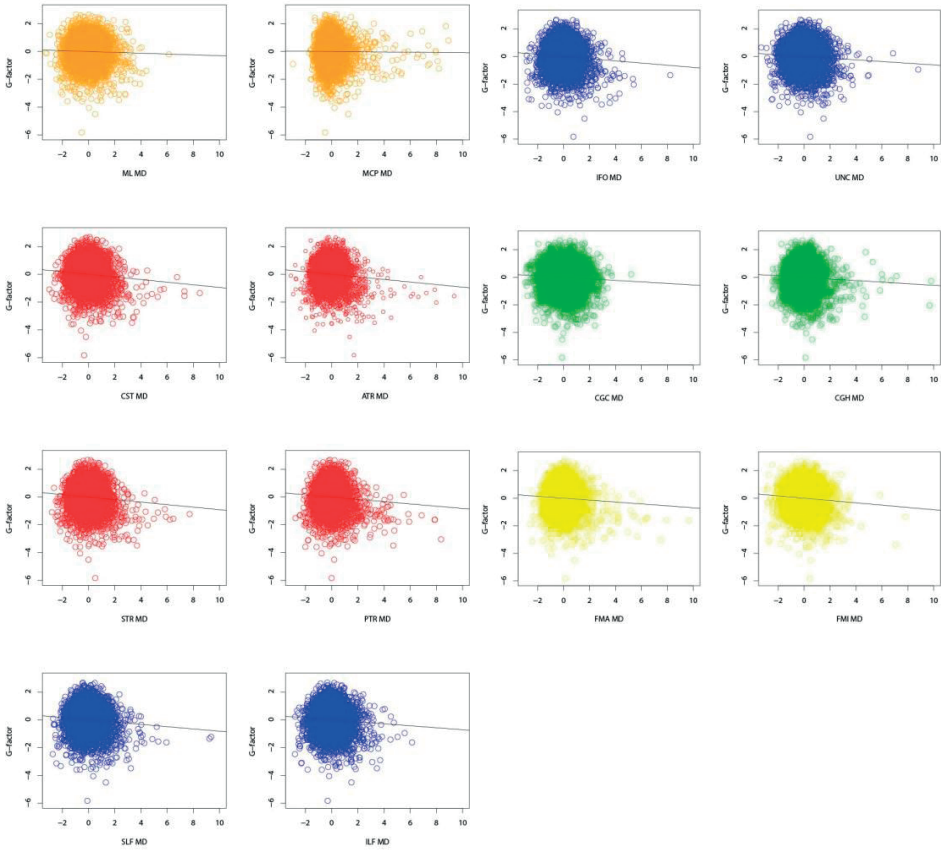

Supplementary Figure A2. Scatterplot correlating tract-specific mean diffusivity with global cognition (g-factor), adjusted for age and sex.

CHAPTER 3.3

Structural connectivity relates to risk of dementia in the general population: evidence for the disconnectivity hypothesis

Lotte G.M. Cremers, F.J. Wolters, Marius de Groot, M. Kamran Ikram, Aad van der Lugt, Wiro J. Niessen, Meike W. Vernooij*, M. Arfan Ikram*

Submitted

**Denotes shared last author*

ABSTRACT

Background The 'disconnectivity hypothesis' postulates that partial loss of connecting white matter fibers between brain regions contributes to the development of dementia, including Alzheimer's disease (AD). Using diffusion-magnetic resonance imaging (MRI) to quantify global and tract-specific white matter microstructural integrity, we tested this hypothesis in a longitudinal population-based setting.

Method Global and tract-specific measures of fractional anisotropy (FA) and mean diffusivity (MD) were obtained in 4,415 non-demented persons (mean age 63.9 years (SD 11.0), 55.0% women) from the prospective population-based Rotterdam Study with brain MRI (2005-2011). We modelled the association of these diffusion measures with risk of dementia (follow-up until 2016), and with changes on repeated cognitive assessment over 5.4 years of follow-up, adjusting for age, sex, education, macrostructural MRI markers, depressive symptoms, cardiovascular risk factors, and *APOE* genotype.

Findings During a mean follow-up of 6.7 years, 101 participants had incident dementia, of whom 83 had AD. Lower global values of FA and higher values of MD associated with an increased risk of dementia (adjusted hazard ratio (95% confidence interval) per standard deviation increase in MD: 1.79 (1.44-2.23)). Similarly, lower global values of FA and higher values of MD related to more cognitive decline in non-demented individuals (difference in global cognition per standard deviation increase in MD (95% CI) was: -0.04 (-0.07;-0.01)). Associations were most profound in the projection, association and limbic system tracts.

Interpretations Structural disconnectivity is associated with and an increased risk of dementia and more pronounced cognitive decline in the general population.

Funding Internationale Stichting Alzheimer Onderzoek, European Union Seventh Framework Programma,VPH-Dare@IT and the STW perspectief programme Population Imaging Genetics (ImaGene).

INTRODUCTION

Dementia is among the leading causes of death and disability worldwide, and its socioeconomic burden on society will continue to increase as the number of persons suffering from dementia is predicted to nearly triple to 131.5 million in 2050.[1] Effective preventive and curative interventions are urgently needed, but their development and timely application is hampered by incomplete understanding of pathophysiology, lack of markers that can identify changes in the very early, subclinical stages of disease and lack of prognostic markers. Subclinical brain changes are thought to occur years, if not decades, prior to onset of clinical symptoms,[2] which is beyond the scope of currently applied subclinical macrostructural imaging markers of neurodegeneration, such as hippocampal volume and presence of white matter hyperintensities.

One of the recent insights in dementia is that brain damage can lead to disruption of brain networks, so called disconnectivity.[3-5] Disconnectivity, which can be investigated using diffusion-magnetic resonance imaging (MRI), seems to occur prior to changes in conventional structural MRI markers such as white matter hyperintensities load in dementia,[6] and is thought to reflect early cerebral white matter damage.[7,8] Previous studies have shown more pronounced disconnectivity both in patients with dementia compared to healthy controls,[9,10] and in relation to more rapid progression in patients with Alzheimer's disease (AD).[11] However, evidence from longitudinal studies for a role of preclinical disconnectivity in the development of dementia is scarce. Two clinical studies among patients with small vessel disease found that network disruption increases the risk of dementia,[12,13] but these studies were hampered by limited precision (observing 18 and 32 cases of dementia, respectively), and it remains undetermined whether findings extend to the wider population without prior TIA or stroke.

Therefore, we aimed to test the disconnectivity hypothesis by investigating whether global and tract-specific disconnectivity are associated with dementia and cognitive decline in a population-based setting.

METHODS

Study population

This study was embedded within the Rotterdam Study, a population-based cohort study including participants of 45 years and older living in Ommoord, a suburb of Rotterdam.[14] The study started in 1990 with 7,983 participants and was extended with 3,011 participants in 2000 and with 3,932 participants in 2006. Participants were examined at baseline with a home interview and an extensive set of examinations in the research center. Follow-up examinations were repeated every 3-4 years. Also, all participants were continuously monitored through electronic linkage of the study

database with their own medical records. All details of the study have been previously described.[14] From 2005 onwards, MRI-scanning was implemented in the core protocol. Between 2005 and 2011, 5,715 participants without contraindications for MRI (metal implants, pacemaker, claustrophobia) were eligible for scanning, of whom 4,888 (86%) underwent a multi-sequence MRI acquisition of the brain, and 4,813 (98%) participants completed the diffusion-weighted sequences. We excluded 245 individuals due to technical scanning issues, e.g. failed segmentations, as well as 38 participants with prevalent dementia and 100 participants with insufficient dementia screening at baseline, resulting in a study sample of 4,430 individuals. Of these individuals, 4,317 persons had detailed cognitive assessment at baseline and 3,402 (79%) had repeated assessment during follow-up examination after on average 5.4 (SD 0.6) years. The Rotterdam Study has been approved by the medical ethics committee according to the Population Study Act Rotterdam Study, executed by the Ministry of Health, Welfare and Sports of the Netherlands. All participants gave written informed consent.

MRI acquisition and processing

Multi-sequence MR imaging was performed on a 1.5 tesla MRI scanner (GE Signa Excite). The imaging protocol has been described extensively elsewhere.[15] The conventional scan protocol consisted of a T1-weighted image, a T2-weighted fluid-attenuated inversion recovery (FLAIR) sequence, and a proton density weighted image.

Scans were spatially co-registered using rigid registration. Scans were segmented with an automated tissue segmentation approach into grey matter, white matter, cerebrospinal fluid (CSF) and background tissue,[16,17] followed by a white matter hyperintensity (WMH) segmentation based on the tissue segmentation and the FLAIR image.[18] Supratentorial intracranial volume (ICV), to correct for head size, was estimated by summing total grey and white matter and CSF volumes.[17] We visually assessed the presence of infarcts on conventional MRI sequences, and in case of involvement of cortical grey matter we classified these as cortical infarcts.

Diffusion-MRI processing and tractography

For diffusion-MRI, we performed a single shot, diffusion-weighted spin echo echo-planar imaging sequence. Maximum b-value was 1000 s/mm^2 in 25 non-collinear directions; three volumes were acquired without diffusion weighting (b-value = 0 s/mm^2). All diffusion data were pre-processed using a standardized pipeline.[19] In short, eddy current and head-motion correction were performed on the diffusion data. The resampled data was used to fit diffusion tensors to compute mean fractional anisotropy (FA) and mean diffusivity (MD) in the normal-appearing white matter, through combination with the tissue segmentation. The diffusion data was also used to segment white matter tracts using a diffusion tractography approach described previously.[20]

We segmented 15 different white matter tracts (12 bilateral, 3 singular) and obtained mean FA and MD in these tracts, with subsequent combination of left and right measures.[20] In general, lower FA and higher MD values are considered indicative of lower microstructural integrity and as such reflecting disconnectivity. Missing data for tract-specific measurements due to tractography or segmentation failures were limited to 33-78 participants (0.8-1.8%) per tract. Tracts were categorized, based on anatomy or presumed function, into brainstem tracts (middle cerebellar peduncle, medial lemniscus), projection tracts (corticospinal tract, anterior thalamic radiation, superior thalamic radiation, posterior thalamic radiation), association tracts (superior longitudinal fasciculus, inferior, longitudinal fasciculus, inferior fronto-occipital fasciculus, uncinated fasciculus), limbic system tracts (cingulate gyrus part of cingulum, parahippocampal part of cingulum) and callosal tracts (forceps major, forceps minor).[20]
We obtained tract volumes and tract WMH volumes by combining the tissue and tract segmentations. Tract-specific WMH volumes were natural-log transformed, to account for their skewed distribution.
Between February 2007 and May 2008, an erroneous swap of the phase and frequency encoding directions for the diffusion acquisition led to a mild ghosting artifact, which was addressed by adjustment in the analysis.[20] There was only partial coverage of one of the brainstem tracts (medial lemniscus) due to incomplete coverage of the cerebellum in the field of view, and we used alternative seed masks for tractography and adjustment in the model to overcome this problem.[20]

Dementia screening and surveillance
All participants were screened for dementia at baseline and during subsequent center visits using the Mini-Mental-State Examination (MMSE) and the Geriatric Mental Schedule (GMS) organic level.[21] Participants with an MMSE score <26 or a GMS score >0 underwent further cognitive examination and informant interview, including the Cambridge Examination for Mental Disorders of the Elderly. In addition, the entire cohort was under continuous surveillance for dementia through electronic linkage of the study database with medical records from general practitioners and the regional institute for outpatient mental health care. Clinical neuroimaging was used when required for dementia subtype diagnosis. A consensus panel led by a consultant neurologist established the final diagnosis in accordance with standard criteria for dementia (DSM-III-R) and Alzheimer's disease (NINCDS-ADRDA). Follow-up until 1st January 2016 was virtually complete (96% of potential person years). Participants were censored at date of dementia diagnosis, death, loss to follow-up, or 1st January 2016, whichever came first.

Assessment of cognitive function

During center visits, all participants underwent routine cognitive assessment comprising a word fluency test (number of animal species within 1 minute), 15-word learning test (immediate and delayed recall of 15 items), letter-digit substitution task (LDST, number of correct digits in 1 minute), Stroop test (error adjusted time in seconds taken for completing the reading, colour naming, and interference tasks), and the Purdue Pegboard task for manual dexterity.[21] To obtain a composite measure of test performance, we calculated the G-factor by principal component analysis,[21] which explained 49-54% of variance in cognitive test scores at each examination round in our population. For each participant, Z-scores were calculated for each test separately, by dividing the difference between individual test score and population mean by the population standard deviation. Scores for the Stroop tasks were inverted such that higher scores indicated better performance.

Other measurements

Information on smoking habits, educational attainment, and use of antihypertensive and lipid-lowering medication was ascertained at baseline by structured questionnaires. Blood pressure was measured twice in sitting position using a random-zero sphygmomanometer and the mean of two readings was used in the analyses. Total serum cholesterol and high-density lipoprotein (HDL) cholesterol were determined in fasting blood samples. Presence of type 2 diabetes at baseline was determined on the basis of fasting serum glucose level (>= 7.0 mmol/l) or, if unavailable, non-fasting serum glucose level (>=11.1 mmol/l) or the use of anti-diabetic medication.[22] Body-mass index (BMI) was calculated, dividing weight in kilograms by the squared height in meters. History of stroke was assessed by interview, and verified in medical records, and participants were continuously monitored for incident stroke through computerized linkage of medical records from general practitioners and nursing home physicians with the study database. We used the validated Dutch version of the Center for Epidemiology Depression Scale (CES-D) for assessment of depressive symptoms.[23]
APOE genotype was determined using polymerase chain reaction on coded DNA samples (original cohort), and using a bi-allelic TaqMan assay (rs7412 and rs429358; expansion cohort). In 179 participants with missing *APOE* status from this blood sampling, genotype was determined by genetic imputation (Illumina 610K and 660K chip; imputation with Haplotype Reference Consortium reference panel [v1.0] with Minimac 3).

Statistical analysis

Analyses included all eligible participants, with the exception of 15 participants whose diffusion measures deviated >7 standard deviations from the mean, leaving 4,415

participants for analysis. We used Cox proportional hazard models to determine the association of global and tract-specific diffusion-MRI measures (FA and MD) with incident dementia. The proportional hazard assumption was met. We assessed risk of dementia per standard deviation increase in FA and MD. We repeated the analyses 1) for Alzheimer disease only, 2) after excluding participants with prevalent stroke while censoring at time of incident stroke, 3) excluding persons with MRI-defined, subclinical cortical infarcts at baseline, and 4) stepwise excluding the first five years of follow-up from the analysis.

We then determined the association of global and tract-specific diffusion-MRI measures with change in cognitive performance using linear regression models. Cognitive test scores at follow-up were adjusted for baseline cognitive test results. These analyses were repeated after exclusion of all participants who developed dementia during follow-up. All models were adjusted for age, sex, education, intracranial volume, white matter volume, and the log-transformed volume of white matter hyperintensities and the correction for swapping gradients and varying field of view (model I), and additionally for education, depressive symptoms (CES-D score), and cardiovascular risk factors (systolic blood pressure, diastolic blood pressure, antihypertensive medication, serum cholesterol, HDL-cholesterol, lipid-lowering medication, diabetes, smoking, and BMI), and *APOE*-ε4 allele carriership (model II).

For the tract-specific analyses, we corrected the p-value (alpha level of 0.05) for multiple comparisons with the number of independent tests on the basis of the variance of the eigenvalues of the correlation matrix of all 30 variables used in the main analysis (i.e. FA and MD for the 15 tracts). The following formula was used: M_{eff}= 1 +(M-1)(1-var (λ_{obs})/M) in which M is the number of variables, λ_{obs} is the variance of the eigenvalues of the correlation matrix,and M_{eff} is the number of independent variables.[24,25] This resulted in an M_{eff} of 17.45, which then, using the Šidák formula (α sidak = 1 - ((1 - α)^(1/M_{eff}))), translated into a significance level of $p<0.0029$ for the tract-specific analyses with dementia as outcome.[24]

For the analyses assessing global diffusion-MRI measures with the separate cognitive tests as outcome, the above-mentioned method generated a significance level of $p<0.008$. For analyses assessing tract-specific diffusion-MRI measures with global cognition and separate cognitive tests as outcome, the adjusted p-value was $p<0.0022$. All analyses were carried out using SPSS Statistics 21.0 (IBM Corp, Armonk, NY, USA) or R version 3.0.3 (packages “GenABEL”, “survival, “stargazer” and “data. table”).

RESULTS

Table 1 presents the baseline characteristics of the study population. Mean age of the 4,415 participants was 63.9 years (SD ±11.1 years), and 55.0% were women. During a median follow-up of 6.8 years (IQR 5.8-8 .0 years), 101 persons developed dementia, of whom 83 had AD.

Table 1. Population characteristics

Characteristic	N= 4,415
Age, years	63.9 (±11.0)
Female	2,426 (55.0 %)
Smoking	
Never	1367 (31.0%)
Former	2120 (48.0%)
Current	928 (21.0%)
Education	
Lower education	1266 (28.7%)
Middle education	2107 (47.7%)
Higher education	1042 (23.6%)
Systolic blood pressure, mmHg	140.0 (±21.5)
Diastolic blood pressure, mmHg	83.2 (±10.9)
Antihypertensive medication	1573 (35.6)
Total cholesterol, mmol/L	5.5 (±1.1)
HDL cholesterol, mmol/L	1.5 (±0.4)
Lipid-lowering medication	1113 (25.2%)
Diabetes mellitus	531 (12.0%)
BMI, kg/m^2	27.4 (±4.1)
Center for Epidemiology Depression Scale score	8 (2-12)
APOE-ε4 carriership	1216 (28.3%)
Mean FA	0.34 (±0.02)
Mean MD	0.74 (±0.03)
Intracranial volume, mL	1142.0 (±116.4)
White matter volume, mL	409.3 (±60.7)
White matter hyperintensities volume, mL	2.90 (1.6-6.3)

Continuous variables are presented as means (±standard deviations) and categorical variables as n (percentages), except for white matter hyperintensities volume and Center for Epidemiology Depression Scale score, which are presented as median (inter-quartile range).
Abbreviations: N:number of participants, HDL:high-density lipoprotein, BMI: body mass index, s;seconds, FA:fractional anisotropy, MD:mean diffusivity x 10^{-3} mm^2/sec, mL: milliliter.

Lower microstructural integrity, reflected in lower values of global FA and higher values of global MD was associated with a higher risk of dementia (fully adjusted hazard ratio [HR], 95% confidence interval (CI), per SD increase in FA: 0.65 (0.52-0.80), and for MD: 1.79 (1.44-2.23) (**Figure 1, Supplementary Table S1**). Results were similar for AD only, and unaltered after excluding participants with prevalent stroke while censoring at time of incident stroke, or excluding participants with subclinical MRI-defined cortical infarcts (**Figure 1, Supplementary Table S1**). Stepwise exclusion of the first five years of follow-up from the analysis did not alter the risk estimates (**Figure 2, Supplementary Table S2**).

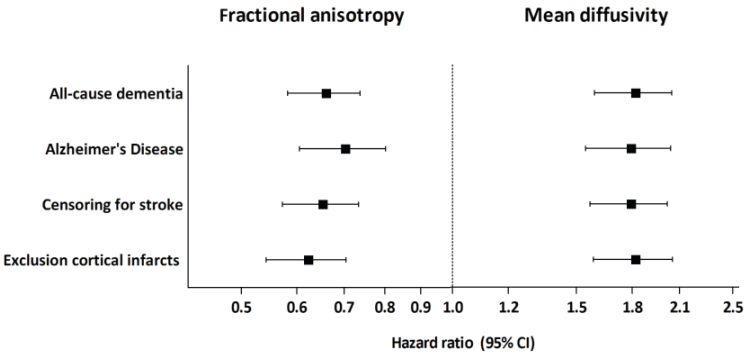

Figure 1. Global mean microstructural integrity and incident dementia

In tract-specific analyses, the strongest associations with dementia risk were observed for MD in the projection tracts, association tracts and limbic system tracts (per SD increase HR of 2.35 (1 .53;3.62) for the superior thalamic radiation, 1.79 (1.36;2.37) for the inferior fronto-occipital fasciculus, and 1.62 (1.41;1.86) for the parahippocampal part of the cingulum respectively (**Table 2, Figure 3**)). Similarly, lower FA in the association tracts and in the limbic system tracts were most profoundly associated

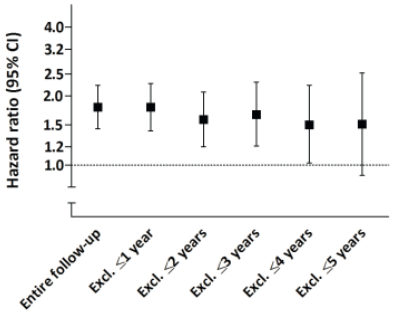

Figure 2. Global mean diffusivity and incident dementia, with stepwise exclusion of the first five years of follow-up

with a higher risk of dementia (per SD increase HR 0.59 (0.45;0.76) for the uncinated fasciculus and HR 0.67 (0.53;0.84) for the parahippocampal part of the cingulum, respectively, in the fully adjusted model (**Table 2**)).

Table 2. Tract-specific white matter microstructure and incident dementia

	Fractional Anisotropy		*Mean Diffusivity*	
White matter tracts	**Model I**	**Model II**	**Model I**	**Model II**
Brainstem tracts				
Middle cerebellar peduncle	1.05 (0.85;1.30)	1.08 (0.87;1.35)	1.05 (0.85;1.30)	1.04 (0.83;1.30)
Medial lemniscus	1.09 (0.86;1.39)	1.11 (0.86;1.44)	1.06 (0.88;1.28)	1.06 (0.87;1.29)
Projection tracts				
Corticospinal tract	1.17 (0.95;1.44)	1.19 (0.96;1.47)	**1.52 (1.13;2.06)**	**1.52 (1.11;2.08)**
Anterior thalamic radiation	0.85 (0.66;1.09)	0.87 (0.67;1.13)	**1.68 (1.23;2.30)***	**1.73 (1.26;2.38)***
Superior thalamic radiation	1.17 (0.95;1.45)	1.20 (0.97;1.50)	**2.29 (1.49;3.52)***	**2.35 (1.53;3.62)***
Posterior thalamic radiation	**0.69 (0.52;0.90)**	**0.74 (0.56;0.97)**	**1.41 (1.15;1.72)***	**1.42 (1.15;1.75)***
Association tracts				
Superior longitudinal fasciculus	0.77 (0.60;1.00)	0.79 (0.60;1.04)	**1.65 (1.30;2.11)***	**1.65 (1.28;2.14)***
Inferior longitudinal fasciculus	0.79 (0.62;1.01)	0.84 (0.65;1.09)	**1.73 (1.36;2.21)***	**1.69 (1.31;2.18)***
Inferior fronto-occipital fasciculus	**0.66 (0.50;0.86)***	**0.71 (0.53;0.93)**	**1.75 (1.34;2.27)***	**1.79 (1.36;2.37)***
Uncinate fasciculus	**0.60 (0.47;0.77)***	**0.59 (0.45;0.76)***	**1.67 (1.39;2.00)***	**1.73 (1.42;2.10)***
Limbic system tracts				
Cingulate gyrus part of cingulum	0.69 (0.54;0.87)	**0.71 (0.55;0.90)**	**1.55 (1.26;1.92)***	**1.58 (1.26;1.97)***
Parahippocampal part of cingulum	**0.67 (0.54;0.84)***	**0.67 (0.53;0.84)***	**1.61 (1.41;1.85)***	**1.62 (1.41;1.86)***
fornix	**0.76 (0.59;0.99)**	0.78 (0.60;1.02)	1.13 (0.80;1.58)	1.06 (0.75;1.50)
Callosal tracts				
Forceps major	**0.77 (0.59;1.00)**	0.79 (0.61;1.04)	1.15 (0.93;1.41)	1.12 (0.90;1.38)
Forceps minor	0.78 (0.60;1.01)	0.80 (0.61;1.06)	**1.38 (1.12;1.71)**	**1.39 (1.11;1.75)**

Data are presented as Hazard ratios (95% CI) per standard deviation increase of FA and MD. Results in bold were significant at $p<0.05$ and those that were starred * at $p<0.0029$. Model I: adjusted for age, sex, education, intracranial volume, white matter volume and the log transformed white matter lesion volume of the investigated tract. Model II: Model I, and additionally adjusted for CES-D score, and cardiovascular risk factors (systolic blood pressure, diastolic blood pressure, antihypertensive medication, serum cholesterol, HDL-cholesterol, lipid lowering medication, diabetes, smoking, BMI) and *apolipoprotein E-ε4 allele* carriership.
Abbreviations: FA: fractional anisotropy, MD; mean diffusivity, WML: white matter lesion, BMI: Body Mass Index, CES-D: Center for Epidemiology Depression Scale score.

The association between global white matter microstructure and cognitive decline is presented in **Table 3**. Higher values of global MD were associated with greater decline in global cognition, driven by worse performance on the Word Fluency Test and Stroop reading and interference subtasks. Results were unaltered by exclusion of all incident dementia cases (**Supplementary Table S3**). Similar associations, albeit somewhat attenuated, were observed for FA.

Table 3. Global white matter microstructure and cognitive decline

	FA	MD
G-factor	0.02 (-0.004;0.041)	**-0.04 (-0.07;-0.01)**
Immediate memory	-0.002 (-0.04;0.03)	-0.03 (-0.07;0.02)
Delayed memory	0.007 (-0.03;0.04)	-0.03 (-0.07;-0.01)
Stroop 1	**0.04 (0.01;0.07)***	**-0.06 (-0.09;-0.02)***
Stroop 2	0.02 (-0.001;0.05)	-0.02 (-0.05;0.02)
Stroop 3	**0.04 (0.01;0.07)***	**-0.09 (-0.12;-0.05)***
Letter-Digit Substitution Task	0.004 (-0.02;0.03)	-0.004 (-0.04;0.03)
Word Fluency Test	0.03 (0.001;0.06)	**-0.06 (-0.10;-0.02)***
Purdue Pegboard	**0.03 (0.005;0.06)**	-0.04 (-0.07;-0.00)

Data are presented as mean difference in Z-score (95% CI) per standard deviation increase of FA and MD. Results in bold were significant at p<0.05 and those that were starred * at p<0.008.

Model adjusted for age, sex, education, intracranial volume, white matter volume and the log transformed white matter lesion volume, CES-D score, and additionally adjusted for cardiovascular risk factors (systolic blood pressure, diastolic blood pressure, antihypertensive medication, serum cholesterol, HDL-cholesterol, lipid lowering medication, diabetes, smoking, BMI) and *apolipoprotein E-ε4 allele* carriership.

Abbreviations: FA: fractional anisotropy, MD; mean diffusivity, WML: white matter lesion, BMI: Body Mass Index, CES-D score: Center for Epidemiology Depression Scale.

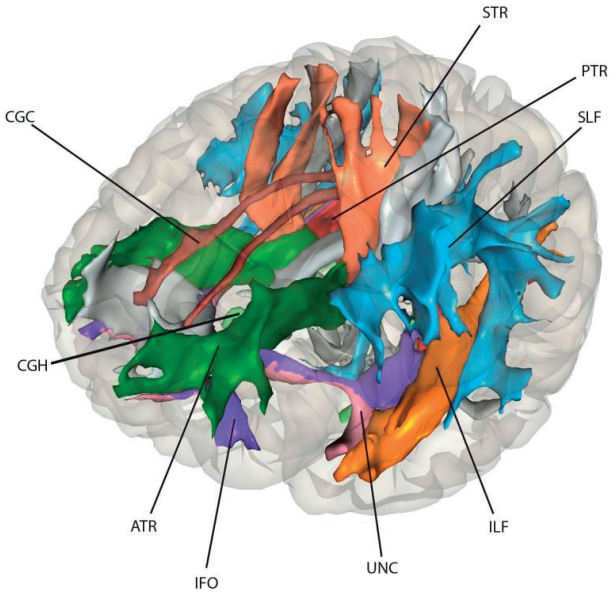

Figure 3. Association of tract-specific diffusion-MRI measures and incident dementia.

Tracts that were significantly associated with dementia risk are color-coded, as represented in the color legend. Other tracts are presented in grey.

Abbreviations:, ATR: anterior thalamic radiation, STR: superior thalamic radiation, PTR: posterior thalamic radiation, SLF: superior longitudinal fasciculus, ILF: inferior longitudinal fasciculus, IFO: inferior-fronto-occipital fasciculus, UNC: uncinate fasciculus, CGC: cingulate gyrus part of cingulum, CGH: parahippocampal part of cingulum.

DISCUSSION

In this longitudinal population-based study, we found that structural disconnectivity is associated with increased risk of dementia and with more pronounced cognitive decline. These associations were most profound for the projection, association and limbic system tracts, and extended into the pre-clinical phase of the disease.

Longitudinal studies provide higher evidence for causal relations. Our main results provide evidence for the 'disconnection hypothesis', which states that loss of brain connections precedes cognitive decline and dementia. In line with this hypothesis, our results suggest that disconnectivity plays a role already in the preclinical stages of dementia. The findings in this study are consistent with previous clinical studies concluding that diffusion-MRI measures in persons with cerebral small vessel disease add in the prediction of cognitive decline and dementia.[12,13] We can now further extend this conclusion to the general population.

Various potential pathways could lead to disconnectivity. A vascular pathway has been proposed in which reduction in white matter perfusion, e.g. due to impaired autoregulation may result in white matter damage.[26] Oligodendrocytes might shrink because of hypoxia and ischaemia in white matter, with subsequent loss of myelin.[27,28] However, in our fully adjusted model we corrected for several cardiovascular risk factors and the estimates did not change substantially. This may be explained by residual confounding (due to age-specific effects of vascular factors or subclinical vascular factors), or a more complex, multifaceted pathway, in which there is a complex interplay of traditional vascular risk factors, hypoxia, and neuro-inflammation.[29] Inflammation-induced disconnectivity may be caused by inflammation-related cytokines (TNF- α, IL-8, IL-10, IFN- γ) and growth factors (IGFBP2, PDGF-BB) which have been associated with a lower integrity of myelin sheaths.[30,31].Yet, reverse causality as an explanation for our findings is very unlikely since the risk estimates did not change after excluding the first five years of follow-up. Also, disconnectivity associated with cognitive decline also in individuals who did not develop dementia during the study duration, suggesting an association already in the preclinical phase of dementia and with normal aging.

We found that structural disconnectivity, indicated by a low FA and high MD throughout the brain, but in particular in the projection, association and limbic system tracts, related to a higher risk of dementia. This is in line with previous research in cross-sectional studies which found lower FA in white matter tracts including the association tracts[32,33] and projection tracts[34,35] associated with dementia. Lower FA values in limbic system tracts (in particular in the parahippocampal cingulum) and the association with dementia, more specifically AD, has been most consistently reported in previous studies.[34,36,37]

A small number of studies reported higher FA values in specific regions in AD.[38,39] This counterintuitive finding may be explained by selective degeneration of a fiber population in regions with crossing white matter tracts, leading to paradoxical higher FA.[40] MD is therefore thought to be a more sensitive and reliable measure in these crossing fiber regions (and therefore also globally),[41] and presumably more sensitive to white matter damage.[9,10] Moreover, in a small group of patients with AD, increases in MD preceded changes in FA which only occurred in a more progressive disease state.[9] Accordingly, in our study we found stronger associations with MD than with FA.

The exact pathological substrate underlying the changes in FA and MD leading to disconnectivity is still unknown. There is pathological evidence that changes in diffusion-MRI measures correlate with myelin damage and axonal count,[42] that myelin is increasingly suggested as an important factor in AD pathology and that myelin breakdown is at the core of the earliest changes involved in dementia.[43] However, the presence of other possible processes such as inflammation generates difficulties to assigning change in diffusion-MRI measures to a specific underlying pathological process causing the observed structural disconnectivity.[44]

Strengths of the study are the population-based setting, the large sample size, the automated publicly available diffusion MRI processing methods that facilitate replication[6], and the longitudinal assessment of cognitive performance with meticulous follow-up for dementia. Some limitations need to be considered. First, the averaging of FA and MD measures over the normal-appearing white matter for analyses discards some spatial information. Second, given the long preclinical phase of dementia, our median follow-up time of 6.8 years is still relatively short, and longer duration studies with repeated imaging are required to further map changes in diffusion-MRI in the process of neurodegeneration. Nevertheless, our results were unaffected by excluding the first five years of follow-up, and independent of macrostructural white matter pathology (white matter hyperintensity volume). Third, although we found associations similar for all-cause dementia and clinical AD, confirmation of subtype diagnosis by biomarkers or pathological examination was not available.

In conclusion, structural disconnectivity increases the risk of dementia and more pronounced cognitive decline. Our study suggests that diffusion-MRI may be useful in risk prediction.

CHAPTER REFERENCES

1. Ferri CP, Prince M, Brayne C, et al. Global prevalence of dementia: a Delphi consensus study. *Lancet.* 2005;366(9503):2112-2117.
2. Jack CR, Jr., Knopman DS, Jagust WJ, et al. Hypothetical model of dynamic biomarkers of the Alzheimer's pathological cascade. *Lancet Neurol.* 2010;9(1):119-128.
3. Reid AT, Evans AC. Structural networks in Alzheimer's disease. *Eur Neuropsychopharmacol.* 2013;23(1):63-77.
4. Daianu M, Dennis EL, Jahanshad N, et al. Alzheimer's Disease Disrupts Rich Club Organization in Brain Connectivity Networks. *Proc IEEE Int Symp Biomed Imaging.* 2013:266-269.
5. O'Sullivan M, Jones DK, Summers PE, Morris RG, Williams SC, Markus HS. Evidence for cortical "disconnection" as a mechanism of age-related cognitive decline. *Neurology.* 2001;57(4):632-638.
6. de Groot M, Verhaaren BF, de Boer R, et al. Changes in normal-appearing white matter precede development of white matter lesions. *Stroke.* 2013;44(4):1037-1042.
7. Nazeri A, Chakravarty MM, Rajji TK, et al. Superficial white matter as a novel substrate of age-related cognitive decline. *Neurobiol Aging.* 2015;36(6):2094-2106.
8. Vernooij MW, Ikram MA, Vrooman HA, et al. White matter microstructural integrity and cognitive function in a general elderly population. *Arch Gen Psychiatry.* 2009;66(5):545-553.
9. Acosta-Cabronero J, Alley S, Williams GB, Pengas G, Nestor PJ. Diffusion tensor metrics as biomarkers in Alzheimer's disease. *PLoS One.* 2012;7(11):e49072.
10. Acosta-Cabronero J, Williams GB, Pengas G, Nestor PJ. Absolute diffusivities define the landscape of white matter degeneration in Alzheimer's disease. *Brain.* 2010;133(Pt 2):529-539.
11. Fu JL, Liu Y, Li YM, Chang C, Li WB. Use of diffusion tensor imaging for evaluating changes in the microstructural integrity of white matter over 3 years in patients with amnesic-type mild cognitive impairment converting to Alzheimer's disease. *J Neuroimaging.* 2014;24(4):343-348.
12. Tuladhar AM, van Uden IW, Rutten-Jacobs LC, et al. Structural network efficiency predicts conversion to dementia. *Neurology.* 2016;86(12):1112-1119.
13. Zeestraten EA, Lawrence AJ, Lambert C, et al. Change in multimodal MRI markers predicts dementia risk in cerebral small vessel disease. *Neurology.* 2017;89(18):1869-1876.
14. Ikram MA, Brusselle GGO, Murad SD, et al. The Rotterdam Study: 2018 update on objectives, design and main results. *Eur J Epidemiol.* 2017;32(9):807-850.
15. Ikram MA, van der Lugt A, Niessen WJ, et al. The Rotterdam Scan Study: design and update up to 2012. *Eur J Epidemiol.* 2011;26(10):811-824.
16. Anbeek P, Vincken KL, van Bochove GS, van Osch MJ, van der Grond J. Probabilistic segmentation of brain tissue in MR imaging. *Neuroimage.* 2005;27(4):795-804.
17. Vrooman HA, Cocosco CA, van der Lijn F, et al. Multi-spectral brain tissue segmentation using automatically trained k-Nearest-Neighbor classification. *Neuroimage.* 2007;37(1):71-81.
18. de Boer R, Vrooman HA, van der Lijn F, et al. White matter lesion extension to automatic brain tissue segmentation on MRI. *Neuroimage.* 2009;45(4):1151-1161.
19. Koppelmans V, de Groot M, de Ruiter MB, et al. Global and focal white matter integrity in breast cancer survivors 20 years after adjuvant chemotherapy. *Hum Brain Mapp.* 2014;35(3):889-899.
20. de Groot M, Ikram MA, Akoudad S, et al. Tract-specific white matter degeneration in aging: the Rotterdam Study. *Alzheimers Dement.* 2015;11(3):321-330.
21. de Bruijn RF, Bos MJ, Portegies ML, et al. The potential for prevention of dementia across two decades: the prospective, population-based Rotterdam Study. *BMC Med.* 2015;13:132.

22. Ligthart S, van Herpt TT, Leening MJ, et al. Lifetime risk of developing impaired glucose metabolism and eventual progression from prediabetes to type 2 diabetes: a prospective cohort study. *Lancet Diabetes Endocrinol.* 2016;4(1):44-51.
23. Beekman AT, Deeg DJ, Van Limbeek J, Braam AW, De Vries MZ, Van Tilburg W. Criterion validity of the Center for Epidemiologic Studies Depression scale (CES-D): results from a community-based sample of older subjects in The Netherlands. *Psychol Med.* 1997;27(1):231-235.
24. Galwey NW. A new measure of the effective number of tests, a practical tool for comparing families of non-independent significance tests. *Genet Epidemiol.* 2009;33(7):559-568.
25. Nyholt DR. A simple correction for multiple testing for single-nucleotide polymorphisms in linkage disequilibrium with each other. *Am J Hum Genet.* 2004;74(4):765-769.
26. Shi Y, Thrippleton MJ, Makin SD, et al. Cerebral blood flow in small vessel disease: A systematic review and meta-analysis. *J Cereb Blood Flow Metab.* 2016;36(10):1653-1667.
27. Ihara M, Polvikoski TM, Hall R, et al. Quantification of myelin loss in frontal lobe white matter in vascular dementia, Alzheimer's disease, and dementia with Lewy bodies. *Acta Neuropathol.* 2010;119(5):579-589.
28. Aboul-Enein F, Rauschka H, Kornek B, et al. Preferential loss of myelin-associated glycoprotein reflects hypoxia-like white matter damage in stroke and inflammatory brain diseases. *J Neuropathol Exp Neurol.* 2003;62(1):25-33.
29. Heppner FL, Ransohoff RM, Becher B. Immune attack: the role of inflammation in Alzheimer disease. *Nat Rev Neurosci.* 2015;16(6):358-372.
30. Benedetti F, Poletti S, Hoogenboezem TA, et al. Inflammatory cytokines influence measures of white matter integrity in Bipolar Disorder. *J Affect Disord.* 2016;202:1-9.
31. Raj D, Yin Z, Breur M, et al. Increased White Matter Inflammation in Aging- and Alzheimer's Disease Brain. *Front Mol Neurosci.* 2017;10:206.
32. Stricker NH, Schweinsburg BC, Delano-Wood L, et al. Decreased white matter integrity in late-myelinating fiber pathways in Alzheimer's disease supports retrogenesis. *Neuroimage.* 2009;45(1):10-16.
33. Damoiseaux JS, Smith SM, Witter MP, et al. White matter tract integrity in aging and Alzheimer's disease. *Hum Brain Mapp.* 2009;30(4):1051-1059.
34. Mayo CD, Mazerolle EL, Ritchie L, Fisk JD, Gawryluk JR, Alzheimer's Disease Neuroimaging I. Longitudinal changes in microstructural white matter metrics in Alzheimer's disease. *Neuroimage Clin.* 2017;13:330-338.
35. Serra L, Cercignani M, Lenzi D, et al. Grey and white matter changes at different stages of Alzheimer's disease. *J Alzheimers Dis.* 2010;19(1):147-159.
36. Zhang Y, Schuff N, Jahng GH, et al. Diffusion tensor imaging of cingulum fibers in mild cognitive impairment and Alzheimer disease. *Neurology.* 2007;68(1):13-19.
37. Kantarci K, Avula R, Senjem ML, et al. Dementia with Lewy bodies and Alzheimer disease: neurodegenerative patterns characterized by DTI. *Neurology.* 2010;74(22):1814-1821.
38. Teipel SJ, Grothe MJ, Filippi M, et al. Fractional anisotropy changes in Alzheimer's disease depend on the underlying fiber tract architecture: a multiparametric DTI study using joint independent component analysis. *J Alzheimers Dis.* 2014;41(1):69-83.
39. Teipel SJ, Stahl R, Dietrich O, et al. Multivariate network analysis of fiber tract integrity in Alzheimer's disease. *Neuroimage.* 2007;34(3):985-995.
40. Douaud G, Jbabdi S, Behrens TE, et al. DTI measures in crossing-fibre areas: increased diffusion anisotropy reveals early white matter alteration in MCI and mild Alzheimer's disease. *Neuroimage.* 2011;55(3):880-890.

41. Jeurissen B, Leemans A, Tournier JD, Jones DK, Sijbers J. Investigating the prevalence of complex fiber configurations in white matter tissue with diffusion magnetic resonance imaging. *Hum Brain Mapp.* 2013;34(11):2747-2766.
42. Beaulieu C. The basis of anisotropic water diffusion in the nervous system - a technical review. *NMR Biomed.* 2002;15(7-8):435-455.
43. Bartzokis G. Age-related myelin breakdown: a developmental model of cognitive decline and Alzheimer's disease. *Neurobiol Aging.* 2004;25(1):5-18; author reply 49-62.
44. Wood TC, Simmons C, Hurley SA, et al. Whole-brain ex-vivo quantitative MRI of the cuprizone mouse model. *PeerJ.* 2016;4:e2632.

Supplementary Table S1. Global white matter microstructure and incident dementia

	Model	FA	MD
All dementia (n=101)	model I	**0.65 (0.53;0.80)**	**1.77 (1.43;2.17)**
	model II	**0.65 (0.52;0.80)**	**1.79 (1.44;2.23)**
AD (n=83)	model I	**0.70 (0.55;0.88)**	**1.71 (1.35;2.16)**
	model II	**0.69 (0.54;0.88)**	**1.76 (1.38;2.24)**
Censoring for stroke (n=98)	model I	**0.65 (0.53;0.80)**	**1.75 (1.41;2.16)**
	model II	**0.64 (0.52;0.80)**	**1.76 (1.42;2.20)**
Exclusion cortical infarcts (n=97)	model I	**0.63 (0.51;0.78)**	**1.75 (1.41;2.17)**
	model II	**0.61 (0.49;0.77)**	**1.79 (1.43;2.24)**

Data are presented as Hazard ratios (95% CI) per standard deviation increase of FA and MD. Results in bold were significant at p<0.05.

Model I: adjusted for age, sex, education, intracranial volume, white matter volume and the log transformed white matter hyperintensity volume.

Model II: Model I, and additionally adjusted for CES-D score, cardiovascular risk factors (systolic blood pressure, diastolic blood pressure, antihypertensive medication, serum cholesterol, HDL-cholesterol, lipid lowering medication, diabetes, smoking, BMI), and *apolipoprotein E-ε4 allele* carriership.

Abbrevations: FA: fractional anisotropy, MD; mean diffusivity, BMI: Body Mass Index, CES-D: Center for Epidemiology Depression Scale score, n=number of cases.

Supplementary Table S2. Global white matter microstructure and incident dementia, incrementally excluding the first five years of follow-up

	Excluding ≤ 1 year (n=4374/88)	Excluding ≤ 2 years (n=4305/74)	Excluding ≤ 3 years (n=4224/56)	Excluding ≤ 4 years (n=4131/41)	Excluding ≤ 5 years (n=3872/25)
FA	**0.63 (0.50;0.78)**	**0.70 (0.54;0.89)**	**0.64 (0.48;0.86)**	0.73 (0.52;1.03)	**0.60 (0.39;0.91)**
MD	**1.77 (1.41;2.21)**	**1.56 (1.20;2.04)**	**1.64 (1.21;2.22)**	**1.49 (1.02;2.16)**	1.58 (0.98;2.54)

Data are presented as Hazard ratios (95% CI) per standard deviation increase of FA and MD after excluding the first 5 years of follow-up. Results in bold p<0.05. Adjusted for age, sex, education, intracranial volume, white matter volume and the log transformed white matter hyperintensity volume.

Abbreviations: FA: fractional anisotropy, MD; mean diffusivity, n; sub-population/number of cases.

Supplementary Table S3. Global white matter microstructural integrity and cognitive decline (after exclusion of all incident dementia cases)

	FA	MD
G-factor	0.01 (-0.01;0.04)	**-0.03 (-0.06;-0.001)**
Immediate memory	-0.007 (-0.04;0.03)	-0.01 (-0.06;0.03)
Delayed memory	0.002 (-0.03;0.03)	-0.02 (-0.06;0.02)
Stroop 1	**0.04 (0.01;0.07)***	**-0.06 (-0.09;-0.02)***
Stroop 2	**0.03 (0.003;0.05)**	-0.02 (-0.05;-0.01)
Stroop 3	**0.04 (0.009;0.06)**	**-0.08 (-0.12;-0.04)***
Letter-Digit Substitution Task	0.005 (-0.02;0.03)	-0.004 (-0.04;0.02)
Word Fluency Test	**0.03 (0.002;0.06)**	**-0.06 (-0.10;-0.02)***
Purdue Pegboard	**0.03 (0.002;0.06)**	-0.03 (-0.06;0.009)

Data are presented as mean difference in Z-score (95% CI) per standard deviation increase of FA and MD. Results in bold were significant at $p<0.05$ and those that were starred * at $p<0.008$.

Model adjusted for age, sex, education, intracranial volume, white matter volume and the log transformed white matter hyperintensity volume, and additionally adjusted for CES-D score, cardiovascular risk factors (systolic blood pressure, diastolic blood pressure, antihypertensive medication, serum cholesterol, HDL-cholesterol, lipid lowering medication, diabetes, smoking, BMI) and *apolipoprotein E-ε4 allele* carriership.

Abbreviations: FA: fractional anisotropy, MD; mean diffusivity, BMI: Body Mass Index, CES-D score: Center for Epidemiology Depression Scale score.

CHAPTER 3.4

White matter microstructure and hearing acuity in older adults: a population-based cross-sectional DTI study

Stephanie Rigters, Lotte G.M. Cremers, M.Arfan Ikram,
Marc P. van der Schroeff, Marius de Groot,
Gennady V. Roschchupkin, Wiro J. Niessen,
Robert J. Baatenburg de Jong, Andre Goedegebure,
Meike W. Vernooij

Neurobiology of Aging 2018

ABSTRACT

To study the relation between the microstructure of white-matter in the brain and hearing function in older adults we carried out a population-based, cross-sectional study. In 2562 participants of the Rotterdam Study, we conducted diffusion tensor imaging to determine the microstructure of the white-matter tracts. We performed pure-tone audiogram and digit-in-noise tests to quantify hearing acuity. Poorer white-matter microstructure, especially in the association tracts, was related to poorer hearing acuity. After differentiating the separate white-matter tracts in the left and right hemisphere, poorer white-matter microstructure in the right superior longitudinal fasciculus and the right uncinate fasciculus remained significantly associated with worse hearing. These associations did not significantly differ between middle-aged (51-69 years old) and older (70-100 years old) participants. Progressing age was thus not found to be an effect modifier. In a voxel-based analysis no voxels in the white matter were significantly associated with hearing impairment.

INTRODUCTION

Progressive sensorineural hearing impairment is a common feature of aging. It is characterized by a gradual decline of hearing thresholds and worse understanding of speech, which seriously affects the quality of life.[1] Although cochlear damage is generally believed to cause age-related hearing impairment, there is strong evidence that age-related hearing impairment also has a central component in its pathogenesis.[2] Moreover, age-related hearing impairment seems to interact with the general cognitive function.[3] Multiple hypotheses on the mechanism between hearing acuity and brain alterations have been outlined. The "common cause hypothesis" describes a mutual factor that affects both hearing acuity as well as brain alterations. This mutual factor could possibly be age, cognition, or an underlying pathological factor such as cardiovascular damage.[4] There are also 2 alternative hypotheses. The "information-degradation hypothesis" describes an indirect effect between hearing and the brain through a shift of cognitive functions. The "sensory-deprivation hypothesis" describes a direct causal relationship in which worse hearing acuity leads to brain alterations.[5] Previous studies using brain imaging have demonstrated that hearing acuity in the aged and middle-aged population relates to morphological brain changes (e.g., gray- or white-matter atrophy.[6,7,8,9] In a previous study in almost 3000 people conducted by our group white-matter atrophy, but not gray-matter atrophy, was associated with age-related hearing impairment.[9] However, apart from the association with gross morphological changes, no conclusion on the underlying white matter microstructure could be made. White-matter microstructure degenerates with aging[10,11] and rates and timing of degradation vary regionally.[12] Reduced organization of white-matter microstructure could repress communication between neurocognitive networks.[13] Previously, auditory and language functions have been ascribed to frontotemporal and parietal white-matter connections[14], especially in the left hemisphere due to functional lateralization. In recent years, diffusion tensor imaging (DTI) has increasingly been used to study brain white-matter tracts. This technique allows for estimation of the microscopic organization of neural tracts by providing information on the diffusion properties of water molecules in the tissue.[15] Parameters that are frequently derived from DTI include fractional anisotropy (FA) and mean diffusivity (MD). Worsening of white-matter integrity is generally reflected in a lower FA and higher MD.[11] The study of Chang et al.was one of the first to investigate the relation between white-matter tracts and hearing function using DTI and pure-tone audiometry.[16] They found a lower FA in the central auditory system in participants with sensorineural hearing impairment. However, they limited their region of interest to the higher auditory system rather than the whole brain. Due to a small sample size, they were not able to correct for confounders. Lin et al. also studied this relation by comparing age-matched participants with hearing impairment

and participants with normal hearing, using DTI and pure-tone audiometry.[17] They also studied the auditory pathway instead of the whole brain and had similar results. Moreover, they found a linear relation between FA and the degree of hearing impairment. Husain et al. conducted a third cross-sectional study and performed DTI on the white matter association tracts.[7] They found a different FA for both hemispheres. The association tracts into and out of the right temporal and frontal cortex had poorer white-matter microstructure in participants with worse hearing thresholds when compared with participants with normal hearing. The same tracts in the left hemisphere were not associated with hearing impairment. These 3 studies have in common that the study samples were small (maximum n = 47), age ranges were wide (between 8 and 85 years old), and authors only focused on specific regions of interest (ROI) in the brain known for their auditory function instead of whole brain analysis. On the contrary, Profant et al. found no significant associations between the organization of white-matter tracts and age-related hearing impairment.[18] They also investigated specific ROIs, and they used an equally small sample size, but they studied relatively old participants (mean age in the older group was 70.4 ± 1.3 years).

Although most of these studies show that microstructural changes in white matter and hearing loss are correlated, some essential issues remain to be investigated.[19] First, ROI's have not consequently been defined, which makes direct comparison of results impossible. It would be useful to additionally study potential changes in brain regions beyond those used for auditory processing. Second, different hearing outcomes have been used (e.g., speech vs. high frequency thresholds) and speech-in-noise ability was not tested. Third, the relationship between cognitive decline, aging, and hearing impairment and their effect on brain structure and function is hard to investigate because of confounding effects. A population-based study could provide an unbiased evaluation of the association between white-matter microstructure and age-related hearing acuity.

To address the above issues, we conducted a large population-based study on community-dwelling older adults. Our primary objective was to analyze the association between the global and tract-specific white-matter microstructure and hearing acuity using DTI. Second, we aimed to investigate the effect of aging on this possible association, because aging is associated with both white matter degeneration and worse hearing acuity. In the analyses, we used both auditory thresholds (low, speech, and high frequencies) and the ability for speech recognition in noise, and we accounted for possible cognitive and cardiovascular covariates. We hypothesized that participants with worse hearing acuity would have a lower FA and higher MD, which corresponds with poorer white-matter microstructure in the tracts. We assumed different outcomes for different tracts, based on anatomy and function, with stronger relations for association tracts directly or indirectly involved in auditory processing such as the superior longitudinal fasciculus, the inferior fronto-occipital fasciculus and the uncinate

fasciculus. Furthermore, since we hypothesized that aging could amplify the effect between white-matter microstructure and hearing acuity, we expected to find a larger effect in older than in middle-aged participants.

METHODS

Study population

This cross-sectional study is based on participants of the population-based Rotterdam Study, an ongoing prospective cohort study on healthy aging.[20] The Rotterdam Study includes inhabitants of 45 years and older of Ommoord, a Rotterdam district. It currently includes 14,926 participants. Participants undergo several measurements every 3-5 years. From 2005 onward, MRI scanning was added to the study protocol[21] and from 2011 onward, audiometry was incorporated as well. We considered eligible participants with brain MRI, including a diffusion-weighted sequence, and audiometry (N = 2665). We excluded those with cortical infarcts on the scan (N = 61), with dementia (N = 25) or with conductive hearing loss (N = 17), leaving 2562 participants for analysis. Dementia was ascertained as previously described using a 3-step protocol.[22] We excluded 104 participants from the analyses concerning the digits-in-noise (DIN) test. They failed to complete the DIN-test or the result was more than 4 standard deviations from the mean, making results less accurate.[23] The Rotterdam Study has been approved by the Medical Ethics Committee of the Erasmus MC and by the Ministry of Health, Welfare and Sports of the Netherlands, implementing the Wet Bevolkingsonderzoek: ERGO (Population Studies Act: Rotterdam Study). All participants provided written informed consent to participate in the study and to obtain information from their treating physicians.

MRI acquisition and processing

Multisequence MRI imaging was performed in a 1.5 Tesla MRI scanner (GE Signa Excite). The MRI protocol included a T1-weighted image (T1w, repetition time 13.8 milliseconds [ms], echo time 2.80 ms, inversion time 400 ms, 96 slices of 1.6 millimeter [mm], matrix 256 x 256), a T2-weighted fluid-attenuated inversion recovery (FLAIR) sequence (repetition time 8000 ms, echo time 120 ms, inversion time 2000 ms, 64 slices of 2.5 mm, matrix 320 x 224), a proton density-weighted image (repetition time 21,300 ms, echo time 17.3 ms, 90 slices of 1.6 mm, matrix 416 x 256), and a spin echo planar diffusion-weighted image (repetition time 8575 ms, echo time 82.6 ms, 35 slices of 3.5 mm, matrix 64 x 96). Maximum b-value was 1000 s/mm^2 in 25 noncollinear directions. Three volumes were acquired without diffusion weighing (b-value = 0 s/mm^2).[21]

A number of preprocessing steps were performed before analysis.[21] In short, structural scans for each participant were spatially coregistered using rigid registration. After brain masking and nonuniformity correction scans were segmented in gray matter, white matter, cerebrospinal fluid, and background tissue using a supervised approach based on a k-nearest neighbor segmentation approach[24,25] on the T1-weighted and proton density images. Intracranial volume, with the exclusion of the cerebellum and surrounding cerebrospinal fluid, was defined by the sum of gray and white matter and cerebrospinal fluid volumes. The brain tissue segmentation method was followed by a white-matter lesion segmentation. This was performed with an in-house developed automated segmentation method using a 2-step protocol which relies on the brain tissue segmentation and the FLAIR image.[26] We used Elastix[27] to correct the diffusion images for subject motion and eddy currents, using an affine registration. Tensors were estimated using a Levenberg-Marquardt algorithm in ExploreDTI.[28] The same motion corrected diffusion data were also used to estimate the probabilistic model required for ProbTrackx tractography.[29] We performed tractography in native space, using standard space seed, target, stop, and exclusion masks as described previously.[30] The probabilistic tractography algorithm was run with default settings (step length 0.5, curvature threshold 0.2, maximum steps 200). Also, the diffusion model estimation (Bedpostx) was run with default options. Cortical infarcts were visually defined as focal parenchymal lesions <3 mm and >15 mm with involvement of cortical gray matter and with signal characteristics equal to CSF on all sequences and with a hyperintensive rim on the FLAIR image.[31] We computed global mean FA and MD in the normal appearing white matter. FA is the degree of anisotropy and is given as a ratio ranging from 0 (isotropic or non-directional) to 1 (unidirectional). MD is expressed in square millimeters per second. Furthermore, we used the diffusion data to segment 15 (of which 12 segmented bilaterally) white-matter tracts using probabilistic tractography as previously described.[32] Tracts were grouped based on anatomy or presumed functional groups into brainstem tracts (middle cerebellar peduncle and medial lemniscus), projection tracts (corticospinal tract, anterior thalamic radiation, superior thalamic radiation, and posterior thalamic radiation), association tracts (superior longitudinal fasciculus, inferior longitudinal fasciculus, inferior fronto-occipital fasciculus, and uncinated fasciculus), limbic system tracts (cingulate gyrus part of cingulum, parahippocampal part of cingulum, and fornix), and callosal tracts (forceps major, forceps minor) in the left and right hemisphere.[32] Due to tractography failures or (visually) rejected segmentations, tract-specific measurements were missing for on average 6.9 participants (ranging from 0 to 61 participants) per tract. We obtained tract-specific diffusion measures (mean FA and mean MD per tract.[32] We standardized global and tract-specific diffusion measures (z-scores). We obtained tract-specific white-matter volumes and tract-specific white-matter lesion volumes (natural log-transformed) by

combining tissue and tract segmentations. Varying seed masks were used to account for partial coverage of the medial lemniscus (one of the brainstem tracts), and this was considered as a potential confounder in the analyses in which the medial lemniscus was investigated.

Voxel-based analysis

Voxel-based analysis (VBA) of DTI data was performed according to the voxel-based morphometry method[33] as previously described.[34] FSL software[35] was used for VBA data processing. All FA and MD maps were nonlinearly registered to the standard FA template from the FSL package with a 1 x 1 x 1 mm^3 voxel resolution. In addition, the Rotterdam Study tract template that was used for analyzing the DTI measures per tract was mapped to MNI space, to assess location of association and compare VBA results with global DTI measures. Participant-specific tract segmentation masks[32] were registered to MNI template in the same way as FA and MD maps and then merged to 1 tract template image. We used 90% probability thresholds to define the tract templates.

Audiometry

All audiometry was performed in a soundproof booth by a single qualified health professional. A clinical audiometer (Decos audiology workstation, version 210.2.6, with AudioNigma interface), TDH-39P earphones and B71 bone conductor were used. Pure-tone audiometry thresholds were measured according to the International Organization for Standardization 8253-1 (International Organization for Standardization, 2010). Air conduction (0.25, 0.50, 1, 2, 4, and 8 kHz) and bone conduction (only 2 frequencies due to limited time: 0.5 and 4 kHz) were tested for both the ears. Masking was done according to the method of Hood.[36] Bone conduction thresholds at 4 kHz were compensated with +10 decibel (dB) afterward.[38] We determined the best hearing ear by calculating the average threshold over all frequencies. If both the ears were equal, right or left was alternately chosen. Of the best hearing ear, we then determined the low (average of 0.25, 0.50 and 1 kHz), speech (average of 0.50, 1, 2 and 4 kHz), and high frequency hearing thresholds (average of 2, 4 and 8 kHz). We excluded participants with an air-bone gap of 15 dB or more to eliminate clinically relevant conductive hearing loss. In addition, the DIN-test was performed to detect the speech recognition ability in noise.[39] Again, this was done for the best hearing ear. The test measures a speech reception threshold by letting participants repeat digit triplets in an automated adaptive procedure and changing the signal to noise ratio according to the correctness of the answer. The speech reception threshold represents a speech-in-noise ratio for 50% correctly repeated triplets. A higher value represents a worse ability of understanding speech in noise. To avoid confounding for peripheral hearing acuity, we

additionally adjusted for the high frequency hearing thresholds in the analyses with the DIN-test.
To avoid confounding for peripheral hearing acuity we additionally adjusted for the high frequency hearing thresholds in the analyses with the DIN-test.

Other covariates
Information on various covariates was collected through a home interview at enrollment of the study, or by recurrent physical examination and blood sampling at the study center. Education was qualified as having completed primary level, secondary level, or higher education. Mini-Mental State Examination (MMSE) score, body mass index, systolic and diastolic blood pressure, diabetes mellitus, cholesterol ratio, smoking habits, and alcohol consumption were reassessed every follow-up visit. Diabetes mellitus was stated present when fasting glucose was 7 mmol/L or more, or (if unavailable) when nonfasting glucose was 11 mmol/L or more, or when participants used antidiabetics. Cholesterol ratio was calculated via the quotient of serum total-cholesterol and high-density cholesterol. Smoking was categorized as never, former, or current. Alcohol consumption was categorized as non-drinker, light consumer (1 unit of alcohol per day for women and 1-2 units of alcohol per day for men) or above average consumer (more than 1 unit of alcohol per day for women and more than 2 units of alcohol per day for men.[40] We used the data on covariates from the same follow-up round as the MRI and audiometry measurements. Except for the MMSE-score, which was registered 1 round earlier.

Statistical analysis
Associations between DTI measurements (FA and MD) and hearing acuity were explored using multivariable linear regression models. Global and tract-specific FA and MD were regarded as independent variables, and pure-tone thresholds and score on the DIN-test as dependent variables. We calculated regression coefficients and 95% confidence intervals (CIs). Significance was set at $p < 0.05$ for the analyses concerning global DTI measurements. To account for multiple testing in the tract-specific analyses, we used the Sidak-correction, which was set at $p < 0.00248$ for the analyses in which we averaged left and right tract-specific measures and set at $p < 0.00156$ for the tract-specific analyses of left and right separately. To adjust for the covariates, we used 2 models. Model 1 was the 'simple' model and adjusted for age, gender, time between DTI and audiometry, intracranial volume, white-matter volume and white-matter lesions (log-transformed, global, or tract-specific). Model 2 was extended with possible confounders on the association between altered white-matter tracts and hearing acuity. Specifically, we investigated the impact of potential vascular confounders, known for their association with altered white matter[32] and hearing acuity.[1] Model 2 further

adjusted for: education, MMSE-score, body mass index, systolic and diastolic blood pressure, the presence of diabetes mellitus, cholesterol ratio, and smoking and alcohol consumption. For analyses involving the medial lemniscus, we additionally adjusted for the varying position of seeds masks. In the analyses on the DIN-test, we adjusted for high frequency hearing loss as well. We repeated the analyses after stratification between middle-aged (51-69 year old) and older participants (70-100 years old). We examined the presence of multicollinearity and found no variance inflation factor larger than 4. For the VBA linear regression models were fitted with voxel values of FA and MD measures as dependent variables and pure-tone thresholds and score on the DIN-test as independent variables. Furthermore, we corrected the VBA models like the DTI models (mentioned previous). For this analysis, all voxels within the white-matter mask were used. To estimate the threshold for significance, a nonparametric permutation test was performed independently for FA and MD. We shuffled the data randomly 5000 times and performed VBA. For every permutation, we saved the minimum p-value. Subsequently, we took the 5th percentile of this minimum p-value distribution to compute the family-wise error p-value threshold, which was 1.21×10^{-7} for FA and 1.23×10^{-7} for MD.[41] To map the significant voxels to the tract location, we created a tract study-specific atlas. Subject-specific tract segmentations[32] were registered to MNI template using FSL software. All these transformed images were merged and divided by number of participants to make a probabilistic tracts template. Due to between-participants variation in tract location, probabilistic templates allowed us to map voxels with different certainty.

Missing data were minimal (0.4% of total data) and were imputed in SPSS using fivefold multiple imputation with an iterative Markov chain Monte Carlo method, based on determinant, outcome, and included variables. Distribution of covariates was similar in the imputed and the nonimputed data set. We pooled the data by aggregating the file in SPSS before analyzing it in R. Data analysis was performed using IBM SPSS Statistics version 21 (IBM, Armonk, NY, USA), and R version 3.1.2 (R Foundation for Statistical Computing, Vienna, Austria).

RESULTS

The demographic characteristics of the 2562 participants are provided in **Table 1**. Hearing thresholds on the pure-tone audiogram were higher toward the higher frequencies, as typically seen in age-related hearing impairment (**Figure 1**).

Table 1. Demographic characteristics of the study population (N = 2,562).

Characteristic	
Age, years	69.3 ± 9.6
Gender, female	1,412 (55.1%)
Education, primary	176 (6.9%)
Education, secondary	1,762 (68.8%)
Education, higher	597 (23.3%)
MMSE score (median, IQR)	29 (27;29)
Body mass index, kg/m^2	27.3 ± 4.0
Systolic blood pressure, mmHg	144 ± 21.4
Diastolic blood pressure, mmHg	84 ± 11.0
Diabetes mellitus, yes	332 (13.0%)
Cholesterol ratio	3.90 ± 1.21
Smoking, never	863 (33.7%)
Smoking, former	1,323 (51.6%)
Smoking, current	368 (14.4%)
Alcohol, never	354 (13.1%)
Alcohol, light drinker	2,077 (77.9%)
Alcohol, above average	222 (8.7%)
FA, global white matter	0.34 ± 0.016
MD, global white matter (x 10^{-3} mm^2/s)	0.75 ± 0.027
PTA low frequencies, dB	17.2 ± 10.7
PTA speech frequencies, dB	24.8 ± 13.6
PTA high frequencies, dB	37.9 ± 19.5
DIN-score* (median, IQR)	-5.0 (-6.4;-2.4)

dB = Decibel; DIN = Digits-in-noise test; FA = Fractional anisotropy; IQR = Inter quartile range; MD = Mean diffusivity; MMSE = Mini-Mental State Examination; PTA = Pure-tone audiometry.
*For DIN N = 2,408.

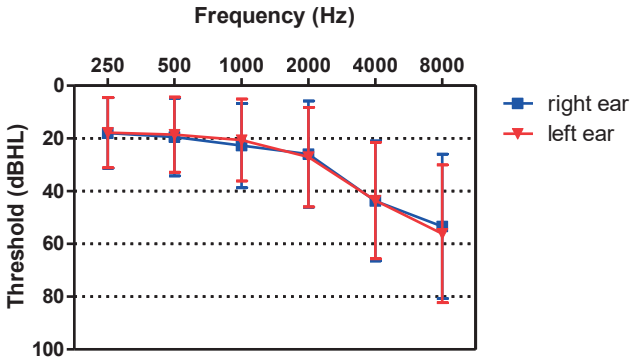

Figure 1. Mean hearing thresholds on the pure-tone audiogram of all participants (N = 2,562). Error bars indicate 95% CI.dBHL = Decibel Hearing Level; Hz = Hertz.

The association between global DTI measures and hearing acuity is presented in **Table 2**. To compare the effect of the DTI measures, the betas of the most important covariates (age, gender, and MMSE-score) are also shown. A lower FA was significantly associated with worse hearing acuity, that is, higher hearing thresholds on the pure-tone audiogram (beta per SD decrease in FA = 0.69 dB, 95% CI 0.24; 1.14) and worse performance on the DIN-test (beta per SD decrease in FA = 0.19 signal to noise ratio, 95% CI 0.05; 0.32). Adjusting for the covariates in model 2 showed stronger associations (beta per SD decrease in FA = 0.86 dB on the pure-tone audiogram, 95% CI 0.41; 1.30 and 0.23 signal to noise ratio on the DIN-test, 95% CI 0.09; 0.37). A higher MD was significantly associated with worse hearing acuity on the pure-tone audiogram for the speech and higher frequencies in model 2. MD and the outcomes of the DIN-test were not significantly associated. Subsequently, we analyzed the association between tract-specific DTI measurements and hearing acuity (**Supplemental Tables 1 and 2**). The association of a lower FA and worse hearing acuity was primarily found in the association tracts: superior longitudinal fasciculus, inferior longitudinal fasciculus, inferior fronto-occipital fasciculus, and uncinate fasciculus (**Table 3**). However, only the association between the superior longitudinal fasciculus and worse hearing on the pure-tone audiogram and the association between the uncinate fasciculus and worse performance on the DIN-test were still significant after the multiple testing correction ($p < 0.0024$).

When differentiating the tracts between left and right hemisphere (**Supplemental Tables 3 and 4**), a lower FA of the right superior longitudinal fasciculus remained significantly ($p < 0.00156$) associated with worse hearing on the pure-tone audiogram. A higher MD of the right uncinate fasciculus was also significantly ($p < 0.00156$) associated with worse hearing on the pure-tone audiogram, whereas the MD of the left and right uncinate fasciculus combined was not (**Supplemental Table 2**). Both significant tracts (superior longitudinal fasciculus and uncinate fasciculus) are displayed by a tractographic reconstruction in **Figure 2** and **Figure 3**. To address our second objective -examining whether there is a different effect caused by progressive aging- we stratified our results into a middle-aged (51-69 years old, n = 1390) and older (70-100 years old, n = 1172) group. The associations between global DTI measurements and pure-tone audiogram were significant in the middle-aged group, but not in the older group. On the other hand, the associations between global DTI measurements and the DIN-test were significant in the older group, but not in the middle-aged group. However, interaction was not significant (**Supplemental Table 5**). Finally, we performed VBA on the white-matter tracts to examine whether specific tract-subregions showed primarily associations with worse hearing acuity. FA and MD in the voxel-based analysis were not associated with hearing acuity on both the pure-tone audiogram and the DIN-test.

Table 2. Association between global DTI measures and hearing acuity.

	PTA (N = 2,562)				DIN (N = 2,408)
	ALL	LOW	SPEECH	HIGH	
↓ in FA (model 1)	**0.69 (0.24; 1.14) 0.002**	**0.42 (0.00; 0.84) 0.049**	**0.72 (0.24; 1.20) 0.003**	**0.97 (0.34; 1.59) 0.002**	**0.19 (0.05; 0.32) 0.008**
↑ in Age, per year	**0.92 (0.86; 0.99) 0.000**	**0.53 (0.47; 0.60) 0.000**	**0.81 (0.74; 0.89) 0.000**	**1.31 (1.21; 1.40) 0.000**	-0.02 (-0.04; 0.00) 0.054
Gender, male	**2.46 (1.51; 3.41) 0.000**	**-1.32 (-2.20;-0.47) 0.003**	**2.29 (1.27; 3.30) 0.000**	**6.25 (4.94; 7.57) 0.000**	**-0.38 (-0.67;-0.08) 0.011**
↓ in FA (model 2)	**0.86 (0.41; 1.30) 0.000**	**0.56 (0.14; 0.97) 0.008**	**0.87 (0.40; 1.36) 0.000**	**1.15 (0.53; 1.78) 0.000**	**0.23 (0.09; 0.37) 0.001**
↑ in Age, per year	**0.90 (0.83; 0.98) 0.000**	**0.51 (0.45; 0.58) 0.000**	**0.80 (0.72; 0.88) 0.000**	**1.30 (1.19; 1.40) 0.000**	-0.02 (-0.04; 0.00) 0.059
Gender, male	**1.97 (0.99; 2.95) 0.000**	**-1.68 (-2.59;-0.77) 0.000**	**1.85 (0.80; 2.90) 0.001**	**5.63 (4.26; 6.99) 0.000**	**-0.39 (-0.70; -0.09) 0.010**
↑ in MMSE, per point	**-0.40 (-0.64;-0.16) 0.001**	**-0.27 (-0.49;-0.04) 0.018**	**-0.33 (-0.59;-0.08) 0.010**	**-0.53 (-0.87;-0.19) 0.002**	**-0.17 (-0.24; -0.09) 0.000**
↑ in MD (model 1)	0.43 (-0.09;0.94) 0.103	0.16 (-0.32;0.63) 0.524	0.41 (-0.14;0.96) 0.140	0.70 (-0.14;0.96) 0.055	0.03 (-0.13;0.18) 0.733
↑ in Age, per year	**0.92 (0.85; 0.99) 0.000**	**0.53 (0.47; 0.60) 0.000**	**0.81 (0.74; 0.89) 0.000**	**1.30 (1.20; 1.40) 0.000**	-0.22 (-0.04; 0.00) 0.075
Gender, male	**2.46 (1.51; 3.41) 0.000**	**-1.33 (-2.22;-0.45) 0.003**	**2.28 (1.26; 3.30) 0.000**	**6.26 (4.94; 7.59) 0.000**	**-0.39 (-0.69; -0.10) 0.008**
↑ in MD (model 2)	**0.58 (0.07; 1.09) 0.026**	0.29 (-0.18;0.77) 0.228	**0.57 (0.02; 1.12) 0.042**	**0.87 (0.15; 1.58) 0.017**	0.07 (-0.09;0.23) 0.377
↑ in Age, per year	**0.90 (0.82; 0.97) 0.000**	**0.51 (0.44; 0.58) 0.000**	**0.80 (0.72; 0.88) 0.000**	**1.29 (1.18; 1.39) 0.000**	-0.02 (-0.04; 0.00) 0.069
Gender, male	**1.99 (1.00; 2.97) 0.000**	**-1.68 (-2.59;-0.76) 0.000**	**1.87 (0.81; 2.92) 0.001**	**5.66 (4.29; 7.03) 0.000**	**-0.40 (-0.71; -0.10) 0.009**
↑ in MMSE, per point	**-0.39 (-0.63;-0.15) 0.001**	**-0.26 (-0.49;-0.04) 0.021**	**-0.33 (-0.59; -0.07) 0.013**	**-0.52 (-0.86;-0.18) 0.002**	**-0.16 (-0.24; -0.09) 0.000**

Outcomes indicate the change in hearing threshold (in decibel) for the PTA and the change in speech reception threshold for the DIN-test per standard deviation change of the DTI measures and most important covariates. Significant findings ($p < 0.05$) are shown in bold and confidence intervals (95%) are shown in brackets.

DIN = Digits-in-noise test; DTI = Diffusion tensor imaging; FA = Fractional anisotropy; MD = Mean diffusivity; MMSE = Mini-Mental State Examination; PTA = Pure-tone audiometry.
All = average threshold 0.25 / 0.50 / 1 / 2 / 4 / 8 kHz, low = average threshold 0.25 / 0.50 / 1 kHz, speech = average threshold 0.50 / 1 / 2 / 4 kHz, high = average threshold 2 / 4 / 8 kHz.
Model 1 is corrected for time between DTI and audiometry, white matter volume (ml), white matter lesion volume (log-transformed), and intracranial volume (ml). Model 2 is corrected as model 1 plus systolic and diastolic blood pressure, body mass index, diabetes mellitus, cholesterol ratio, education, score on the Mini-Mental State Examination, smoking, and alcohol consumption.
In the DIN-analyses high frequency hearing loss was also accounted for.

Table 3. Association between the FA of the association tracts and hearing acuity.

	PTA (N = 2,562)				DIN (N = 2,408)
	ALL	LOW	SPEECH	HIGH	
SLF (model 1)	0.70 (0.20; 1.19) 0.005	0.37 (-0.09; 0.83) 0.114	0.62 (0.09; 1.15) 0.021	1.02 (0.34; 1.71) 0.003	0.00 (-0.15; 0.15) 0.994
SLF (model 2)	**0.84 (0.35; 1.34)*** **0.000**	0.49 (0.03; 0.95) 0.036	0.76 (0.24; 1.29) 0.004	**1.20 (0.52; 1.89)*** **0.000**	0.04 (-0.11; 0.19) 0.571
ILF (model 1)	0.58 (0.11; 1.05) 0.015	0.42 (-0.02; 0.85) 0.060	0.57 (0.07; 1.07) 0.026	0.74 (0.09; 0.74) 0.026	0.08 (-0.07; 0.22) 0.287
ILF (model 2)	0.62 (0.16; 1.09) 0.008	0.46 (0.03; 0.89) 0.037	0.62 (0.12; 1.12) 0.015	0.79 (0.14; 1.44) 0.017	0.10 (-0.05; 0.24) 0.182
IFO (model 1)	0.59 (0.10; 1.08) 0.018	0.43 (-0.03; 0.89) 0.066	0.65 (0.12; 1.17) 0.016	0.75 (0.07; 1.44) 0.031	0.13 (-0.03; 0.28) 0.102
IFO (model 2)	0.67 (0.18; 1.16) 0.007	0.50 (0.04; 0.95) 0.033	0.73 (0.20; 1.25) 0.006	0.84 (0.16; 1.53) 0.015	0.15 (0.00; 0.30) 0.049
UNC (model 1)	0.28 (-0.21; 0.77) 0.257	0.19 (-0.26; 0.65) 0.405	0.34 (-0.19; 0.86) 0.208	0.37 (-0.31; 1.05) 0.283	0.19 (0.04; 0.34) 0.011
UNC (model 2)	0.41 (-0.08; 0.90) 0.097	0.30 (-0.16; 0.75) 0.198	0.46 (-0.06; 0.98) 0.084	0.52 (-0.15; 1.20) 0.128	**0.23 (0.08; 0.38)*** **0.002**

Outcomes indicate the change in hearing threshold (in decibel) for the PTA and the change in speech reception threshold for the DIN-test per standard deviation decrease of FA. Significant results ($\alpha < 0.05$) are shown in normal font, results that survived multiple testing ($p < 0.00156$) are shown in bold and with *. Confidence intervals (95%) are shown in brackets.

DIN = Digits-in-noise test; DTI = Diffusion tensor imaging; FA = Fractional anisotropy; IFO = Inferior fronto-occipital fasciculus; ILF = Inferior longitudinal fasciculus; PTA = Pure-tone audiometry; SLF = Superior longitudinal fasciculus; UNC = Uncinate fasciculus.
All = average threshold 0.25 / 0.50 / 1 / 2 / 4 / 8 kHz, low = average threshold 0.25 / 0.50 / 1 kHz, speech = average threshold 0.50 / 1 / 2 / 4 kHz, high = average threshold 2 / 4 / 8 kHz.
Model 1 is corrected for age, sex, time between DTI and audiometry, white matter volume, white matter lesions volume (log-transformed), and intracranial volume (ml). Model 2 is corrected as model 1 plus systolic and diastolic blood pressure, body mass index, diabetes mellitus, cholesterol ratio, education, score on Mini-Mental State Examination, smoking, and alcohol consumption.
In the DIN-analyses high frequency hearing loss was also accounted for.

To address our second objective – examining whether there is a different effect caused by progressive aging– we stratified our results into a middle-aged (51-69 years old, n = 1,390) and older (70-100 years old, n = 1,172) group. The associations between global DTI measurements and pure-tone audiogram were significant in the middle-aged group, but not in the older group. On the other hand, the associations between global DTI measurements and the DIN-test were significant in the older group, but not in the middle-aged group. However, interaction was not significant (**Supplemental Table 5**).

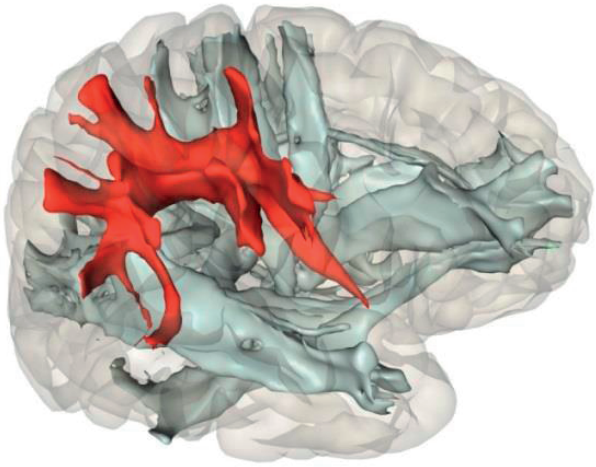

Figure 2. Tractographic reconstruction of the right superior longitudinal fasciculus, sagittal view.

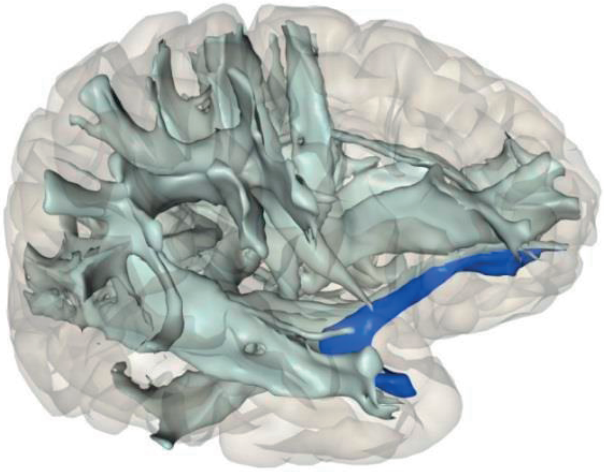

Figure 3. Tractographic reconstruction of the right uncinate fasciculus, sagittal view.

Finally, we performed VBA on the white matter tracts to examine whether specific tract-subregions showed primarily associations with worse hearing acuity. FA and MD in the voxel-based analysis were not associated with hearing acuity on both the pure-tone audiogram and the DIN-test.

DISCUSSION

Our objective was to investigate the association between brain white-matter microstructure and hearing acuity in middle-aged and older adults in a large population-

based study. We found that poorer white-matter microstructure, in particular in association tracts, was significantly associated with worse hearing acuity. Altered white-matter microstructure in the right superior longitudinal fascisulus and the right uncinate fasciculus were associated with worse hearing acuity, when differentiating for the white-matter tracts in the left and right hemisphere. Progressive aging did not seem to be an effect modifier. In the VBA there were no single voxels in the white-matter tracts that were significantly associated with hearing acuity. Our results contribute to the discussion on how white-matter microstructure and hearing acuity are related. We found an association in specific auditory and language-related tracts. This could argue against the "common cause hypothesis". Otherwise, we would have expected more widespread changes throughout the brain. Moreover, we corrected our analyses for potential confounders and possible components of the "common cause hypothesis", such as age and hypertension. The fact that we still found significant associations between poorer white-matter microstructure and worse hearing acuity makes the "common cause hypothesis" as the main explanation less likely. We acknowledge that we might not have included several unknown confounders. Altered white-matter microstructure was both associated with worse hearing on the pure-tone audiogram as well as worse hearing on the DIN-test, which reflects central auditory processing and cognitive skills.[41] The brain alterations may thus have an effect on higher auditory and cognitive functions. This would plead for the "information-degradation hypothesis" over a mere loss of sensory deprivation with worse hearing. To further explore the stated hypotheses, a comparative neuroimaging study in hearing impaired participants with or without hearing aids may help narrow possible pathways. Different white-matter tracts have a variable susceptibility to age-related structural decline.[10] This could be caused by the location and function of the tracts. It also suggests that different tracts may play a different role in age-related diseases. We found that primarily association tracts, among these the superior longitudinal fasciculus and uncinate fasciculus, were related to hearing acuity. Association tracts connect the different cortical regions of the same hemisphere and are typically located in watershed areas, implying that their blood supply relies on small and deep lenticulostriate arteries. Association tracts may therefore be more vulnerable to insults and vascular damage.[42] The superior longitudinal fasciculus connects the frontal lobe with the temporal, parietal and occipital lobe. Multiple processes, such as language, emotion, and attention have been ascribed to the superior longitudinal fasciculus.[43] The uncinate fasciculus is an association tract that connects the limbic regions in the frontal lobe to the temporal lobe.[44] Its function is not exactly clear, however it seems to be involved in limbic tasks such as emotional processing and memory, including linguistic-related tasks such as naming people[45], semantic processing such as mnemonic associations[46] and better overall language development in children.[47] This is interesting, since we found an association with the

uncinate fasciculus and our speech-in-noise test. A lower FA in the right superior longitudinal fasciculus in hearing impaired participants was also found by Husain et al.[7] They also found associations with the inferior fronto-occipital tract, the corticospinal tract, and the anterior thalamic radiation. However, the authors only published p-values and no raw data, making direct comparison of effect sizes not possible. They did not find an association with the uncinate fasciculus. They did not perform a test on speech recognition in noise, such as the DIN-test, for which we primarily found an association with the uncinate fasciculus. This association could suggest that this tract is involved in higher order auditory function, including certain verbal memory functions needed to recall the digits in noise. Our second objective was to investigate the effect of aging on the association between white-matter microstructure and hearing acuity. We hypothesized a possible progression of white matter damage in worse hearing acuity with age. Besides correcting for age as a possible confounder in multivariable models 1 and 2, we also stratified our results between middle-aged and older participants to investigate if age is a possible effect modifier. We found no significant interaction, despite the fact that increased FA was significantly associated with a worse outcome on the DIN-test in the older group, whereas in the middle-aged group, this significant association was found in the pure-tone thresholds. Thus, progressive aging does not seem to act as an effect modifier. Profant et al. likewise noticed the differences in the relation between FA and hearing acuity among younger and older participants.[18] Although they compared their older group with a much younger group (mean age 67.9 vs. 24.3) than ours, they also did not find a significant effect. We suggest further research on this relation by performing longitudinal studies, since cross-sectional studies do not allow age changes within individuals to be studied. To our knowledge, we performed the largest study so far on tract-specific white-matter microstructure and hearing acuity. Furthermore, we tried to optimize the design. First, we investigated the whole brain instead of the central auditory system and thereby provided an overview of the brain. Second, we explored both peripheral and central hearing function. A pure-tone audiogram reflects more on the peripheral auditory function, whereas a speech-in-noise test informs on higher functions of the auditory system. Third, the tract-specific measurements were performed with fully automated and publicly available methods.[10] Finally, we corrected for cognition and cardiovascular risk factors.[19] Still, our study has several limitations. Within the tracts that we have studied, there was no specific auditory tract. This we tried to preempt by additionally performing an analysis on the voxel level using voxel-based morphometry. No significant voxels were found when we used 90% probability thresholds to define the tract templates (corresponding voxels had to belong to a tract in 90% of the participants). When lowering these thresholds to 10%, we found significant voxels in areas that belong to the right superior fasciculus and right inferior longitudinal fasciculus. However, this

means that in only 10% of the participants this was a predefined white-matter tract by the anatomical template. We made the choice for a 90% threshold so we were sure that we looked at white-matter tracts and not at voxels possibly belonging to other brain areas. An explanation for finding different results with the tract-specific and voxel-based analysis may be that due to multiple comparisons corrections, the threshold for the voxel-based analysis is too conservative. To detect significant voxels, a bigger sample size would be required. To decrease the number of tests, another method with low resolution can be used, such as for example tract profiles estimation[48] Third, our study was performed with 25 diffusion gradient directions, and this may have lowered the precision to detect crossing fiber populations. However, probabilistic tractography was performed with a good reproducibility of 0.89.[32] Therefore, we are confident that we could reconstruct the tracts of our interest accurately. Unfortunately, it was not possible to differentiate in our specific-tract data for subcomponents, for example, the 3 segments of the SLF that are presumed to have different functions.[49] Finally, the study design is cross-sectional, making it impossible to state a conclusion on the direction of the effect. Therefore, longitudinal research is required.

CONCLUSION

In 2562 participants of the Rotterdam Study, poorer white-matter microstructure was associated with worse hearing acuity, specifically in the right superior longitudinal fasciculus and uncinate fasciculus. Progressive aging was not found to be an effect modifier.

CHAPTER REFERENCES

1. Gates, G.A., Mills, J.H. Presbyacusis. Lancet 2005;366:1111-1120. doi: 10.1016/S0140-6736(05)67423-5.
2. Humes, L.E., Dubno, J.R., Gordon-Salant, S., Lister, J.J., Cacace, A.T., Cruickshanks, K.J., Gates, G.A., Wilson, R.H., Wingfield, A. Central presbycusis: a review and evaluation of the evidence. J Am Acad Audiol. 2012;23:635-666. doi: 10.3766/jaaa.23.8.5.
3. Taljaard, D.S., Olaithe, M., Brennan-Jones, C.G., Eikelboom, R.H., Bucks, R.S. The relationship between hearing impairment and cognitive function: a meta-analysis in adults. Clin Otolaryngol. 2016;41:718-729. doi: 10.1111/coa
4. Mudar, R.A., Husain, F.T. Neural alterations in acquired age-related hearing loss. Front Psychol. 2016;7:828. doi: 10.3389/fpsyg.2016.00828.
5. Wong, P.C., Ettlinger, M., Sheppard, J.P., Gunasekera, G.M., Dhar, S. Neuroanatomical characteristics and speech perception in noise in older adults. Ear Hear 2010;31:471-479. doi: 10.1097/AUD.0b013e3181d709c2.
6. Eckert, M.A., Cute, S.L., Vaden, K.I.Jr., Kuchinsky, S.E., Dubno, J.R. Auditory cortex signs of age-related hearing loss. J Assoc Res Otolaryngol. 2012;13:703-713. doi: 10.1007/s10162-012-0332-5.
7. Husain, F.T., Medina, R.E., Davis, C.W., Szymko-Bennett, Y., Simonyan, K., Pajor, N.M., Horwitz, B. Neuroanatomical changes due to hearing loss and chronic tinnitus: a combined VBM and DTI study. Brain Res. 2011;19:74-88. doi: 10.1016/j.brainres.2010.10.095.
8. Peelle, J.E., Troiani, V., Grossman, M., Wingfield, A. Hearing loss in older adults affects neural systems supporting speech comprehension. J Neurosci. 2011;31:12638-12643. doi: 10.1523/JNEUROSCI.2559-11.2011.
9. Rigters, S.C., Bos, D., Metselaar, M., Roshchupkin, G.V., Baatenburg de Jong, R.J., Ikram, M.A., Vernooij, M.W., Goedebure, A. Hearing impairment is associated with smaller brain volume in aging. Fron. Aging Neurosci. 2017;9. doi: 10.3389/fnagi.2017.00002
10. De Groot, M., Cremers, L.G., Ikram, M.A., Hofman, A., Krestin, G.P., van der Lugt, A., Niessen, W.J., Vernooij, M.W. White matter degeneration with aging: longitudinal diffusion MR imaging analysis. Radiology 2016;279:532-541. doi: 10.1148/radiol.2015150103.
11. Yap, Q.J., The, I., Fusar-Poli, R., Sum, M.Y., Kuswanto, C., Sim, K. Tracking cerebral white matter changes across the lifespan: insights from diffusion tensor imaging studies. J Neural Transm. 2013;120:1369-1395. doi: 10.1007/s00702-013-0971-7.
12. Lebel, C., Gee, M., Camicioli, R., Wieler, M., Martin, W., Beaulieu, C. Diffusion tensor imaging of white matter tract evolution over the lifespan. Neuroimage. 2012;60:340-352. doi: 10.1016/j.neuroimage.2011.11.094.
13. Salat, D.H. The declining infrastructure of the aging brain. Brain Connect. 2011;4:279-293. doi: 10.1089/brain.2011.0056.
14. Parker, G.J., Luzzi, S., Alexander, D.C., Wheeler-Kingshott, C.A., Ciccarelli, O., Lambon Ralph, M.A. Lateraization of ventral and dorsal auditory-language pathways in the human brain. Neuroimage 2005;24:656-666. doi: 10.1016/j.neuroimage.2004.08.047.
15. O'Donnell, L.J., Westin, C.F. An introduction to diffusion tensor image analysis. Neurosurg Clin N Am. 2011;22:185-196. doi: 10.1016/j.nec.2010.12.004
16. Chang, Y., Lee, S.H., Lee, Y.H., Hwang, M.J., Bae, S.J., Kim, M.N., Lee, J., Woo, S., Lee, H., Kang, D.S. Auditory neural pathway evaluation on sensoneurinal hearing loss using diffusion tensor imaging. Neuroreport. 2004;15:1699-1703. doi: 10.1097/01.wnr.0000134584.10207.1a.

17. Lin, Y., Wang, J., Wu, C., Wai, Y., Yu, J., Ng, S. Diffusion tensor imaging of the auditory pathway in sensoneurinal hearing loss: changes in radial diffusivity and diffusion anisotropy. J Magn Reson Imaging 2008;28:598-603. doi: 10.1002/jmri.21464.
18. Profant, O., Ŝkoch, A., Balogová, Z., Tintěra, J., Hlinka J., Syka, J. Diffusion tensor imaging and MR morphometry of the central auditory pathway and auditory cortex in ageing. Neuroscience 2014;260: 87-97. doi: 10.1016/j.neuroscience.2013.12.010.
19. Cardin, V. Effects of Aging and adult-onset hearing loss on cortical auditory regions. Front Neurosci. 2016. doi: 10.3389/fnins.2016.00199.
20. Hofman, A., Brusselle, G.G., Darwish Murad, S., van Duijn, C.M., Franco, O.H., Goedegebure, A., Ikram, M.A., Klaver, C.C., Nijsten, T.E., Peeters, R.P., Stricker, B.H., Tiemeier, H.W., Uitterlinden A.G., Vernooij, M.W. The Rotterdam Study: 2016 objectives and design update. Eur J Epidemiol. 2015;30:661-708. doi: 10.1007/s10654-015-0082-x.
21. Ikram, M.A., van der Lugt, A., Niessen, W.J., Koudstaal, P.J., Krestin, G.P., Hofman, A. The Rotterdam Scan Study: design update 2016 and main findings. Eur J Epidemiol. 2015;30:1299-1315. doi: 10.1007/s10654-015-0105-7.
22. De Bruijn, R.F., Bos, M.J., Portegies, M.L., Hofman, A., Franco, O.H., Koudstaal, P.J., Ikram, M.A. The potential for prevention of dementia across two decades: the prospective, population-based Rotterdam Study. BMC Med. 2015;13:132. doi: 10.1186/s12916-015-0377-5.
23. Smits, C., Houtgast, T. Measurements and calculations on the simple up-down adaptive procedure for speech-in-noise tests. J Acoust Soc Am. 2006;120:1608-1621. doi: 10.1121/1.2221405.
24. Anbeek, P., Vincken, K.L., van Bochove, G.S., van Osch, M.J., van der Grond, J. Probabilistic segmentation of brain tissue in MR imaging. Neuroimage 2005;27:795-804. doi: 10.1016/j.neuroimage.2005.05.046.
25. Vrooman, H.A., Cocosco, C.A., van der Lijn, F., Stokking, R., Ikram, M.A., Vernooij, M.W., Breteler, M.M., Niessen, W.J. Multi-spectral brain tissue segmentation using automatically trained k-Nearest-Neighbor classification. Neuroimage 2007;37:71-81. doi: 10.1016/j.neuroimage.2007.05.018.
26. De Boer, R., Vrooman, H.A., van der Lijn, F., Vernooij, M.W., Ikram, M.A., van der Lugt, A., Breteler, M.M., Niessen, W.J. White matter lesion extension to automatic brain tissue segmentation on MRI. Neuroimage 2009;45:1151-1161. doi: 10.1016/j.neuroimage.2009.01.011.
27. Klein, S., Staring, M., Pluim, J.P. Comparison of gradient approximation techniques for optimalisation of mutual information in nonrigid registration. Medical Imaging 2005;192. doi: 10.1117/12.565277.
28. Leemans, A., Jeurissen, B., Sijbers, J., Jones, D. ExploreDTI: a graphical toolbox for processing, analyzing, and visualizing diffusion MR data. 17th Annual Meeting of Intl Soc Mag Reson Med. 2009.
29. Smith, S.M., Jenkinson, M., Woolrich, M.W., Beckmann, C.F., Behrens, T.E., Johansen-Berg, H., Bannister, P.R., De Luca, M., Drobnjak, I., Flitney, D.E., Niazy, R.K., Saunders, J., Vickers, J., Zhang, Y., De Stefano, N., Brady, J.M., Matthews, P.M. Advances in functional and structural MR image analysis and implementation as FSL. Neuroimage 2004;23:S208-219. doi: 10.1016/j.neuroimage.2004.07.051.
30. De Groot, M., Vernooij, M.W., Klein, S., Ikram, M.A., Vos, F.M., Smith, S.M., Niessen, W.J., Andersson, J.L. Improving alignment in tract-based spatial statistics: evaluation and optimization of image registration. Neuroimage 2013;75:400-411. doi: 10.1016/j.neuroimage.2013.03.015.
31. Vernooij, M.W., Ikram, M.A., Tanghe, H.L., Vincent, A.J., Hofman, A., Krestin, G.P., Niessen, W.J., Breteler, M.M., van der Lugt, A. Incidental findings on brain MRI in the general population. N Engl J Med. 2007;357:1821-1828. doi: 10.1056/NEJMoa070972.

32. De Groot, M., Ikram, M.A., Akoudad, S., Krestin, G.P., Hofman, A., van der Lugt, A., Niessen, W.J., Vernooij, M.W. Tract-specific white matter degeneration in aging: the Rotterdam Study. Alzheimers Dement. 2015;11:321-330. doi:10.1016/j.alz.2014.06.011.
33. Ashburner, J., Friston, K.J. Voxel-based morphometry –the methods. Neuroimage 2000;11:805-821. doi: 10.1006/nimg.2000.0582.
34. Roshchupkin, G.V., Adams, H.H., van der Lee, S.J., Vernooij, M.W., van Duijn, C.M., Uitterlinden, A.G., van der Lugt, A., Niessen, W.J., Ikram, M.A. Fine-mapping the effects of Alzheimer's disease risk loci on brain morphology. Neurobiol. Aging 2016;48:204-211. doi: 10.1016/j.neurobioaging.2016.08.024.
35. Smith, S.M., Jenkinson, M., Woolrich, M.W., Beckmann, C.F., Behrens, T.E., JohansenBerg, H., Bannister, P.R., De Luca, M., Drobnjak, I., Flitney, D.E., Niazy, R.K., Saunders, J., Vickers, J., Zhang, Y., De Stefano, N., Brady, J.M., Matthews, P.M., 2004. Advances in functional and structural MR image analysis and implementation as FSL. Neuroimage 23, S208eS219.
36. Hood, J.D. The Principles and practice of bone conduction audiometry: A review of the present position. Laryngoscope 1960;70:1211-1228. doi: 10.1288/00005537-196009000-00001.
37. Margolis, R.H., Eikelboom, R.H., Johnson, C., Ginter, S.M., Swanenpoel de, W., Moore, B.C. False air-bone gaps at 4 kHz in listeners with normal hearing and sensorineural hearing loss. Int J Audiol. 2013;52:526-532. doi: 10.3109/14992027.2013.792437.
38. Koole, A., Nagtegaal, A.P., Homans, N.C., Hofman, A., Baatenburg de Jong, R.J., Goedegebure, A. Using the digits-in-noise test to estimate age-related hearing loss. Ear Hear. 2010;37:508-513. doi: 10.097/AUD.0000000000000282.
39. Dawson, D.A., Room, R. Towards agreement on ways to measure and report drinking patterns and alcohol-related problems in adult general population surveys: the Skarpö conference overview. J Subst Abuse. 2000;12:1-21. doi:10.1016/S0899-3289(00)00037-7.
40. Churchill, G.A., Doerge, R.W. Empirical threshold values for quantitative trait mapping. Genetics 1994;138:963-971.
41. Pichora-Fuller, M.K., Souza, P.E. Effects of aging on auditory processing of speech. Int J Audiol. 2003;42:11-16. doi: 10.3109/14992020309074638.
42. Rosano, C., Abebe, K.Z., Aizenstein, H.J., Boudreau, R., Jennings, J.R., Venkatraman, V., Harris, T.B., Yaffe, K., Satterfield, S., Newman, A.B. Longitudinal systolic blood pressure characteristics and integrity of white matter tracts in a cohort of very old black and white adults. Am J Hypertens. 2015;3:326-334. doi: 10.1093/ajh/hpu134.
43. Kamali, A., Flanders, A.E., Brody, J., Hunter, J.V., Hasan, K.M. Tracing superior longitudinal fasciculus connectivity in the human brain using high resolution diffusion tensor tractography. Brain Struct Funct. 2014;219:269-281. doi: 10.1007/s00429-012-0498-y.
44. Von Der Heide, R.J., Skipper, L.M., Klobusicky, E., Olson, I.R. Dissecting the uncinate fasciculus: disorders, controversies and a hypothesis. Brain 2013;136:1692-1707. doi: 10.1093/brain/awt094.
45. Papagno, O. Naming and the role of the uncinated fasciculus in language function. Curr Neurol Neurosci Rep. 2011;11:553-559. doi: 10.1007/s11910-011-0219-6.
46. Hau, J., Sarubbo, S., Houde, J.C., Girard, G., Deledalle, C., Crivello, F., Zago, L., Mellet, E., Jobard, G., Joliot, M., Mazoyer, B., Tzourio-Mazoyer, N., Descoteaux, M., Petit, L. Revisting the human uncinated fasciculus, its subcomponents and asymmetries with stem-based tractography and microdissection calication. Brain Struct Funct. 2017;222:1645-1662.
47. Travis, K.E., Adams, J.N., Kovachy, V.N., Ben-Shachar, M., Feldman, H.M. White matter properties differ in 6-year old readers and pre-readers. 2017;222:1685-1703. doi: 10.1007/s00429-016-1302-1.

48. Yeatman, J.D., Dougherty, R.F., Myall, N.J., Wandell, B.A., Feldman, H.M. Tract profiles of white matter properties: automating fiber-tract quantification. PLoS One 2012;7:e49790. doi: 10.1371/journal.pone.0049790.
49. Makris, N., Kennedy, D.N., McInernet, S., Sorensen, A.G., Wang, R., Caviness, V.S Jr., Pandya, D.N. Segmentation of subcomponents within the superior longitudinal fascicle in humans: a quantative, in vivo, DT-MRI-study. Cereb Cortex. 2005;15:854-869. doi: 10.1093/cercor/bhh186.

SUPPLEMENTAL MATERIAL

CHAPTER 3.5

Lower microstructural integrity of brain white matter is related to higher mortality

Lotte G.M*. Cremers, Sanaz Sedaghat*, Marius de Groot, Albert Hofman, Aad van der Lugt, Wiro J. Niessen, Oscar H. Franco, Abbas Dehghan, M. Arfan Ikram, Meike W. Vernooij

Neurology 2015

**Denotes equal contribution*

ABSTRACT

Objective To investigate the association of cerebral white matter microstructural integrity with mortality.

Methods We included 4294 individuals, free from stroke and dementia (mean age 63.6 years, 44% male) from the population-based Rotterdam Study (2006-2011). Diffusion-MRI was used to assess the microstructural integrity of the white matter, both globally and for specific white matter tracts. Fractional anisotropy (FA) and mean diffusivity (MD) were the parameters used to quantify white matter integrity. All-cause mortality and cause-specific mortality was recorded with a median follow-up time of 5.4 year and 4.6 years, respectively. Cox regression models, adjusted for age, sex, *APOE*-ε4 allele carriership, cardiovascular risk factors and macrostructural MRI changes, were used to estimate hazard ratios.

Results During the follow-up time 216 (5.0%) participants died from all causes, 31 (0.7%) from cardiovascular causes and 102 (2.4%) individuals died of non-cardiovascular causes. Each standard deviation (SD) decrease in FA and each SD increase in MD was associated with a 1.37 fold (95%CI: 1.20, 1.57) and a 1.49 fold (95%CI: 1.28, 1.75) higher hazard of all-cause mortality, respectively. The associations were more prominent with cardiovascular mortality rather than non-cardiovascular mortality. In tract-specific analyses, we observed that association tracts were more prominently related to mortality.

Conclusions Our findings suggest that impairments in cerebral white matter, even at early stages, are not limited to adverse brain outcomes and they are related to mortality especially from cardiovascular causes.

INTRODUCTION

Brain white matter plays a major role in brain functioning e.g. in cognitive function and motor function.[1,2] One of the manifestations of white matter damage is the emergence of white matter hyperintensities, a common finding on MRI.[3] Several studies reported a link between presence of white matter hyperintensities and adverse health outcomes, as well as shorter survival.[4-6] However, it seems that white matter hyperintensities could constitute only the "tip of the iceberg" of white matter pathology, and changes in the microstructure of white matter develop long before appearance of white matter hyperintensities on MRI.[7] Diffusion-MRI is a sensitive MRI technique, to quantify subtle changes in the white matter microstructure. Fractional anisotropy (FA) and mean diffusivity (MD) are commonly used diffusion-MRI parameters. Generally, lower FA and higher MD are associated with poorer white matter microstructural integrity. Given the prominent role of white matter hyperintensities not only in development and progression of brain disorders as dementia and stroke[8,9] but also in poor survival[10], it is of great importance to study early changes in white matter before white matter hyperintensities form.[11] Therapeutic approaches and life style changes in early phase might help to prevent further progression of impairments in white matter microstructural integrity.[11,12]
We hypothesized that early stage white matter pathologies are associated with shorter survival. We investigated the association of cerebral microstructural integrity with mortality. Previous studies showed that different white matter tracts have differences in vulnerability to degeneration.[13,14] Therefore, we assessed whether regional differences in white matter microstructural integrity had differential effects on mortality.

METHODS

Population

The present study is embedded within the framework of the Rotterdam Study, an ongoing prospective population-based study, among inhabitants of Ommoord, a district of Rotterdam in the Netherlands. The design of the Rotterdam Study has been described previously.[15,16] Since 2005, brain MRI is implemented into the study protocol of the Rotterdam Study. Between 2006 and 2011, out of 5430 non-demented eligible participates, 4841 persons underwent a structural and diffusion-MRI of the brain. We excluded 53 scans due to incomplete acquisitions, 112 scans due to artifacts hampering automated processing, 135 scans due to failed tissue segmentation, and 160 scans due to presence of cortical infarcts (MRI-defined). We additionally excluded participants with history of clinical stroke (n=87). Persons with cortical infarcts and stroke were excluded from all analyses because tissue loss and the gliosis surrounding infarcts may influence image registration resulting in unreliable WMH segmentation volumes. This

resulted in 4294 participants for both global and tract-specific analyses (age range: 45.7-100.0).

Standard Protocol Approvals, Registrations, and Patient Consents

The Rotterdam Study has been approved by the medical ethics committee according to the Population Study Act Rotterdam Study, executed by the Ministry of Health, Welfare and Sports of the Netherlands. A written informed consent was obtained from all participants.[15]

MRI acquisition, processing and inspection

Brain MRI scanning was performed on a 1.5T MRI scanner (GE Signa Excite). Scan protocol and sequence details are described extensively elsewhere.[16] For the diffusion scan, a single shot, diffusion weighted spin echo echo-planar imaging sequence was performed (maximum b-value was 1000 s/mm^2 in 25 non-collinear directions, three volumes were acquired without diffusion weighting (b-value = 0 s/mm^2)).[16] The T1-weighted, proton, density-weighted and the fluid-attenuated inversion recovery scans were used for automated segmentation of grey matter, white matter, white matter hyperintensities (WMH), which was extended with a post-processing WMH segmentation approach.[17-19] All segmentation results were visually inspected and, if needed manually corrected. Supratentorial intracranial volume (ICV) was estimated by summing grey and white matter, and CSF volumes.[17] Cortical infarcts were rated on structural sequences, and in case of involvement of cortical grey matter, they were classified as cortical infarcts. Lacunes were defined as focal hyperintensities (size ≥3 and < 15 mm) with the signal intensity of CSF on all sequences, and when located supratentorially with a hyperintense rim on fluid-attenuated inversion recovery (FLAIR) sequence. To differentiate lacunar infarcts from dilated perivascular spaces, symmetry of the lesions, sharp demarcation and absence of a hyperintense rim on the FLAIR sequence supported presence of a dilated perivascular space.[20] Cerebral microbleeds were rated on a three-dimensional T2*-weighted gradient-recalled echo MRI scan as focal areas of very low signal intensity.[16]

Diffusion-MRI processing and tractography

All diffusion data were pre-processed using a standardized pipeline (including correction for motion and eddy currents), obtaining global mean FA and MD in the normal-appearing white matter (voxels with WMH were excluded from the global analysis). White matter tracts were segmented using a probabilistic diffusion tractography approach described previously.[21] In tract-specific analyses voxels with WMH were not excluded. We segmented 14 different white matter tracts (11 tracts were present in the left and right hemispheres), and obtained participant specific median scores for FA

and MD inside each white matter tracts, with subsequent combination of left and right measures. The resulting tract-specific means were standardized.[21] Tracts were categorized based on anatomy, into brainstem tracts, projection tracts, association tracts, limbic system tracts, and callosal tracts.[22] The tract segmentations were used to obtain tract-specific white matter volumes, and by combining tissue and tract segmentations we obtained tract-specific WMH volumes.

Mortality

Deaths (in and out-hospital) were reported on a weekly basis through the automatic linkage with General Practitioner (GP) files. In addition, central registry of the municipality in Rotterdam was checked bimonthly for information on vital status. For participants moved outside the research area, the GPs were the primary source of information, complemented by the municipality records in the place of residence. This also includes people in nursing homes. For cause-specific mortality, research physicians reviewed all available information (from general practitioner and hospital records) and coded the events according to the International Classification of Diseases, 10th edition (ICD-10). Death due to cardiovascular mortality was classified as ICD-10 codes I00-I99 and death due to other reasons was recorded as non-cardiovascular mortality. A consensus panel, led by a physician with expertise in cardiovascular disease, decided the final cause of death according to ICD-10 codes using standardized definitions. Follow-up was completed until July 4, 2014 and January 1, 2013 for total mortality and cause-specific mortality, respectively.[23]

Cardiovascular risk factors

After a resting period of five minutes, blood pressure was measured twice in a single visit using a random-zero sphygmomanometer. Total and high density lipoprotein (HDL) cholesterol levels were determined using an automated enzymatic method. Information on smoking and antihypertensive and lipid lowering medication was based on home interviews. Smoking was categorized in never, former and current smoking. Cardiovascular disease was considered as a history of myocardial infarction, or coronary revascularization procedures.[23] Diabetes mellitus was defined by use of blood glucose lowering medication or a fasting serum glucose level equal to or greater than 7.0 mmol/l.[7] Apolipoprotein E (*APOE*) ε4 allele carriership was assessed on coded genomic DNA samples.

Statistical analysis

Due to a skewed distribution of volume of WMH, we natural-log transformed WMH volumes. Associations of white matter microstructural integrity (global and tract-specific) with all-cause mortality were evaluated using Cox proportional hazard models.

To take into account the competing risk, for cardiovascular and non-cardiovascular mortality we used a competing risk approach (R package "riskRegression").
We performed the analyses in four models. In the first model we adjusted for age, and sex. In the second model, analyses were adjusted additionally for cardiovascular risk factors including systolic blood pressure, diastolic blood pressure, antihypertensive medication, total and HDL cholesterol, lipid-lowering medication, smoking, history of coronary heart disease, diabetes mellitus, body mass index, and *APOE*-ε4 allele carriership. In the third model, we adjusted for age, sex, macrostructural white matter changes ((tract-specific) white matter volume, and log transformed (tract-specific) volume of white matter hyperintensities), intracranial volume, presence of microbleeds, and presence of lacunar infarcts. In both the global and tract-specific analysis we adjusted for WMH volume to control for possible partial volume effects and to single out real microstructural changes.[7] Model four was adjusted for all covariates from first, second and third models. Tract-specific analyses were performed with model three.[21] Since the cerebellum could not always be fully incorporated in the diffusion scan leading to a varying coverage of the brainstem tracts (mainly medial lemniscus), we additionally controlled for this factor in the tract-specific analyses of the medial lemniscus.[22] Linearity and proportionality assumptions were met for all analyses. We performed multiple imputation for missing data in the covariates (< 12% for all covariates), using a Markov Chain Monte Carlo method and we used the imputed data for all the analyses.
We inspected the mortality rates per 1000 person-years in tertiles of FA and MD, and to take into account the differences in age and sex, we made tertiles of FA and MD based on the residuals of FA and MD regressed against age and sex. We additionally used the Kaplan-Meier method to estimate cumulative mortality curves of all-cause mortality associated with the tertiles of FA and MD. To investigate whether damage to the microstructural integrity of white matter is associated with mortality due to causes other than neurological diseases, we performed a series of sensitivity analyses. First, participants with interim dementia or clinically reported stroke were censored to rule out the influence of new cases of dementia and stroke during follow-up on the association of FA and MD with all-cause mortality.[24] Second, we repeated the association of FA and MD with cardiovascular mortality after excluding deaths due to stroke.
For the tract-specific analysis we used Šidák correction to correct for multiple comparisons, after estimating the number of independent tests,[25] resulting in $p < 0.0037$ as the significance threshold for an alpha value of 0.05. All analyses were carried out using SPSS 20.0.2 for Windows or R version 2.15.0.

RESULTS

Baseline characteristics of the participants are presented in **Table 1**. Comparing eligible and non-eligible participants, we observed that excluded participants were older and had higher loads of cardiovascular risk factors **(Table e-1)**.

Table 1. Baseline characteristics

Baseline characteristics	**N= 4294**
Age, years	63.6 (11.0)
Age of death, years	72.6 (11.9)
Men	1906 (44.4)
Systolic blood pressure, mmHg	139.0 (21.5)
Diastolic blood pressure, mmHg	83.1 (10.8)
Antihypertensive medication	1463 (34.1)
Total cholesterol, mmol/l	5.5 (1.0)
HDL cholesterol, mmol/l	1.4 (0.4)
Lipid-lowering medication	1014 (23.6)
Smoking	
Current	878 (20.4)
Former	2060 (48.0)
History of coronary heart disease	256 (6.0)
Diabetes mellitus	393 (9.2)
Body mass index, kg/m^2	27.4 (4.1)
*APOE-ε*4 allele carrier	1140 (28.4)
White matter volume, mL	403.3 (60.8)
Volume of white matter hyperintensities, mL	4.4 (2.4,8.8)
Intracranial volume, mL	1340.0 (132.9)
Cerebral microbleeds	779 (18.1)
Lacunar infarcts	93 (2.2)
Fractional anisotropy	0.34 (0.01)
Mean diffusivity, 10^{-3} mm^2/s	0.74 (0.03)

Categorical variables are presented as numbers (percentages), continuous variables as means (standard deviations) and volume of white matter hyperintensities is presented as median (interquartile range).
The following variables had missing data: blood pressure (n=90), blood pressure lowering medication (n=78), smoking (n=69), lipid-lowering medication (n= 48), HDL: high density lipoprotein cholesterol (n=520), total cholesterol (n= 518), body mass index (n=82), diabetes (n=125), history of coronary heart disease (n=44), *APOE-ε*4 allele carrier (n=273).
Abbreviation: *APOE*: Apolipoprotein E.Comparing eligible and non-eligible participants, we observed that excluded participants were older and had higher loads of cardiovascular risk factors **(Table e-1)**.

During the median [interquartile range] follow-up time of 5.4 [3.6-5.9] years, 216 (5%) participants died. For cause-specific mortality, during the median [interquartile range] follow-up time of 4.6 [3.3-5.7] years, 31 (0.7%) individuals died of cardiovascular causes

and 102 (2.4%) participants died from non-cardiovascular causes. All-cause mortality rates in participants with low, middle and high tertiles of FA and MD are shown in **Figure 1**.

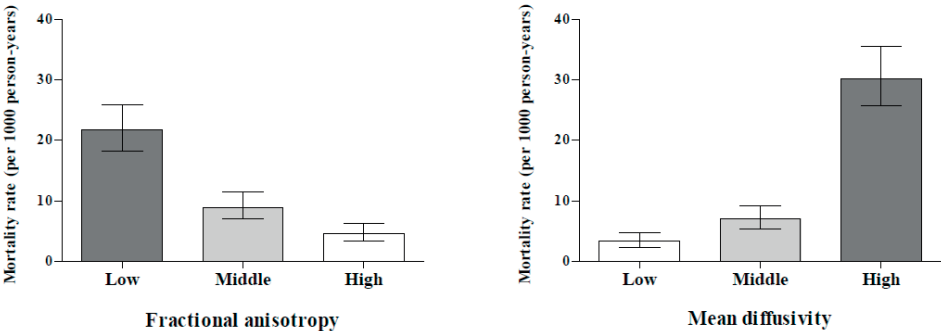

Figure 1

In model I, adjusted for age and sex, decrease in FA and increase in MD was associated with higher hazard of all-cause mortality. Adjustments for cardiovascular risk factors, macrostructural MRI changes and presence of lacunar infarcts and microbleeds attenuated the associations minimally (**Table 2)**.

Table 2. The association between white matter microstructural integrity and mortality

	All-cause mortality	
	Hazard ratio* (95% CI) N=4294 (216)	**p value**
Fractional anisotropy		
Model I	1.37 (1.20, 1.57)	<0.001
Model II	1.31 (1.15, 1.49)	<0.001
Model III	1.27 (1.10, 1.48)	0.001
Model IV	1.24 (1.10, 1.43)	0.004
Mean diffusivity		
Model I	1.49 (1.28, 1.75)	<0.001
Model II	1.39 (1.19, 1.63)	<0.001
Model III	1.39 (1.17, 1.66)	<0.001
Model IV	1.32 (1.11, 1.56)	0.002

*Hazard ratios and 95% CI are calculated per standard deviation decrease in fractional anisotropy and per standard deviation increase in mean diffusivity.

Model I: Adjusted for age, and sex.

Model II: Model I + systolic blood pressure, diastolic blood pressure, antihypertensive medication, smoking, total cholesterol, high density lipoprotein cholesterol, lipid-lowering medication, diabetes mellitus, history of coronary heart disease, *APOE-ε*4 allele carrier, and body mass index.

Model III: Model I + intracranial volume, white matter volume, logarithm of white matter lesion volume, presence of microbleeds, and presence of lacunar infarcts.

Model IV: Model I+ II + III

Abbreviation: CI: confidence interval, *APOE*: Apolipoprotein E.

Each SD decrease in FA was associated with 1.99-fold increased hazard of cardiovascular mortality (95% CI: 1.44, 2.77), in the age and sex adjusted model. Further adjustments did not change our findings. There was no association between FA and non-cardiovascular mortality (all p>0.05). Similarly, each SD higher MD was associated with 1.84-fold increased hazard of cardiovascular mortality (95%CI: 1.26, 2.68). After adjustments for cardiovascular risk factors and macrostructural MRI changes and presence of lacunar infarcts and microbleeds, the associations attenuated and were no longer significant (p= 0.207). Higher MD was associated with increased hazard of non-cardiovascular mortality (HR: 1.31, 95%CI: 1.04, 1.65), but the association was no longer significant after further adjustments (**Table 3**).

Table 3. The association of white matter microstructural integrity and cardiovascular and non-cardiovascular mortality

	Cardiovascular mortality		**Non-cardiovascular mortality**	
	Hazard ratio* (95% CI) N=4294 (31)	**p value**	**Hazard ratio* (95% CI) N=4294 (102)**	**p value**
Fractional anisotropy				
Model I	1.99 (1.44, 2.77)	<0.001	1.19 (0.98, 1.44)	0.079
Model II	1.81 (1.28, 2.57)	0.001	1.13 (0.93, 1.38)	0.206
Model III	1.62 (1.12, 2.34)	0.010	1.07 (0.87, 1.33)	0.513
Model IV	1.53 (1.04, 2.24)	0.029	1.04 (0.84, 1.28)	0.735
Mean diffusivity				
Model I	1.84 (1.26, 2.68)	0.001	1.31 (1.04, 1.65)	0.021
Model II	1.66 (1.10, 2.49)	0.015	1.22 (0.97, 1.54)	0.085
Model III	1.48 (0.96, 2.30)	0.077	1.12 (0.86, 1.46)	0.381
Model IV	1.34 (0.85, 2.13)	0.207	1.07 (0.82, 1.38)	0.620

*Hazard ratios and 95% CI are calculated per standard deviation decrease in fractional anisotropy and per standard deviation increase in mean diffusivity.

Model I: Adjusted for age, and sex.

Model II: Model I + systolic blood pressure, diastolic blood pressure, antihypertensive medication, smoking, total cholesterol, high density lipoprotein cholesterol, lipid-lowering medication, diabetes mellitus, history of coronary heart disease, *APOE-ε4* allele carrier, and body mass index.

Model III: Model I + intracranial volume, white matter volume, logarithm of white matter lesion volume, presence
of microbleeds, and presence of lacunar infarcts.

Model IV: Model I+ II + III

Abbreviation: CI: confidence interval; *APOE:* Apolipoprotein E.

Kaplan-Meier survival curves showed that individuals with low FA and high MD had the highest cumulative mortality rate (**Figure e-1**).

In the tract-specific analyses, we observed that for all tracts, MD was more prominently related to mortality than FA. For FA, after correcting for multiple testing, lower microstructural integrity in the different white matter tracts was not associated with mortality. For MD, the association between lower tract-specific white matter microstructural integrity and mortality seemed to be present throughout the brain; however, it was more prominent in the association tracts (**Table 4** and **Figure e-2**).

Excluding participants with interim dementia or stroke did not change our observations (**Table e-2**). Similarly, excluding stroke death did not change the association of FA and MD with cardiovascular mortality (**Table e-3**).

Table 4. Associations of tract-specific white matter microstructural integrity and mortality

	Fractional Anisotropy	**Mean diffusivity**
	Hazard ratio* (95% CI)	Hazard ratio* (95% CI)
Tracts in brainstem		
Middle cerebellar peduncle	1.04 (1.27, 0.86)	1.08 (0.95, 1.22)
Medial lemniscus [a]	1.03 (1.22, 0.87)	**1.21 (1.06, 1.37)***
Projection tracts		
Corticospinal tract	1.06 (1.22, 0.93)	**1.29 (1.11, 1.49)***
Anterior thalamic radiation	1.05 (1.23, 0.89)	**1.17 (1.00, 1.37)**
Superior thalamic radiation	1.06 (1.22, 0.93)	**1.21 (1.05, 1.38)**
Posterior thalamic radiation	1.19 (1.43, 1.00)	1.10 (0.95, 1.27)
Association tracts		
Superior longitudinal fasciculus	**1.20 (1.41, 1.03)**	**1.28 (1.13, 1.46)***
Inferior longitudinal fasciculus	1.09 (1.30, 0.92)	**1.28 (1.09, 1.49)***
Inferior fronto-occipital fasciculus	**1.25 (1.49, 1.04)**	1.24 (1.05, 1.45)
Uncinate fasciculus	**1.27 (1.49, 1.06)**	**1.35 (1.15, 1.57)***
Limbic system tracts		
Cingulate gyrus part of cingulum	1.09 (1.28, 0.93)	**1.27 (1.10, 1.47)***
Parahippocampal part of cingulum	1.14 (1.30, 0.97)	1.00 (0.91, 1.10)
Callosal tracts		
Forceps major	**1.28 (1.52, 1.06)**	1.08 (0.96, 1.23)
Forceps minor	**1.23 (1.49, 1.02)**	**1.24 (1.06, 1.45)**

*Hazard ratios and 95% CI, calculated per standard deviation decrease in fractional anisotropy and increase in mean diffusivity, adjusted for age, sex, intracranial volume, white matter volume, volume of white matter hyperintensities, presence of microbleeds, and presence of lacunar infarcts.

Results in bold are significant at $p<0.05$.

Results in bold and * were significant after correction for multiple testing ($p< 3.7 \times 10^{-3}$).

Abbreviation: CI: confidence interval.

DISCUSSION

We showed that among community-dwelling individuals, lower microstructural integrity of cerebral white matter is related to an increased mortality, independent of cardiovascular risk factors, macrostructural MRI changes (white matter volume and the log transformed volume of white matter hyperintensities), and presence of lacunar infarcts and microbleeds. The association was more prominent with cardiovascular mortality rather than non-cardiovascular mortality. Furthermore, we found that lower white matter microstructure in the association tracts most strongly related to mortality.
White matter is a key component of the brain consisting of glial cells and myelinated axons that transmit signals mostly between various regions of the brain and spinal cord.[2] White matter accounts for nearly half of the brain volume and its microstructural integrity is crucial for normal brain function.[7] White matter damage represented as white matter hyperintensities and white matter atrophy is reported to be related to a higher risk of mortality.[4,10,26] The association between more subtle, microstructural changes in white matter can provide a better insight into cerebral white matter pathology, but this has not yet been investigated in a population-based setting. Virtanen et al., in pre-operative patients with peripheral arterial disease, showed that microstructural changes in white matter are linked to a worse cardiorespiratory and metabolic profile and an increased risk of mortality.[27] In this study we showed that this finding can be extended to the general population free of dementia and stroke.
We observed that poorer white matter microstructural integrity was associated with higher all-cause, cardiovascular, and non-cardiovascular mortality, but most prominently with cardiovascular mortality. A possible explanation for this observation could be that white matter is more prone to vascular insults.[28,29] Shared cardiovascular risk factors such as hypertension and diabetes might play a role in this association. Adjusting for cardiovascular risk factors attenuated the associations; but the findings persisted. This might indicate that at least part of the association is driven by cardiovascular risk factors that could not be measured, or represent the very initial phase of atherosclerotic processes. Rather than cardiovascular risk factors, one of the important pathologies that would influence white matter integrity is neurodegenerative diseases such as Alzheimer's disease. Although we excluded the dementia cases from the analyses, we cannot exclude the possibility that impairment in the white matter integrity could be related to (preclinical) neurodegenerative processes, in particular in the association tracts.
Available literature suggests that damage to cerebral white matter is not only associated with deterioration in cerebral functions such as cognition, sensory or motor function but also with disturbances in regulation of endocrine and autonomic nervous systems throughout the body.[30] Disturbances in white matter microstructural integrity

may therefore influence a variety of functions throughout the body that may result in a higher risk of mortality, also due to causes other than neurological diseases.[6,30] This is in line with our observation that adjusting for macrostructural-MRI changes (white matter volume, and log transformed volume of white matter hyperintensities) and excluding neurological diseases (interim stroke and dementia) did not change our findings. Moreover, the association between white matter microstructure and cardiovascular mortality persisted even after excluding cerebrovascular related mortality, indicating that the association was not mainly driven by cerebrovascular diseases.

In the tract specific analyses, we observed that MD was more prominently associated with mortality than FA. The disparity in associations between FA, MD and mortality might indicate that FA and MD reflect different pathophysiologies. The exact processes underlying the changes in FA and MD are still not known. However, it is hypothesized that FA is dominated by tract coherence and axonal loss, and MD by (volume of) interstitial or extracellular fluid.[31,32] Besides a biological difference, MD seems to be a more sensitive diffusion-MRI measure in regions with crossing tracts.[33]

The associations found with MD were widespread in the brain, but more apparent to the association tracts, which may be explained by the variable susceptibility to vascular damage between different tracts. Previous research has shown that there is a differential vulnerability of white matter tracts in aging. The association tracts are more prone to insult and degeneration in later life; however, the exact mechanism explaining this differential sensitivity remains unclear.[13,14] A possible explanation could be the location of the association tracts in watershed areas, making these tracts more vulnerable to insult and vascular damage leading to faster degeneration.

Strengths of this study include the large sample size and its population-based design. Furthermore, the availability of extensive data on cardiovascular risk factors and macrostructural MRI-markers enabled us to control for potential confounders. Limitations of this study should be acknowledged. In the tract-specific analysis we used median FA and MD and this disposes spatial information compared to a voxel-based technique. Also, varying field of views relative to the cerebellum resulted in less accurate measurements and therefore less reliable conclusions on brain stem tracts. The diffusion tensor model in regions with crossing fibers can result in unreliable diffusion-MRI measures particularly for FA. In contrast to FA, MD seems to be a more reliable measure in crossing fiber regions.[33] Although we used probabilistic tractography, and excluded tracts veering off into neighboring tract, our results with FA might have been influenced in crossing fiber regions. Furthermore, we computed tract-specific volumes to correct analyses for tract-specific atrophy and for partial volume effects in the segmentations. However, we cannot totally rule out the influence of partial volume averaging of CSF on our results. Follow-up time for cause-specific mortality was shorter than mortality from all causes; this might have led to an underestimation of the association between

white matter integrity and cause-specific mortality. Although our findings were independent of several cardiovascular risk factors, roles of other potential confounders such as physical activity, dietary factors, inflammation, and carotid disease on the association between white matter integrity and mortality need to be further tested.

Our findings suggest that the adverse effects of impairments in cerebral white matter integrity, even at early stages, are not limited to neurocognitive outcomes and they can also put individuals at higher risk of mortality especially from cardiovascular causes. This might call for further studies unravelling the mechanisms behind the link between white matter integrity and survival.

CHAPTER REFERENCES

1. Chanraud S, Zahr N, Sullivan EV, Pfefferbaum A. MR diffusion tensor imaging: a window into white matter integrity of the working brain. *Neuropsychology review.* 2010;20(2):209-225.
2. Fields RD. White matter matters. *Scientific American.* 2008;298(3):42-49.
3. de Leeuw FE, de Groot JC, Achten E, et al. Prevalence of cerebral white matter lesions in elderly people: a population based magnetic resonance imaging study. The Rotterdam Scan Study. *Journal of neurology, neurosurgery, and psychiatry.* 2001;70(1):9-14.
4. Debette S, Beiser A, DeCarli C, et al. Association of MRI markers of vascular brain injury with incident stroke, mild cognitive impairment, dementia, and mortality: the Framingham Offspring Study. *Stroke; a journal of cerebral circulation.* 2010;41(4):600-606.
5. Henneman WJ, Sluimer JD, Cordonnier C, et al. MRI biomarkers of vascular damage and atrophy predicting mortality in a memory clinic population. *Stroke; a journal of cerebral circulation.* 2009;40(2):492-498.
6. Sabayan B, van der Grond J, Westendorp RG, van Buchem MA, de Craen AJ. Accelerated progression of white matter hyperintensities and subsequent risk of mortality: a 12-year follow-up study. *Neurobiology of aging.* 2015.
7. de Groot M, Verhaaren BF, de Boer R, et al. Changes in normal-appearing white matter precede development of white matter lesions. *Stroke.* 2013;44(4):1037-1042.
8. Gordon BA, Najmi S, Hsu P, Roe CM, Morris JC, Benzinger TL. The effects of white matter hyperintensities and amyloid deposition on Alzheimer dementia. *Neuroimage Clin.* 2015;8:246-252.
9. Windham BG, Deere B, Griswold ME, et al. Small Brain Lesions and Incident Stroke and Mortality: A Cohort Study. *Ann Intern Med.* 2015;163(1):22-31.
10. Ikram MA, Vernooij MW, Vrooman HA, Hofman A, Breteler MM. Brain tissue volumes and small vessel disease in relation to the risk of mortality. *Neurobiology of aging.* 2009;30(3):450-456.
11. Pantoni L. Cerebral small vessel disease: from pathogenesis and clinical characteristics to therapeutic challenges. *The Lancet. Neurology.* 2010;9(7):689-701.
12. Fazekas F, Wardlaw JM. The origin of white matter lesions: a further piece to the puzzle. *Stroke; a journal of cerebral circulation.* 2013;44(4):951-952.
13. Bender AR, Volkle MC, Raz N. Differential aging of cerebral white matter in middle-aged and older adults: A seven-year follow-up. *Neuroimage.* 2016;125:74-83.
14. Kochunov P, Williamson DE, Lancaster J, et al. Fractional anisotropy of water diffusion in cerebral white matter across the lifespan. *Neurobiol Aging.* 2012;33(1):9-20.
15. Hofman A, Brusselle GG, Darwish Murad S, et al. The Rotterdam Study: 2016 objectives and design update. *Eur J Epidemiol.* 2015;30(8):661-708.
16. Ikram MA, van der Lugt A, Niessen WJ, et al. The Rotterdam Scan Study: design update 2016 and main findings. *Eur J Epidemiol.* 2015;30(12):1299-1315.
17. de Boer R, Vrooman HA, van der Lijn F, et al. White matter lesion extension to automatic brain tissue segmentation on MRI. *Neuroimage.* 2009;45(4):1151-1161.
18. Koppelmans V, de Groot M, de Ruiter MB, et al. Global and focal white matter integrity in breast cancer survivors 20 years after adjuvant chemotherapy. *Hum Brain Mapp.* 2014;35(3):889-899.
19. Vrooman HA, Cocosco CA, van der Lijn F, et al. Multi-spectral brain tissue segmentation using automatically trained k-Nearest-Neighbor classification. *Neuroimage.* 2007;37(1):71-81.
20. Adams HH, Cavalieri M, Verhaaren BF, et al. Rating method for dilated Virchow-Robin spaces on magnetic resonance imaging. *Stroke.* 2013;44(6):1732-1735.

21. de Groot M, Ikram MA, Akoudad S, et al. Tract-specific white matter degeneration in aging: the Rotterdam Study. *Alzheimers Dement.* 2015;11(3):321-330.
22. de Groot M, Vernooij MW, Klein S, et al. Improving alignment in Tract-based spatial statistics: evaluation and optimization of image registration. *NeuroImage.* 2013;76:400-411.
23. Leening MJ, Kavousi M, Heeringa J, et al. Methods of data collection and definitions of cardiac outcomes in the Rotterdam Study. *Eur J Epidemiol.* 2012;27(3):173-185.
24. Akoudad S, Portegies ML, Koudstaal PJ, et al. Cerebral Microbleeds Are Associated With an Increased Risk of Stroke: The Rotterdam Study. *Circulation.* 2015;132(6):509-516.
25. Nyholt DR. A simple correction for multiple testing for single-nucleotide polymorphisms in linkage disequilibrium with each other. *American journal of human genetics.* 2004;74(4):765-769.
26. Bokura H, Kobayashi S, Yamaguchi S, et al. Silent brain infarction and subcortical white matter lesions increase the risk of stroke and mortality: a prospective cohort study. *Journal of stroke and cerebrovascular diseases : the official journal of National Stroke Association.* 2006;15(2):57-63.
27. Virtanen S, Utriainen KT, Parkkola R, et al. White matter damage of the brain is associated with poor outcome in vascular surgery patients with claudication: a pilot study. *European journal of vascular and endovascular surgery : the official journal of the European Society for Vascular Surgery.* 2014;48(6):687-693.
28. Maillard P, Seshadri S, Beiser A, et al. Effects of systolic blood pressure on white-matter integrity in young adults in the Framingham Heart Study: a cross-sectional study. *The Lancet. Neurology.* 2012;11(12):1039-1047.
29. Rosano C, Abebe KZ, Aizenstein HJ, et al. Longitudinal systolic blood pressure characteristics and integrity of white matter tracts in a cohort of very old black and white adults. *American journal of hypertension.* 2015;28(3):326-334.
30. Ulrich-Lai YM, Herman JP. Neural regulation of endocrine and autonomic stress responses. *Nature reviews. Neuroscience.* 2009;10(6):397-409.
31. Maclullich AM, Ferguson KJ, Reid LM, et al. Higher systolic blood pressure is associated with increased water diffusivity in normal-appearing white matter. *Stroke.* 2009;40(12):3869-3871.
32. Vernooij MW, Ikram MA, Vrooman HA, et al. White matter microstructural integrity and cognitive function in a general elderly population. *Arch Gen Psychiatry.* 2009;66(5):545-553.
33. Jeurissen B, Leemans A, Tournier JD, Jones DK, Sijbers J. Investigating the prevalence of complex fiber configurations in white matter tissue with diffusion magnetic resonance imaging. *Hum Brain Mapp.* 2013;34(11):2747-2766.

Table e-1. Baseline characteristics of included and excluded participants

Baseline characteristics	Participated N= 4294	Not participated N=1136	P-value
Age, years	63.6 (11.0)	68.0 (12.2)	<0.001
Men	1906 (44.4)	470 (41.4)	0.128
Systolic blood pressure, mmHg	139.0 (21.5)	144.6 (24.5)	0.017
Diastolic blood pressure, mmHg	83.1 (10.8)	83.6 (11.8)	0.548
Antihypertensive medication	1463 (34.1)	555 (48.9)	0.005
Total cholesterol, mmol/l	5.5 (1.0)	5.3 (1.1)	<0.001
HDL cholesterol, mmol/l	1.4 (0.4)	1.4 (0.4)	0.009
Lipid-lowering medication	1014 (23.6)	368 (33.2)	<0.001
Smoking			
Current	878 (20.4)	236 (21.3)	<0.001
Former	2060 (48.0)	545 (48.0)	
History of coronary heart disease	256 (6.0)	105 (9.2)	0.100
Diabetes mellitus	393 (9.2)	145 (12.8)	0.009
Body mass index, kg/m^2	27.4 (4.1)	27.9 (5.1)	<0.001

Table e-2. The association of white matter microstructural integrity and mortality excluding participants with interim stroke and dementia

	Total mortality	
	Hazard ratio* (95% CI) N=4219 (198)	p value
Fractional anisotropy		
Model I	1.35 (1.17, 1.56)	<0.001
Model II	1.31 (1.14, 1.51)	<0.001
Model III	1.27 (1.09, 1.49)	0.003
Mean diffusivity		
Model I	1.51 (1.27, 1.79)	<0.001
Model II	1.44 (1.21, 1.72)	<0.001
Model III	1.43 (1.18, 1.72)	<0.001

*Hazard ratios and 95% CI are calculated per standard deviation decrease in fractional anisotropy and per standard deviation increase in mean diffusivity.

Model I: Adjusted for age, and sex.

Model II: Model I + systolic blood pressure, diastolic blood pressure, antihypertensive medication, smoking, total cholesterol, high density lipoprotein cholesterol, lipid-lowering medication, diabetes mellitus, history of coronary heart disease, *APOE-ε*4 allele carrier, and body mass index.

Model III: Model I + intracranial volume, white matter volume, logarithm of volume of white matter hyperintensities, presence of microbleeds, and presence of lacunar infarcts.

Abbreviation: CI: confidence interval, *APOE*: Apolipoprotein E.

Table e-3. The association of white matter microstructural integrity and cardiovascular mortality excluding death from stroke

	Cardiovascular mortality	
	Hazard ratio* (95% CI) N=4289 (26)	**p value**
Fractional anisotropy		
Model I	1.85 (1.29, 2.67)	0.001
Model II	1.61 (1.10, 2.35)	0.014
Model III	1.61 (1.07, 2.41)	0.023
Mean diffusivity		
Model I	1.89 (1.24, 2.88)	0.003
Model II	1.66 (1.04, 2.65)	0.032
Model III	1.63 (1.01, 2.65)	0.046

*Hazard ratios and 95% CI are calculated per standard deviation decrease in fractional anisotropy and per standard deviation increase in mean diffusivity.

Model I: Adjusted for age, and sex.

Model II: Model I + systolic blood pressure, diastolic blood pressure, antihypertensive medication, smoking, total cholesterol, high density lipoprotein cholesterol, lipid-lowering medication, diabetes mellitus, history of coronary heart disease, *APOE-ε*4 allele carrier, and body mass index.

Model III: Model I + intracranial volume, white matter volume, logarithm of volume of white matter hyperintensities, presence of microbleeds, and presence of lacunar infarcts.

Abbreviation: CI: confidence interval, *APOE*: Apolipoprotein E.

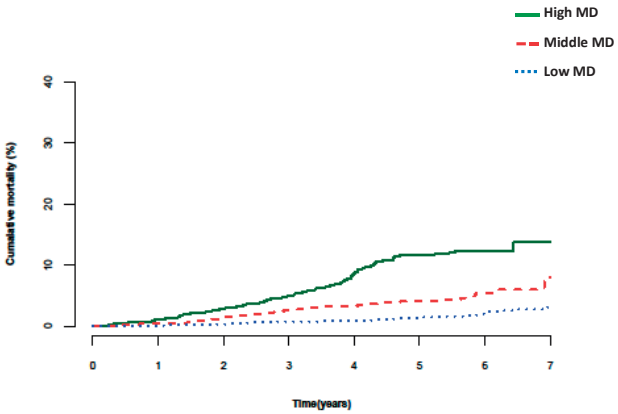

A) Fractional anisotropy

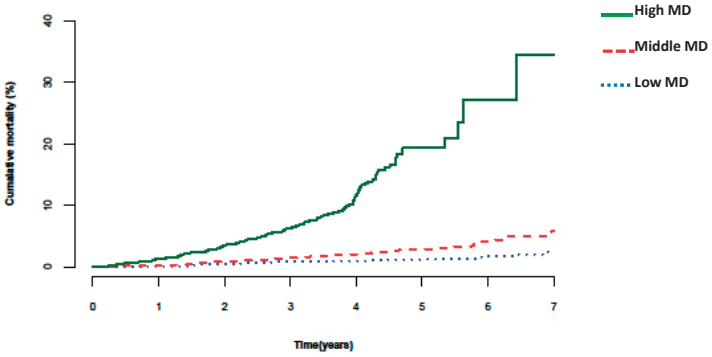

B) Mean diffusivity

Figure e-1.

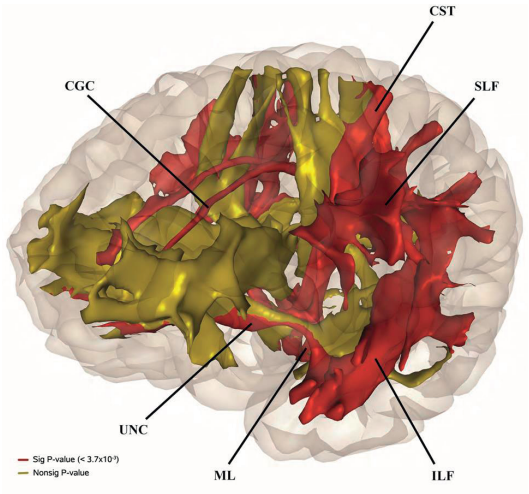

Figure e-2.

CHAPTER 3.6

Genetic variation underlying cognition and its relation with neurological outcomes

Lotte G.M. Cremers*, Maria J. Knol*,
Alis Heshmatollah*, M. Kamran Ikram,
Andre Uitterlinden, Cornelia M. van Duijn,
Wiro J. Niessen, Meike W. Vernooij, M. Arfan Ikram,
Hieab H.H. Adams

Submitted

**Denotes equal contribution*

ABSTRACT

Background General cognition in adults shows variation due to brain and cognitive reserve, and degenerative components. A recent genome-wide association study identified genetic variants for general cognitive function in 148 independent loci. The relation of these variants with cognitive decline, the incidence of dementia, parkinsonism and stroke, and brain imaging is still unknown. Here, we aimed to elucidate these associations.

Methods This study was conducted within the population-based Rotterdam Study (mean age 65.3±9.9 years, 58.0% women). We used lead variants for general cognitive function to construct a polygenic score (PGS). Additionally, we excluded genetic variants previously associated with intracranial volume and educational attainment at multiple significance thresholds to eliminate the brain and cognitive reserve component.

Results A higher PGS including all lead variants (N=170) was related to a cognitive decline, higher educational attainment and larger intracranial volume. No association was found with daily functioning, or the incidence of dementia, parkinsonism or stroke. Excluding genetic variants associated with the cognitive and brain reserve component caused an attenuation of nearly all associations found.

Conclusion This study suggests that genetic variants associated with general cognitive function represent both reserve and degenerative components of cognitive performance.

INTRODUCTION

General cognitive function represents the ability to perform tasks across different cognitive domains. The development of the nervous system shapes an important part of the inter-individual variation in general cognitive function, with neurodegenerative processes increasingly contributing later in life.[1,2] The developmental component of cognition can be referred to as reserve and is subdivided into cognitive reserve and brain reserve. Cognitive reserve stands for a more efficient use of neural networks, or use of alternate networks, and is estimated with educational attainment; brain reserve represents a quantitative buffer of neural networks, of which intracranial volume is a marker.[3] As such, general cognition is a mixed construct consisting of both reserve and degenerative components[1], that has relevance for clinical outcomes with an important cognitive component, such as daily functioning, dementia, parkinsonism, and stroke.
Recently, the highly polygenic architecture of general cognitive function was partly elucidated by the identification of genetic variants in 148 independent loci (Davies et al. in press) One approach to provide more insight into underlying pathways, is to unravel the relation of these variants with markers of both reserve and degenerative components of general cognitive function. The association of these variants with specific clinical outcomes linked to accelerated cognitive decline could additionally contribute to understanding these pathways.
Brain changes may be a plausible biological substrate to explain possible underlying pathways between these genetic variants and cognitive performance, and subsequent clinical outcomes. Structural brain magnetic resonance imaging (MRI), including diffusion-MRI, is a suitable method for investigating brain changes that are important for cognition and related outcomes.[4-7]
In this population-based study, we aimed to elucidate the association of the recently identified genetic variants for general cognitive function with cognitive decline, measures of daily functioning, the risk of neurological disorders, and structural neuroimaging.

METHODS

Study population

This study was conducted within the framework of the Rotterdam Study, an ongoing population-based cohort study located in the Netherlands with the aim to investigate causes and determinants of diseases in the elderly.[8] This cohort was initiated in 1990 and extended in 2000 and 2006, with a total of 14926 participants aged 45 years and older who undergo examinations every three to four years. Assessment of dementia, parkinsonism including PD, and stroke has been performed since the start of the study.

In 2002, an extensive cognitive test battery was added to the core protocol. MRI scanning was implemented in the study protocol from 2005 onwards.[9] Out of 14926 subjects, genotyping was successfully performed in 11496 participants. **Figure 1** gives an overview of the selection of participants for the different analyses, presented in a flowchart. After application of the exclusion criteria, different subgroups of participants remained for different analyses (**Figure 1**). According to the Population Study Act Rotterdam Study, the Ministry of Health, Welfare and Sports of the Netherlands has given approval for the Rotterdam Study. All participants have given written informed consent.[8]

Genotyping

The Illumina 550K, 550K duo and 610 quad arrays were used for genotyping. Samples with a call rate below 97.5% were removed, as well as gender mismatches, excess autosomal heterozygosity, duplicates or family relations, ethnic outliers, variants with call rates lower than 95.0%, failing missingness test, Hardy-Weinberg equilibrium p-value smaller than 10^{-6} and allele frequencies smaller than 1%. Genotypes were imputed using MaCH/minimac software to the 1000 Genomes phase I version 3 reference panel.

Polygenic score

We made a polygenic score (PGS) for all participants using the 178 lead single nucleotide polymorphisms (SNPs) with the corresponding effect sizes as described by Davies *et al.*(in press) Variants that were not available in the reference panel and variants with an $r^2<0.30$ were excluded (N=7 and N=1, respectively). For the remaining genetic variants (N=170), the allele dosage was multiplied by the reported effect estimate. Subsequently, the weighted effects of all variants were added up and the resulting polygenic scores were standardized into Z-scores.

Furthermore, we aimed to differentiate the reserve component of general cognitive function from the degenerative effects. Therefore, we calculated additional PGSs where variants associated with educational attainment and intracranial volume were removed using multiple p-value thresholds. For each variant, we used the lowest p-value threshold for either educational attainment or intracranial volume. The p-values were extracted from the summary statistics of a GWAS on educational attainment performed in 120000 individuals, and a GWAS on intracranial volume performed in 32438 individuals.[10] For all 170 variants included in the abovementioned PGS, information was available in both the educational attainment and intracranial volume GWAS. The different p-value thresholds for the association with educational attainment and intracranial volume, with the corresponding number of variants that remained, and the explained variance of the G-factor in our dataset are shown in **Supplementary**

Table S1. When applying the strictest p-value threshold (p>0.05), 36 genetic variants remained.

Cognitive test battery

The Mini-Mental State Examination (MMSE) was assessed as a measure of global cognitive function. Additionally, cognitive function was assessed using multiple cognitive tests: the 15-word learning test (15-WLT), the Stroop test (consisting of reading, color naming and interference tasks, error-adjusted scores), the Letter-Digit Substitution Task (LDST), the Word Fluency Test (using animal categories) and the Purdue pegboard (PPB) task for the left hand, right hand and both hands.[2,11-14] A measure of general cognitive function ("G-factor") was obtained through principal component analysis on the delayed recall score of the 15-WLT, Stroop interference test, Letter-Digit Substitution Task, Word Fluency Task and the Purdue Pegboard test, as described previously.[2] The G-factor explained 53.4% and 51.9% of the variance in cognitive test scores in our population at baseline and follow-up visit, respectively. Z-scores were calculated in order to make comparable test results. Self-reported years of education was used as a measure of educational attainment.

Assessment of daily functioning

Two components of daily functioning were assessed: basic activities of daily living (BADL) and instrumental activities of daily living (IADL). The Dutch version of the Stanford Health Assessment Questionnaire was used to measure BADL[15] and IADL was measured using the Dutch version of the Instrumental Activities of Daily Living scale.[16] To prevent selective loss of data, IADL items scored as non-applicable were imputed using the variables age, sex, BADL scores and all other available IADL items. Both BADL and IADL scores were standardized into Z-scores. Lower scores correspond to better daily functioning.

Assessment of clinical outcomes

The assessment of dementia, parkinsonism (including PD) and stroke were previously described in detail.[17-19] In summary, history of these clinical outcomes was assessed during the baseline interview. Participants were screened at baseline and subsequent center visits for dementia with the MMSE and the Geriatric Mental Schedule organic level, and for signs of parkinsonism. Participants with a positive screening were further examined and were evaluated by a panel led by an experienced neurologist who made the definitive diagnosis. After enrollment, participants were continuously monitored for dementia, parkinsonism and stroke through automated linkage of the study database with files from general practitioners. Follow-up for parkinsonism (including

PD) was available until the 1st January 2015 and for dementia and stroke until the 1st January 2016.

MRI acquisition and processing

We performed a multi-sequence brain MRI scan on a 1.5 tesla research dedicated MRI scanner (GE Signa Excite). Imaging details are provided elsewhere.[26] In short, the scan protocol included a T1-weighted image, a T2-weighted fluid-attenuated inversion recovery (FLAIR) sequence, a proton density weighted image and a spin echo echo planar diffusion weighted image for the diffusion-MRI. Scans were segmented into grey matter, white matter, white matter lesion volume, cerebrospinal fluid and background tissue.[20,21] We estimated supratentorial intracranial volume by summing total grey and white matter volume and cerebrospinal fluid.[20]

For the diffusion-MRI, three volumes were performed without diffusion weighting (b-value=0 s/mm^2, maximum b-value was 1000 s/mm^2). Diffusion tensors were computed using ExploreDTI to obtain fractional anisotropy (FA) and mean diffusivity (MD) in normal-appearing white matter voxels. We segmented fifteen white matter tracts using probabilistic tractography and atlas-based masking.[22] Tracts were grouped based on anatomic location or presumed function into brain stem tracts, projection tracts, association tracts, limbic system tracts and callosal tracts. Tract-specific FA and MD but also white matter volumes and white matter lesion volumes in specific tracts were obtained as previously described.[22]

In general, a lower FA and a higher MD are indicative of lower microstructural white matter integrity

Data analysis

Linear regression models were used to assess the associations between the PGS and cognitive function and daily functioning cross-sectionally and longitudinally by means of change in cognitive and daily functioning over time. Cox proportional hazard models were used to study the association between the PGS and the incidence of dementia, parkinsonism, and stroke. The proportional hazards assumption and linearity assumption were met. We used linear regression models to study the relation between the PGS and volumetric brain outcomes and white matter microstructural integrity. All models were adjusted for age and sex. Models assessing change in cognitive function or daily functioning over time were additionally adjusted for baseline measurements, and time between baseline and follow-up visit. Models that assessed the relation between the PGS and volumetric brain outcomes were adjusted for intracranial volume when the outcome was not intracranial volume, and additionally for white matter and white matter lesion volume in the analyses with white matter microstructural integrity. The abovementioned analyses were repeated for all genetic variants separately.

Since outcomes for the different analyses may be correlated, we used permutation testing in order to assess the number of independent outcomes for each subsection. Based on this information, we defined the multiple testing p-value thresholds for the different analyses, namely $p<0.0038$ for the cross-sectional and $p<0.0040$ for the longitudinal analyses of cognitive performance and daily functioning; $p<0.0101$ for the volumetric and global diffusion-MRI brain measures, and $p<0.0022$ for the tract-specific diffusion-MRI analyses; and $p<0.0129$ for the clinical outcomes. For the analyses of the genetic variants separately, we additionally used the Bonferroni correction for multiple testing, using the formula k/170 with k representing the p-value threshold as obtained by permutation testing. Analyses were performed using the IBM SPSS Statistics 21 and R 3.4.0 software.

RESULTS

Genotyping data was available for 11496 individuals, with a mean age of 65.3±9.9 years, of which 58.0% was women. A flowchart for the inclusion of participants in the different analyses is shown in **Figure 1**. An overview of the characteristics of the study population for the different analyses are shown in **Table 1**.

Table 1. Study characteristics*

Characteristic	Sample									
	Cognition and ADL N=5262	Brain imaging N=3710	Dementia		Parkinson's disease		Parkinsonism		Stroke	
			N=11070	n=1444	N=10588	n=126	N=10826	n=258	N=11391	n=1220
Age, years	64.0±9.1	64.0 (11.0)	64.8±9.5	72.0±8.0	64.6±9.4	69.2±8.7	64.9±9.7	70.7±8.8	65.1±9.8	70.4±8.7
Female, % (N)	57.4 (3022)	55.0 (2039)	57.6 (6376)	68.0 (982)	57.3 (6065)	46.8 (59)	57.4 (6219)	52.3 (135)	58.2 (6436)	58.9 (718)
Follow-up time, years	6.1±0.6	-	12.2±6.4	11.3±6.3	12.4±6.5	7.8±5.9	12.3±6.5	7.7±5.8	12.3±6.6	9.4±5.9

*Values are expressed in mean±standard deviation unless stated otherwise; N is the total number of people for whom this characteristic is assessed; n is the number of cases.
Abbreviations: activities of daily living (ADL).

Cognitive performance and daily functioning

Figure 2, panel A shows the association between the genetic variants for general cognitive function and cognitive performance, daily functioning and educational attainment. An increase in the PGS was significantly associated with a higher G-factor ($\beta=0.08$, $p=9.6x10^{-14}$), as well as with individual cognitive tests, except for the PPB test. The PGS was also significantly associated with more years of education ($\beta=0.29$,

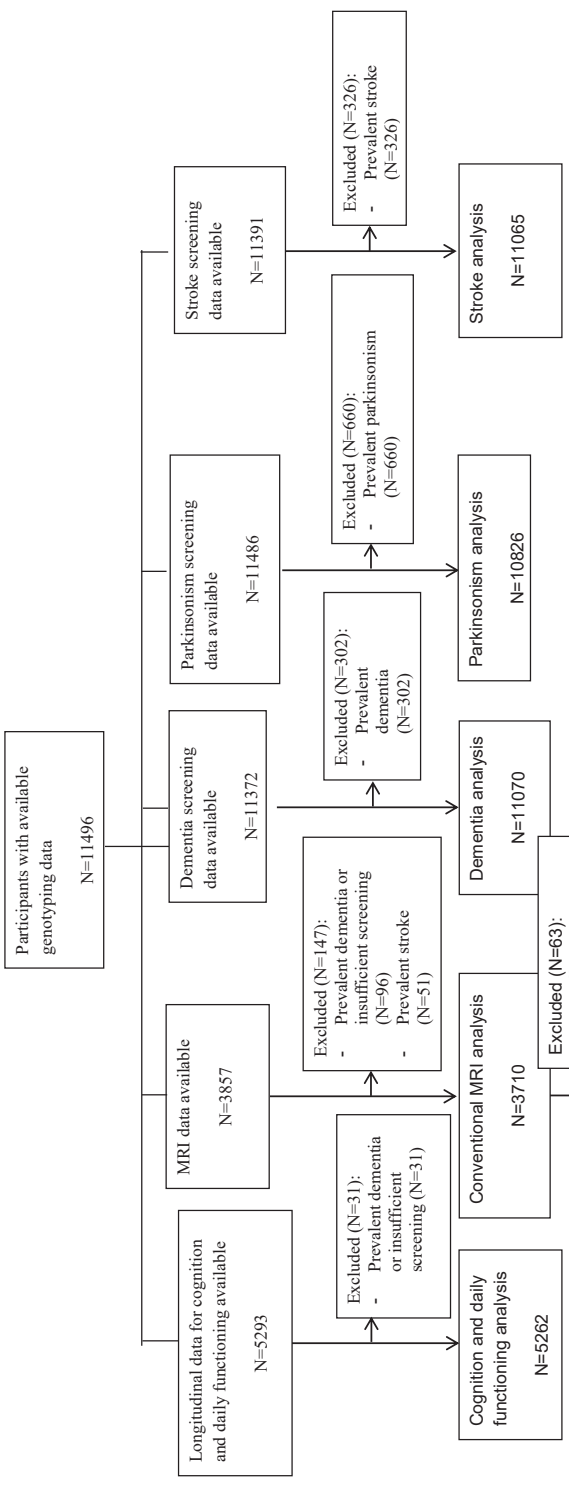

Figure 1. Flowchart presenting the in- and exclusions of participants in the different analyses.
Abbreviations: Magnetic Resonance Imaging (MRI).

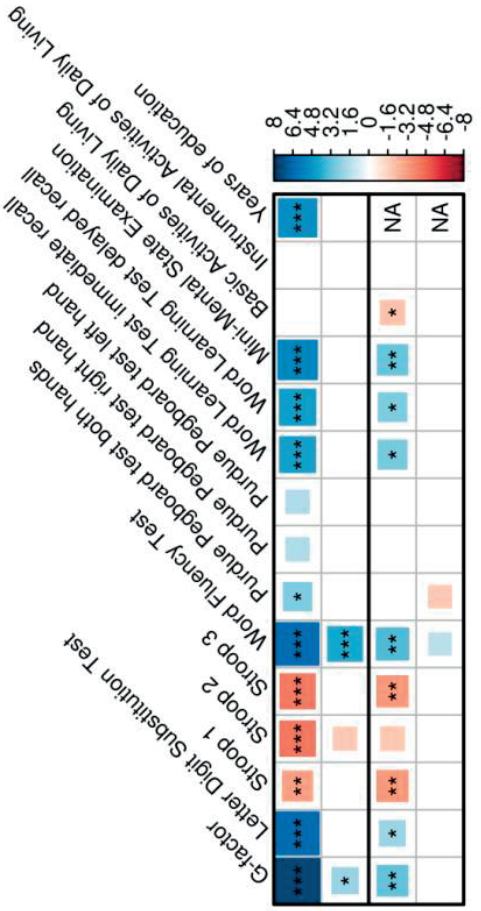

Figure 2. Association of G-factor genetic variants with (decline in) cognition and daily functioning, and educational attainment.

$p=5.2x10^{-7}$). No association with daily functioning was found. All associations attenuated after removing variants associated with the reserve component of cognition. No individual variant was significantly associated with any of the outcomes.

Figure 2, panel B shows that the PGS was associated with less decline in cognitive function ($\beta_{\Delta G\text{-factor}}=0.027$, $p=1.5x10^{-3}$). The PGS was also associated with less decline in BADL, although this was not significant after multiple comparison adjustments. Removing variants associated with educational attainment and intracranial volume resulted in an attenuation of the effects. In the single-variant analysis, no variant reached statistical significance for the association with cognitive decline or change in daily functioning.

Clinical outcomes

No significant association was found between the PGS and any of the clinical outcomes (**Figure 3**). Out of all 170 individual variants, none was significantly associated with the risk of one of dementia, parkinsonism or stroke. An increased risk for dementia was found after excluding variants associated with the reserve component at a $p>0.05$ threshold (hazard ratio 1.06, $p=0.040$), although this did not survive correction for

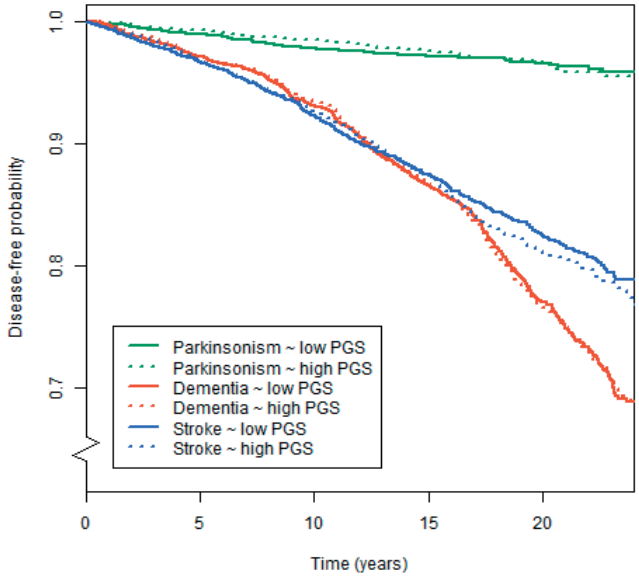

Figure 3. Polygenic scores for general cognitive function and disease-free probability for dementia, parkinsonism and stroke.

Kaplan-Meier curves presenting the association between low (i.e. below the median) and high (above the median) polygenic scores and the disease-free probability over time for dementia, parkinsonism, and stroke.

multiple testing.

Brain MRI markers

Figure 4 shows the results of the association of PGS with brain tissue volumes and global white matter microstructural integrity. We found that a higher PGS was significantly related to a larger intracranial volume (b=0.05, $p=7.5x10^{-4}$), but not with the other volumetric and global white matter microstructural integrity (**Figure 4**). At a nominal significance level, a higher PGS was associated with a higher FA in the medial lemniscus, and a lower MD in the inferior-fronto-occipital fasciculus and the posterior thalamic radiation, but this did not survive correction for multiple testing (data not shown). Removing genetic variants associated with the reserve component of cognition caused a weakening of the associations. No individual variant reached the significance threshold for the association with any of the brain imaging markers.

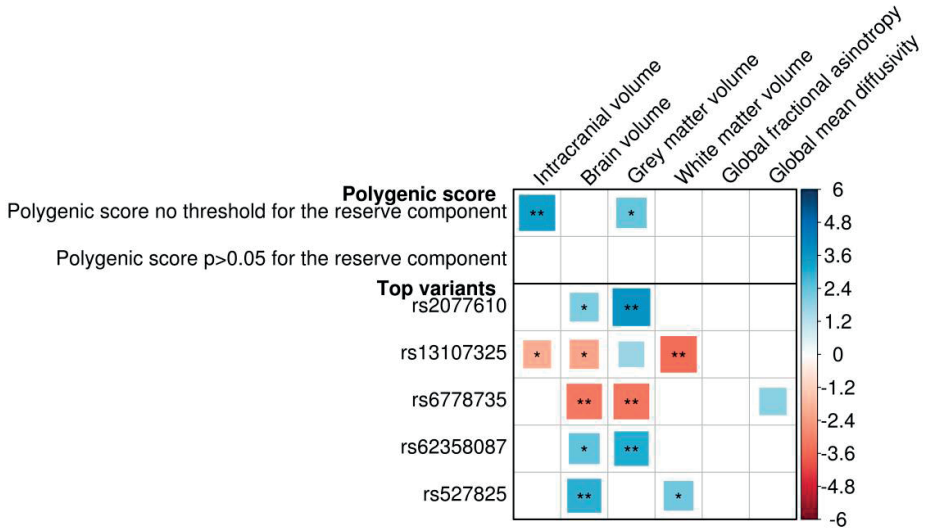

Figure 4. Association between genetic variants for general cognitive function and several brain imaging markers. Association between genetic variants for general cognitive function and both volumetric and global white matter microstructural integrity markers. Two polygenic scores are presented, one including all independent lead variants, and one only including variants with a p>0.05 for the association with the reserve component of cognition, which consists of cognitive reserve (educational attainment) and brain reserve (intracranial volume). Also, the five top genetic variants for the association with these brain imaging markers are presented. Positive associations depicted in blue correspond to a larger volume or a better white matter microstructural integrity. Larger blocks indicate higher t-values. Significance levels are indicated by asterisks: *p<0.05, nominally significant; **p<0.0101, adjusted for the number of independent traits as calculated through 10,000 permutations; ***$p<5.9 \times 10^{-5}$ (0.0101/170), additionally adjusted for the number of genetic variants.

Association between genetic variants for general cognitive function and cognitive function and daily functioning at one point in time, as well as years of education (panel A), and change in cognitive performance and daily functioning over time (panel B), adjusted for age and sex. Two polygenic scores are presented, one including all independent

lead variants, and one only including variants with a p>0.05 for the association with the reserve component of cognition, which consists of cognitive reserve (educational attainment) and brain reserve (intracranial volume). Larger blocks indicate higher t-values. Higher scores indicate better performance, except for the Stroop test, the Basic Activities of Daily Living and Instrumental Activities of Daily Living. Significance levels are indicated by asterisks: *p<0.05, nominally significant; **p<0.0038 (**Figure 2, panel A**) or p<0.0040 (**Figure 2, panel B**), adjusted for the number of independent traits as calculated through 10000 permutations; ***p<2.2 x 10^{-5} (**Figure 2, panel A**; 0.0038/170) or p<2.4 x 10^{-5} (**Figure 2, panel B**; 0.0040/170), additionally adjusted for the number of genetic variants.

DISCUSSION

In this population-based study among middle-aged and elderly persons, a PGS based on recently identified genetic variants for global cognition was associated with better global cognitive performance, better performance on individual cognitive tests, less cognitive decline, more years of education and a larger intracranial volume. We found no significant association with (decline in) daily functioning, the incidence of dementia, parkinsonism and stroke, or with any of the other global or white matter tract-specific brain imaging markers.

Cognitive decline is an important marker for the progression of neurodegenerative diseases.[23-25] Therefore, we related the genetic variants for global cognition to longitudinal assessments of cognitive and functional outcomes in our study and found that a PGS based on these genetic variants was associated with cognitive performance both cross-sectionally and longitudinally. This indicates that the genetic variants can partially explain inter- as well as intra-individual differences in cognition, and is supportive that a degenerative pathway underlies these identified genetic variants. However, no significant relation was found between the PGS and the risk of dementia, parkinsonism or stroke in this study. If anything, we saw a nominally significant association with the incidence of dementia, but the direction of effect was not as expected, i.e. a higher PGS associated with better cognitive function showed an increase in dementia risk. However, since this association did not survive correction for multiple testing, no strong conclusions should be drawn from this finding, and validation in other studies is needed. To our knowledge there are as yet no other studies that have investigated the association between these genetic variants and cinical outcomes. Previous studies did show an association between cognitive function and dementia, parkinsonism, Parkinson's disease (PD) and stroke, both before and after diagnosis.[7,24,26-29] Also, disease-specific genetic variants for these disorders have been associated with cognitive functioning.[30-33] This may indicate that cognitive decline as seen in abovementioned (prodromal) clinical

outcomes is mainly caused by disease-specific variants rather than variants for general cognitive function. In addition, it is possible that our study did not have enough power to detect a significant association with the incidence of the clinical outcomes due to the relatively small number of cases.

We also found that a higher PGS was related to a larger intracranial volume and higher educational attainment, both reflecting early brain growth and therefore suitable as markers for brain and cognitive reserve.[34,35] Brain reserve is partially determined by genetics[36-38] and is suggested to be protective against cognitive decline.[39]

Thus, our findings are supportive that the genetic variants act through both the reserve and neurodegenerative pathway. However due to absence of an association between the PGS and clinical outcomes, we attempted to enrich the degenerative component of the PGS by filtering out genetic variants hat are associated with intracranial volume and educational attainment. By applying this filter, nearly all associations for the different analyses were attenuated, supporting the suggestion that the genetic variants mainly represent the reserve component of cognitive performance. However, removing genetic variants associated with the reserve component may also eliminate degenerative components of the PGS if some variants are pleiotropic, possibly leading to an underpowered study for detecting an effect of the PGS. A more robust method would be to run a genome-wide association study (GWAS) with cognitive decline as an outcome instead of using cross-sectional measurements of cognitive performance, preferably in an elderly population since neurodegeneration mainly occurs later in life. However, longitudinal measurements such as those in the present study are only available in a fraction of the samples with cross-sectional assessments, which at present impedes GWAS discoveries for cognitive decline.

Strengths of this study are the population-based setting, the longitudinal assessment of cognitive function and daily functioning, the availability of structural brain imaging, and the long follow-up period for dementia, parkinsonism and stroke. We also need to consider limitations. It should be noted that the Rotterdam Study was part of the discovery cohort for the general cognitive function GWAS (Davies et al). However, since this was only a small proportion of the total sample size (2.0%), we do not expect that this influenced our findings to a large amount. This also leads to the limitation that the effect estimates in the summary statistics of the GWAS are based on the effect estimates of many different populations, and they may not be the correct estimates for the Dutch population as present in the Rotterdam Study.

In conclusion, we found that the PGS of general cognitive function was associated with cognitive performance, cognitive decline, intracranial volume and educational attainment, but not with daily functioning, neurological disorders, or the other brain imaging markers. Based on our results we postulate that the genetic variants identified for general cognitive function are acting mainly through the reserve pathway of cogni-

tion, but also affect the degenerative pathway. Further genetic studies of cognitive decline in elderly individuals can provide more insight into the degenerative pathway.

Chapter references

1. Gerstorf D, Ram N, Hoppmann C, Willis SL, Schaie KW. Cohort differences in cognitive aging and terminal decline in the Seattle Longitudinal Study. Dev Psychol. 2011 Jul;47(4):1026-41. PubMed PMID: 21517155. PMCID: PMC3134559.
2. Hoogendam YY, Hofman A, van der Geest JN, van der Lugt A, Ikram MA. Patterns of cognitive function in aging: the Rotterdam Study. Eur J Epidemiol. 2014 Feb;29(2):133-40. PubMed PMID: 24553905.
3. Groot C, van Loenhoud AC, Barkhof F, van Berckel BNM, Koene T, Teunissen CC, et al. Differential effects of cognitive reserve and brain reserve on cognition in Alzheimer disease. Neurology. 2018 Jan 9;90(2):e149-e56. PubMed PMID: 29237798. Epub 2017/12/15. eng.
4. Cremers LG, de Groot M, Hofman A, Krestin GP, van der Lugt A, Niessen WJ, et al. Altered tract-specific white matter microstructure is related to poorer cognitive performance: The Rotterdam Study. Neurobiol Aging. 2016 Mar;39:108-17. PubMed PMID: 26923407.
5. Squarzoni P, Tamashiro-Duran J, Souza Duran FL, Santos LC, Vallada HP, Menezes PR, et al. Relationship between regional brain volumes and cognitive performance in the healthy aging: an MRI study using voxel-based morphometry. J Alzheimers Dis. 2012;31(1):45-58. PubMed PMID: 22504316.
6. Taki Y, Kinomura S, Sato K, Goto R, Wu K, Kawashima R, et al. Correlation between gray/white matter volume and cognition in healthy elderly people. Brain Cogn. 2011 Mar;75(2):170-6. PubMed PMID: 21131121.
7. Weinstein G, Beiser AS, Decarli C, Au R, Wolf PA, Seshadri S. Brain imaging and cognitive predictors of stroke and Alzheimer disease in the Framingham Heart Study. Stroke. 2013 Oct;44(10):2787-94. PubMed PMID: 23920020. PMCID: PMC3974341.
8. Ikram MA, Brusselle GGO, Murad SD, van Duijn CM, Franco OH, Goedegebure A, et al. The Rotterdam Study: 2018 update on objectives, design and main results. Eur J Epidemiol. 2017 Sep;32(9):807-50. PubMed PMID: 29064009. PMCID: 5662692. Epub 2017/10/25. eng.
9. Ikram MA, van der Lugt A, Niessen WJ, Koudstaal PJ, Krestin GP, Hofman A, et al. The Rotterdam Scan Study: design update 2016 and main findings. Eur J Epidemiol. 2015 Dec;30(12):1299-315. PubMed PMID: 26650042. PMCID: PMC4690838.
10. Okbay A, Beauchamp JP, Fontana MA, Lee JJ, Pers TH, Rietveld CA, et al. Genome-wide association study identifies 74 loci associated with educational attainment. Nature. 2016 May 26;533(7604):539-42. PubMed PMID: 27225129. PMCID: PMC4883595.
11. Folstein MF, Folstein SE, McHugh PR. "Mini-mental state". A practical method for grading the cognitive state of patients for the clinician. J Psychiatr Res. 1975 Nov;12(3):189-98. PubMed PMID: 1202204.
12. Golden CJ. Identification of brain disorders by the Stroop Color and Word Test. J Clin Psychol. 1976 Jul;32(3):654-8. PubMed PMID: 956433.
13. Lezak MD, Howieson DB, Loring DW. Neuropsychological assessment. 4th ed. New York: Oxford University Press; 2004.
14. Tiffin J, Asher EJ. The Purdue pegboard; norms and studies of reliability and validity. J Appl Psychol. 1948 Jun;32(3):234-47. PubMed PMID: 18867059.
15. Fries JF, Spitz PW, Young DY. The dimensions of health outcomes: the health assessment questionnaire, disability and pain scales. J Rheumatol. 1982 Sep-Oct;9(5):789-93. PubMed PMID: 7175852.
16. Lawton MP, Brody EM. Assessment of older people: self-maintaining and instrumental activities of daily living. Gerontologist. 1969 Autumn;9(3):179-86. PubMed PMID: 5349366.

17. de Bruijn RF, Bos MJ, Portegies ML, Hofman A, Franco OH, Koudstaal PJ, et al. The potential for prevention of dementia across two decades: the prospective, population-based Rotterdam Study. BMC Med. 2015 Jul 21;13:132. PubMed PMID: 26195085. PMCID: 4509699. Epub 2015/07/22. eng.
18. Darweesh SK, Koudstaal PJ, Stricker BH, Hofman A, Ikram MA. Trends in the Incidence of Parkinson Disease in the General Population: The Rotterdam Study. Am J Epidemiol. 2016 Jun 1;183(11):1018-26. PubMed PMID: 27188952. Epub 2016/05/18. eng.
19. Wieberdink RG, Ikram MA, Hofman A, Koudstaal PJ, Breteler MM. Trends in stroke incidence rates and stroke risk factors in Rotterdam, the Netherlands from 1990 to 2008. Eur J Epidemiol. 2012 Apr;27(4):287-95. PubMed PMID: 22426770. PMCID: 3370158. Epub 2012/03/20. eng.
20. Vrooman HA, Cocosco CA, van der Lijn F, Stokking R, Ikram MA, Vernooij MW, et al. Multi-spectral brain tissue segmentation using automatically trained k-Nearest-Neighbor classification. Neuroimage. 2007 Aug 01;37(1):71-81. PubMed PMID: 17572111.
21. de Boer R, Vrooman HA, van der Lijn F, Vernooij MW, Ikram MA, van der Lugt A, et al. White matter lesion extension to automatic brain tissue segmentation on MRI. Neuroimage. 2009 May 01;45(4):1151-61. PubMed PMID: 19344687.
22. de Groot M, Ikram MA, Akoudad S, Krestin GP, Hofman A, van der Lugt A, et al. Tract-specific white matter degeneration in aging: the Rotterdam Study. Alzheimers Dement. 2015 Mar;11(3):321-30. PubMed PMID: 25217294.
23. Razani J, Bayan S, Funes C, Mahmoud N, Torrence N, Wong J, et al. Patterns of deficits in daily functioning and cognitive performance of patients with Alzheimer disease. J Geriatr Psychiatry Neurol. 2011 Mar;24(1):23-32. PubMed PMID: 21164171.
24. Williams-Gray CH, Foltynie T, Brayne CE, Robbins TW, Barker RA. Evolution of cognitive dysfunction in an incident Parkinson's disease cohort. Brain. 2007 Jul;130(Pt 7):1787-98. PubMed PMID: 17535834.
25. Darweesh SK, Verlinden VJ, Stricker BH, Hofman A, Koudstaal PJ, Ikram MA. Trajectories of prediagnostic functioning in Parkinson's disease. Brain. 2017 Feb;140(2):429-41. PubMed PMID: 28082300.
26. Darweesh SKL, Wolters FJ, Postuma RB, Stricker BH, Hofman A, Koudstaal PJ, et al. Association Between Poor Cognitive Functioning and Risk of Incident Parkinsonism: The Rotterdam Study. JAMA Neurol. 2017 Sep 25. PubMed PMID: 28973176.
27. Rajan KB, Aggarwal NT, Wilson RS, Everson-Rose SA, Evans DA. Association of cognitive functioning, incident stroke, and mortality in older adults. Stroke. 2014 Sep;45(9):2563-7. PubMed PMID: 25104848. PMCID: PMC4146653.
28. Verlinden VJA, van der Geest JN, de Bruijn R, Hofman A, Koudstaal PJ, Ikram MA. Trajectories of decline in cognition and daily functioning in preclinical dementia. Alzheimers Dement. 2016 Feb;12(2):144-53. PubMed PMID: 26362597.
29. Pal G, O'Keefe J, Robertson-Dick E, Bernard B, Anderson S, Hall D. Global cognitive function and processing speed are associated with gait and balance dysfunction in Parkinson's disease. J Neuroeng Rehabil. 2016 Oct 28;13(1):94. PubMed PMID: 27793167. PMCID: PMC5084375.
30. Harris SE, Malik R, Marioni R, Campbell A, Seshadri S, Worrall BB, et al. Polygenic risk of ischemic stroke is associated with cognitive ability. Neurology. 2016 Feb 16;86(7):611-8. PubMed PMID: 26695942. PMCID: PMC4762420.
31. Morley JF, Xie SX, Hurtig HI, Stern MB, Colcher A, Horn S, et al. Genetic influences on cognitive decline in Parkinson's disease. Mov Disord. 2012 Apr;27(4):512-8. PubMed PMID: 22344634. PMCID: PMC3323737.

32. Nombela C, Rowe JB, Winder-Rhodes SE, Hampshire A, Owen AM, Breen DP, et al. Genetic impact on cognition and brain function in newly diagnosed Parkinson's disease: ICICLE-PD study. Brain. 2014 Oct;137(Pt 10):2743-58. PubMed PMID: 25080285. PMCID: PMC4163033.
33. Verhaaren BF, Vernooij MW, Koudstaal PJ, Uitterlinden AG, van Duijn CM, Hofman A, et al. Alzheimer's disease genes and cognition in the nondemented general population. Biol Psychiatry. 2013 Mar 01;73(5):429-34. PubMed PMID: 22592056. Epub 2012/05/18. eng.
34. Negash S, Xie S, Davatzikos C, Clark CM, Trojanowski JQ, Shaw LM, et al. Cognitive and functional resilience despite molecular evidence of Alzheimer's disease pathology. Alzheimers Dement. 2013 May;9(3):e89-95. PubMed PMID: 23127468. PMCID: PMC3640705.
35. Coffey CE, Saxton JA, Ratcliff G, Bryan RN, Lucke JF. Relation of education to brain size in normal aging: implications for the reserve hypothesis. Neurology. 1999 Jul 13;53(1):189-96. PubMed PMID: 10408558.
36. Bartley AJ, Jones DW, Weinberger DR. Genetic variability of human brain size and cortical gyral patterns. Brain. 1997 Feb;120 (Pt 2):257-69. PubMed PMID: 9117373.
37. Tramo MJ, Loftus WC, Stukel TA, Green RL, Weaver JB, Gazzaniga MS. Brain size, head size, and intelligence quotient in monozygotic twins. Neurology. 1998 May;50(5):1246-52. PubMed PMID: 9595970.
38. Adams HH, Hibar DP, Chouraki V, Stein JL, Nyquist PA, Renteria ME, et al. Novel genetic loci underlying human intracranial volume identified through genome-wide association. Nat Neurosci. 2016 Dec;19(12):1569-82. PubMed PMID: 27694991. PMCID: PMC5227112.
39. Satz P. Brain reserve capacity on symptom onset after brain injury: a formulation and review of evidence for threshold theory. Neuropsychology. 1993;7(3):273–95.

Supplementary Table S1. P-value thresholds for the association with educational attainment and intracranial volume, and corresponding number of genetic variants remaining.

Threshold p-value for the association with educational attainment and intracranial volume	Number of variants remaining	Explained variance G-factor
No threshold	170	0,00656
$P>5e^{-8}$	149	0,00593
$P>1e^{-7}$	146	0,00607
$P>1e^{-6}$	144	0,00594
$P>1e^{-5}$	135	0,00507
$P>1e^{-4}$	121	0,00431
$P>1e^{-3}$	101	0,00299
P>0.01	70	0,00186
P>0.05	36	0,00062

CHAPTER 3.7

Predicting global cognitive decline in the general population using the Disease State Index

Lotte G.M. Cremers*, Wyke Huizinga*, Wiro J. Niessen, Gabriel P. Krestin, M. Arfan Ikram, Jyrki Lötjönen, Stefan Klein**, Meike W.Vernooij**

Submitted

**Denotes equal contribution*

***Denotes shared last author*

ABSTRACT

Background Identifying persons at risk for cognitive decline may aid in early detection of persons at risk of dementia and to select those that would benefit most from therapeutic or preventive measures for dementia.

Objective In this study we aimed to validate whether cognitive decline in the general population can be predicted with multi-variate data using a previously proposed supervised classification method: Disease State Index (DSI).

Methods We included 2,542 participants, non-demented and without mild cognitive impairment at baseline, from the population-based Rotterdam Study (mean age 60.9 ± 9.1 years). Participants with significant global cognitive decline were de- fined as the 5% of participants with the largest cognitive decline per year. We trained DSI to predict occurrence of significant global cognitive decline using a large variety of baseline features. Prediction performance was assessed as area under the receiver operating characteristic curve (AUC), using 500 repetitions of 2-fold cross-validation experiments.

Results A mean AUC (95% confidence interval) for DSI prediction was 0.78 (0.77 - 0.79) using only age as input feature. When using all available features, a mean AUC of 0.77 (0.75 - 0.78) was obtained. Without age, and with age-corrected features and feature selection on MRI features, a mean AUC of 0.70 (0.63 - 0.76) was obtained, showing the potential of other features besides age.

Conclusion The best performance in the prediction of global cognitive decline in the general population by DSI was obtained using only age as input feature. Other features showed potential, but did not improve prediction. Future studies should evaluate whether the performance could be improved by new features, e.g., longitudinal features, and other prediction methods.

INTRODUCTION

It is well established that neuropathological brain changes related to dementia accumulate over decades, and that the disease has a long preclinical phase. This may facilitate early disease detection and prediction.[1] A large amount of body of literature on potential features and risk factors for dementia exists. However, clinicians often struggle to integrate all the data obtained from a single patient for diagnostic or prognostic purposes. Therefore, there is a need for information technologies and computer-based methods that support clinical decision making.[2] Disease State Index (DSI) is a supervised machine learning method intended to aid clinical decision making.[3] This method compares a variety of patient variables with those variables from previously diagnosed cases, and computes an index that measures the similarity of the patient to the diagnostic group studied. The DSI method has previously been tested in specific patient populations and has shown to perform reasonably well in the early prediction of progression from mild cognitive impairment (MCI) to Alzheimer's disease and has been successful in the classification of different dementia subtypes [3–6]. In a recent study DSI has been validated in a population-based setting to predict late-life dementia.[7] Identification of persons at risk for global cognitive decline may aid in early detection of persons at risk of dementia and may help to develop therapeutic or preventive measures to postpone or even prevent further cognitive decline and dementia.[8] This is especially important since previous research has shown that preventive interventions for dementia were more effective in persons at risk than in unselected populations.[9, 10] We therefore used DSI to predict global cognitive decline in the general population to select the persons at risk. The main aim of this study was to investigate whether multi-variate data can predict global cognitive decline in the general population. If a high risk group can be selected from the general population, a population screening program for this group might facilitate early detection of dementia. We evaluated the prediction performance using several sets of clinical features and features derived brain images acquired with magnetic resonance imagaging (MRI), to assess whether the prediction is dependent on the combination of the input features. DSI was chosen as a classification method because this method is able to handle datasets with missing data, which is often the case in population study datasets. Also, this method has been succesfully applied in previous studies and performed comparable to other state-of-the-art classificiers.[4, 7, 11]

MATERIALS AND METHODS

Study population

We included participants from three independent cohorts within the Rotterdam Study (RS), a prospective population-based cohort study in a suburb of Rotterdam

that investigates the determinants and occurrence of diseases in the middle-aged and elderly population.[12] Brain MRI-scanning was implemented in the study protocol since 2005.[13] The Rotterdam Study has been approved by the medical ethics committee according to the Population Study Act Rotterdam Study, executed by the Ministry of Health,Welfare and Sports of the Netherlands. Written informed consent was obtained from all participants.[14] We used data from RS cohorts I, II and III, of which each consists of multiple subcohorts. In this study a subcohort of RS cohort I, II and III were used, to which we refer as sI, sII and sIII, respectively. Baseline features of sI were collected during 2009-2011 and sII were collected during 2004-2006. The participants of the both cohorts were 55 years or older. For RS cohort III participants were 45 years or older at time of inclusion. Baseline features of sIII were collected during 2006-2008. Participants with prevalent dementia, mild cognitive impairment (MCI) and MRI defined cortical infarcts at baseline were excluded for all analyses. In total, 4328 participants with baseline information on cognition, MRI and other features were included. Baseline MRI was acquired on average 0.3± 0.45 years after collecting the non-imaging features. Furthermore, diffusion-MRI was acquired. However, for a subset of 680 participants in RS cohort II diffusion-MRI data was obtained on average 3.5±0.2 years later than the other baseline MRI features. Longitudinal data on global decline was available for 2542 out of 4328 participants. The follow-up cognitive assessment was on average 5.7±0.6 years after the baseline visit.

Disease State Index

Prediction was performed with DSI.[3] This classifier derives an index indicating the disease state of the partici- pant under investigation based on the available features of that participant. DSI has two major advantages: 1) it can cope with missing data and 2) it gives an interpretable result because DSI also provides a decision tree that can be quite well explained.

DSI classifier is composed of the components: fitness and relevance.[3] Let N be the total number of negatives, P the total number of positives, $FN(x)$ the number of false negatives, and $FP(x)$ the number of false positives, when x is used as classification cut-off. Then the fitness function is estimated for each feature i as:

$$f_i(x) = \frac{FNR_i(x)}{FNR_i(x) + \mathrm{FPR}_i(x)} - \frac{FN_i(x)}{FN_i(x) + \frac{P}{N} FP_i(x)} \quad (1)$$

where $FNR(x) = FN(x)/P$ is the false negative rate and $FPR(x) = FP(x)/N$ is the false positive rate in the training data when the feature value x is used as the classification cut-off. The fitness automatically accounts for the imbalance in class size making implicitly both classes equal in size, as the fraction P/N in the denominator scales the negative class (related to $FP(x)$) to correspond the size of the positive class. The fitness function is a classifier where the values < 0.5 imply negative class and > 0.5 positive class. The relevance of each feature is estimated by:

$$R = \max\{\text{sensitivity} + \text{specificity} - 1, 0\}, \quad (2)$$

which measures how good the feature is in differentiating the two classes. The lower the overlap between the distributions of positives and negatives, the higher R. Finally, DSI is computed from the equation:

$$\mathrm{DSI} = \frac{\sum_i R_i f_i}{\sum_i R_i} \quad (3)$$

DSI is a value between zero and one; somebody is classified as positive if DSI > 0.5 and as negative if DSI < 0.5. DSI is an ensemble classifier, meaning that it combines multiple independent classifiers (fitness functions) defined for each feature separately. Because of that, DSI can tolerate missing data. Features can be grouped in a hierarchical manner. The final DSI is a combination of the levels in the hierarchy. The fitness, relevance and their combination as a composite DSI are repeated recursively by grouping the data until a single DSI value is obtained.[11] Therefore, the final DSI, which is used for the classification, depends on the hierarchy structure, as a different structure leads to a different averaging of the feature combinations. The top-level part of the hierarchy defined for this study is shown in **Figure 1**.

Baseline features

Figure 1 shows the used categories of features in hierarchical manner. Please note that not all individual features are shown in this figure. The sections below describe all the used features (indicated in bold font) in detail.

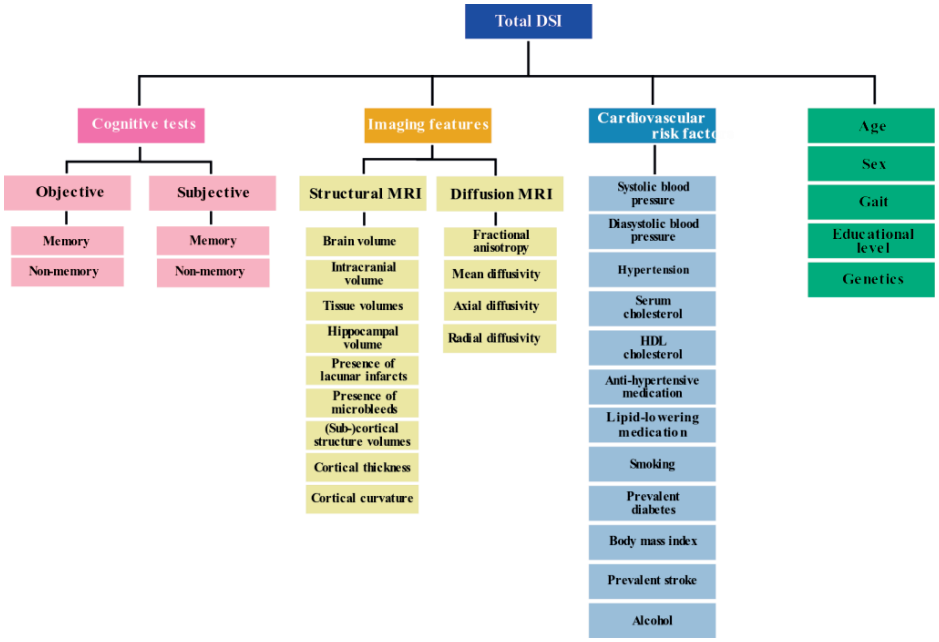

Figure 1. Feature categories shown in a hierarchy as used by the DSI. Please note that not all individual features are included in this graph

MRI features

Multi-sequence MR imaging was performed on a 1.5 Tesla MRI scanner (GE Signa Excite). The imaging protocol and sequence details were described extensively elsewhere.[13] Morphological imaging was performed with T1- weighted, proton density-weighted and fluid-attenuated inversion recovery (FLAIR) sequences. These sequences were used for an automated tissue segmentation approach to segment scans into grey matter, white matter, cere- brospinal fluid (CSF) and background tissue.[15] **Intracranial volume (ICV)** (excluding the cerebellum and surrounding CSF cerebellar) was estimated by summing total grey and white matter and CSF. Brain tissue segmentation was complemented with a **white matter lesion** segmentation based on the tissue segmentation and the FLAIR image with extraction of white matter lesion voxels by intensity thresholding.[16] We obtained **(sub)cortical struc- ture volumes**, **cortical thickness**, and **curvature** of the cortex and hippocampal volume using the publicly avail- able FreeSurfer 5.1 software [17–19]. For **cerebral blood flow** measurements, we performed a 2D phase-contrast imaging as previously described.[20] In short, blood flow velocity (mm/sec) was calculated based on regions of interest (ROI) drawn on the phase-contrast images in the carotid arteries and basilar artery at a level just under the skull base. The value of mean signal intensity in each ROI reflected the flow velocity with the cross-sectional area of the vessel. Flow was calculated by multiplying

the average velocity with the cross-sectional area of the vessel.[20] A 3D T2*-weighted gradient-recalled echo was used to image **cerebral microbleeds**. Microbleeds were defined as focal areas of very low signal intensity, smaller than 10 mm in size and were rated by one of five trained raters who were blinded to other MRI sequences and to clinical data.[21, 22] **Lacunar infarcts** were defined as focal parenchymal lesions >3 mm and < 15 mm in size with the same signal characteristics as cerebrospinal fluid on all sequences and with a hyperintense rim on the FLAIR image (supratentorially). Probabilistic tractography was used to segment 15 different white matter tracts in diffusion-weighted MR brain images, and we obtained **mean FA**, **mean MD**, **axial** and **radial diffusivity** inside each white matter tract.[23]

Cardiovascular risk factors

Cardiovascular risk factors were based on information derived from home interviews and physical examinations during the center visit. **Blood pressure** was measured twice at the right brachial artery in sitting position using a random-zero sphygmomanometer. We used the mean of two measurements in the analyses. Information on the use of **antihypertensive medication** was obtained by using questionnaires and by checking the medication cabinets of the participants. Hypertension was defined as a systolic blood pressure >140 mmHg or a diastolic blood pressure
>90 mmHg or the use of anti-hypertensive medication at baseline. **Serum total cholesterol and high-density lipoprotein (HDL) cholesterol** were measured in fasting serum, taking lipid-lowering medication into account.
Smoking was assessed by interview and coded as never, former and current. **Body-mass index (BMI)** is defined as weight kilograms divided by height in meters squared. **Diabetes mellitus** status was defined as a fasting serum glucose level (>7.0 mmol/l) or, if unavailable, non-fasting serum glucose level (>11.1 mmol/l) or the use of anti-diabetic medication.[14] **Alcohol consumption** was acquired in a questionnaire. **Prevalent stroke** was ascertained as previously described.[24] **Educational level** was assessed during a home interview and was categorized into 7 categories, ranging from primary education only to university level.[14]

APOE-ε4 allele carriership

APOE-E4 allele carriership was assessed on coded genomic DNA samples.[25] APOE-genotype was in Hardy- Weinberg equilibrium. APOE-E4 allele carriership was coded positive in case of one or two APOE-E4 alleles.

Gait features

Gait was assessed by three walking tasks over a walkway: “normal walk”, “turn” and “tandem walk” (heel to toe).[26] Using a principal component analysis we obtained the

following gait factors which we used by DSI: **Rhythm**, **Variability**, **Phases**, **Pace**, **Base of Support**, **Tandem**, and **Turning**.[27]

Baseline cognitive function

We included the following **objective memory** and **non-memory** cognitive tests: **15-Word Learning Test imme- diate** and **delayed recall**,[28] **Stroop tests** (**reading**, **color-naming** and **interference**),[29, 30] **The Letter-Digit Substitution Task**,[31] **Word Fluency Test**,[32] and the **Purdue Pegboard test**.[33] **Subjective cognitive complaints** were evaluated by interview. This interview included three questions on mem- ory (difficulty remembering, forgetting what one had planned to do, and difficulty finding words), and three questions on everyday functioning (difficulty managing finances, problems using a telephone, and difficulty getting dressed).[34]

Outcome: definition of cognitive decline

A g-factor was constructed by a principal component analysis on the delayed recall score of the 15-Word Learning Test, Stroop interference Test, Letter-Digit Substitution Task, Word Fluency Test, and the Purdue Pegboard test.[34] Cognitive decline was defined by the g-factor from the follow-up visit minus the g-factor from the baseline visit resulting in a delta g-factor. Since the follow-up time was not the same for each participant, the delta g-factor was divided by the follow-up time to obtain global cognitive decline per year. Significant global cognitive decline (yes/no) was defined as belonging to the 5% of participants with the highest cognitive decline (delta g-factor) per year. In the used dataset, consisting of 2,542 participants, this resulted in 127 participants with a positive class label.

Evaluation experiments

Prediction performance evaluation

The performance of DSI in predicting occurrence of global cognitive decline was evaluated using cross-validation. The area under the receiver-operator curve (AUC) was determined using 500 repetitions of 2-fold cross-validation (CV) experiments. This means that with each repetition 50% of the study dataset was used for training and the other 50% was used for testing, and vice versa, keeping the class ratio in the training and test set equal. We report the mean AUC, and the uncertainty of the mean expressed by its 95% confidence interval, derived from the 1000 resulting AUC values. The confidence interval was determined with the corrected resampled t-test for CV estimators of the generalization error.[35] AUCs were considered significantly different if the 95% confidence interval of their difference did not contain zero.

Since global cognitive decline per year is age dependent, we expect that age is an important feature for the prediction. We therefore include **age** as feature in the model.

However, since other features might depend on age, correcting these features might improve the prediction performance.[36] We therefore also assessed the prediction performance using age-corrected features. We corrected the non-binary features for age using a linear regression model.[37] We evaluated four different models:

I age was included and no age-correction was performed on thenon-binary features
II age was excluded and no age-correction was performed on the non-binary features
III age was included and non-binary features, except age, were corrected for age
IV age was excluded and non-binary features, except age, were corrected for age.

To assess whether the performance of DSI was dependent on the combination of input features, we evaluated various feature combinations. In each cross-validation experiment the feature set was expanded with a feature or category of features. We analyzed four of such cumulative feature sets, differing in the order in which the feature set was expanded. Additionally, we analyzed MRI features separately and a set including all features but age.

Relevance analysis

To gain insight into the relevance weight that DSI assigns to each feature, we calculated the feature relevance distribution over the 500 repetitions of 2-fold CV, for the top-level feature categories of the hierarchy: age, sex, cognitive tests, cardiovascular risk factors, gait, education, genetics, and MRI features.

Feature selection on MRI features

In this study, hundreds of MRI features were extracted from images. It is likely that many of those features are not very efficient in detecting cognitive decline. Typically feature selection is applied to exclude poor features which may induce noise to the classifier. In DSI, weighting with relevance supresses the effect of such features. If the number of features is high, their cumulative effect may, however, be remarkable. Previous results have shown that when including many features with a low relevance, the performance of DSI may decrease.[7] We therefore included an experiment evaluating the effect of feature selection on MRI features using their relevance. Due to averaging, feature noise reduces in higher levels of the feature hierarchy. The relevance of top-level feature categories may therefore be higher than lower-level, individual features. Therefore, due to the selection on the individual features, the top-level features may drop out, despite their high relevance. To prevent entire top-level feature categories to drop out of the model, we chose to only apply feature selection on the MRI features, which made up 80% of all input features, before selection. The relevance of the MRI features was determined on the entire dataset, before training. MRI features were selected by thresholding the relevance. Subsequently, an AUC distribution was

determined in 10 repetitions of 2-fold CV. The following relevance thresholds were chosen: $t \in \{0.0, 0.01, \ldots, 0.09, 0.1\}$. For each threshold we assessed three feature sets in which the relevance-based feature selection on the MRI features was applied: 1) all features, 2) all features but age, and 3) MRI features only.

Sub-group analyses

As subjects close to the decision boundary (DSI ~0.5) are more likely to be misclassified, we evaluated classification performance when only accepting/providing the classification for test subjects with low (<0.2) or high (>0.8) DSI. In this way, the subjects with 0.2 < DSI < 0.8 are disregarded, which, in a clinical case, would mean that there is no diagnosis possible for these cases. We computed the AUC of this sub-group for DSI using all available features, both with age-correction and without age-correction. Furthermore, we performed a sensitivity analysis in which the diffusion-MRI of 680 participants in RS cohort II were ignored, because this data was obtained on average 3.47± 0.15 years later than the other baseline MRI features.

RESULTS

Table 1 presents the characteristics of the study population. The mean age of the participants was 60.9 ± 9.1 years and 55.6% were females.

Prediction performance

Figure 2a shows the mean AUC (95% confidence interval) for several combinations of features in predicting global cognitive decline, without correcting the non-binary features for age. Each color represents an expanding set of used input features, where the most left set is only MRI features and the most right set is all features except age. When using only MRI features, the AUC was 0.75 (0.70 - 0.80). When using only age as baseline feature, the AUC was 0.78 (0.74 - 0.83). Using additional features on top of age resulted in an equal or slightly lower AUC (differences not statistically significant). When using all available features with DSI, the AUC was 0.77 (0.72 - 0.82). The mean AUC of DSI without age as baseline predictor was 0.75 (0.70 - 0.80).

Figure 2b shows the mean AUC (95% confidence interval) for the same combinations of features as in **Figure 2**a, but here the non-binary features were corrected for age. The AUC for MRI features only was significantly lower with age-correction compared to without age correction, with an AUC of 0.55 (0.50 - 0.61). For the other feature sets, the AUC of the models where age correction was applied was not statistically significantly different, compared to not using age correction. When the effect of age was totally removed from the model, i.e. model iv, the AUC was 0.65 (0.58 - 0.73).

Table 1 Baseline characteristics

Feature	R_{nac}	R_{nac}	Positive R_{ac}(N=127)	Control N=2415)
Age, years	0.38	-	71.2 (10.1)	60.3 (8.7)
Sex, female	0.01	-	73 (54.5%)	1340 (55.6%)
Objective cognitive test results	0.28	0.16	-	-
Word Learning Test immediate recall	0.09	0.02	7.7 (2.2)	8.1 (2.0)
Word Learning Test delayed recall	0.05	0.04	7.9 (2.9)	8.2 (2.8)
Reading subtask of Stroop test, s	0.20	0.03	17.2 (2.7)	16.3 (2.9)
Color naming subtask of Stroop test, s	0.18	0.06	23.6 (3.6)	22.3 (4.0)
Interference subtask of Stroop test, s	0.32	0.10	53.8 (20.3)	44.0 (13.0)
Letter-Digit Substitution Task, number of correct digits	0.15	0.00	29.7 (6.7)	32.2 (6.2)
Word Fluency Test, number of animals	0.04	0.08	23.2 (5.7)	23.8 (5.7)
Purdue Pegboard test, number of pins placed	0.15	0.07	10.3 (2.1)	10.9 (1.7)
Mini-mental-state examination	0.14	0.11	27.8 (1.7)	28.4 (1.5)
Education[1]	0.07	0.07	3 (1-3)	3 (2-5)
Cardiovascular risk factors	0.34	0.27	-	-
Alcohol[1], glasses per week	0.06	0.04	3.5 (0.3-5.5)	5.5 (1.0-5.5)
Systolic blood pressure, mmHg	0.24	0.04	146.2 (20.3)	135.9 (19.6)
Diastolic blood pressure, mmHg	0.00	0.02	82.8 (9.4)	82.4 (10.6)
Blood pressure lowering medication	0.26	-	51 (38.3%)	284 (11.9%)
Body Mass Index, kg/m^2	0.07	0.07	28.2 (4.4)	27.4 (4.1)
Serum cholesterol, mmol/L	0.11	0.12	5.4 (0.9)	5.6 (1.1)
HDL-cholesterol, mmol/L	0.04	0.09	1.4 (0.4)	1.5 (0.4)
Lipid lowering medication	0.13	-	46 (34.6%)	510 (21.3%)
Smoking	0.08	0.08	-	-
Never	-	-	49 (36.6%)	746 (31.2%)
Former	-	-	54 (40.3%)	1154 (48.2%)
Current	-	-	31 (23.1%)	492 (20.6%)
Diabetes mellitus, presence	0.09	-	24 (18.2%)	220 (9.2%)
APOE-E4 allele carriership	0.02	-	39 (30.2%)	639 (28.3%)
MRI features	0.41	0.25	-	-
Intra-cranial volume, mL	0.03	0.00	1137 (119)	1144 (113)
Brain tissue volume	0.38	0.08	-	-
White matter volume, mL	0.13	0.01	390 (60)	419 (57)
Gray matter volume, mL	0.10	0.01	522 (54)	537 (52)
CSF volume, mL	0.29	0.07	223 (53)	186 (46)
Brain region volume	0.35	0.12	-	-
Hippocampus volume, mL	0.23	0.09	6.4 (0.8)	6.8 (0.7)
White matter lesion volume[1], mL	0.31	0.08	4.5 (2.5-9.4)	2.4 (1.4-4.3)
Cerebral microbleeds, presence	0.09	-	33 (24.6%)	370 (15.6%)
Lacunar infarcts, presence	0.04	-	10 (7.5%)	72 (3.0%)
Global FA	0.17	0.07	0.3 (0.02)	0.3 (0.01)

Table 1 Baseline characteristics (*continued*)

Feature			Positive	Control
	R_{nac}	R_{nac}	R_{ac}(N=127)	N=2415)
Global MD,10^{-3} mm^2/s	0.33	0.07	0.8 (0.03)	0.7 (0.03)
Global cortical thickness, mm	0.08	0.01	2.4 (0.2)	2.5 (0.1)
Gait	0.19	0.17	-	-

Baseline features of the study population and their relevances. The relevances were computed on the entire dataset. Continuous variables are presented as mean (standard deviation) and categorical variables as *n* (percentages).*Abbreviations*: N; number of participants, HDL; high-density lipoprotein, s; seconds, FA; fractional anisotropy, MD; mean diffusivity 10^{-3} mm2/s. CSF; cerebrospinal fluid. *Symbols*: R_{nac}; relevance when feature was not corrected for age, R_{ac}; relevance when feature was age-corrected. 1Education, alcohol and white matter lesion volume are presented as median (inter-quartile range).

Relevance analysis

Figure 3 shows the relevance weight per feature category when the non-categorical features were corrected for age prior to computing DSI and without age-correction. Without age-correction, the features with the best discriminating abilities according to their relevance weights were MRI features (0.42 (0.33 - 0.51)), age (0.39 (0.27 - 0.51)), cognitive tests (0.35 (0.24 - 0.45)) and cardiovascular risk factors (0.34 (0.26 - 0.43)). When correcting the non- binary features, except age, for age, the most discriminating features were age (0.39 (0.27 - 0.51)), MRI features (0.37 (0.24 - 0.51)), and cognitive tests (0.32 (0.17 - 0.47)).

Feature selection on MRI features

Feature selection for MRI features had no effect on the AUC in any of the three feature sets, when the non-binary features were not corrected for age (**Figure 4A)**. The AUC did increase after MRI feature selection when the non-binary features, except age, had been corrected for age (**Figure 4B**), with the optimal *t* being 0.07 (see **Figure 4**b). For $t = 0.07$, the AUC increased from 0.55 (0.50 - 0.61) to 0.62 (0.58 - 0.67) when only MRI features were included in the model. When using all features, the AUC increased from 0.75 (0.70 - 0.79) to 0.77 (0.73 - 0.82), and when using all features but age, the AUC increased from 0.65 (0.58 - 0.73) to 0.70 (0.63 - 0.76).

Sub-group analyses

When only taking into account the extreme cases, i.e. cases for which $0.2 < DSI < 0.8$ (~40% of the total dataset, i.e.~1000 subjects), the mean AUC increased to 0.82 (0.76 - 0.88) using age as input feature only. Again in this group, additional features did not significantly improve the performance of DSI (results not shown). Ignoring the diffusion-MRI features of 680 participants of whom this data was acquired on average 3.47 ± 0.15 years later than the assessment of the other baseline MRI features did not change AUC significantly compared to the performance in the total population (results not shown).

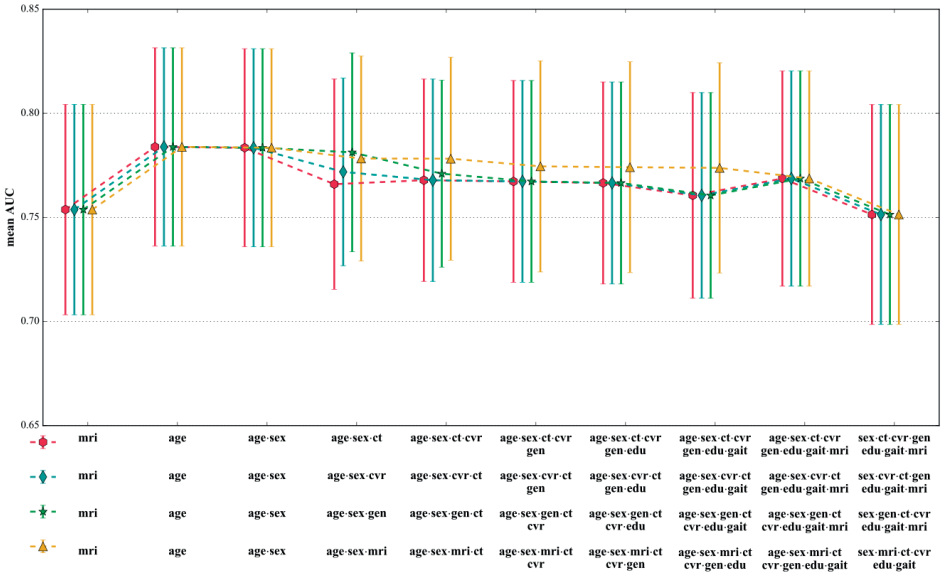

Figure 2A. Mean AUC for several combinations of features without correcting the non-binary features for age**.** Features are accumulated in four different orders, indicated by color and symbol. The bars indicate the confidence interval. Short-hand notations are used for several features: cognitive tests (ct), cardiovascular risk factors (cvr), MRI features (mri), genetics (APOE-E4 carrier-ship) (gen), and educational level (edu)

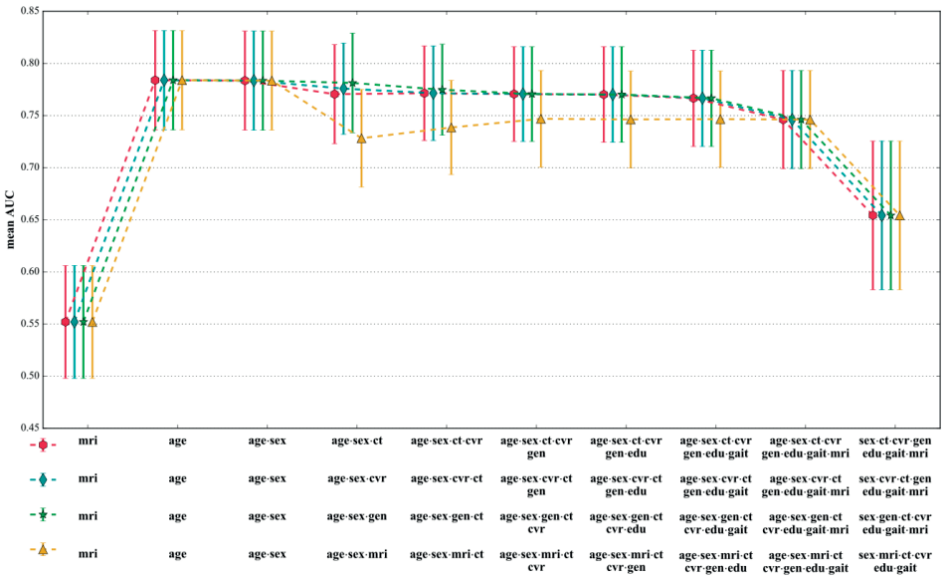

Figure 2B is with the non-binary features corrected for age. Features are accumulated in four different orders, indicated by color and symbol. The bars indicate the confidence interval. Short-hand notations are used for several features: cognitive tests (ct), cardiovascular risk factors (cvr), MRI features (mri), genetics (APOE-E4 carrier-ship) (gen), and educational level (edu).

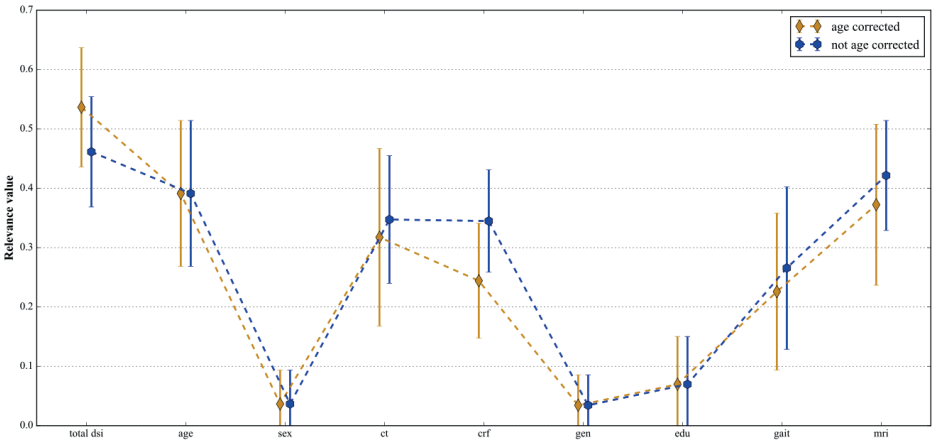

Figure 3. Mean relevance weight *R* and 95% confidence interval for the top-level features categories. The blue line shows the case where the non-binary features were non corrected for age and the golden line shows the case where the non-binary features were age-corrected.

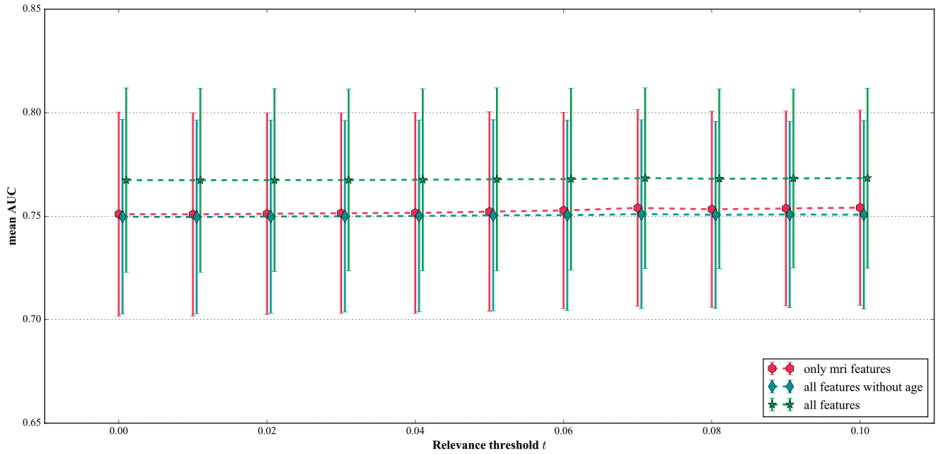

Figure. 4A. Mean AUC for several combinations of features where the MRI features were selected based on their relevance without correcting the non-binary features for age**.**

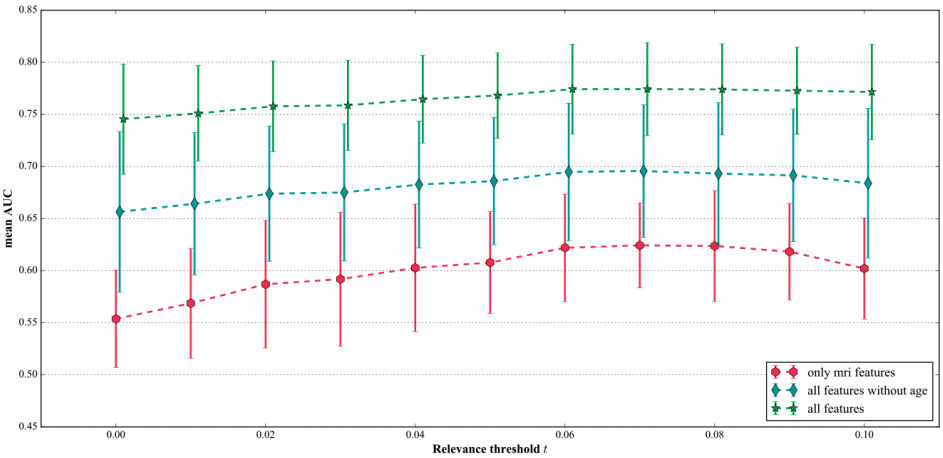

Figure 4B is with the non-binary features corrected for age. Features with $R < t$ were excluded.

DISCUSSION

The objective of this study was to assess whether global cognitive decline can be predicted using multi-variate data with the previously proposed DSI. We found the best prediction performance, evaluated with AUC, using only age as input feature. Adding more features to DSI did not improve its performance in predicting global

cognitive decline as defined in this study. Overall performance of DSI in the prediction of global cognitive decline (mean AUC 0.78) was comparable to previously reported performances of DSI for prediction of dementia[7] in the population-based CAIDE study, consisting of 2000 participants who were randomly selected from four separate, population-based samples, originally studied in midlife (1972, 1977, 1982, or 1987),[38] and to other population-based prediction models of dementia.[39] In this study we included a large number of heterogeneous features. Age was the most important feature for predicting global cognitive decline using DSI, yielding the highest AUC. This was further supported by the observation that the performance of DSI reduced when using all features except age. Our finding that age is the single strongest predictor for cognitive decline is in line with published prediction models for dementia, that invariably assign the highest weight to age.[40] We found that the relevance R, which indicates how well a feature can discriminate between persons who will develop cognitive decline and those who will not, was highest for MRI features (0.42) followed by age (0.39). DSI, however, performed worse when using only MRI features, compared to using only age. We speculate that the high relevance of the MRI features may be explained by age-specific effects that are captured in these MRI features, which is supported by our finding that MRI feature relevance (0.37) and DSI performance dropped when adjusting MRI features for age. When the non-binary features were age-corrected and age was not included in the model, the mean AUC was 0.65, still significantly better than chance (0.5), indicating that relevant information for predicting global cognitive decline could be present in the other features. In this study, however, they did not improve the predicting performance when added to age. To our surprise we found that APOE-4 allele carrier-ship had a low relevance weight and did not improve the performance of DSI, even though it is the best known genetic risk factor for AD. This is in contrast to a previous study focusing on the progression from MCI to AD, which found APOE-genotype to have high predictive value.[41] It may be that our study population was too young to show effect of APOE on prediction (mean age 60.9), since the risk progression effect of APOE-4 allele carriership has been described to peak between ages 70 and 75 years.[42] The relevance-based feature selection on the MRI features showed an increase in the AUC, but only when the nonbinary features were corrected for age. A possible explanation is that without age correction, the AUC is strongly driven by the age-factor that is present in the MRI features. In this case, less and different features were excluded compared to the age-corrected models, causing the selection to have no effect on the prediction performance. However, after removal of these age-specific effects by age correction, performance can be increased by removal of irrelevant features. When age was totally excluded from the model iv (age was excluded and age correction was applied to the non-binary features), an AUC of 0.70 was obtained, showing the potential of the other features. One limitation of

this analysis is that the relevance computation and threshold selection was done on the entire dataset, i.e. the training data was included in these computations. Therefore, AUC increase due to application of the relevance threshold might be overestimated, but can be seen as an upper limit. The overall conclusions do not change.
To our knowledge, this is the first population-based study testing the supervised machine learning DSI tool for prediction of global cognitive decline. Strengths of our study include the population-based design, large sample size and availability of an extensive set of features. However, limitations of our dataset need to be considered. We constructed a g-factor as a measure of global cognition and participants without complete cognitive data were excluded.This might have caused some selection bias towards relatively healthy subjects. Also, mortality and drop-out was not taken into account. Persons who are lost to follow-up usually have a poorer health status and are therefore more likely to develop cognitive decline or die before onset of cognitive decline. The exclusion of these ssumingly more severe cases might have lowered the performance of DSI. The result that age is the main predictor for cognitive decline indicates that the age distribution of the subjects with cognitive decline differs from the entire set of subjects. Hence age could be used to select people at risk of cognitive decline. However, when screening for significant cognitive decline, an age-dependent threshold on cognitive decline might be needed, e.g. using the 5% percentile of the cognitive decline as function of age, to detect young people at risk of developing dementia. The usage of such an age-dependent threshold will be part of future research.
Finally, it should be noted that cognitive decline is not equivalent to neurodegeneration/dementia and may result from other causes 260 as well, due to conditions affecting the participant's cognition at the time of the cognitive assessment, normal human variability and normal aging. Nevertheless, being able to predict cognitive decline would be a step forward in selecting people for therapy or prevention.

Conclusion and future work

Based on our results we can conclude that age is the most important predictor for cognitive decline in the general population using DSI. Other features showed having potential, but did not improve prediction performance. A next step could be to use longitudinal features in DSI, as these might improve its prediction performance. To validate whether our findings are not due to limitations of DSI, also other methods need to be evaluated in this prediction challenge. Finally, to be able to detect younger people at risk of significant global cognitive decline in future studies, thresholds for cognitive decline should be carefully chosen depending on the population, for example be age-adjusted.

CHAPTER REFERENCES

1. C.R. Jack, D.S. Knopman, W.J. Jagust, R.C. Petersen, M.W. Weiner, P.S. Aisen, L.M. Shaw, P. Vemuri, H.J. Wiste, S.D. Weigand, T.G. Lesnick, V.S. Pankratz, M.C. Donohue and J.Q. Trojanowski, Tracking pathophysiological processes in Alzheimer´s disease: an up300 dated hypothetical model of dynamic biomarkers, Lancet Neurology 12(2) (2013), 207–216.
2. S. Kloppel, C.M. Stonnington, J. Barnes, F. Chen, C. Chu, C.D. Good, I. Mader, L.A. Mitchell, A.C. Patel, C.C. Roberts, N.C. Fox, C.R. Jack, J. Ashburner and R.S. Frackowiak, Accuracy of dementia diagnosis: a direct comparison between radiologists and a computerized method, Brain 131(11) (2008), 2969–2974.
3. J. Mattila, J. Koikkalainen, A. Virkki, A. Simonsen, M. van Gils, G. Waldemar, H. Soininen, J. Lötjönen and the Alzheimer's Disease Neu305 roimaging Initiative., A disease state fingerprint for evaluation of Alzheimer's disease, Journal of Alzheimer's Disease 27(1) (2011), 163–176.
4. J. Mattila, H. Soininen, J. Koikkalainen, D. Rueckert, R.Wolz, G.Waldemar and J. Lötjönen, Optimizing the diagnosis of early Alzheimer's disease in mild cognitive impairment subjects, Journal of Alzheimer's Disease 32(4) (2012), 969–979.
5. A. Hall, J. Mattila, J. Koikkalainen, J. Lötjönen, R. Wolz, P.H. Scheltens, G.B. Frisoni, M. Tsolaki, F. Nobili, Y. Freund-Levi, L. Minthon, L. Frölich, H.J. Hampel, P.T. Visser and H. Soininen, Predicting progression from cognitive impairment to Alzheimer's disease with the Disease State Index, Current Alzheimer Research 12(1) (2015), 69–79.
6. M.A.M. noz-Ruiz, A. Hall, J. Mattila, J. Koikkalainen, S.K. Herukka, R. Vanninen, Y. Liu, J. Lötjönen, H.S. H and the Alzheimer's Disease Neuroimaging Initiative., Comparing predictors of conversion to Alzheimer's disease using the disease state index, Neurodegenerative Diseases 13(2–3) (2014), 200–202. 7 T. Pekkala, A. Hall, J. Lötjönen, J. Mattila, H. Soininen, T. Ngandu, T. Laatikainen, M. Kivipelto and A. Solomon, Development of a Late-Life Dementia Prediction Index with Supervised Machine Learning in the Population-Based CAIDE Study, Journal of Alzheimer's Disease 55(3) (2017), 1055–1067.
8. J.A. Blumenthal, P.J. Smith, S. Mabe, A. Hinderliter, K. Welsh-Bohmer, J.N. Browndyke, P.H. Lin, W. Kraus, P.M. Doraiswamy, J. Burke and A. Sherwood, Lifestyle and Neurocognition in Older Adults with Cardiovascular Risk Factors and Cognitive Impairment, Psychoso-matic Medicine 79(6) (2017), 719–727.
9. E.P.M. van Charante, E. Richard, L.S. Eurelings, J.W. van Dalen, S.A. Ligthart, E.F. van Bussel, M.P. Hoevenaar-Blom, M. Vermeulen and W.A. van Gool, Effectiveness of a 6-year multidomain vascular care intervention to prevent dementia (preDIVA): a cluster-randomised controlled trial, Lancet 388(10046) (2016), 797–805.
10. T. Ngandu, J. Lehtisalo, A. Solomon, E. Levälahti, S. Ahtiluoto, R. Antikainen, L. Bäckman, T. Hänninen, A. Jula, T. Laatikainen, J. Lind325 ström, F. Mangialasche, T. Paajanen, S. Pajala, M. Peltonen, R. Rauramaa, A. Stigsdotter-Neely, T. Strandberg, J. Tuomilehto, H. Soininen and M. Kivipelto, A 2 year multidomain intervention of diet, exercise, cognitive training, and vascular risk monitoring versus control to prevent cognitive decline in at-risk elderly people (FINGER): a randomised controlled trial, Lancet 385(9984) (2015), 2255–2263.
11. J. Mattila, J. Koikkalainen, A. Virkki, M. van Gils, J. Lötjönen and for the Alzheimer's Disease Neuroimaging Initiative, Design and Application of a Generic Clinical Decision Support System for Multiscale Data, IEEE Transactions on Biomedical Engineering 59(1) (2012), 234–240.
12. M.A. Ikram, G.G. Brusselle, S.D. Murad, C.M. van Duijn, O.H. Franco, A. Goedegebure, C.C.W. Klaver, T.E.C. Nijsten, R.P. Peeters, B.H. Stricker, H. Tiemeier, A.G. Uitterlinden, M.W. Vernooij

and A. Hofman, The Rotterdam Study: 2018 update on objectives, design and main results, European Journal of Epidemiology 32(9) (2017), 807–850.

13. M.A. Ikram, A. van der Lugt, W.J. Niessen, P.J. Koudstaal, G.P. Krestin, A. Hofman, D. Bos and M.W. Vernooij, The Rotterdam Scan Study: design update 2016 and main findings, European Journal of Epidemiology 30(12) (2015), 1299–1315.
14. A. Hofman, G.G. Brusselle, S.D. Murad, C.M. van Duijn, O.H. Franco, A. Goedegebure, M.A. Ikram, C.C.K.T.E.C. Nijsten, R.P. Peeters, B.H. Stricker, H.W. Tiemeier, A.G. Uitterlinden and M.W. Vernooij, The Rotterdam Study: 2016 objectives and design update, European Journal of Epidemiology 30(8) (2015), 661–708.
15. H.A. Vrooman, C.A. Cocosco, F. van der Lijn, R. Stokking, M.A. Ikram, M.W. Vernooij, M.M. Breteler and W.J. Niessen, Multi-spectral brain tissue segmentation using automatically trained k-Nearest-Neighbor classification, NeuroImage 37(1) (2007), 71–81.
16. R. de Boer, H.A. Vrooman, F. van der Lijn, M.W. Vernooij, M.A. Ikram, A. van der Lugt, M.M. Breteler and W.J. Niessen, White matter lesion extension to automatic brain tissue segmentation on MRI, NeuroImage 45(4) (2009), 1151–1161.
17. A.M. Dale, B. Fischl and M.I. Sereno, Cortical surface-based analysis. I. Segmentation and surface reconstruction, NeuroImage 9(2) (1999), 179–194.
18. R.S. Desikan, F. Ségonne, B. Fischl, B.T. Quinn, B.C. Dickerson, D. Blacker, R.L. Buckner, A.M. Dale, R.P. Maguire, B.T. Hyman, M.S. Albert and R.J. Killiany, An automated labeling system for subdividing the human cerebral cortex on MRI scans into gyral based regions of interest, NeuroImage 31(3) (2006), 968–980.
19. B. Fischl, D.H. Salat, E. Busa, M. Albert, M. Dieterich, C. Haselgrove, A. van der Kouwe, R. Killiany, D. Kennedy, S. Klaveness, A. Montillo,N. Makris, B. Rosen and A.M. Dale, Whole brain segmentation: automated labeling of neuroanatomical structures in the human brain, Neuron 33(3) (2002), 341–355.
20. M.W. Vernooij, A. van der Lugt, M.A. Ikram, P.A.Wielopolski, H.A. Vrooman, A. Hofman, G.P. Krestin and M.M. Breteler, Total cerebral blood flow and total brain perfusion in the general population: the Rotterdam Scan Study, Journal of Cerebral Blood Flow & Metabolism 28(2) (2008), 412–419.
21. G. Roob, R. Schmidt, P. Kapeller, A. Lechner, H.P. Hartung and F. Fazekas, MRI evidence of past cerebral microbleeds in a healthy elderly population, Neurology 52(2) (1999), 991–994.
22. M.W. Vernooij, A. van der Lugt, M.A. Ikram, P.A. Wielopolski, W.J. Niessen, A. Hofman, G.P. Krestin and M.M. Breteler, Prevalence andrisk factors of cerebral microbleeds: the Rotterdam Scan Study, Neurology 70(14) (2008), 1208–1214.
23. M. de Groot, M.A. Ikram, S. Akoudad, G.P. Krestin, A. Hofman, A. van der Lugt, W.J. Niessen and M.W. Vernooij, Tract-specific white matter degeneration in aging: the Rotterdam Study, Alzheimer's & Dementia 11(3) (2015), 321–330.
24. S. Akoudad, M.L. Portegies, P.J. Koudstaal, A. Hofman, A. van der Lugt, M.A. Ikram and M.W. Vernooij, Cerebral Microbleeds Are Associated With an Increased Risk of Stroke: The Rotterdam Study, Circulation 132(6) (2015), 509–516.
25. P.R. Wenham, W.H. Price and G. Blandell, Apolipoprotein E genotyping by one-stage PCR, Lancet 337(8750) (1991), 1158–1159.
26. L. Lahousse, V.J. Verlinden, J.N. van der Geest, G.F. Joos, A. Hofman, B.H. Stricker, G.G. Brusselle and M.A. Ikram, Gait patterns in COPD: the Rotterdam Study, European Respiratory Journal 46(1) (2015), 88–95.

27. V.J. Verlinden, J.N. van der Geest, Y.Y. Hoogendam, A. Hofman, M.M. Breteler and M.A. Ikram, Gait patterns in a community-dwelling population aged 50 years and older, Gait Posture 37(4) (2013), 500–505.
28. M.L. Bleecker, K. Bolla-Wilson, J. Agnew and D.A. Meyers, Age-related sex differences in verbal memory, Journal of Clinical Psychology 44(3) (1988), 403–411.
29. I. Goethals, K. Audenaert, F. Jacobs, E. Lannoo, C.V. de Wiele, H. Ham, A. Otte, K. Oostra and R. Dierckx, Cognitive neuroactivation using SPECT and the Stroop Colored Word Test in patients with diffuse brain injury, Journal of Neurotrauma 21(8) (2004), 1059–1069.
30. C.J. Golden, Identification of brain disorders by the Stroop Color and Word Test, Journal of Clinical Psychology 32(3) (1976), 654–658.
31. M.D. Lezak, Neuropsychological assessment in behavioral toxicology–developing techniques and interpretative issues, Scandinavian Journal of Work, Environment & Health 10(Suppl 1) (1984), 25–29.
32. K.A. Welsh, N. Butters, R.C. Mohs, D. Beekly, S. Edland, G. Fillenbaum and A. Heyman, The Consortium to Establish a Registry for Alzheimer's Disease (CERAD). Part V. A normative study of the neuropsychological battery, Neurology 44(4) (1994), 609–614.
33. J. Desrosiers, R. Hébert, G. Bravo and E. Dutil, The Purdue Pegboard Test: normative data for people aged 60 and over, Disability and Rehabilitation 17(5) (1995), 217–224.
34. Y.Y. Hoogendam, A. Hofman, J.N. van der Geest, A. van der Lugt and M.A. Ikram, Patterns of cognitive function in aging: the Rotterdam Study, European Journal of Epidemiology 29(2) (2014), 133–140.
35. C. Nadeau and Y. Bengio, Inference for the Generalization Error, Machine Learning 52(3) (2003), 239–281.
36. F. Falahati, D. Ferreira, H. Soininen, P. Mecocci, B. Vellas, M. Tsolaki, I. Kłoszewska, S. Lovestone, M. Eriksdotter, L.-O. Wahlund, A. Simmons, E. Westman, for the AddNeuroMed consortium and the Alzheimer´s Disease Neuroimaging Initiative, The effect of age correction on multivariate classification in Alzheimer´s disease, with a focus on the characteristics of incorrectly and correctly classified subjects, Brain Topography 29(2) (2016), 296–307.
37. J. Koikkalainen, H. Pölönen, J. Mattila, M. van Gils, H. Soininen, J. Lötjönen and the Alzheimer's Disease Neuroimaging Initiative, Improved Classification of Alzheimer's Disease Data via Removal of Nuisance Variability, PLoS One 7(2) (2012), 31112.
38. M. Rusanen, M. Kivipelto, E. Levälahti, T. Laatikainen, J. Tuomilehto, H. Soininen and T. Ngandu, Heart diseases and long-term risk of dementia and Alzheimer's disease: a population-based CAIDE study., Journal of Alzheimer's disease 42(1) (2014), 183–191.
39. M. Kivipelto, T. Ngandu, T. Laatikainen, B. Winblad, H. Soininen and J. Tuomilehto, Risk score for the prediction of dementia risk in 20 years among middle aged people: a longitudinal, population-based study, Lancet Neurology 5(9) (2006), 735–741.
40. B.C. Stephan, C. Tzourio, S. Auriacombe, H. Amieva, C. Dufouil, A. Alpérovitch and T. Kurth, Usefulness of data from magnetic resonance imaging to improve prediction of dementia: population based cohort study, The British Medical Journal 350 (2015), 2863.
41. L.C. Löwe, C. Gaser, K. Franke and for the Alzheimer's Disease Neuroimaging Initiative, The Effect of the APOE Genotype on Individual BrainAGE in Normal Aging, Mild Cognitive Impairment, and Alzheimer's Disease, PLoS One 11(7) (2016), 0157514.
42. L.W. Bonham, E.G. Geier, C.C. Fan, J.K. Leong, L. Besser, W.A. Kukull, J. Kornak, O.A. Andreassen, G.D. Schellenberg, H.J. Rosen, W.P. Dillon, C.P. Hess, B.L. Miller, A.M. Dale, R.S. Desikan

and J.S. Yokoyama, Age-dependent effects of APOE_4 in preclinical Alzheimer's disease, Annals of Clinical and Translational Neurology 3(9) (2016), 668–677.

CHAPTER 4

General discussion

MAIN FINDINGS AND INTERPRETATION

General Discussion

The main objectives of my thesis were to study determinants of white matter microstructural changes as assessed with Diffusion-Tensor-Imaging (DTI), and to study the role of white matter microstructural changes in age related brain diseases such as cognitive decline, dementia, and neurovascular disease.
In this chapter, I will first discuss my main findings and I will consider possible pathways underlying the found associations and additionally some methodological considerations. Next, I will discuss the implications of the findings with respect to clinical practice and finally I will discuss future perspectives.

Main findings

Determinants of white matter microstructural integrity

Chapter 2 in this thesis describes the different determinants of white matter microstructural changes globally but also in specific tracts. I started with a longitudinal analysis for the establishment of reference values of change in DTI-measures in aging. Since the brain is not an isolated organ but is connected with all other organs in our body, I was also interested in the systemic influences on the brain by different organ systems, such as the kidneys, the lungs and the thyroid gland. To explore whether microvascular pathology could be one of the possible pathways leading to lower white matter microstructural integrity I also studied the association between retinal vessels and microstructural changes in this chapter.
I found lower white matter microstructural integrity in most parts of the brain normal-appearing white matter after two years of follow-up in normal aging. Also, reduced kidney function associated with lower white matter microstructural integrity throughout the brain. Retinal vessel diameters was linked to white matter microstructure by means that larger venules and narrower arteries associated with a poorer white matter microstructural integrity. Reduced lung function was linked to lower white matter microstructural integrity in particular in the association tracts. In the last chapter I found an age-dependent association between thyroid hormones and white matter microstructural integrity: in younger individuals higher levels of free thyroxine (FT4) were associated with larger total brain volumes (mainly white matter volume) and a better white matter microstructural integrity and in older persons higher FT4 associated with smaller total brain volumes and a poorer white matter microstructural integrity.
The results reported in **chapter 2** indicate that aging and systemic influences of (subclinical) disease outside the brain are consistently associated with reduced white

matter microstructural integrity. What underlies these associations? There are various potential pathways, supported by the different chapters in my thesis.

First, a vascular etiologic pathway has often been hypothesized.[1] Vascular brain pathology may lead to a reduction in white matter perfusion, for example due to impaired autoregulation, resulting in white matter damage.[2-5] Another mechanism may be that the presence of vascular factors, not causing direct damage, interact with another degenerative process and worsen pathologic effects.[6] Yet another possibility is that shared vascular risk factors such as hypertension and diabetes explain the association between (subclinical) disease outside the brain and subclinical brain changes. This latter mechanism is especially feasible in situations in which small vessels for example in the kidney or retina and brain are similar with anatomical and hemodynamic similarities.[7] My findings in **chapter 2.2** indeed confirmed a role of vascular factors. The association between kidney function and cerebral white matter microstructure attenuated after adjusting for cardiovascular risk factors, indicating that the association was partly driven by cardiovascular factors. Furthermore, I found effect-modification by hypertension in the association between kidney function and lower white matter microstructural integrity. In addition, my findings in **chapter 2.3** in which retinal vessel calibres associated with white matter microstructural integrity, suggest a microvascular pathway underlying the white matter microstructural changes. However, both in **chapter 2.1**, focussing on aging and white matter microstructure, and in **chapter 2.5** assessing the relation of thyroid hormones and brain morphology, adjusting for cardiovascular risk factors did not change the estimates marginally. This may be explained by residual confounding (e.g. unmeasured factors, age-specific effects of vascular factors or subclinical vascular factors or a genetic predisposition). However, a non-vascular pathway should be considered as well. For example, free radical injury has been suggested to associate with white matter changes on DTI.[8] This could be one of the alternative pathways explaining the association of thyroid function with lower white matter volume and lower white matter microstructural integrity in elderly. Oxidative stress has also been proposed as one of the possible factors in the pathophysiology of age-related diseases such as dementia.[9,10] Alternatively, direct toxic influences on the brain for example due to high thyroid hormone levels could underlie some of the found associations. Hypoxia, resulting in metabolic decreases and decline of cerebral perfusion is another possible pathway causing morphologic brain changes,[11] as we suggested in **chapter 2.4** in which reduced lung function was associated with lower white matter microstructural integrity. Also, systemic inflammation which may induce chronic inflammation of the vessel wall leading to lower white matter microstructural integrity is another potential mechanism leading to white matter microstructural damage as described in **chapter 2.4**.[12,13]

Apart from all above mentioned possible pathways, a more complex, multifaceted pathway needs to be considered in which there is an interplay between vascular factors, hypoxia, and inflammation.[14] Future research can help to elucidate these possible pathways. Longitudinal analyses are needed to draw conclusions on directionality of associations. More in-depth measurements of cerebral perfusion and autoregulation may shed more light on the hypotheses on hypoperfusion and hypoxia. Mediation analyses with the inclusion of possible mediators such as inflammatory markers can help to study disease causal pathways. Also, hypothesis-free genome-wide association studies can uncover novel genes and pathways involved in age-related brain pathology.

White matter microstructural integrity and cognitive decline, mild cognitive impairment, dementia and hearing loss

When focusing on white matter microstructure and age-related brain diseases, my most important finding was that white matter microstructural integrity both globally and in various tracts related to cognitive function and risk of dementia, and that this association was more pronounced for some tracts than for others. I found that reduced white matter microstructural integrity throughout the brain, but mainly in the association and projection tracts related to poorer cognition. In a longitudinal analysis, I found a similar pattern, again that in particular the association, projection and limbic system tracts related to risk of dementia and with more pronounced cognitive decline. In addition, the white matter microstructure of in particular the association tracts was related to mortality. The found associations remained after adjusting for macrostructural white matter changes such as white matter atrophy and white matter hyperintensity and thus support the hypothesis that white matter microstructural integrity is an earlier and potentially more sensitive marker of white matter damage.

What underlies these associations?

The role of vascular factors in the association of white matter microstructural integrity and age-related brain diseases seems evident. Indeed, in **chapter 3.1**, I found that cardiovascular risk factors were related to mild cognitive impairment, a transitional stage between aging and dementia. Besides cardiovascular risk factors, also markers of small vessel disease such as white matter hyperintensities were related to MCI, and these results indicate the important role of vascular factors in early phases of age-related diseases such as dementia. Also, in an additional analysis in **chapter 3.3** (data not published) we found overall and age-specific associations of cardiovascular risk factors (i.e. hypertension, hypercholesterolaemia, current smoking, diabetes, and body mass index) with global white matter microstructural integrity from middle age on as depicted in **Figure 1**. In addition, low white matter microstructural integrity was mainly related to cardiovascular mortality as described in **chapter 3.5**. However, some

of the found associations did not attenuate after adjustments for cardiovascular risk factors, as we described in **chapter 3.2 and 3.3** in which we focused on tract-specific white matter microstructural integrity and the association with cognition and dementia. Also, adjusting for cardiovascular risk factors did not change the estimates substantially studying white matter microstructural integrity and hearing loss in **chapter 3.4**. Hearing loss possibly adds to the cognitive load of a vulnerable brain leading to white matter microstructural brain changes.[15] Also other mechanisms, as we described above, should be considered in contributing to the found associations and this need to be further investigated in future research.

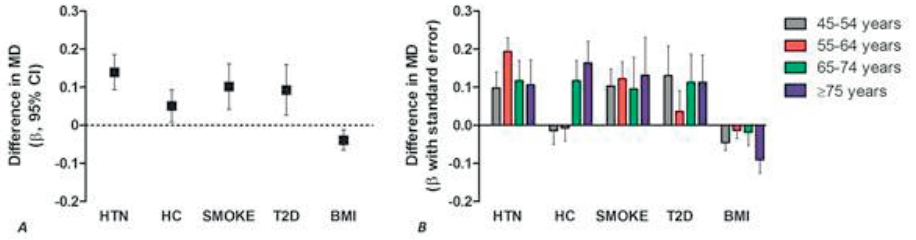

Figure 1

Cognitive performance consists of developmental and degenerative components.[16] Recently, the highly polygenic architecture of cognition was partly elucidated by the identification of genetic variants in ninety-nine independent loci (Davies et al, in press). We aimed to elucidate the associations of the genetic variants underlying cognition with cognitive decline, daily functioning, dementia, parkinsonism and stroke. Brain changes may be an intermediate between the genetic variants and the different endpoints and therefore we also studied the link between the genetic variants and brain imaging markers including DTI-measures globally and tract-specific. A higher polygenic score (PGS) was associated with cognitive decline. No association was found with daily functioning, the incidence of dementia, parkinsonism or stroke. A higher PGS was related to a larger intracranial volume and higher educational attainment and associated with a better white matter microstructure in the posterior thalamic radiation, inferior-fronto-occipital fasciculus and in the parahippocampal part of the cingulum. These white matter tracts have been associated with cognitive performance previously.[17] This study suggests that the studied genetic variants associated with cognition represent both developmental and degenerative components of cognitive performance. This indicates that the results in **chapter 3.2 and 3.3** assessing the relation of white matter microstructural integrity and cognition and dementia, apart from neurodegeneration can also be partly explained by developmental influences.

To investigate the potential clinical use of advanced imaging markers we aimed to evaluate a previously proposed prediction tool, namely the Disease State Index

(DSI)[18], to predict cognitive decline using (advanced) imaging and non-imaging features, including global and tract-specific DTI -measures. Though for several of the brain imaging markers that were introduced in the DSI, independent associations with risk of cognitive decline and dementia had been described,[19-21] their added value in the prediction model was disappointingly low. Best performance of the prediction of global cognitive decline was obtained using only age as input feature. Adding additional input features to the DSI did not improve prediction of global cognitive decline in the general population. This is in concordance with a previous population based study, concluding that MRI markers on top of age and other conventional risk variables did not improve the prediction of all cause dementia.[22] This indicates that more work is needed in the domain of disease prediction modeling of dementia and other age-related brain diseases, and that specifically in the field of imaging markers we may need to focus more on either fine-grained advanced imaging features such as functional MRI measures, multimodality imaging[23] or the use of other analytical approaches such as deep learning algorithms[24] in medical image analysis.

Methodological considerations related to studies in this thesis

Population-based study design

The studies discussed in this thesis were conducted within the Rotterdam Study, a prospective population based cohort study starting in 1990, including inhabitants of the district Ommoord of the city Rotterdam, aged 45 years and over, designed to study determinants and prognosis of chronic diseases in elderly.[25] Participants are considered to be a random sample from the general population, which reduces the possibility of selection bias and thus increases generalizability of the results. However, it must be noted that the participants of the Rotterdam Study are mostly Caucasians, making the results only generalizable to similar populations. In order to participate, in particular for the MRI, inhabitants of Ommoord needed to visit the research centre. Therefore, the healthy volunteer effect (another form of selection bias) cannot be ruled out, since it is likely that participants with poorer health did not participate. The inclusion of relatively healthy persons however will most likely lead to an underestimation of the found effect estimates. The entire cohort of the Rotterdam study is under continuous surveillance for outcomes such as dementia and mortality through electronic linkage of the study database with medical records from the general practitioners and the regional institute for outpatient mental health care. This minimizes loss to follow-up and reduces the healthy volunteer effect. The longitudinal analyses presented in this thesis, studying the association between white matter microstructure and dementia or mortality, are therefore less likely influenced by selection bias.

Differential misclassification or measurement error is a form of information bias which might have influenced our resuls, since it is likely that DTI-measures were less accurately measured in older persons, in persons with preclinical dementia or brain atrophy due to motion artifacts.

Confounding, a situation in which an association between exposure and outcome is distorted by the presence of another third variable[26], can be prevented by restriction, stratification or adjustment. In this thesis we performed multivariable adjusted regression models to account for several potential confounders, mainly vascular factors. Yet, variables included in the model that do not meet the criteria for potential confounders (e.g. intermediates) can introduce over-adjustments bias.[27] This may have influenced our results, since white matter microstructural changes may be intermediates in the relation between vascular factors and different outcomes such as dementia. I present a basic model and additionally a model including vascular factors in most of the presented studies in this thesis to assess the potential role of this over-adjustments bias effect. Most of the studies described in this thesis were performed with data that was acquired cross-sectionally. Due to the cross-sectional design, no conclusions can be drawn on the directionality of causality of the associations presented in this thesis. However, **chapter 3.3** is a longitudinal study on the relation between white matter microstructural integrity and dementia and cognitive decline. To address potential reverse causality, we repeated this analysis after stepwise exclusion of the first five years of follow-up. The risk estimates did not change, therefore it is very unlikely that the associations were driven by (subclinical) dementia cases (reverse causality).
The studies described in this thesis were conducted within large sample sizes and this reduces the chance on false positive findings in comparison to smaller imaging studies.

Imaging protocol
From 2005 onwards, MRI was implemented in the study protocol and a dedicated research scanner, undergoing a QA protocol keeping the system unchanged (no major updates or upgrades) was installed in the Rotterdam Study research center.[28] Since this is a population-based study there is a restriction of time, costs and inconvenience for the participants which needs to be balanced with the relevance and quality of the acquired imaging data. In the design of the scan protocol the time constraint, contrast and resolution requirements were taking into account. Back in 2005, when the MRI protocol was designed, the number of gradient directions was chosen to best fit the optimized protocol proposed by Jones et al.[29] taking time limits and the number of slices permitted into account. Acquisition parameters have been left unchanged since the start of the study to ensure longitudinal data stability and comparability over time. We acknowledge the fact that the spatial resolution for the diffusion acquisition used

in this thesis was relatively lower than current standards and we are aware of the lower precision to detect crossing fiber populations using 25 gradient directions. However, probabilistic tractography within the Rotterdam Study was performed with fully automated methods, publicly available methods[30] with a good reproducibility. The median R^2 of the reproducibility of the FA measurements was 0.89, in participants scanned twice within two weeks.[31] Therefore there is no reason to assume that our diffusion-weighted MRI protocol severely affected the ability to accurately reconstruct tracts of interest. We however used aggregated diffusion measures and averaging of FA and MD measures and this might discard some spatial information.

Underlying tissue properties

The diffusion of water molecules in the brain is dependent on multiple factors, including the underlying white matter microstructural integrity, which is believed to be predominantly determined by the alignment and diameter of white matter tracts and their myelin.[32] The diffusion profiles of water molecules in the brain, based on diffusion-weighted MRI measures, give indirect information about the underlying tissue or white matter microstructural integrity of the brain. Fractional anisotropy (FA) and mean diffusivity (MD) are the two most commonly used diffusion-weighted MRI measures. However, to what extent diffusion tensor imaging measures may be informative about the exact underlying tissue structure is still under debate. Generally it is assumed that lower FA and higher MD are associated with lower white matter microstructural integrity and there is pathological evidence that changes in these DTI-measures correlate with myelin damage and axonal loss.[32] Previously it was suggested that axial and radial diffusivity (two other DTI-measures) could disentangle whether changes in the white matter microstructure were due to axonal loss or due to myelin loss. However, the presence of other possible processes such as inflammation generates difficulties to assigning change in diffusion-MRI measures to a specific underlying pathological process (e.g. myelin loss) causing the observed lower microstructural integrity.[33] Yet based on previous research (including animal studies)[34], the found associations in this thesis, but also on the fact that white matter microstructural changes precede white matter macrostructural changes[35] we can assume that changes in diffusion-weighted MRI measures are pointing towards brain pathology of any kind.

Furthermore, it is now widely recognized that voxels with complex configurations are a challenge for DTI. The “crossing fiber problem” typically refers to the situation with two or more differentially oriented fiber bundles contributing to the diffusion-weighted MRI signal leading to incorrect DTI estimates and failure of the tractography. Previous research showed that up to 90% of the cerebral white matter voxels contain crossing fibres.[36] Interpretation of DTI-measures therefore must be done with caution. Until now the crossing fiber problem appears to be a fundamental limitation of DTI that

comes with the complexity of brain tissue, rather than a technical problem that can be overcome with a higher spatial resolution.[37]

Differential effect and vulnerability of white matter tracts

Previous studies found a differential vulnerability to decline for different white matter tracts and stated that the association tracts are most vulnerable to decline and aging.[38,39] Also in this thesis I found that the microstructural integrity of primarily the association tracts was associated with the studied determinants and outcomes in this thesis. A possible explanation could be the location of the association tracts in watershed areas, making these tracts more vulnerable to vascular damage leading to more pronounced loss of white matter microstructural integrity. Tract-specific analyses may thus have added value in providing novel etiological insight into structural brain pathology, the location of brain microstructural damage with relation to age-related brain outcomes and may help to unravel underlying pathways. In this thesis I also found that different association tracts were related to different outcomes. For example the white matter microstructure of association tracts related to hearing impairment were in particular the superior longitudinal fasciculus and the uncinate fasciculus, while the white matter microstructure of the inferior-fronto-occipital fasciculus associated most strongly with cognitive performance. This possibly points towards disease-specific effects which can be detected using tract-specific analyses, with interesting possibilities towards risk stratification and early disease prevention.

However, future studies are needed to replicate our findings to see whether these tract-specific differences are true findings initiated by disease or initiated by technical issues (e.g. the association tracts are larger tracts, making tractography less sensitive to partial volume effects compared to smaller tracts).[40]

Clinical implications and future research

In this thesis I contributed to the establishment of reference values of change in DTI-measures in aging. Furthermore, I highlight the added value of (tract-specific) DTI-measures over conventional MRI markers to study determinants and outcomes of white matter disease. This further supports the observation that macrostructural markers only represent the tip of the iceberg of the white matter damage. More etiological knowledge can be obtained using (tract-specific) DTI. I found tract-specific differences; among the 15 white matter tracts, the association tracts most often related to age-related brain outcomes such as cognitive performance. This may have clinical implications, since knowledge on tract-specific effects on cognition may inform clinicians to predict which cognitive domains may be most affected depending on the location of (focal) white matter damage, e.g. in chronic pathology or in an acute setting such as an acute stroke. Also, given the importance of recognizing pathways leading to

age-related brain diseases our results may aid in developing new biomarkers and may lead to better recognition of persons at risk**.**
Reduced kidney function and lung function were both associated with cognitive impairment. Based on the results presented in this thesis we suggest that white matter microstructural changes possibly mediate the association between different determinants (e.g. kidney function and lung function) and age-related brain diseases such as cognitive impairment. The traditional approach to mediation analysis is to adjust for the mediator in regression analysis. However, recently alternative analytic methods have been introduced to improve the interpretation of mediation analyses.[41] Future research should incorporate these methods to investigate whether changes in white matter microstructural integrity actual mediate the association of several determinants with age-related outcomes.

Although several associations were found between white matter microstructure and age-related brain diseases, this does not necessarily indicate that these markers are of value in disease prediction as shown in the DSI study we performed. Thus, a logical next step before clinical implementation of imaging markers is to investigate the added value of imaging markers including DTI for the prediction of age-related diseases. Prediction models other than the DSI tool, in the general population but also in specific patient populations, need to be tested and used as reference model to verify whether imaging markers including DTI-measures when added to the model can improve prediction of age-related diseases such as dementia.
Also, prediction of age-related diseases is calling for more advanced analytical approaches such as deep learning algorithms or machine learning methods, since extracted, often aggregated imaging markers so far do not improve prediction performance on top of age.

Concluding remarks
In this thesis I contributed to the establishment of reference values of change in DTI-measures in aging. I investigated different determinants of white matter microstructural changes, and studied the relation of white matter microstructure with age-related brain diseases. In this chapter I gave an overview of the main results, discussed methodological considerations regarding the performed studies and mentioned some clinical implications and directions for future research. The white matter microstructure of the association tracts seems to be most sensitive to decline. Although several associations were found between white matter microstructure and age-related brain diseases, the use of (global and tract-specific) DTI-measures to support clinical decision-making and prediction of age-related brain diseases needs further steps, which should focus on

prediction modelling, inclusion of more fine-grained imaging features, or the use of other analytical and methodological approaches.

REFERENCES

1. Gons RA, van Oudheusden LJ, de Laat KF, et al. Hypertension is related to the microstructure of the corpus callosum: the RUN DMC study. *J Alzheimers Dis.* 2012;32(3):623-631.
2. Burzynska AZ, Preuschhof C, Backman L, et al. Age-related differences in white matter microstructure: region-specific patterns of diffusivity. *Neuroimage.* 2010;49(3):2104-2112.
3. Maillard P, Seshadri S, Beiser A, et al. Effects of systolic blood pressure on white-matter integrity in young adults in the Framingham Heart Study: a cross-sectional study. *Lancet Neurol.* 2012;11(12):1039-1047.
4. Yau PL, Hempel R, Tirsi A, Convit A. Cerebral white matter and retinal arterial health in hypertension and type 2 diabetes mellitus. *Int J Hypertens.* 2013;2013:329602.
5. Wolters FJ, de Bruijn RF, Hofman A, Koudstaal PJ, Ikram MA, Heart Brain Connection Collaborative Research G. Cerebral Vasoreactivity, Apolipoprotein E, and the Risk of Dementia: A Population-Based Study. *Arterioscler Thromb Vasc Biol.* 2016;36(1):204-210.
6. Honig LS, Tang MX, Albert S, et al. Stroke and the risk of Alzheimer disease. *Arch Neurol.* 2003;60(12):1707-1712.
7. O'Rourke MF, Safar ME. Relationship between aortic stiffening and microvascular disease in brain and kidney: cause and logic of therapy. *Hypertension.* 2005;46(1):200-204.
8. Back SA, Kroenke CD, Sherman LS, et al. White matter lesions defined by diffusion tensor imaging in older adults. *Ann Neurol.* 2011;70(3):465-476.
9. Zhou X, Li Y, Shi X, Ma C. An overview on therapeutics attenuating amyloid beta level in Alzheimer's disease: targeting neurotransmission, inflammation, oxidative stress and enhanced cholesterol levels. *Am J Transl Res.* 2016;8(2):246-269.
10. von Arnim CAF, Gola U, Biesalski HK. More than the sum of its parts? Nutrition in Alzheimer's disease. *Nutrition.* 2010;26(7-8):694-700.
11. Antonelli Incalzi R, Marra C, Giordano A, et al. Cognitive impairment in chronic obstructive pulmonary disease--a neuropsychological and spect study. *J Neurol.* 2003;250(3):325-332.
12. Benedetti F, Poletti S, Hoogenboezem TA, et al. Inflammatory cytokines influence measures of white matter integrity in Bipolar Disorder. *J Affect Disord.* 2016;202:1-9.
13. Raj D, Yin Z, Breur M, et al. Increased White Matter Inflammation in Aging- and Alzheimer's Disease Brain. *Front Mol Neurosci.* 2017;10:206.
14. Heppner FL, Ransohoff RM, Becher B. Immune attack: the role of inflammation in Alzheimer disease. *Nat Rev Neurosci.* 2015;16(6):358-372.
15. Livingston G, Sommerlad A, Orgeta V, et al. Dementia prevention, intervention, and care. *Lancet.* 2017;390(10113):2673-2734.
16. Gerstorf D, Ram N, Hoppmann C, Willis SL, Schaie KW. Cohort differences in cognitive aging and terminal decline in the Seattle Longitudinal Study. *Dev Psychol.* 2011;47(4):1026-1041.
17. Cremers LG, de Groot M, Hofman A, et al. Altered tract-specific white matter microstructure is related to poorer cognitive performance: The Rotterdam Study. *Neurobiol Aging.* 2016;39:108-117.
18. Pekkala T, Hall A, Lotjonen J, et al. Development of a Late-Life Dementia Prediction Index with Supervised Machine Learning in the Population-Based CAIDE Study. *J Alzheimers Dis.* 2017;55(3):1055-1067.
19. Wolters FJ, Zonneveld HI, Hofman A, et al. Cerebral Perfusion and the Risk of Dementia: A Population-Based Study. *Circulation.* 2017;136(8):719-728.

20. Debette S, Beiser A, DeCarli C, et al. Association of MRI markers of vascular brain injury with incident stroke, mild cognitive impairment, dementia, and mortality: the Framingham Offspring Study. *Stroke.* 2010;41(4):600-606.
21. Akoudad S, Wolters FJ, Viswanathan A, et al. Association of Cerebral Microbleeds With Cognitive Decline and Dementia. *JAMA Neurol.* 2016;73(8):934-943.
22. Stephan BC, Tzourio C, Auriacombe S, et al. Usefulness of data from magnetic resonance imaging to improve prediction of dementia: population based cohort study. *BMJ.* 2015;350:h2863.
23. Liu X, Chen K, Wu T, Weidman D, Lure F, Li J. Use of multimodality imaging and artificial intelligence for diagnosis and prognosis of early stages of Alzheimer's disease. *Transl Res.* 2018.
24. Litjens G, Kooi T, Bejnordi BE, et al. A survey on deep learning in medical image analysis. *Med Image Anal.* 2017;42:60-88.
25. Ikram MA, Brusselle GGO, Murad SD, et al. The Rotterdam Study: 2018 update on objectives, design and main results. *Eur J Epidemiol.* 2017;32(9):807-850.
26. Hajian Tilaki K. Methodological issues of confounding in analytical epidemiologic studies. *Caspian J Intern Med.* 2012;3(3):488-495.
27. Jager KJ, Zoccali C, Macleod A, Dekker FW. Confounding: what it is and how to deal with it. *Kidney Int.* 2008;73(3):256-260.
28. Ikram MA, van der Lugt A, Niessen WJ, et al. The Rotterdam Scan Study: design update 2016 and main findings. *Eur J Epidemiol.* 2015;30(12):1299-1315.
29. Jones DK, Simmons A, Williams SC, Horsfield MA. Non-invasive assessment of axonal fiber connectivity in the human brain via diffusion tensor MRI. *Magn Reson Med.* 1999;42(1):37-41.
30. de Groot M, Vernooij MW, Klein S, et al. Improving alignment in Tract-based spatial statistics: evaluation and optimization of image registration. *Neuroimage.* 2013;76:400-411.
31. de Groot M, Ikram MA, Akoudad S, et al. Tract-specific white matter degeneration in aging: the Rotterdam Study. *Alzheimers Dement.* 2015;11(3):321-330.
32. Beaulieu C. The basis of anisotropic water diffusion in the nervous system - a technical review. *NMR Biomed.* 2002;15(7-8):435-455.
33. Wood TC, Simmons C, Hurley SA, et al. Whole-brain ex-vivo quantitative MRI of the cuprizone mouse model. *PeerJ.* 2016;4:e2632.
34. van Tilborg E, van Kammen CM, de Theije CGM, van Meer MPA, Dijkhuizen RM, Nijboer CH. A quantitative method for microstructural analysis of myelinated axons in the injured rodent brain. *Sci Rep.* 2017;7(1):16492.
35. de Groot M, Verhaaren BF, de Boer R, et al. Changes in normal-appearing white matter precede development of white matter lesions. *Stroke.* 2013;44(4):1037-1042.
36. Jeurissen B, Leemans A, Tournier JD, Jones DK, Sijbers J. Investigating the prevalence of complex fiber configurations in white matter tissue with diffusion magnetic resonance imaging. *Hum Brain Mapp.* 2013;34(11):2747-2766.
37. Schilling K, Gao Y, Janve V, Stepniewska I, Landman BA, Anderson AW. Can increased spatial resolution solve the crossing fiber problem for diffusion MRI? *NMR Biomed.* 2017;30(12).
38. Bender AR, Volkle MC, Raz N. Differential aging of cerebral white matter in middle-aged and older adults: A seven-year follow-up. *Neuroimage.* 2016;125:74-83.
39. Kochunov P, Williamson DE, Lancaster J, et al. Fractional anisotropy of water diffusion in cerebral white matter across the lifespan. *Neurobiol Aging.* 2012;33(1):9-20.
40. Vos SB, Jones DK, Viergever MA, Leemans A. Partial volume effect as a hidden covariate in DTI analyses. *Neuroimage.* 2011;55(4):1566-1576.

41. Valeri L, VanderWeele TJ. SAS macro for causal mediation analysis with survival data. *Epidemiology.* 2015;26(2):e23-24.

CHAPTER 5

Summary & Samenvatting

ENGLISH SUMMARY

As our life expectancy rises, the prevalence of common age-related brain diseases such as cognitive decline, dementia and neurovascular disease will increase. Effective preventive and curative interventions are scarce, whilst causative factors remain largely unknown. The role of cerebral white matter in age-related diseases has been established. However, macrostructural white matter changes, which are visible on a conventional MRI, constitute only the tip of the iceberg of the white matter pathology that have occurred. Recently, it has become possible to investigate white matter microstructural changes, thought of as an earlier and more sensitive markers, using diffusion-weighted MRI. It is hypothesized that white matter microstructural damage lead to loss of communication between different cortical networks, resulting in 'disconnectivity' leading to age-related brain diseases. Population data on determinants of white matter microstructural changes globally but in particular in specific white matter tracts in middle-aged and elderly persons were scarce.

The aims of the studies described in this thesis were to study determinants of global and tract-specific white matter microstructural damage, and to investigate the link between white matter microstructural damage and age-related brain diseases. The studies were embedded within the Rotterdam Study, which is a large population-based cohort study since 1990, investigating causes and consequences of diseases in the elderly.

In **chapter 2** determinants (in which we focused on aging and systemic influences on the brain) of white matter microstructural changes were described. To establish reference values of change in diffusion-weighted MRI measures in aging we performed a longitudinal analysis in **chapter 2.1**. I found loss of white matter microstructural integrity widespread in the brain. Global fractional anisotropy (FA) decreased, MD increased after 2 years of follow-up. The small vessels in kidney and retina are similar with anatomical and hemodynamic similarities. In **chapter 2.2 and chapter 2.3** I found that both kidney function and retinal vessel calibers associated with white matter microstructural integrity respectively. The association between reduced kidney function and poorer white matter microstructure was throughout the brain and partly driven by cardiovascular risk factors. In **chapter 2.3** I found that wider venules and narrower arterioles were related to reduced white matter microstructural integrity. This suggests that white matter microvascular damage is more widespread than visually detectable as white matter hyperintensities. In **chapter 2.4** focusing on lung function and white matter microstructure we found tract-specific differences. Reduced lung function related to a low white matter microstructural integrity, in particular in the association tracts. This may be explained by the location of the association tracts in watershed areas making these tracts more susceptible to vascular damage. In **chapter 2.5** the association between thyroid hormones and brain changes was assessed. I found

an age-dependent effect of free thyroxine (FT4). Higher FT4 levels were associated with larger brain volumes and higher white matter microstructural integrity in younger individuals, but not in the elderly. Adjusting for cardiovascular risk factors did not change the estimates marginally pointing towards other pathways explaining the found association.

Chapter 3 of this thesis was dedicated to the relation of white matter microstructural integrity and age-related brain diseases. Higher age, stroke and cardiovascular risk factors were related to mild cognitive impairment (MCI) in **chapter 3.1**. In addition, persons with MCI, in particular amnestic MCI had larger white matter hyperintensity load, poorer global white matter microstructural integrity and more lacunar infarcts than cognitively healthy participants. These results highlight the importance of vascular factors in early phases of dementia. Next, in **chapter 3.2** I investigated the link between white matter microstructure and cognition and found that reduced white matter microstructural integrity throughout the brain, but mainly in the association and projection tracts related to poorer cognition. A similar pattern was found in **chapter 3.3** in which white matter microstructural integrity across the whole brain, but in particular in the association, projection and limbic system tracts related to risk of dementia and with more pronounced cognitive decline. These results indicate that there is an association already in the preclinical phase of dementia and suggest that diffusion-weighted MRI may be useful in risk stratification or even prediction. Since hearing loss is considered a risk factor for dementia, we also studied the relation of white matter microstructural integrity and hearing acuity in middle-aged and elderly persons. In **chapter 3.4** I found that poorer white-matter microstructure, in particular in auditory and language-related association tracts, was significantly associated with worse hearing acuity. In **chapter 3.5** I investigated how white matter microstructural integrity was related to all-cause and cardiovascular mortality in persons free from stroke and dementia. Persons with a lower microstructural integrity, mainly in the association tracts, were at a higher risk of mortality. The associations were most profound for cardiovascular mortality indicating that white matter microstructural integrity is prone to vascular insults. In **chapter 3.6** I aimed to elucidate the associations of the genetic variants underlying cognition with cognitive decline, daily functioning, dementia, parkinsonism, stroke and brain imaging markers. The genetic variants associated with cognition related to cognitive decline, larger intracranial volume, higher educational attainment and associated with a better white matter microstructure. This study suggests that these genetic variants represent both the developmental and degenerative components of cognitive performance. In **chapter 3.7** I tried to make the first step to the clinical implication of brain imaging markers and aimed to evaluate a previously proposed prediction tool namely the Disease State Index (DSI) to predict cognitive decline using imaging and non-imaging features. Best performance of the prediction of global cognitive decline was obtained

using only age as input feature. Adding additional imaging markers did not improve prediction. This calls for other prediction tools, more advanced imaging markers or other analytical approaches in the prediction of age-related diseases.

Finally in **chapter 4** I discuss the main findings of this thesis, methodological considerations, clinical implications, and I make recommendations for future research. My conclusions were firstly that systemic influences relate to a lower white matter microstructural integrity via different pathways. Proposed mechanisms are vascular factors, hypoxia, oxidative stress, inflammation, genetics, or a multifaceted interplay of the previous mentioned mechanisms. Secondly, white matter microstructural integrity (mainly in the association tracts) plays a role in several age-related brain diseases such as cognitive decline, mild cognitive impairment, dementia and hearing loss. Thirdly, using a previously proposed prediction tool, using imaging features on top of age did not improve the prediction of cognitive decline, calling for other prediction tools, more advanced imaging markers or other analytical approaches in prediction modelling.

NEDERLANDSE SAMENVATTING

De levensverwachting van mensen neemt toe en als een gevolg daarvan zullen ook vaak voorkomende aan veroudering-gerelateerde hersenziekten zoals cognitieve achteruitgang, dementie en vasculaire hersenziekten gaan toenemen. Er is nog relatief weinig bekend over de oorzaken van aan veroudering-gerelateerde ziekten en ook preventieve en curatieve interventies zijn schaars. Dat de witte stof van de hersenen een rol speelt in aan veroudering-relateerde hersenziekten is inmiddels aangetoond. Macrostructurele witte stof veranderingen, welke zichtbaar zijn op een conventionele MRI, laten vaak maar een klein gedeelte zien van de opgetreden witte stof schade. Met behulp van een geavanceerde magnetic resonance imaging (MRI) techniek, namelijk een diffusie-gewogen MRI kan men tegenwoordig in een vroeg stadium al kleine veranderingen van de witte stof opsporen die nog niet voor het blote oog waarneembaar zijn en die dus kunnen dienen als vroege markers voor witte stof schade. De hypothese is dat deze microstructurele witte stof veranderingen ervoor zorgen dat verschillende corticale gebieden in de hersenen minder goed met elkaar kunnen communiceren, resulterend in disconnectiviteit wat uiteindelijk kan leiden tot cognitieve klachten en andere aan veroudering-gerelateerde hersenziekten. Bevolkingsstudies in personen van middelbare en oudere leeftijd die deze microstructurele veranderingen van de witte stof globaal, maar ook in specifieke witte stof banen hebben bestudeerd zijn schaars.
Het doel van het onderzoek beschreven in dit proefschrift was om met behulp van diffusie-gewogen MRI verschillende factoren van microstructurele witte stof veranderingen te onderzoeken en de relatie van deze microstructurele witte stof veranderingen met aan veroudering-gerelateerde hersenziekten in beeld te brengen. Dit onderzoek heb ik uitgevoerd binnen de Rotterdam Studie, een grote bevolkingsstudie uitgevoerd onder inwoners van middelbare en oudere leeftijd van de wijk Ommoord in Rotterdam.
In **hoofdstuk 2** beschrijf ik verschillende determinanten (met focus op de invloed van ouder worden en op systemische invloeden op het brein) van microstructurele witte stof veranderingen. Om referentie waarden van verandering van diffusie-gewogen MRI maten in verouderende hersenen vast te kunnen stellen heb ik in **hoofdstuk 2.1** een longitudinale studie verricht. Ik vond een verslechterde microstructurale witte stof integriteit in vrijwel het gehele brein. Global fractionele anisotropie (FA) nam af, de gemiddelde diffusiviteit (MD) nam toe na 2 jaar.
De kleinste bloedvaten in de nier, retina en de hersenen tonen veel anatomische en hemodynamische overeenkomsten. In **hoofdstuk 2.2 en 2.3** respectievelijk vond ik dat zowel nierfunctie als de diameters van de retinale vaten geassocieerd zijn met microstructurele witte stof veranderingen. De associatie tussen verminderde nierfunctie en een verminderde witte stof integriteit was diffuus aanwezig in het brein, dus niet in bepaalde witte stof banen in het bijzonder, en werd deels verklaard door cardiovasculaire

risicofactoren. In **hoofdstuk 2.3** vond ik dat wijdere retinale venulen (kleine aders) en nauwere arteriolen (kleine slagaders) gerelateerd zijn aan een verminderde microstructurele witte stof integriteit. Dit suggereert dat microvasculaire witte stof veranderingen uitgebreider zijn dan wordt gezien als witte stof hyperintensiteit. In **hoofdstuk 2.4** onderzocht ik de relatie tussen longfunctie en witte stof microstructurele integriteit en vond ik verschillen tussen witte stof banen. Verminderde longfunctie relateerde aan een verminderde witte stof microstructurele integriteit, en dan met name van de associatie vezels. Dit zou mogelijk verklaard kunnen worden door de anatomische locatie van de associatie vezels in waterscheidingsgebieden, waardoor deze witte stof vezels mogelijk meer gevoelig zijn voor vasculaire schade. In **hoofdstuk 2.5** vond ik een leeftijdsafhankelijk effect van het schildklierhormoon vrij thyroxine (FT4). Hogere waarden van FT4 waren geassocieerd met grotere brein volumes en een betere microstructuur van de witte stof in jongere personen, maar niet in oudere mensen. De resultaten werden niet beïnvloed door het corrigeren voor cardiovasculaire factoren en dit wijst erop dat ook andere mechanismen een rol spelen in de gevonden associatie.
Hoofdstuk 3 in dit proefschrift is gewijd aan de relatie tussen witte stof microstructuur en aan leeftijds-gerelateerde hersenziekten. Hogere leeftijd, een herseninfarct in de voorgeschiedenis en het hebben van cardiovasculaire risicofactoren waren gerelateerd aan milde cognitieve stoornis (MCI) in **hoofdstuk 3.1**. Daarbij hadden personen met MCI, in het bijzonder amnestische MCI een groter witte stof hyperintensiteit volume, een slechtere globale microstructurele witte stof integriteit en meer lacunaire infarcten dan cognitief gezonde mensen. Deze resultaten onderstrepen het belang van vasculaire factoren in de vroege fase van dementie. Vervolgens heb ik in **hoofdstuk 3.2** gekeken naar de relatie tussen witte stof microstructuur en cognitief functioneren. Verminderde witte stof microstructuur in het gehele brein, maar met name in de associatie en projectie vezels relateerde aan een verminderd cognitief functioneren. Een vergelijkbaar patroon werd gevonden in **hoofdstuk 3.3** waarin een slechtere witte stof microstructuur in vrijwel het gehele brein maar ook met name in de associatie, projectie en limbische vezels relateerde aan een verhoogd risico op dementia en een verhoogde afname in cognitief functioneren. Deze resultaten indiceren dat er al een associatie is in de preklinische fase van dementie en suggereren dat diffusie-gewogen MRI bruikbaar kan zijn voor risico predictie.
Gehoorverlies wordt gezien als een risicofactor voor dementia en daarom heb ik ook de relatie tussen witte stof microstructuur en gehoorverlies bestudeerd in middelbare en oudere personen. In **hoofdstuk 3.4** vond ik dat een slechtere witte stof microstructuur, met name in aan gehoor en spraak gerelateerde associatie vezels associeerde met een slechtere gehoorfunctie.
In **hoofdstuk 3.5** heb ik onderzocht hoe microstructurele witte stof integriteit relateerde aan sterfte in personen zonder beroerte of dementia. Personen met een mindere

witte stof microstructurele integriteit hadden een hoger risico op sterfte, met name cardiovasculaire sterfte en dit onderstreept nog verder dat de microstructuur van de witte stof gevoelig is voor vasculaire schade.
In **hoofdstuk 3.6** was het doel om de associaties van genetische varianten onderliggend aan cognitie te bestuderen met cognitieve achteruitgang, dagelijks functioneren, dementie, parkinsonisme, beroerte en MRI markers van het brein. De bestudeerde genetische varianten hingen samen met cognitieve achteruitgang, een groter brein volume en een betere educatie. Dit suggereert dat deze genetische varianten zowel de ontwikkelingscomponent als de degeneratieve component van cognitie representeren. Mijn bevindingen in **hoofdstuk 3.2 en 3.3**, gericht op de relatie tussen witte stof microstructuur en cognitie en dementie, worden dus mogelijk naast neurodegeneratie ook deels verklaard door ontwikkelingsfactoren.
In **hoofdstuk 3.7** wilde ik de eerste stap maken naar de klinische bruikbaarheid van brein MRI markers en had ik als doel om een eerder voorgestelde predictie methode genaamd de 'Disease State Index' te gebruiken om cognitieve achteruitgang te voorspellen aan de hand van verschillende markers inclusief MRI markers. Ik vond dat leeftijd de belangrijkste predictor was en dat andere predictors geen toegevoegde waarde hadden in de voorspelling van cognitieve achteruitgang bovenop leeftijd. Dit geeft aan dat voor de predictie van aan verouderings-gerelateerde hersenziekten andere predictie methoden, meer geavanceerdere MRI markers of andere analytische methoden nodig zijn.
Tenslotte, in **hoofdstuk 4** bespreek ik de belangrijkste bevindingen, de methodologische limitaties en de klinische implicaties van dit proefschrift en geef ik suggesties voor verder onderzoek. Mijn belangrijkste conclusies zijn: ten eerste: systemische invloeden buiten het brein zijn consistent geassocieerd met een mindere witte stof microstructurele integriteit. Mogelijke mechanismen zijn via vasculaire factoren, hypoxie, oxidatieve stress, inflammatie, een genetische predispositie of een samenspel van deze mogelijke mechanismen. Ten tweede, de witte stof microstructuur van met name de associatie vezels spelen een rol in vele aan veroudering gerelateerde hersenziekten zoals cognitieve achteruitgang, MCI, dementie en gehoorsverlies. Ten derde, gebruikmakend van een eerder voorgestelde predictie methode, was leeftijd de belangrijkste predictor voor cognitieve achteruitgang en hadden MRI markers bovenop leeftijd geen toevoegde waarde. Dit roept aan tot andere predictie methoden, meer geavanceerde imaging maten of andere analytische methoden.

CHAPTER 6

Appendices

PhD PORTFOLIO

Name PhD Student:	Lotte Cremers
Erasmus MC Department:	Epidemiology and Radiology & Nuclear Medicine
Research School:	Netherlands Institute for Health Sciences
PhD Period:	August 2013 – November 2017
Supervisors:	Prof. dr. M.A. Ikram, Prof. dr. M.W. Vernooij

1. PhD training	**Year**	**ECTS**
Research skills		
Master of Science in Clinical epidemiology, NIHES	2013-2015	70
Integrity in Science (Erasmus MC)	2014	0.3
The Course on R (4 days). Postgraduate School MolMed, Rotterdam	2014	2
International conferences		
Alzheimer's Association International Conference 2014, Copenhagen, Denmark: poster presentation	2014	1.3
Association of Radiology Conference 2014, 's Hertogenbosch, the Netherlands: oral presentation	2014	1.0
Annual meeting of the Radiological Society of North America 2015, Chicago, USA: oral presentation	2015	1.5
VasCog 2016, Amsterdam, the Netherlands: poster presentation	2016	1.0
European Congress of Radiology 2017, Vienna, Austria: oral presentation	2017	1.5
In depth courses, seminars and workshops		
Weekly research seminars, department of epidemiology, Erasmus MC	2013-2016	4.0
FSL course FMRIB, Oxford, United Kingdom	2014	2.0
fMRI & DTI course, Basel, Switserland	2015	2.0
2. Teaching activities		
Assisting in the Junior Med School	2015	2.0
Jury Junior Med School	2016	2.0
Supervising master student J. Verbruggen Microbleed location is related to white matter lesion morphology	2016	4.0
3. Other		
Reviewer		
Reviewing activities for peer-reviewed journals	2015-present	1.0

LIST OF PUBLICATIONS

White matter degeneration in aging; a longitudinal diffusion-MRI analysis: de Groot M**, Cremers LGM**, Ikram MA., Hofman A., Krestin GP, van der Lugt A., Niessen WJ, Vernooij MV. Radiology 2016 May 279 (2): 532-41.

Kidney function and microstructural integrity of brain white matter: Sedaghat S, **Cremers LGM**, de Groot M, Hoorn EJ, Hofman A, van der Lugt A, Franco OH, Vernooij MW, Dehghan A, Ikram MA. Neurology 2015 Jul 14: 85(2):154-61.

Retinal microvasculature and white matter microstructure: The Rotterdam Study. Mutlu U, **Cremers LGM**, de Groot M, Hofman A, Niessen WJ, van der Lugt A, Klaver CC, Ikram MA, Vernooij MW, Ikram MK. Neurology 2016 sept 6; 87(10):1003-10.

Reduced lung function is associated with poorer brain white matter microstructure. **Cremers LGM**, Lahousse L, de Groot M, Roshchupkin GV, Krestin GP, Niessen WJ, Stricker BH, Ikram MA, Brussele GG, Vernooij MW. *Submitted.*

Age dependent association of thyroid function with brain morphology and microstructural organization: evidence from brain imaging.
Cremers LGM*,Chaker L*, Cremers GM*, Korevaar TIM, de Groot M, Dehghan A, Franco OH, Niessen WJ, Ikram MA, Peeters RP, Vernooij MW. Neurobiology of Aging 2018 Jan;61:44-51.

Determinants, MRI correlates, and prognosis of mild cognitive impairment: The Rotterdam Study.
Cremers LGM*, de Bruijn RF*, Akoudad S*, Hofman A, Niessen WJ, van der Lugt A, Koudstaal PJ, Vernooij MW, Ikram MA. Journal of Alzheimers disease 2014;42 Suppl 3:S239-49.

Altered tract-specific white matter microstructure is related to poorer cognitive performance: The Rotterdam Study.
Cremers LGM, de Groot M, Hofman A, Krestin GP, van der Lugt A, Niessen WJ, Vernooij MW, Ikram MA. Neurobiology of Aging 2016 mar;39:108-17.

Structural connectivity relates to risk of dementia in the general population: evidence for the disconnectivity hypothesis.
Cremers LGM, Wolters FJ, de Groot M, Ikram MK, van der Lugt A, Niesesn WJ, Vernooij MW*, Ikram MA*. *Submitted.*

White matter microstructure and hearing acuity in older adults: a population-based cross-sectional DTI study.
Rigters SC, **Cremers LGM**, Ikram MA, van der Schroeff MP, de Groot M, Roshchupkin GV, Niessen WJ, Baatenburg de Jong RJ, Goedegebure A, Vernooij MW. Neurobiology of aging 2018 Jan;61:124-131.

Lower microstructural integrity of brain white matter is related to higher mortality. **Cremers LGM***, Sedaghat S*, de Groot A, van der Lugt A, Niessen WJ, Franco OH, Dehghan A, Ikram MA, Vernooij MW. Neurology 2016 Aug 30; 87(9);927-34.

Genetic variation underlying cognition and its relation with neurological outcomes. **Cremers LGM***, Knol MJ*, Heshmatollah A*, Ikram MK, Uitterlinden AG, van Duijn CM, Niessen WJ, Vernooij MW, Ikram MA, Adams HHH. *Submitted*

Predicting global cognitive decline in the general population using the Disease State Index. **Cremers LGM***, Huizinga W*, Niessen WJ, Krestin GP, Poot DHJ, Ikram MA, Lötjönen J, Klein S**, Vernooij MW**.
Submitted

Retinal neurodegeneration and brain MRI markers: the Rotterdam Study.
Mutlu U, Bonnemaijer PWM, Ikram MA, Colijn JM, **Cremers LGM**, Buitendijk GHS, Vingerling JR, Niessen WJ, Vernooij MW, Klaver CCW, Ikram MK.
Neurobiology of Aging 2017 Dec 60;183-191.

Tract-specific white matter microstructure and gait in humans.
Verlinden VJ, de Groot M, **Cremers LGM**, van der Geest JN, Hofman A, Niessen WJ, van der Lugt A, Vernooij MW, Ikram MA.
Neurobiology of Aging 2016 Jul: 43: 164-73.

White matter lesions relate to tract-specific reductions in functional connectivity.
Langen CD, Zonneveld HI, White T, Huizinga W, **Cremers LGM**, de Groot M, Ikram MA, Niessen WJ, Vernooij MW.
Neurobiology of Aging 2017 Mar, 51: 97-103.

Prevalence, clinical management, and natural course of incidental findings on brain MR images: the population-based Rotterdam Scan Study
Bos D, Poels MM, Adams HH, Akoudad S, **Cremers LGM**, Zonneveld HI, Hoogendam YY, Verhaaren BF, Verlinden VJ, Verbruggen JG, Peymani A, Hofman A, Krestin GP, Vincent AJ, Feelders RA, Koudstaal PJ, van der Lugt A, Ikram MA, Vernooij MW.
Radiology 2016 Nov: 281(2): 507-515.

Genetic determinants of unruptured intracranial aneurysms in the general population.
Peymani A, Adams HH, **Cremers LGM**, Krestin G, Hofman A, van Duijn CM, Uitterlinden AG, van der Lugt A, Vernooij MW, Ikram MA.
Stroke 2015 Oct: 46(10): 2961-4.

Determinants of calcification growth in atherosclerotic carotid arteries; a serial multidetector CT angiography study.
Van Gils MJ, Bodde MC, **Cremers LGM**, Dippel DW, van der Lugt A.
Atherosclerosis 2013 Mar: 227(1): 95-9.

DANKWOORD

Het zit erop! Wat is de tijd voorbij gevlogen. Ik heb met veel inspirerende mensen mogen samenwerken en heb van velen mogen leren. In dit dankwoord wil ik een aantal personen in het bijzonder bedanken.

Mijn beide promotoren, professor Meike Vernooij en professor Arfan Ikram wil ik op de eerste plaats bedanken.
Beste Meike, zoals ik je al vaker heb gezegd, wat een powervrouw ben jij. Je social skills, intellect en perfectionisme zijn bewonderenswaardig. Daarnaast ben je altijd bereikbaar, meedenkend en ontzettend lief. Bedankt daarvoor en voor alle begeleiding die ik de afgelopen jaren van jou heb gekregen! Fijn om je straks ook weer in de kliniek te treffen en ik kijk nu al zo uit naar 7 december.
Beste Arfan, onze tijd samen in de kliniek als AIOS radiologie vergeet ik nooit! Nu slechts een aantal jaren later ben je én hoogleraar, én afdelingshoofd van de afdeling Epidemiologie in het Erasmus MC. Jouw epidemiologische kennis, altijd briljante ideeën, en scherpe opmerkingen hebben me enorm geholpen waarvoor veel dank.
Ik heb het als een voorrecht beschouwd dat ik in jullie groep heb mogen deelnemen.

Ook gaat mijn hartelijke dank uit naar mijn promotiecommissie voor het willen uitwisselen van gedachten over mijn proefschrift. Speciale dank aan de leden van de leescommissie: professor Peter Koudstaal, professor Frank-Erik de Leeuw en dr. Stefan Klein. Dank voor jullie moeite en inzet hiervoor!

Dank professor Gabriel Krestin, dr. Winnifred van Lankeren en professor Aad van der Lugt voor alle kansen en mogelijkheden die jullie me hebben geboden de afgelopen jaren.

Natuurlijk wil ik ook alle deelnemers van de Rotterdam Studie bedanken voor hun deelname. Lydia Buist en Pauli van Eldik, dank voor jullie inzet. Ook de rest van het ERGO team wil ik hartelijk bedanken. Zonder jullie was er ook geen proefschrift! Ik vond het altijd gezellig om uitschrijfdienst te doen en waardeerde de gezellige praatjes en de lekkere croissantjes en krentenbollen. Dank jullie allemaal!

Lieve Marius, jij bent de grondlegger van de DTI in de Rotterdam Studie. Zonder jou was dit proefschrift er nooit geweest! Je bent een warm persoon. Dank voor onze prettige samenwerking en gesprekken.

Wat een fijne tijd was het op de 28e! Lieve Rens en Renée, onze perfecte combinatie van persoonlijkheden in kamer 2807 was het recept voor 3 jaar lang plezier. Lieve Rens, mijn roomie en maatje! Toen jij wegging was het niet meer hetzelfde. Ik ben blij dat ik je nog op regelmatige basis zie en op de hoogte ben en blijf van het reilen en zeilen van jouw leven.
Frenkie, een lunchloopje doet een mens goed. Dank voor de gezellige gesprekken! Tot in de kliniek.
Ook mijn andere collega's van de afdeling Epidemiologie wil ik bedanken: Hazel, Sanaz, Tavia, Hieab, Gena, Thom, Silvan, Alis, Eline, Hoyan, Maria, Nina, Lana, Sander, Layal, Kimberly, Pinar, Unal, Noor, Saloua, Sirwan, Vincent, Marileen, Jeremy, Saima, Stephanie, Lies, Daniel en Jasper. Dank jullie wel!
Gabrielle Bakker, ook jij bedankt voor al je hulp de afgelopen jaren.
Ik vond het gezellig met jullie, mastermeuk buddies.

Wyke, ik vond het altijd heel prettig met jou samenwerken en ook de VPH-DARE-IT reisjes met jou waren een feestje! Ook na onze promotie blijven we elkaar zien. Ik leef met alles met jullie mee.
Mijn dank gaat ook uit naar alle andere collega's van de Biomedical Imaging Group Rotterdam.

Dank collega's van de afdeling radiologie & nucleaire geneeskunde voor een warm welkom bij mijn terugkeer in de kliniek.

Lieve vriendinnetjes, Angel, Femke, Daphne, Vera, Marthe, Merel, Lara, Renske, Ikram, Simone, Dorian, hopelijk vanaf nu weer meer tijd om samen te borrelen en dingen te ondernemen!

Mijn paranimfen, Selma Andrade, lieve Sel, mijn allerbeste vriendinnetje! Geen dankwoord is lang genoeg om te beschrijven wat wij allemaal hebben meegemaakt. Jij kent mij als geen ander en alle hoogtepunten en dieptepunten van ons leven hebben we samen gedeeld. Ik word blij van jou!
Pauline Croll, lieve Paulientje (b.. t…), het leek wel liefde op het eerste gezicht! Ik ken geen vrouw die grappiger is dan jij. Fijn om jou nu ook als paranimf achter me te hebben staan en ik hoop dat we elkaar ook in de toekomst heel vaak blijven zien.

Ko Mast, wat heb jij mij geholpen de afgelopen jaren. Ik wil je oprecht bedanken voor alles wat je voor me hebt gedaan. Zonder jou had ik geen meubelzaak naast mijn studie kunnen runnen. Ik mis onze gesprekken op zaterdag.

Natuurlijk wil ik ook mijn (schoon)familie bedanken.
Rob en Kitty, Joost en ik zijn jullie heel erg dankbaar. De afgelopen twee jaar hebben wij nog meer gemerkt hoe jullie onvoorwaardelijk achter ons staan, ieder gat bij ons dichten en ons helpen waar nodig. Dank! Oma Toos, bedankt voor de mooie momenten.

Jeroen, mijn grote broer. Wij delen een passie! Wellicht niet puur toeval gezien onze achternaam? Uren kunnen wij hier samen over kletsen. Iedereen heeft een springplank nodig zegt men en jij was dat voor mij. Dank hiervoor.

Sara lieve zus, 2017 was niet jouw en ons jaar. Je hebt je er zo hard doorheen geknokt. Nu op naar betere tijden en een nieuwe start in Weesp. Dank voor het er altijd zijn. Ik ben trots op jou!

En dan natuurlijk mijn ouders, lieve papa en mama, bedankt voor alle mogelijkheden die jullie me altijd hebben gegeven. Ik heb veel aan jullie te danken. Wat hebben wij een onbezorgde jeugd gehad dankzij jullie!

Joost, schat en liefde van mijn leven. Wat zijn wij een topteam samen, op alle vlakken! Ik blijf om je lachen en heb zin in de toekomst met jou en onze kleine man.

Vins, wat een prachtig mannetje ben je toch! Volg je hart……

ABOUT THE AUTHOR

Lotte Gertruda Marianne Cremers was born on March 2nd 1983 in Boxmeer, the Netherlands. After graduating at the Elzendaal College in Boxmeer in 2001, she went on to study medicine at the Erasmus Medical Center in Rotterdam and graduated with honours in 2010. During this period she lived in Australia for one year. Furthermore, she participated in a research project on hypokalaemia at the department of Internal Medicine at the Erasmus Medical Center under the supervision of prof.dr. B. Zietse.

In 2010, she started her residency at the department of Radiology and Nuclear Medicine at the Erasmus Medical Center in Rotterdam and at the Albert Schweitzer hospital in Dordrecht. In 2013 she started a PhD research project on 'Structural Brain Connectivity in Aging and Neurodegeneration' at the Neuroepidemiology department of the Erasmus Medical Center (supervision: prof. dr. M.A. Ikram and prof.dr. M.W Vernooij), which resulted in this thesis. During this period she participated in the Research Master program in Health Sciences with specialization in Clinical Epidemiology provided by the Netherlands Institute of Health Sciences (NIHES). From February 2018 onwards, she continued her residency at the Radiology and Nuclear Medicine Department at the Erasmus Medical Center (head: prof. dr. G.P. Krestin and under supervision of dr. W. van Lankeren) and is planning to differentiate into neuroradiology and breast imaging.